4. SITE 608[1]

Shipboard Scientific Party[2]

HOLE 608

Date occupied: 13 July 1983 (0730 hr.)

Date departed: 17 July 1983 (1230 hr.)

Time on hole: 4 days, 5 hr.

Position: 42°50.205′N; 23°05.252′W

Water depth (sea level; corrected m, echo sounding): 3526

Water depth (rig floor; corrected m, echo sounding): 3541.8

Bottom felt (m, drill pipe): 3533.6

Penetration (m): 530.9

Number of cores: 59

Total length of cored section (m): 530.9

Total core recovered (m): 428.03

Core recovery (%): 80.6

Oldest sediment cored:
Sub-bottom depth (m): 515.4
Nature: dolomite-bearing calcareous mudstone
Age: upper middle Eocene, NP16, ~ 42 Ma
Measured velocity (km/s): 2.26

Basement:
Sub-bottom depth (m): 515.4 (top); 530.9 (bottom)
Nature: basalt
Velocity range (km/s): 4.27

HOLE 608A

Date occupied: 17 July 1983 (1419 hr.)

Date departed: 18 July 1983 (1600 hr.)

Time on hole: 1 day 1 hr.

Position: 42°50.205′N; 23°05.252′W

Water depth (sea level; corrected m, echo sounding): 3526

Water depth (rig floor; corrected m, echo sounding): 3541.8

Bottom felt (m, drill pipe): 3533.6

Penetration (m): 146.4

Number of cores: 16

Total length of cored section (m): 146.4

Total core recovered (m): 144.04

Core recovery (%): 98.4

Oldest sediment cored:
Sub-bottom depth (m): 146.4
Nature: foraminiferal–nannofossil ooze
Age: uppermost Miocene
Measured velocity (km/s): 1.536

Basement: not reached

Principal results: Site 608 is on the southern flank of the King's Trough tectonic complex. Hole 608 was continuously cored with the variable-length hydraulic piston corer (VLHPC) and extended core barrel (XCB) to basement at 530.9 m sub-bottom. Hole 608A was continuously cored with the VLHPC, providing overlap to refusal at 146.4 m sub-bottom. Core recovery was generally over 90%, but very low recoveries in isolated cores within 100 m of basement place the average recovery for Hole 608 at 81%, versus 98% for Hole 608A.

A stratigraphically continuous sequence of Quaternary (NN21) through mid-upper Oligocene sediments was recovered to 455 m sub-bottom (NP24). At this level a major hiatus occurs, representing a time period of up to 9.7 m.y. No other major hiatuses have been detected. Between about 465 and 455 m sub-bottom, the sediments contain mixed middle to lower Oligocene and Eocene (reworked) faunas. Below about 465 m sub-bottom a mid-upper Eocene (NP17) to upper middle Eocene (NP16) sediment sequence lies upon basalt at 515.4 m sub-bottom. Two cores were taken in this basaltic basement to a terminal depth of 530.9 m. Paleomagnetic and lithologic tie-lines in the overlapping VLHPC part of the section indicate that a complete composite section appears to have been recovered through the Quaternary and lower Pliocene to at least 120 m sub-bottom (NN12).

Dolomite-bearing calcareous mudstone above basement and dolomitic marlstone through the middle Eocene give way upsection to marly nannofossil chalk containing graded volcaniclastic beds and volcanic ash layers in the upper Eocene. Eocene accumulation rates averaged 11.8 m/m.y. Immediately above the Eocene–Oligocene hiatus is an interval of marly nannofossil chalk with flaser structures and a chalk conglomerate, displaying soft-sediment deformation structures, that is interpreted as consisting of debris flows. The hiatus is interpreted to be of tectonic origin, because it is recorded as an angular unconformity in seismic profiles and may be correlated with a regional volcanic event.

The remaining upper Oligocene, all of the Miocene, and most of the Pliocene make up a sequence of chalks to oozes that are marly up to the middle Miocene and almost pure calcium carbonate above. Within this thick pelagic sequence, another tectonic event is recognized. The marly chalks of the lower Miocene (NN3/NN2) at around 320 to 406 m sub-bottom display flaser structures and microfaulting with slickensides. Maximum sediment instability is recognized at 369 to 375 m, where another chalk conglomerate occurs. This is again considered a debris-flow deposit. Sedimentation rates during the late Oligocene and early Miocene aver-

---

[1] Ruddiman, W. F., Kidd, R. B., Thomas, E., et al., *Init. Repts. DSDP*, 94: Washington (U.S. Govt. Printing Office).

[2] William F. Ruddiman (Co-Chief Scientist), Lamont-Doherty Geological Observatory, Dept. of Geological Sciences, Columbia University, Palisades, NY 10964; Robert B. Kidd (Co-Chief Scientist), Institute of Oceanographic Sciences, Surrey GU8 5UB, United Kingdom (present address: Ocean Drilling Program, Texas A&M University, College Station, TX 77843-3469); Ellen Thomas (Science Representative), Deep Sea Drilling Project, Scripps Institution of Oceanography, La Jolla, CA (present address: Lamont-Doherty Geological Observatory, Dept. of Geological Sciences, Columbia University, Palisades, NY 10964; Jack G. Baldauf, Paleontology and Stratigraphy Branch, U.S. Geological Survey, Menlo Park, CA (present address: Ocean Drilling Program, Texas A&M University, College Station, TX 77843-3469); Bradford M. Clement, Lamont-Doherty Geological Observatory, Palisades, NY (present address: Ocean Drilling Program, Texas A&M University, College Station, TX 77843-3469); James F. Dolan, Dept. of Earth Sciences, University of California, Santa Cruz, Santa Cruz, CA 95060; Margaret R. Eggers, Dept. of Geology, University of South Carolina, Columbia, SC 29208; Philip R. Hill, Atlantic Geoscience Center, Geological Survey of Canada, Bedford Institute of Oceanography, Dartmouth, Nova Scotia B2Y 4A2 Canada; Lloyd D. Keigwin, Jr., Dept. of Geology and Geophysics, Woods Hole Oceanographic Institution, Woods Hole, MA 02543; Margie Mitchell, Geological Research Div., Scripps Institution of Oceanography, La Jolla, CA 92093; Isabelle Philipps, Laboratoire de Géologie et Océanographie, Université de Bordeaux I, 33605 Talence Cedex France; Frank Robinson, Lamont-Doherty Geological Observatory, Palisades, NY 10964; Sassan A. Salehipour, Ocean Engineering No. 2, University of Rhode Island, Kingston, RI 02882; Toshiaki Takayama, Dept. of Geology, Kanazawa University, Kanazawa 920 Japan; Gerhard Unsold, Geologisch-Paläontologisches Institut, Universität Kiel, D-2300 Kiel, Federal Republic of Germany; Philip P. E. Weaver, Institute of Oceanographic Sciences, Surrey GU8 5UB, United Kingdom.

aged 10 m/m.y. Rates dropped slightly in the uppermost part of the lower Miocene to 8.6 m/m.y. They double through the middle Miocene and upper Miocene to Pliocene, averaging 19 m/m.y.

Glacial-interglacial carbonate cycles begin at around 76 m sub-bottom in the lower Pliocene and continue to the top of the hole. Ice rafting, characterized by dispersed glacial erratic dropstones, is first detected at about this depth. These observations suggest that the date at which initiation of glaciation was recorded at this location was about 2.47 Ma (top of the Gauss). Average sedimentation rates through the glacial-interglacial cycles increased to about 34 m/m.y., presumably because of increased sediment input from ice rafting.

BACKGROUND AND OBJECTIVES

Introduction

Within the original series of sites planned as the North Atlantic paleoenvironmental transect, Site 3 (Site 608) was located at the site of *Vema* Piston Core *V*29-179, near the axis of the Mid-Atlantic Ridge at latitude 44°N. The prime objective of drilling at this site on Leg 94 was to examine fluctuations of the Polar Front and sea-surface temperature history through the Neogene. A later proposal to the Ocean Paleoenvironment Panel (OPP) recommended that a site be drilled somewhat farther south and east, on the flanks of King's Trough (42°50′N; 23°05′W). Here the aim was to determine the geologic history of the intraplate King's Trough tectonic complex. A continuous stratigraphic record was required through the Paleogene to basement on a flank of the complex for comparison with rock-core and dredge-haul data from within the complex itself (Kidd, et al., 1982; Stebbins and Thompson, 1978; Cann, 1971; Ramsay, 1970). Sediment cores taken around the proposed location had recovered a record of continuous deposition during the late Pleistocene and showed that the site had been just astride the southernmost penetration of polar water during glacial periods (Weaver, 1983). OPP considered that an eastward shift of the site to the King's Trough area would compromise slightly some of the paleoenvironmental objectives of the third site of the latitudinal transect, but that it would have the advantages of both meeting the tectonic objectives and providing a deep hole in which to extend the time scale of the transect through the Paleogene. The shift of site also created one new paleoenvironmental opportunity: to test for east-west differences in polar-front movement and sea-surface temperature change along an otherwise largely north-south portion of the transect.

Regional and Tectonic Setting

King's Trough is a complex of roughly parallel basins and ridges situated 700 km northeast of the Azores (Fig. 1). The complex extends at an angle to the Mid-Atlantic Ridge in a west-northwest/east-southeast direction, from 19° to 25°W (Laughton 1965; Searle and Whitmarsh, 1978). The summits of the main flanking ridges are above 2000 m water depth, but the major intervening trough is anomalously deep for this part of the North Atlantic, at greater than 4400 m (Fig. 2). All basins are bounded by inward-facing faults striking at about 120° (Kidd et al., 1982).

The origin of this intraplate tectonic complex has been in dispute for over 15 years, despite the relatively abun-

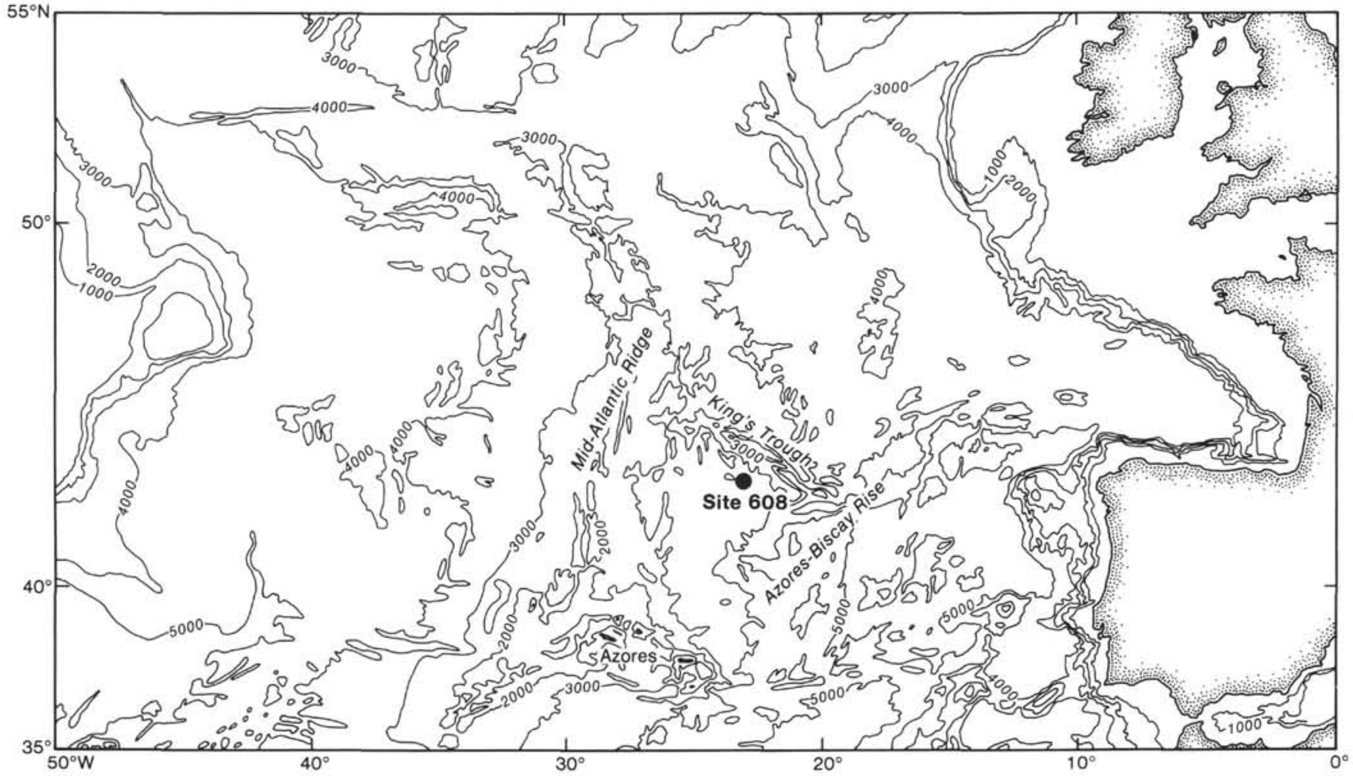

Figure 1. Location of the King's Trough complex and Site 608. Bathymetry in meters (after Kidd et al., 1982).

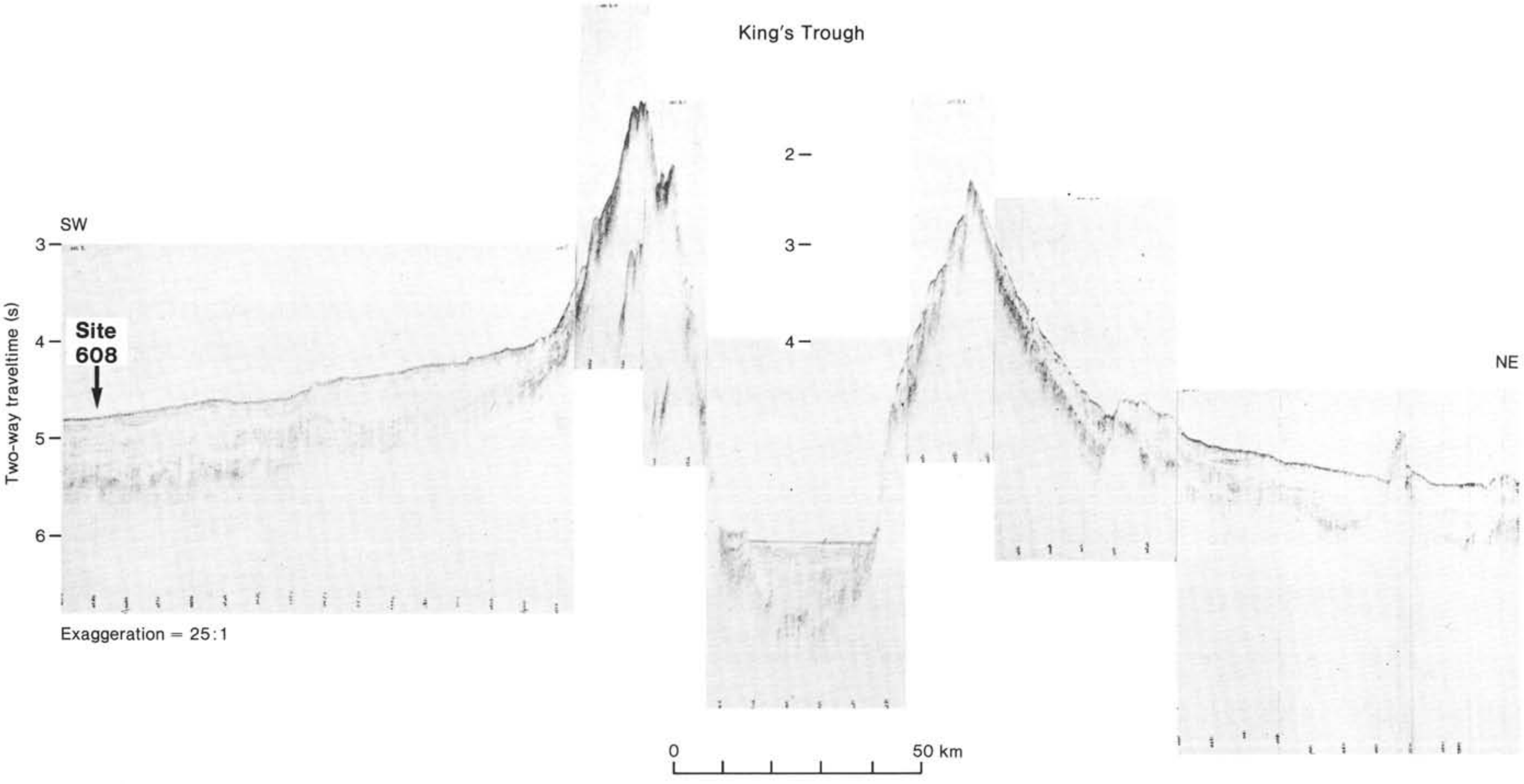

Figure 2. *Discovery* Cruise 54 seismic profile of the King's Trough complex, showing the location of Site 608.

dant geophysical and geological data available for the area (Fig. 3). Matthews et al. (1969) thought that King's Trough had formed by north-northeast/south-southwest compression, and Le Pichon and Sibuet (1971) suggested that this process occurred in the late Eocene with some subsequent, mainly vertical motion. Cann (1971), after dating a metamorphic event at Palmer Ridge from dredge hauls at the eastern end of the complex, suggested that the formation of King's Trough began much later, in the late Oligocene, as a short-lived plate boundary. Williams and McKenzie (1971) thought King's Trough resulted from the elimination of a bend in the Mid-Atlantic Ridge in the late Paleocene to early Eocene, whereas Vogt and Avery (1974) suggested that increased mantle plume discharge in the late Oligocene caused formation of a new plate boundary.

Searle and Whitmarsh (1978) showed from seismic refraction and gravity data that the flanks of King's Trough have a somewhat thicker than average crust that causes a shallowing of the seafloor in the region. They also noted a mirror image of this shallowing on the western side of the Mid-Atlantic Ridge. They suggested that the regional shallowing resulted from a hot spot situated at the Ridge between the times of magnetic Anomalies 24 and 6a (21 to 56 Ma; Berggren, Kent, and Flynn, in press). Magnetic isochrons showed that the maximum lateral displacement allowable within the complex would have been 30 to 50 km (dextral) at Anomalies 24 and 25, but that there was no strike-slip movement over approximately the last 56 m.y. (see Miles and Kidd, this volume). Searle and Whitmarsh (1978) proposed that the deep trough itself was formed primarily by extension; from "backtracking curves" they concluded that the flanking ridges were probably subaerial at some time in their history.

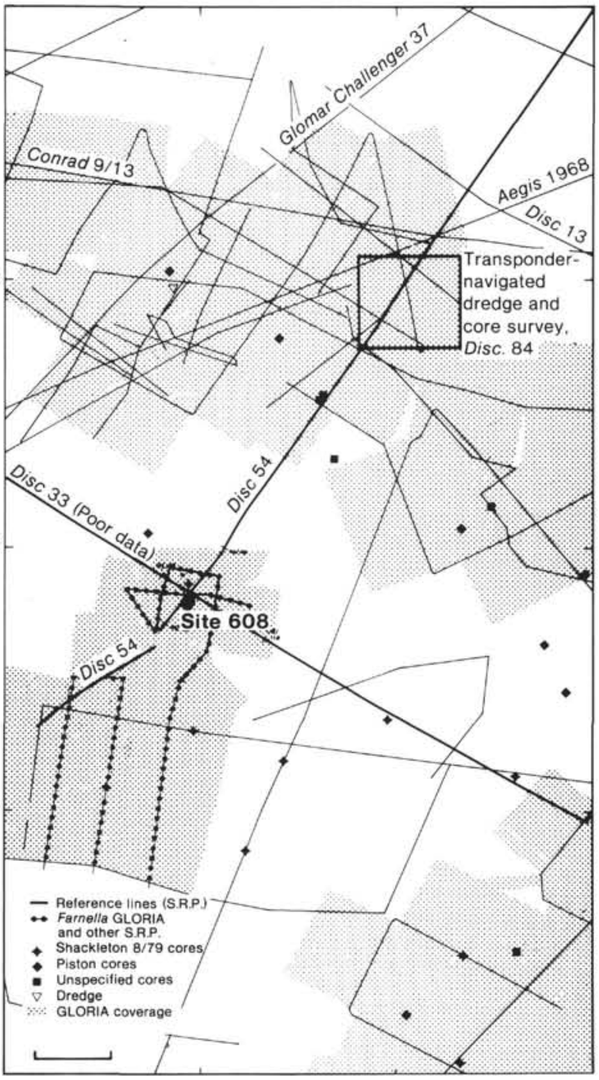

Figure 3. Site survey data for Leg 94, Site 608. S.R.P. = seismic reflection profile.

Kidd et al. (1982) used a long-range sidescan sonar survey of the region as control for new bathymetric and geologic maps of the area and for transponder-navigated dredging and rock-coring operations on the fault-bound inner flanks of the main trough (see back-pocket Figs. 3 and 4, Kidd and Ramsey, this volume). The sampling showed that basaltic volcanism, dated at 52 ± 6 Ma, was responsible for formation of the acoustic basement recognized as magnetic Anomaly 21. During a period of volcanic activity, ashes and tuffs were deposited near sea level in the late Oligocene and early Miocene. Upper Eocene and middle Miocene chalks make up the remainder of the *in situ* material dredged from the trough walls. Kidd et al. (1982) proposed a hypothesis involving uplift of a "hot-spot"-generated aseismic ridge by about 2 km during the early Oligocene. They suggested that intraplate rifting occurred during the early Miocene and resulted in the formation of the deep internal troughs, after deposition of the ashes and tuffs.

A site survey run in March 1982 over the proposed Site 3A by the Institute of Oceanographic Sciences (Wormley, U.K.) showed that sediment thicknesses around the site vary from 0.2 to 0.9 s (two-way traveltime), although they generally are about 0.5 to 0.6 s (see also Jacobs, this volume). The site chosen was over a small knoll in the basement, where the sediment thickness could be expected to be just over 500 m (0.5 s). A new magnetic anomaly map of this southern flank of King's Trough, completed just before the cruise, included data from this 1982 *Farnella* survey. These data put the chosen knoll just east of magnetic Anomaly 18, so we could expect a basement age in the older part of the range 41.29 to 42.73 Ma (see Miles and Kidd, this volume).

Site Objectives

1. Tectonic history. The primary objective of drilling at Site 608 was to recover a continuous stratigraphic section, to basement, on the southern (outer) flank of King's Trough, to be related to the sampling from the fault scarps within the complex. In addition, we hoped to date a regional mid-sediment reflector that might correlate with the hypothesized tectonic uplift of the complex. Evidence of volcanic activity during the Neogene would provide further constraints on hypotheses about formation of this intraplate feature.

2. Neogene paleoenvironments. Site 608 represents the third site in the latitudinal paleoenvironment transect, and thus, within the VLHPC part of the hole, would provide a record of the 23,000-, 41,000-, and 100,000-yr. cycles of thermal response to glaciation. Again, recovering a section to study high-resolution paleontologic, isotopic, and paleomagnetic stratigraphy was a major goal at the site.

3. *Paleogene stratigraphy*. Site 608 was the only site scheduled to terminate in oceanic basement. Thus other important biostratigraphic objectives depended upon recovery of its projected Eocene and Oligocene record.

4. *Other objectives*. The site was to be drilled on the northern edge of an area selected as a pelagic carbonate environment suitable for international studies of the feasibility of subseabed radioactive waste disposal. An ancillary objective at Site 608 was to provide samples for studies of the sedimentary sequence below levels accessible to scientists through conventional piston coring. Specific studies examined sediment permeability, shear strength, and pore-water chemistry (see Wilson and Miles, this volume).

OPERATIONS

Site Approach

Glomar Challenger left the area of Site 607 at about 0500 hr.[3] on Monday, 11 July. A course of 068° was set to cross the Mid-Atlantic Ridge toward Site 608, 560 km north of the Azores. The vessel arrived at a way point in the general vicinity of the site at 0415 hr. on Wednesday, 13 July and slowed to 8 knots while altering course to 090°. The west-to-east course was planned to follow an air-gun profile that had been run during the *Farnella* site survey in March 1982 (Fig. 4). Features on this earlier seismic record were clearly identifiable on the *Challenger's* records, and a satellite navigation fix at 0510 hr. put us on target (Fig. 5). The 13-kHz beacon was therefore dropped on the first pass over the proposed site at 0555 hr., and the ship was immediately slowed for retrieval of the seismic gear. Soon after returning to lock on to the beacon, a second satellite fix confirmed the location of the site as correct (42°50.2′N; 23°05.2′W). The site sits above a small knoll in the basement, over which the sediment thins from about 0.6 s (two-way traveltime) to about 0.45 s (500 m) on both the *Farnella* and the *Challenger* profiles.

Positioning over the beacon was completed by 0730 hr. on 13 July, and we were running in the hole until 1330 hr. A quarter of an hour was assigned to rigging the VLHPC, and we felt for bottom between 1345 hr. and 1500 hr. One water core was recovered; the next barrel was damaged when it was set down too hard. Eventually a good mudline core was recovered, arriving on deck at 1615 hr. and containing 6.97 m of nannofossil marl and ooze. We cored continuously with the VLHPC until Core 608-16 (Table 1).

Core 608-3 (16.6–26.2 m sub-bottom) was shot twice because the first time this interval was shot the flapper core catcher stuck open and there was no recovery. The second attempt recovered 9.43 m. Over-pulls of 5000 lbf. were experienced on Cores 608-3 and 608-6, and 10,000 lbf. on Cores 608-10, 608-14, and 608-15, in sticky nannofossil oozes. Eventually a 40,000-lbf. over-pull on Core 608-16 resulted in our having to wash over for retrieval. No shattering of liners was experienced at Site 608.

The XCB coring extended into basement to 530.9 m sub-bottom (Cores 608-17 through 608-57). The sediment became increasingly lithified; cores were split using the saw beginning with Core 608-26 (233.3–242.9 m sub-bottom). Nevertheless, recovery averaged over 90% to at least 380 m sub-bottom. One exception occurred when we tried a "Geoset" cutting shoe in the rapidly hardening chalks at about 300 m. Core 608-33 recovered only 3.66 m of chalk when its catcher jammed. We immediately switched back to the soft-formation cutting shoe.

Continued XCB coring on 16 July resulted in variable recovery through hard chalk. Sometimes cored intervals were washed away; sometimes the cutting shoe would jam. Again, the Geoset shoe was tried, this time with a slip-ring core catcher. Core 608-47, however, resulted in no recovery; the core had slipped out entirely. Core 608-51 recovered only the core-catcher sample, and the subsequent (Eocene) Cores 608-52 and 608-53 were found to have single large glacial-erratic pebbles set within a disturbed zone at their tops. Erratic pebbles dropping downhole past the drill bit may have caused recovery problems.

A number of minor excursions from the 13-kHz beacon throughout the day may also have impeded core recovery somewhat. The weather and sea conditions did not appear adverse, but ship positioning was erratic. At 2200 hr., a 16-kHz beacon was dropped; after placing in offsets of 270 ft. north and 610 ft. east, we began operating on this beacon at 2315 hr (16 July). Positioning improved considerably thereafter. Cores 608-55 and 608-56 had recovered only core-catcher samples from the interval 502.1 to 511.7 m prior to the beacon change. The next core, 608-57, recovered 4.5 m and entered basaltic basement.

Despite the use of a soft cutting tool for Core 608-57, we recovered 70 cm of fairly fresh vesicular basalt with calcite veins. Two further cores were taken using a diamond bit, but both recovered less than a meter of basalt. Total basalt recovery was 2.2 m out of 16.2 m cored. Total penetration at Site 608 was 530.9 m.

The weather remained fairly good, with overcast skies and relatively calm sea conditions, during operations on the hole, apart from a period in the early hours of 14 July when winds from the north were gusting to 30 knots. The ship remained remarkably stable, however, throughout this interval.

The last core from Hole 608 arrived on deck at 1102 hr. on 17 July, and we began pulling out of the hole. The mudline was cleared at 1230 hr. and the offsets on the 16-kHz beacon were reduced, making Hole 608A 670 ft. and 247° true from Hole 608. The spud-in at Hole 608A came at 1419 hr., and a 2.35-m-long first core arrived on deck at 1455 hr. A direct correlation could be made between the base of the Holocene at Holes 608 and 608A,

---

[3] All times are local (ship's time); difference from GMT, 2 hr.

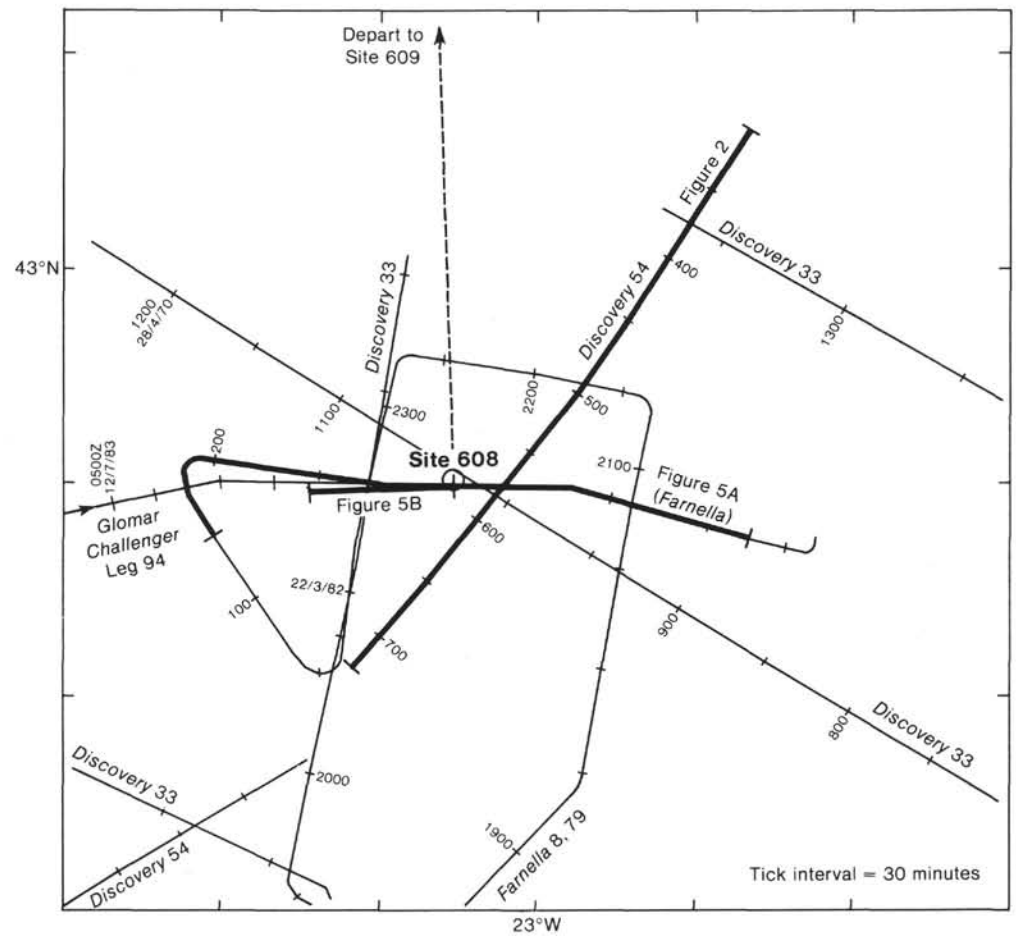

Figure 4. *Glomar Challenger* approach and departure, Site 608. Tracks of part of Figure 2 as well as of Figures 5A and 5B are indicated.

and we were content that we would have the offset required to achieve overlapping cored intervals for the two holes (see Ruddiman et al., this volume).

Continuous VLHPC coring extended to 146.4 m sub-bottom in Hole 608A (Table 1). A 40,000-lbf. over-pull was experienced on Core 608A-16 (136.8–146.4 m sub-bottom), and this was washed over to effect retrieval. This core arrived on deck at 0923 hr. on 18 July, and we began pulling out of the hole. The mudline was cleared at 1010 hr. and the bit was on deck at 1505 hr. Weather conditions were good throughout operations on Hole 608A.

By 1540 hr. we were underway and streaming the seismic gear. A short southeasterly run was made so that we could record first a seismic profile over the beacon, and then a long south-to-north profile across the western end of the King's Trough complex before setting course for Site 609.

SEDIMENT LITHOLOGY

Description of Units

Two holes were cored at Site 608. Hole 608 was continuously cored with the VLHPC to 151 m with about 95% recovery and about 2% of the section disturbed by coring. Below 151 m in Hole 608, the XCB continuously cored to basement (at 515.4 m), where two cores were cut in basalt (T.D. = 530.9 m). The upper 275 m of XCB coring gave 86% recovery with about 1% disturbance, whereas below 425 m recovery fell to 45% with 6% disturbance. Overall recovery was 81% at Hole 608. Hole 608A provided HPC overlap to 146 m depth, with 98% recovery and 1% coring disturbance.

Sediments at Site 608 vary from nearly pure pelagic oozes and chalks to dominantly terrigenous sediments. Seven sedimentary lithologic units and a basalt unit were recognized (Table 2, Fig. 6).

Lithologic Unit I consists of 76 m of alternating calcareous oozes and marls, which correspond to glacial–interglacial changes in climate during the late Pliocene and Quaternary. Sediments are dominantly white to very light gray nannofossil ooze and foraminiferal–nannofossil ooze, with very light brown marly foraminiferal–nannofossil ooze. The lightest sediments (white) in the upper part of Unit I are nearly pure nannofossil oozes frequently bounded by sharp contacts. All other contacts are usually blurred by bioturbation. The distortion of sharp lithologic contacts, flowed layers, and inclined bedding, which occurs in Cores 608-8, -7, -6, and 608A-6, may not be drilling-related (see Takayama and Sato, this volume). Throughout Site 608, bioturbation is most evident in the darker sediments and across contacts between contrasting colors, whereas white sediments are

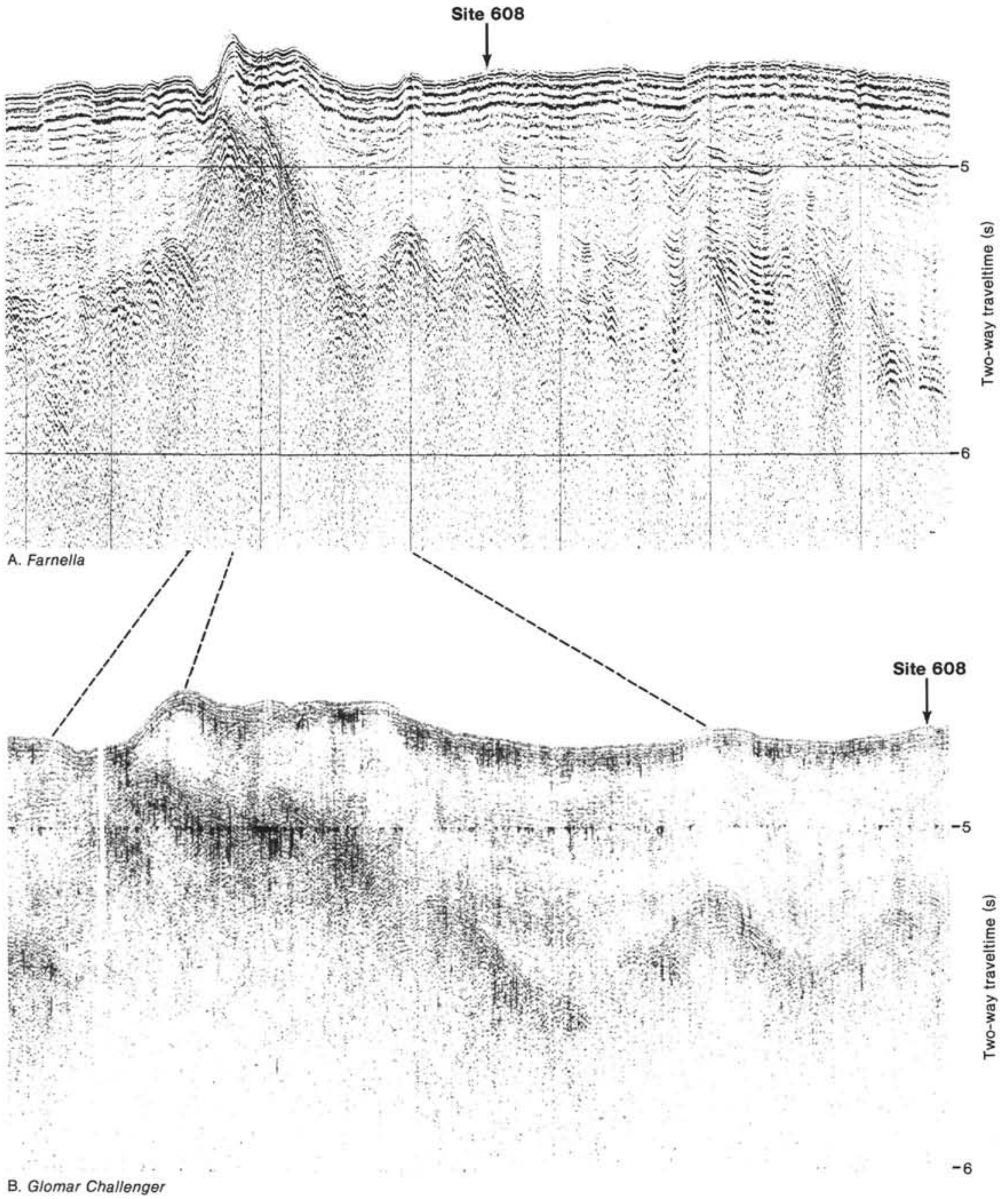

Figure 5. Comparison of seismic records from (A) the *Farnella* and (B) the *Glomar Challenger* in the vicinity of Site 608. Figure 4 indicates the position of the *Glomar Challenger* and *Farnella* profiles.

uniform. Unit I has the most variable carbonate content, with a range of 45 to 95%.

Thin gray, pale green, and pale blue laminae are common throughout Unit I. It is not known whether these are primary or post-depositional (diagenetic) features, but smear-slide analyses indicate more pyrite in these intervals. Pyrite is also evident within and around burrows (as halos) and as pieces up to 1 cm in diameter and several centimeters in length. Such pieces are clearly burrow casts. There are occasional foraminiferal sands and intervals rich in volcanic ash and glass. These features are commonly a few centimeters thick, and are dispersed by bioturbation. A noteworthy exception is a foraminiferal sand almost 1 m thick at about 57 m depth in Hole 608 (Section 608-7-2). This is interpreted as a pelagic turbidite because it fines upward. It was not found in Hole 608A. Where volcanic ash is abundant, the sediment is dark green to olive (Section 608A-2-4). Pieces of pumice occur rarely in Unit I, and glacial dropstones are common in the darker-colored intervals. The dropstones are basaltic, metamorphic, and acid igneous clasts.

Unit II is white to very light gray calcareous ooze and chalk of Miocene–Pliocene age with high carbonate content (90–95%). It is distinguished from the overlying unit

Table 1. Coring summary, Site 608.

Core	Date (July, 1983)	Time (hr.)	Depth from drill floor (m) Top Bottom	Depth below seafloor (m) Top Bottom	Length cored (m)	Length recovered (m)	Recovery (%)
Hole 608							
1	13	1615	3533.6-3540.6	0.0-7.0	7.0	6.97	99.6
2	13	1810	3540.6-3550.2	7.0-16.6	9.6	9.15	95.3
3	13	2040	3550.2-3559.8	16.6-26.2	9.6	9.43	98.5
4	13	2213	3559.8-3569.4	26.2-35.8	9.6	9.62	100.0
5	13	2334	3569.4-3579.0	35.8-45.4	9.6	8.82	91.2
6	14	0055	3579.0-3588.6	45.4-55.0	9.6	9.31	97.1
7	14	0206	3588.6-3598.2	55.0-64.6	9.6	9.26	96.5
8	14	0315	3598.2-3607.8	64.6-74.2	9.6	8.36	87.1
9	14	0450	3607.8-3617.4	74.2-83.8	9.6	7.92	82.5
10	14	0550	3617.4-3627.0	83.8-93.4	9.6	9.35	97.4
11	14	0704	3627.0-3636.6	93.4-103.0	9.6	9.02	94.0
12	14	0821	3636.6-3646.2	103.0-112.6	9.6	9.02	94.0
13	14	0931	3646.2-3655.8	112.6-122.2	9.6	8.81	91.8
14	14	1120	3655.8-3665.4	122.2-131.8	9.6	8.35	87.0
15	14	1227	3665.4-3675.0	131.8-141.4	9.6	9.11	94.9
16[b]	14	1400	3675.0-3684.6	141.4-151.0	9.6	9.52	99.2
17	14	1511	3684.6-3690.1	151.0-156.5	5.5	5.52	100.4
18	14	1630	3690.1-3699.7	156.5-166.1	9.6	8.41	87.6
19	14	7146	3699.7-3709.3	166.1-175.7	9.6	8.22	85.6
20	14	1905	3709.3-3718.9	175.7-185.3	9.6	9.33	97.2
21	14	2020	3718.9-3728.5	185.3-194.9	9.6	7.20	75.0
22	14	2137	3728.5-3738.1	194.9-204.5	9.6	8.22	85.6
23	14	2255	3738.1-3747.7	204.5-214.1	9.6	9.77	101.8[a]
24	15	0005	3747.7-3757.3	214.1-223.7	9.6	9.59	99.9
25	15	0140	3757.3-3766.9	223.7-233.3	9.6	9.72	101.3[a]
26	15	0300	3766.9-3776.5	233.3-242.9	9.6	8.04	83.7
27	15	0425	3776.5-3786.1	242.9-252.5	9.6	9.63	100.3
28	15	0540	3786.1-3795.7	252.5-262.1	9.6	8.82	91.9
29	15	0650	3795.7-3805.3	262.1-271.7	9.6	9.10	94.8
30	15	0816	3805.3-3814.9	271.7-281.3	9.6	7.62	79.4
31	15	0926	3814.9-3824.5	281.3-290.9	9.6	9.16	95.4
32	15	1048	3824.5-3834.1	290.9-300.5	9.6	8.19	85.3
33	15	1212	3834.1-3843.7	300.5-310.1	9.6	3.66	38.1
34	15	1337	3843.7-3853.3	310.1-319.7	9.6	8.89	92.6
35	15	1447	3853.3-3862.9	319.7-329.3	9.6	9.01	93.9
36	15	1610	3862.9-3872.5	329.3-338.9	9.6	8.32	86.7
37	15	1726	3872.5-3882.1	338.9-348.5	9.6	9.27	96.6
38	15	1840	3882.1-3891.7	348.5-358.1	9.6	9.02	98.8
39	15	2020	3891.7-3901.3	358.1-367.7	9.6	6.24	65.0
40	15	2155	3901.3-3910.9	367.7-377.3	9.6	8.52	88.7
41	15	2315	3910.9-3920.5	377.3-386.9	9.6	9.94	103.5[a]
42	16	0035	3920.5-3930.1	386.9-396.5	9.6	7.34	76.5
43	16	0202	3930.1-3939.7	396.5-406.1	9.6	7.48	77.9
44	16	0323	3939.7-3949.3	406.1-415.7	9.6	5.52	57.5
45	16	0455	3949.3-3958.9	415.7-425.3	9.6	9.45	98.4
46	16	0610	3958.9-3968.5	425.3-434.9	9.6	5.75	60.0
47	16	0737	3968.5-3978.1	434.9-444.5	9.6	0.0	0.0
48	16	0902	3978.1-3987.7	444.5-454.1	9.6	9.64	100.4
49	16	1027	3987.7-3995.3	454.1-461.7	7.6	5.82	76.6
50	16	1224	3995.3-4000.9	461.7-467.3	5.6	4.82	86.1
51	16	1348	4000.9-4006.9	467.3-473.3	6.0	0.25	4.2
52	16	1541	4006.9-4016.5	473.3-482.9	9.6	5.32	55.4
53	16	1735	4016.5-4026.1	482.9-492.5	9.6	2.52	26.2
54	16	1910	4026.1-4035.7	492.5-502.1	9.6	6.55	68.2
55	16	2128	4035.7-4041.3	502.1-507.7	5.6	0.08	1.4
56	16	2326	4041.3-4045.3	507.7-511.7	4.0	0.05	1.2
57	17	0145	4045.3-4048.3	511.7-514.7	3.0	4.50	150.0[a]
58	17	0642	4048.3-4054.9	514.7-521.3	6.6	0.67	10.1
59	17	1102	4054.9-4063.9	521.3-530.9	9.0	0.84	8.8
					530.9	428.03	80.6%
Hole 608A							
1	17	1455	3533.0-3535.4	0.0-2.4	2.4	2.35	97.9
2	17	1612	3535.4-3545.0	2.4-12.0	9.6	9.67	100.0
3	17	1714	3545.0-3554.6	12.0-21.6	9.6	9.80	100.0
4	17	1816	3554.6-3564.2	21.6-31.2	9.6	9.83	100.0
5	17	1928	3564.2-3573.8	31.2-40.8	9.6	9.31	97.0
6	17	2033	3573.8-3583.4	40.8-50.4	9.6	9.68	100.0
7	17	2150	3583.4-3593.0	50.4-60.0	9.6	9.28	96.7
8	17	2320	3593.0-3602.6	60.0-69.6	9.6	9.39	97.8
9	18	0045	3602.6-3612.2	69.6-79.2	9.6	9.49	98.8
10	18	0145	3612.2-3621.8	79.2-88.8	9.6	9.80	100.0
11	18	0315	3621.8-3631.4	88.8-98.4	9.6	9.27	96.6
12	18	0435	3631.4-3641.0	98.4-108.0	9.6	8.81	91.8
13	18	0545	3641.0-3650.6	108.0-117.6	9.6	9.47	98.6
14	18	0647	3650.6-3660.2	117.6-127.2	9.6	9.54	99.4
15	18	0756	3660.2-3669.8	127.2-136.8	9.6	9.17	95.5
16[b]	18	0923	3669.8-3679.4	136.8-146.4	9.6	9.18	95.6
					146.4	144.04	98.4%

[a] More recovery than drilled, because there were problems with excursions from hole. Lost position in hole after Core 608-55.

[b] 40,000-lbf. over-pull on Cores 608-16 and 608A-16; see text for explanation.

Table 2. Lithologic units at Site 608.

Unit	Subunit	Lithology	Sub-bottom interval (m)
I		Alternating nannofossil oozes and marls	0-76
II	A	White nannofossil ooze and foraminiferal nannofossil ooze	76-220
	B	White nannofossil chalk	220-257
III		White nannofossil chalk with green and gray laminae	257-320
IV		Nannofossil chalk with flaser chalk, chalk conglomerate, and microfaults	
	A	Foraminiferal-nannofossil chalk, gray and green	320-339
	B	Foraminiferal-nannofossil chalk, pale brown	339-377
	C	Marly nannofossil chalk	377-406
V		Marly nannofossil chalk	
	A	No faulting or flaser chalk	406-444.5
	B	Tannish white to very pale brown, with flattened burrows	444.5-454
	C	Flaser chalk	454-462
VI		Marly nannofossil chalk with graded volcaniclastic beds and disseminated ash intervals	462-514
VII		Dolomitic marlstone	514-515.4
1		Vesicular basalt	515.4-530.9

by the reduced frequency of color changes. Two subunits are recognized on the basis of a gradual change from ooze to chalk. Subunit IIA (76–220 m) is foraminiferal–nannofossil ooze to 122 m and nannofossil ooze below. The only significant colors other than the basic white to very light gray occur in occasional light green, gray, and greenish gray laminae. A graded foraminiferal sand (30 cm thick) occurs at about 115 m in Hole 608. A similar (50-cm) sand bed occurs in Hole 608A about 5 m deeper, and these appear to be the same turbidite. Unit II sediments are virtually featureless below 140 m depth.

Chalk beds first appear at 170 m in Unit IIA, and with increasing frequency at around 195 m. By 220 m, Unit II is dominantly chalk; Subunit IIB begins at this level and ends at 257 m. Section 608-26-4 was the first section to be split with the saw (depth 237.8 m), resulting in less distortion of sedimentary features. Sediment fracturing was first apparent in Subunit IIB. It is unclear how much sediment fracturing resulted from the drilling process, but some must be natural, because Section 608-26-4 has traces of pyrite along fracture faces.

Unit III is white nannofossil chalk of Miocene age, and extends to 320 m. It is recognized by the abrupt appearance of frequent green and gray laminae. The chalk is commonly brecciated by drilling into "biscuits" large enough to retain their stratigraphic order and to be sampled, so that drilling disturbance is considered minimal. Carbonate content (85–95%) appears to be a little lower than in Unit II, but there are too few data to confirm this. Zoophycos burrows first occur in Unit III chalks some 20 m below the level at which cores were first split with the saw. They are frequent throughout Unit III, so their appearance is probably not due to a change in the method of core splitting.

Unit IV is an 86-m sequence (320–406 m) of Miocene nannofossil chalk with microfaults and sediment flow

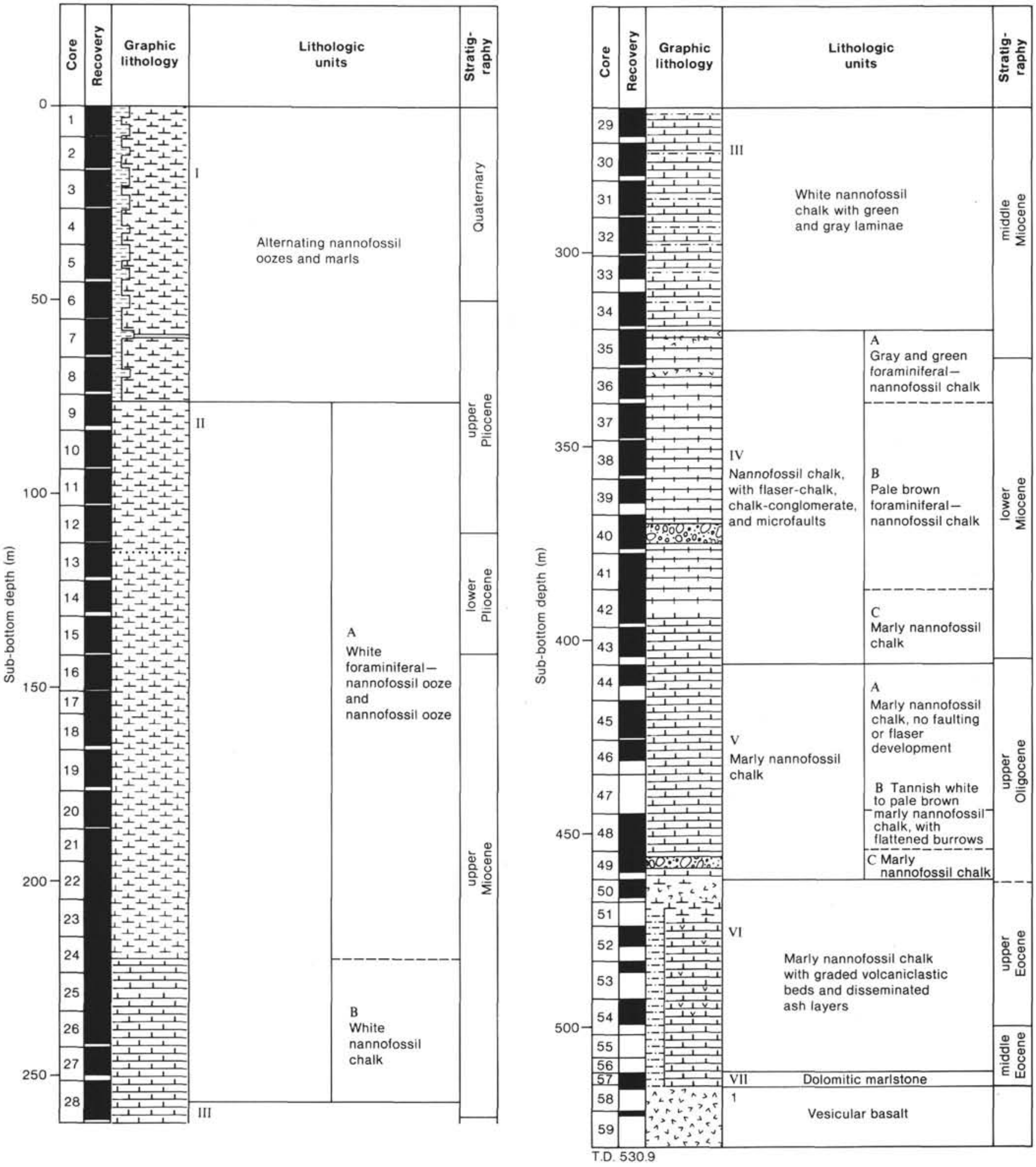

Figure 6. Recovery and lithologic units recognized at Site 608.

structures. It has slightly less carbonate (80–85%) than Unit III, and is divisible into three subunits. Subunit IVA is a foraminiferal nannofossil chalk that reaches 339 m. It is white to yellowish gray, light greenish gray, and light gray. Intervals throughout this subunit are rich in volcanic ash and glass, probably accounting for the gray and greenish color. Faulting first becomes evident within this subunit at 322 m; slickensides sometimes accompany the microfaults. Other evidence of sediment movement is subhorizontal streaming of burrows, which in one instance (333 m) are crosscut by an undistorted Zoophycos burrow.

Subunit IVB (339–377 m) is also a foraminiferal-nannofossil chalk; it differs from Subunit IVA in color (white and pale brown). Dolomite first becomes a significant component in Subunit IVB, and flaser chalks, slickensides, and microfaulting become more common. Near the base of this subunit (370 m) is a thick (2.5-m) chalk conglomerate, along with three thin beds of similar lithology. Clasts in the conglomerate are subangular to rounded marly chalk, rich in volcanic material.

Subunit IVC (377–406 m) is a marly nannofossil chalk with continued evidence of sediment flow. It changes from white and very faint tan to white and light greenish gray.

Unit V is 56 m of upper Oligocene marly nannofossil chalk, from 406 to 462 m. Subunit VA is similar in lithology to Subunit IVC, but without microfaulting or evidence of sediment flow. It begins light greenish gray, changes to pinkish and yellowish gray at 418 m, and gradually changes to tannish white and very pale brown. Subunit VB is a tannish white to very pale brown interval (Core 608-48), within which burrow mottles become progressively flattened. By 453.6 m, they show the first signs of "smearing," which is followed downsection by filamentous, wavy bedding (see Hill, this volume).

Flaser chalk structures become pronounced in Subunit VC, a yellow white to very pale brown marly nannofossil chalk. This chalk has numerous sand- to fine gravel-sized clasts of dispersed volcanic ash and an ash-bearing marly chalk conglomerate. X-ray diffraction (XRD) revealed phillipsite in this subunit, possibly reflecting nearby volcanism or erosion of preexisting volcanic material.

Unit VI (462–514 m) is a marly nannofossil chalk with graded layers and disseminated ash intervals. The top of this unit approximates the Eocene/Oligocene boundary. It is reduced in carbonate content (50–80%) compared with overlying units, and is easily distinguished by frequent layers of very dark gray and dark green. These dark layers are commonly graded and made up of volcaniclastic material: volcanic glass, feldspars, tuff clasts, pyroxene, olivine, and so on. Smectite was detected by X-ray diffraction, indicating the alteration of tuff and glass. Blocks of chalk are commonly broken by microfaulting, with slickensides evident (476 and 478 m).

Unit VII is 1.4 m of dolomitic mudstone overlying basalt. Its color is pale brown to dark grayish brown, and it has very low percentages of carbonate (20%). Dolomite rhombs are present in smear slides, as well as in the sand-sized fraction, where they occasionally have grown on the tests of foraminifers. Smear slides also reveal the presence of manganese micronodules, corroborated by the presence of the manganese carbonate mineral rhodochrosite (detected by XRD). X-ray diffraction also shows the presence of mixed-layer clays (smectites) resulting from the alteration of volcanic ash and basalts.

Basalt (Unit 1) was recovered in Cores 608-57 through -59 (515.4–530.9 m[4]). The basalt is fine-grained with small (3-mm) phenocrysts of altered olivine and plagioclase. Alteration to a depth of 1 cm, with a thin rind of glass (1–2 mm), is evident on the uppermost piece recovered. Vesicles throughout are mostly 1 mm in diameter, although occasionally they are as large as 3 mm. Cutting through the basalts are veins of cream-colored carbonate with conchoidal fractures. This may indicate incipient replacement by chert. The uppermost carbonate vein contains identifiable nannofossils, showing that it results from alteration of sediment caught within the basalt.

Volcaniclastic Lithologies

Two types of volcaniclastic sediments are recognized in Hole 608: disseminated ash layers and graded volcaniclastic layers; numerous beds are heavily bioturbated, however, so that two types cannot always be clearly distinguished.

Disseminated Ash Beds

These beds occur frequently in the top 454 m of the section but cannot be distinguished except by the identification of small amounts of volcanic glass in smear slides. Below 454 m, the concentration of volcanic debris increases dramatically. Distinct, several-centimeters-thick beds of chalk, with ash concentrations, can be identified (Fig. 7). The volcanic content of these beds consists predominantly of fine, sand-sized, clear, vesicular glass and subordinate amounts of tuff clasts. Large feldspar laths and occasional mafic minerals such as olivine and pyroxene are also present as single clasts.

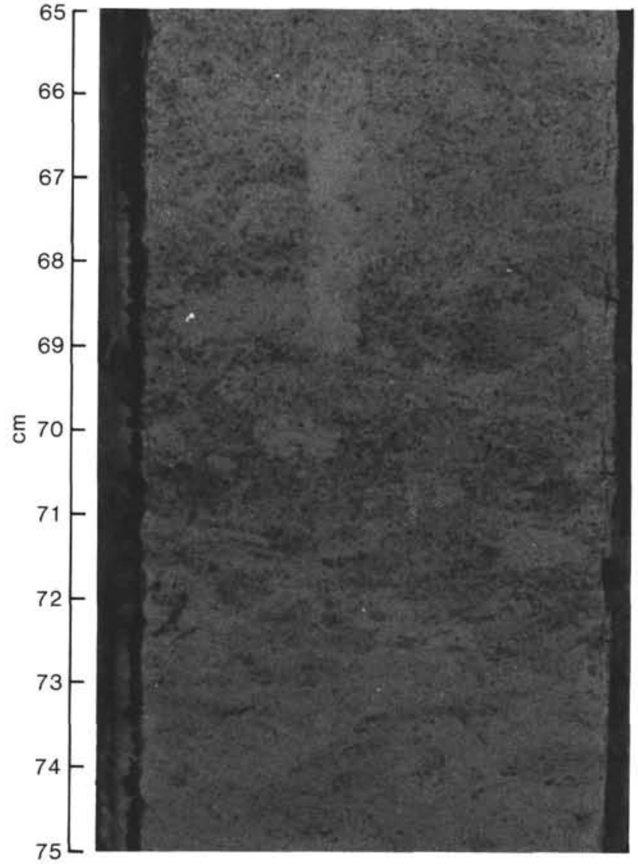

Figure 7. Disseminated ash in chalk (Sample 608-50-1, 65–75 cm).

---

[4] See Table 1; Core 608-57 recovery was 150%.

These ash layers are interpreted as having been deposited directly from subaerial eruptions in the vicinity of the drill site. The beds may represent a period of several thousand years over which a particular volcanic center was active, or single eruptions that have been disseminated within the chalk by bioturbation.

Graded Ash Beds

Associated with the disseminated ash beds in Unit VI, sharp-based, graded beds of volcaniclastic material are common (Fig. 8). These beds may be up to 5 cm thick, and grade from medium sand to clayey silt. The upper part of the graded bed is usually strongly bioturbated, and the characteristically green volcaniclastic beds grade gradually into the lighter chalk.

The sandy lower parts of the graded beds consist mainly of tuff clasts with relatively few large grains of feldspar, usually welded to tuff fragments. The clasts are moderately rounded to well rounded, indicating substantial current transport.

These graded beds are interpreted as turbidite deposits transported from an upslope location. The sands contain no indicators of the water depth from which they were derived.

Other volcaniclastic turbidite beds within Unit VI, although so bioturbated that the sharp base has been destroyed, can be identified by their distinctive green color and their composition and size grading.

Redeposited Carbonate Beds

Within the background chalk lithology, several intervals can be identified where remobilization and redeposition of the chalk has taken place. On the basis of clast composition, two major groups of such beds can be distinguished: foraminiferal sands and allochthonous and flaser chalks.

Foraminiferal Sands

These occur in Units I and II. They consist almost entirely of foraminiferal tests within sharp-based graded beds up to 82 cm thick (Section 608-7-2). Beds of this thickness are uncommon; more typically, the beds are only a few centimeters thick or are merely partings. The foraminifers are dominantly planktonic, but the benthic assemblage is very similar (diverse, deep-water) to that in the surrounding ooze. Pyrite is often associated with the foraminiferal sands and commonly concentrated in the basal, coarsest parts of the beds, although in one bed (Fig. 9) the pyrite is also concentrated in laminae

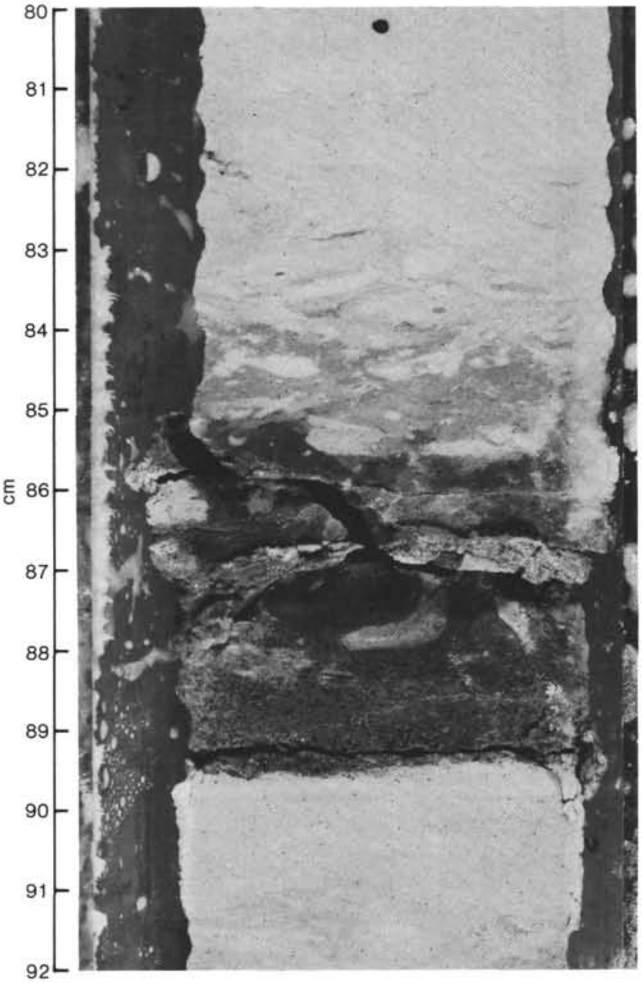

Figure 8. Graded ash bed in chalk sequence (Sample 608-50-2, 80–92 cm). Note bioturbated top.

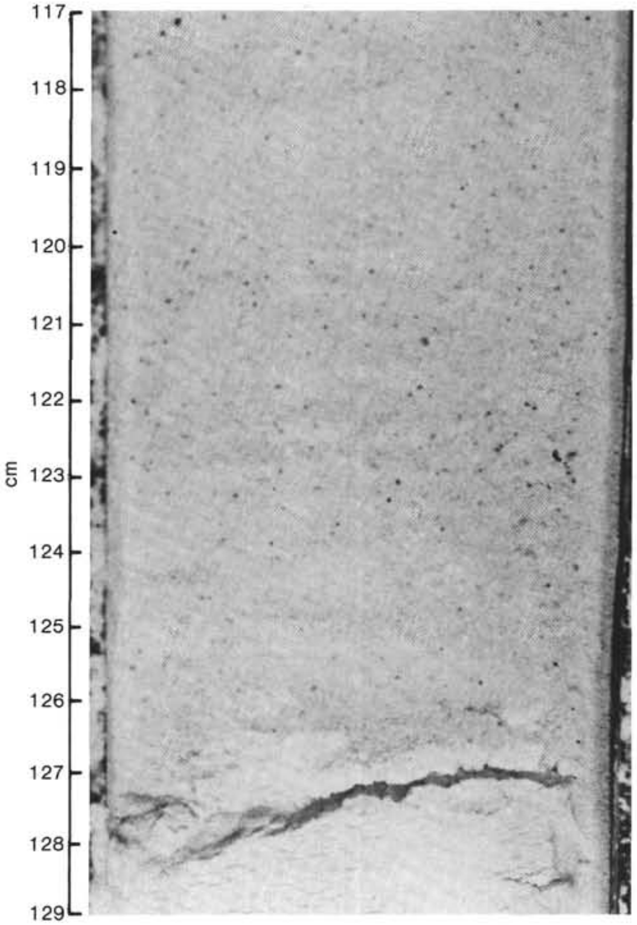

Figure 9. Graded foraminiferal sand bed (Sample 608A-14-2, 117–129 cm). Note pyrite concentrations (darker laminae).

above the base. It is not clear whether the pyrite formed before the foraminiferal tests were transported, and was concentrated by dynamic sorting, or formed after deposition, as a result of increased porosity in the coarser layers of the bed.

The sorting and graded nature of the beds suggests deposition from a waning current. A turbidite origin is most likely for the thick beds, but it is possible that the thin beds and partings may have resulted from winnowing by bottom-current activity.

Allochthonous and Flaser Chalks

Units IV and VC contain several intervals of redeposited chalk. Chalk clast conglomerates containing clasts up to 3 cm wide (width of core prohibits identification of larger clasts with near-horizontal long axes) are found in beds up to 70 cm thick in Cores 608-40 and 608-49. Upper and lower boundaries are generally difficult to define, owing to the similarity of the surrounding beds and conglomerate matrix. Most of the conglomerates are matrix-supported, and are interpreted as debris-flow deposits. A single clast-supported conglomerate overlies a possible debris flow at 457 m (Fig. 10) and shows crude fining upward to a thin ash-rich sand interval, which is in turn overlain by a burrowed chalk with a few sandy laminae. The thin (8-cm) overlying bed is interpreted as a turbidite, which may have been directly related to the underlying debris flow. A possibly deformed bed, showing very irregular lithologic contacts, is seen in Unit IV, Core 608-36 (Fig. 11). It is not clear whether these contacts represent large-scale bioturbation or fold deformation of previously bioturbated sediment. A Zoophycos burrow that crosscuts the irregular contacts indicates that deformation must have occurred while the sediment was relatively soft (see Hill, this volume).

Chalk units where the burrowed chalk lithology has a distinctive flaser appearance are common in Units IV and V. Burrows become elongated in the horizontal plane until they resemble discontinuous laminae or lenses (Fig. 12). The intervening chalk matrix is smeared out into stringerlike partings between the lensoid burrows. Flaser chalks from other areas have been described (Garrison and Kennedy, 1977), and have been variously interpreted. However, they are related to post-depositional compaction and solution (Garrison and Kennedy, 1977). It is possible that the distribution of flaser chalks may be related to gravitational or tectonic deformation (Mimran, 1975; see also Hill, this volume).

PHYSICAL PROPERTIES

The physical properties measured on samples from Site 608 are shown in Figures 13A through 13H. The measured values of dry water content, wet water content, porosity, and void ratio (Fig. 13A–13H) decrease with depth. The uppermost values probably were 100% in the surface sediments and decreased to 53% at 50 m. Values of measured water content stay constant at about 47% for sediments below 100 m. Two lithologic changes in the sediment at depths of around 80 m (glacial cycles to preglacial ooze) and 220 m (ooze to chalk) are recognizable by concurrent increases in water content. Wet water contents show the same trend.

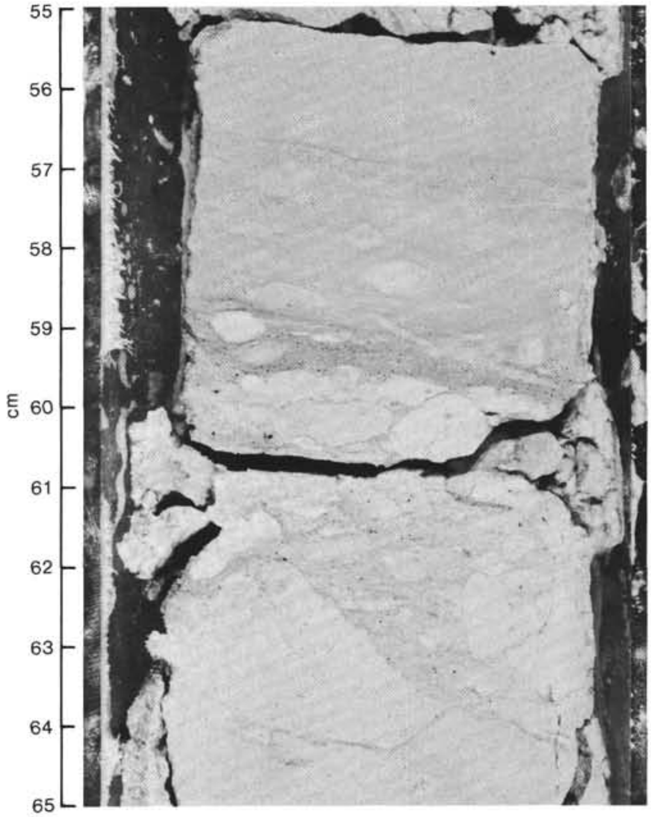

Figure 10. Crudely graded, clast-supported chalk conglomerate with bioturbated, ash-rich top (Sample 608-49-2, 55–65 cm).

The measured porosity and void-ratio values obtained from Hole 608 samples (Figs. 13C and 13D) decrease from 60 to 70% porosity and a void ratio of 2 to 2.5 at the surface to 59% porosity and a void ratio of 1.5 at a depth of 50 m. Deeper sediments have a constant porosity value of 56% and a void ratio of 1.3.

Grain densities of Site 608 samples fall between 2.5 and 2.7 g/cm^3 (Fig. 13E).

Measured values of wet-bulk density increase irregularly from 1.5 g/cm^3 at the surface to 1.7 g/cm^3 at 50 m. Deeper sediments have a wet bulk density of about 1.76 g/cm^3 (Fig. 13F).

Values of sonic velocity in the sediment begin at 1.5 km/s over the first 250 m and increase linearly from 1.5 km/s at 250 m to 2.2 km/s at 500 m. The sonic velocity of the basalt is 4.2 km/s at sub-bottom depths greater than 500 m (Fig. 13G).

Shear-strength values (Fig. 13H) increase with depth, from 70 g/cm^2 at the surface to over 350 g/cm^2 at 50 m sub-bottom depth. Measured values of shear strength show a major shift toward lower values at about 60 m.

The specific gravity of basalt was determined, by weighing in air and in water, as 2.57 g/cm^3, which approximates other values for the specific gravity of basalt.

SEISMIC STRATIGRAPHY

On departure from Site 608, we ran an air-gun profile across the beacon in a south-to-north direction and obtained an improved record of the seismic reflectors at the site. The original north–south *Discovery* 54 profile

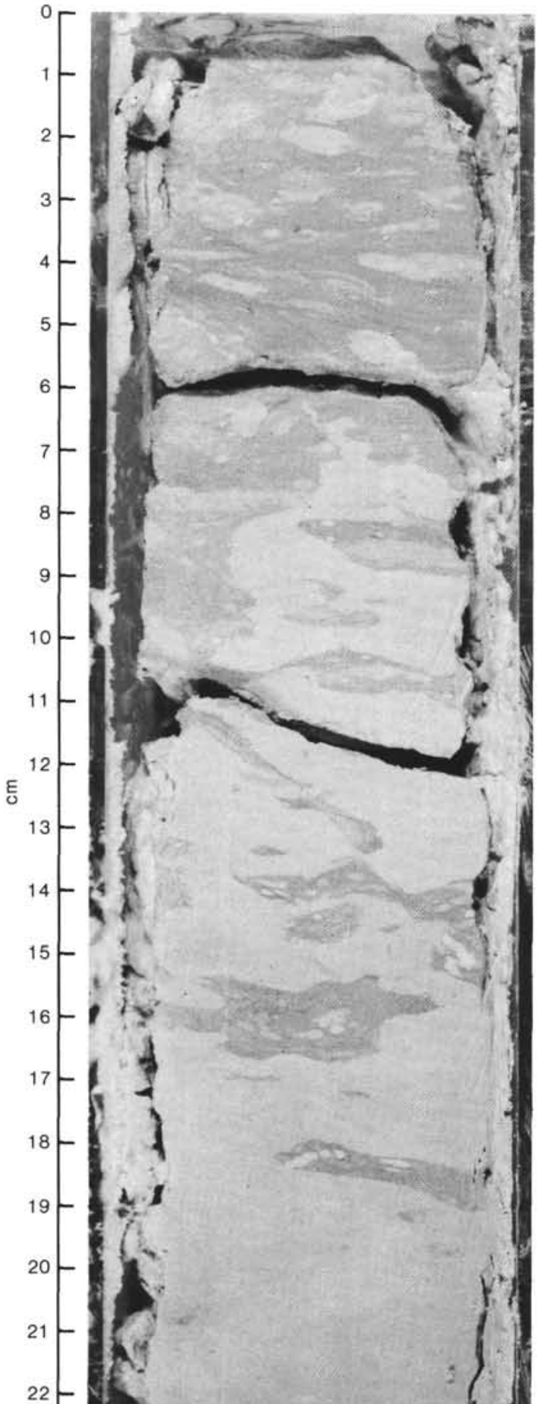

Figure 11. A possibly deformed bed (Sample 608-36-6, 0-25 cm), showing crosscutting Zoophycos burrow (see text for discussion).

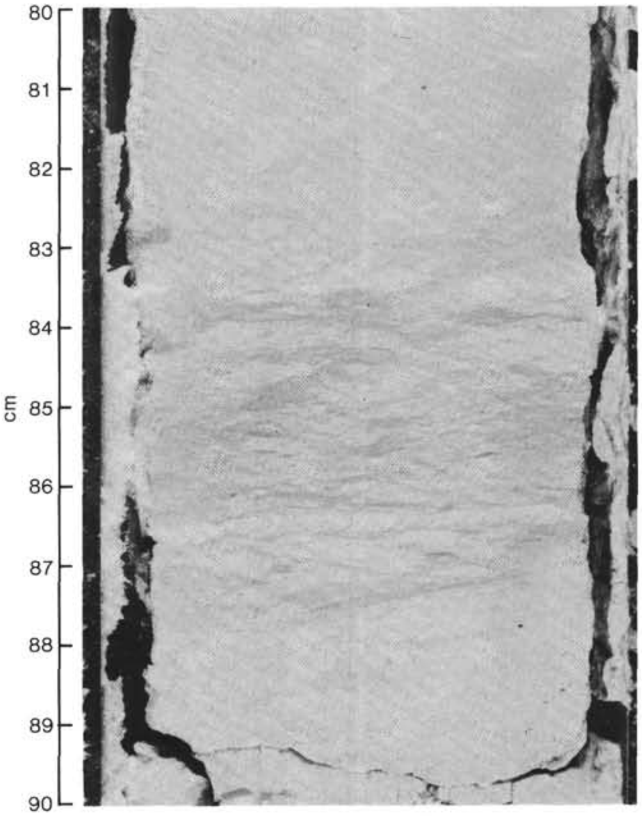

Figure 12. Well-developed flaser chalk (Sample 608-38-2, 80-90 cm). Note possibly flattened Zoophycos burrows (broken Spreiten?).

(Fig. 2) used for the site proposal showed clear reflectors within the sediment section that have since been traced extensively over the south flank of King's Trough (Kidd and Ramsay, this volume). East-west profiles invariably show the deeper of these regional reflectors less clearly (Fig. 5).

The total thickness of sediment on acoustic basement is measured at between 0.45 and 0.6 s (two-way traveltime) in the vicinity of the site (see Jacobs, this volume). This later profile over the beacon puts it at 0.5 s (Fig. 14).

The seismic section in Figure 14 can be divided into six acoustic units. The upper unit (A) consists, as at our first two sites, of acoustically reverberant reflectors that are wavy in form and blend together because they are closely spaced. This reflective unit extends from the surface to 0.07 s sub-bottom. Units B, C, and D make up most of the section and are relatively transparent compared with the other acoustic units. The interval is divided into three parts because the middle Unit C gives a slightly more coherent return than the two more transparent units, B and D. Acoustic Unit B extends from 0.07 to 0.12 s sub-bottom, Unit C from 0.12 to 0.28 s, and D from there to 0.37 s sub-bottom. Immediately above acoustic basement is a distinctive stratified unit (E: 0.37-0.50 s).

Hole 608 penetrated to basalt at 515.4 m sub-bottom and terminated at 530.9 m. Using the seismic velocity of 1.9 km s^{-1} measured for the lower parts of the sediment sequence, basement could have been expected at 526 m, and this was confirmed by our recovery of pillow basalts there.

Making similar calculations for the other acoustic unit boundaries, again employing measured seismic velocities

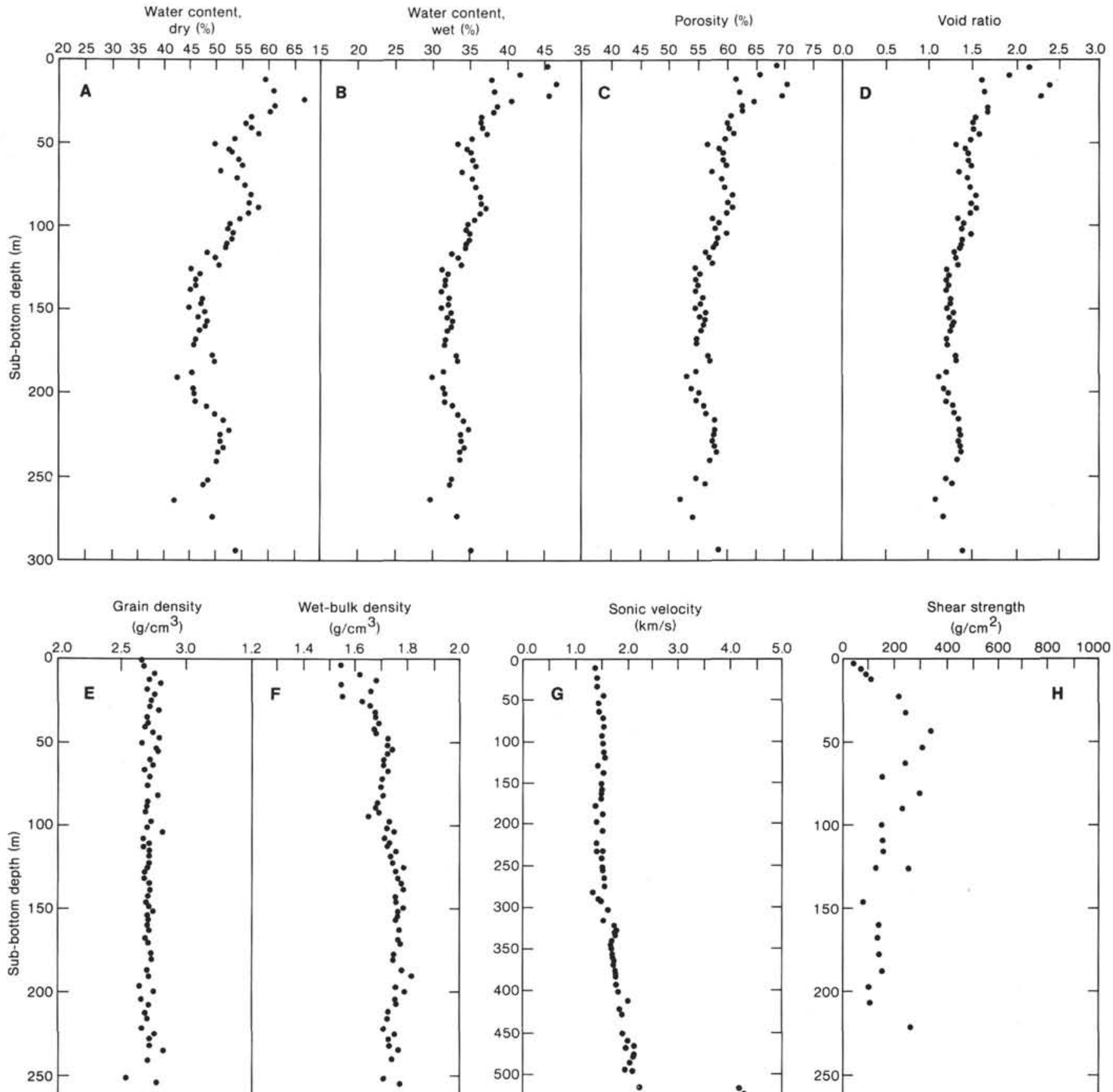

Figure 13. A–H. Physical properties at Site 608.

for the sediments, a direct correlation with the lithologic units is not forthcoming (Fig. 14). It would appear reasonable, however, to assume that acoustic Unit A represents the interval of glacial/interglacial cycles (lithologic Unit I). Acoustic Unit E probably represents the Eocene volcaniclastic sequence recovered below a major hiatus, because this unit is clearly unconformable with the overlying sequence on the records.

The generally transparent nature of the other three units probably reflects the ooze and chalk sequences of the Pliocene and Miocene. The more coherent nature of acoustic Unit C may in some way reflect the soft sediment deformation and microfaulting that characterizes lithologic Unit IV. The top of acoustic Unit C, at about 0.12 s, is at the same level as an acoustic change in the *Farnella* east–west profile (Fig. 5). In places, the bound-

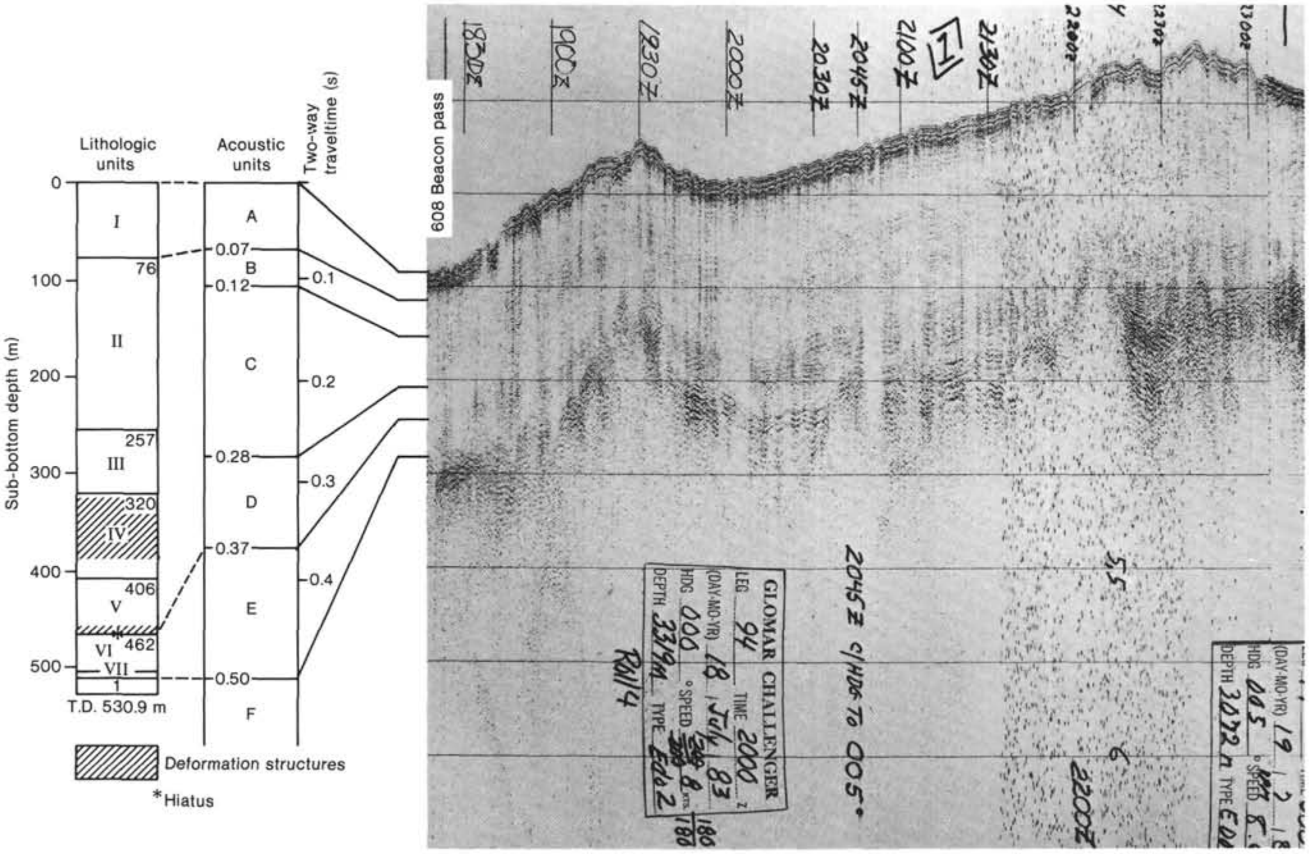

Figure 14. Seismic stratigraphy and comparison with lithologic units at Site 608.

ary can be seen to have an unconformable relationship with acoustic Units B and A above; see the eastern (i.e., the right-hand) side of Figure 5A.

BIOSTRATIGRAPHY

Hole 608 was continuously cored to basement at 530.9 m sub-bottom depth. Hole 608A was continuously piston-cored to 146.4 m sub-bottom. A stratigraphically continuous sequence of Quaternary through mid-upper Oligocene sediments was recovered, below which there was a long hiatus, and below that, mid-upper Eocene to upper middle Eocene sediments overlying basalt. Between about 455 and 465 m sub-bottom (spanning the hiatus), the nannofossil and planktonic foraminiferal biostratigraphic data are conflicting. Nannofossils and planktonic foraminifers are generally abundant throughout, and are well preserved in the Quaternary and Pliocene and moderately to poorly preserved in the Miocene, Oligocene, and Eocene. Benthic foraminifers are rare throughout, but generally diverse, with good preservation in the upper 200 m and variable preservation below. Diatoms occur only in the Quaternary, upper Pliocene, and middle Miocene.

Figure 15 shows a breakdown of the stratigraphy, based on paleontological and paleomagnetic data (see Baldauf et al., this volume, for an updated version). The Quaternary/Pliocene boundary is placed at 50 m in Hole 608 and 54 m in Hole 608A by derivation from the sedimentation rate curve. The lower Pliocene/upper Pliocene boundary is placed at 109 m in Hole 608 and 104 m in Hole 608A, on the basis of paleomagnetics and nannofossils. The best fit on the sedimentation rate curve is obtained using paleomagnetic data; the poor fit of some paleontological dates may be due to reworking or to inaccurate dating of the datum levels.

The following boundaries were determined using biostratigraphic and paleomagnetic criteria (see Baldauf et al., this volume):

Boundary	Sub-bottom depth (m)
Pliocene/Miocene	142
late/middle Miocene	247
middle/early Miocene	328
Miocene/Oligocene	404

The hiatus between the mid-upper Oligocene and mid-upper Eocene sediments occurs between Sample 608-49,CC and Section 608-50-2, on the basis of nannofossil ages. Sample 608-49,CC contains a mixed assemblage of Eocene and Oligocene calcareous nannofossils. Benthic foraminifers suggest a boundary between Samples 608-48,CC and 608-50-2, 100–102 cm. Samples 608-49,CC and 608-50-1, 100–102 cm contain a mixed Eocene–Oligocene assemblage. The planktonic foraminifers suggest a boundary between 608-48,CC and 608-49,CC.

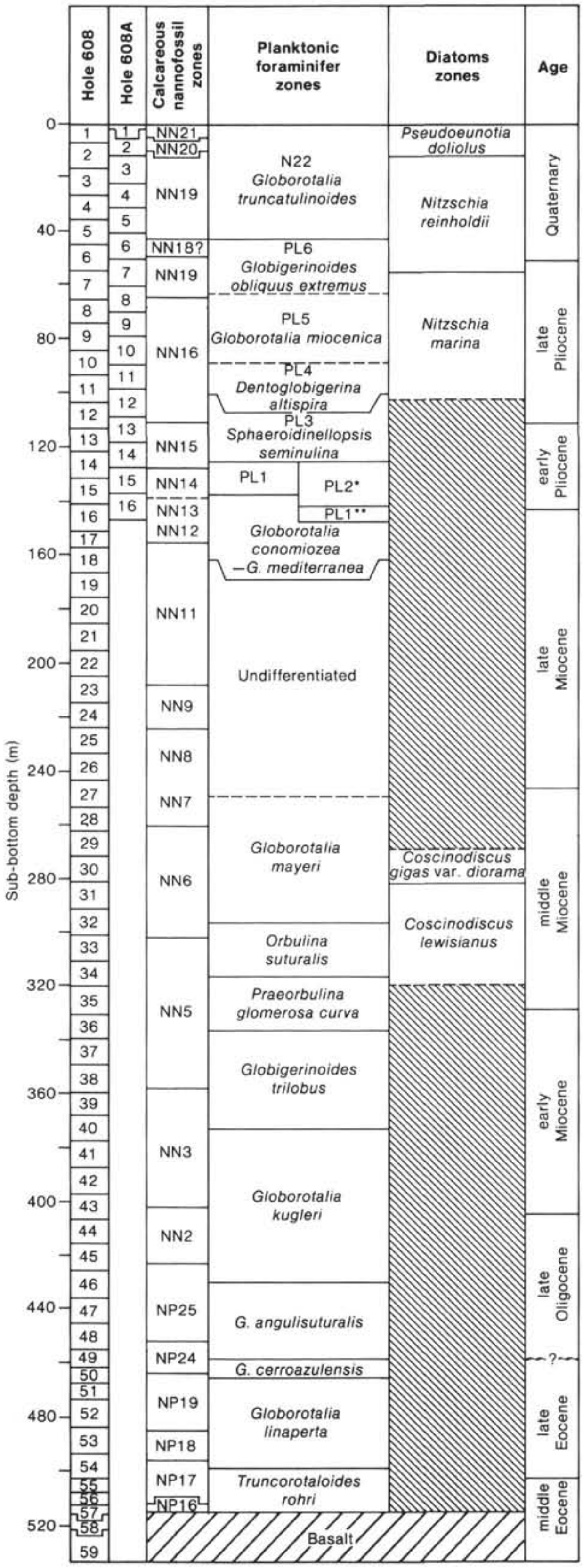

Figure 15. Biostratigraphic summary, Site 608 (for updated version, see Baldauf et al., this volume).*Zone PL2 in Hole 608A only. **Zone PL1 in Hole 608A. Hachures in the Diatom column indicate samples that are barren or contain rare non-age-diagnostic fragments.

Calcareous Nannofossils

At Site 608, Quaternary, Pliocene, Miocene, upper to middle Oligocene, and upper Eocene sediments were recognized by using calcareous nannofossils. All samples examined, except one from the lowest part of Hole 608, contain abundant calcareous nannoplankton assemblages.

Quaternary

The youngest coccolith assemblage at this site belongs to NN21, the *Emiliania huxleyi* Zone, which occurs in Sample 608-1,CC, where abundant *Emiliania huxleyi* and *Gephyrocapsa oceanica* occur together. The uppermost sample from Hole 608A, Sample 608A-1,CC, was assigned to the NN20 *Gephyrocapsa oceanica* Zone on the basis of the coccolith assemblage without *E. huxleyi* and *Pseudoemiliania lacunosa*. The presence of abundant *P. lacunosa* and the absence of discoasters place Samples 608-2,CC to 608-4,CC and 608A-2,CC to 608A-5,CC in the NN19 *Pseudoemiliania lacunosa* Zone. Among these samples, Sample 608-4,CC has no *Gephyrocapsa oceanica* and Sample 608A-5,CC contains no gephyrocapsid specimens. Therefore the former belongs to Bukry's (1973) *Gephyrocapsa caribbeanica* Subzone (CN13b) and the latter to the *Emiliania annula* Subzone (CN13a). These two samples are assigned to the lowermost Pleistocene. In this zone, LADs (last-appearance datums) of *Helicosphaera sellii* and *Calcidiscus macintyrei* are recognized.

Pliocene–Miocene

The Pliocene/Pleistocene boundary is clearly recognized in Hole 608A between Samples 608A-5,CC and 608A-6,CC, below which *Discoaster brouweri* occurs continuously. Sample 608A-6,CC contains abundant *Crenalithus doronicoides, Coccolithus pelagicus*, and *Helicosphaera carteri*, together with a few *Discoaster brouweri* and *D. triradiatus*, and therefore is assigned to the uppermost Pliocene NN18 *Discoaster brouweri* Zone. Below this sample, the assemblage is characterized by the occurrences of various discoasters such as *D. brouweri, D. pentaradiatus, D. surculus, D. asymmetricus*, and *D. tamalis*. On the basis of the absence of *Reticulofenestra pseudoumbilica*, Samples 608A-7,CC to 608A-12,CC are all placed in the upper Pliocene NN16 *Discoaster surculus* Zone, as are Samples 608-5,CC and 608-7,CC, which contain the same assemblage. The lack of discoasters and gephyrocapsid specimens in Sample 608-7,CC seems to place it in the lowest NN19. The interval in lower Core 608-5 and upper Core 608-6 is characterized by mixed floras; this interval is probably slumped (see Takayama and Sato, this volume). The presence of *D. brouweri, D. pentaradiatus*, and *D. surculus* places Samples 608-8,CC through 608-11,CC in the NN16 *Discoaster surculus* Zone. Although small *Reticulofenestra* showing strong affinities with *R. pseudoumbilica* were observed in the overlying zone, typical *R. pseudoumbilica* first occurs in Samples 608-12,CC and 608A-13,CC. Thus Samples 608-12,CC, 608A-13,CC, and 608A-14,CC are assigned to the lower Pliocene NN15 *Reticulofenestra pseudoumbilica* Zone. *Sphenolithus abies* occurs in Samples 608-13,CC and 608A-14,CC, somewhat below the extinction level of *R. pseudoumbilica*. The assemblage in Sample 608-14,CC is characterized by the common occurrence of *Amaurolithus tricorniculatus, A. primus*, and *A. delicatus*, together with various discoasters such as *Discoaster brouweri, D. pentaradiatus, D. surculus, D. variabilis*, and *D. asymmetricus;* this places this sample in the lower Pliocene NN14 *Discoaster asymmetricus* Zone. The same assemblage is found in Samples 608A-14,CC and 608A-15,CC. The underlying NN13 *Ceratolithus rugosus* Zone, characterized by the presence of *Ceratolithus rugosus* and absence of *Discoaster asymmetricus*, could not be recognized, because *Ceratolithus* is very rare or absent in both holes. Thus Samples 608-15,CC, 608-16,CC, and 608A-16,CC are tentatively placed in the NN12 *Amaurolithus tricorniculatus* Zone. Among them, Sample 608A-16,CC contains fairly abundant *Discoaster challengeri.* On the basis of the occurrences of *Discoaster quinqueramus*, the *Discoaster quinqueramus* Zone (NN11) is represented from Sample 608-17,CC on down to Sample 608-22,CC. The first-appearance datums (FAD) of *Discoaster pentaradiatus* and *D. surculus* are recognized in the upper and the middle part of this zone. Although the number of specimens is limited, the occurrence of *Discoaster hamatus* seems to place Samples 608-23,CC and 608-24,CC in the upper Miocene NN9 *Discoaster hamatus* Zone. The NN10 *Discoaster calcaris* Zone is therefore missing at this site. On the basis of the occurrence of a few specimens of *Discoaster kugleri* in Samples 608-25,CC through 608-27,CC, these samples are assigned to the middle Miocene NN7 *Discoaster kugleri* Zone. This assignment is supported by the existence of the LAD of *Coccolithus miopelagicus* within this zone. Because *Catinaster coalitus*, one of the important marker species for the middle Miocene, is not recognized, the NN8 *Catinaster coalitus* Zone could not be clearly delineated at this site. *Cyclicargolithus floridanus* occurs continuously below Sample 608-28,CC. According to Bukry's (1973) zonation, the LAD of *Cyclicargolithus floridanus* coincides with the FAD of *Discoaster kugleri*, which designates the boundary between NN7/NN6. Therefore, Samples 608-28,CC through 608-32,CC are all placed in the NN6 *Discoaster exilis* Zone. Samples 608-33,CC to 608-37,CC contain nannofloras characterized by the comparatively abundant occurrence of *Sphenolithus heteromorphus* together with *Sphenolithus abies, Cyclicargolithus floridanus, Coccolithus pelagicus, C. miopelagicus, Helicosphaera granulata, Discoaster exilis*, and *D. variabilis*, and are referred to the middle to lower Miocene NN5 *Sphenolithus heteromorphus* Zone. *Sphenolithus belemnos* first occurs in Sample 608-38,CC. Thus Samples 608-38,CC through 608-42,CC are assigned to the lower Miocene NN3 *Sphenolithus belemnos* Zone. An additional six samples (608-38-2, 83–84 cm; 608-38-3, 38–40 cm; 608-38-3, 97–98 cm; 608-38-3, 102–103 cm; and 608-38-3, 104–105 cm) are all placed in the NN5 *Sphenolithus heteromorphus* Zone on the basis of the occurrence of *Sphenolithus heteromorphus* and the absence of *Helicosphaera ampliaperta*. Therefore, between Samples 608-38-3, 104–105 cm and 608-38,CC, the NN4 *Helicosphaera ampliaperta* Zone (16.3–18.2 Ma) is missing (see Takayama and Sato; and Baldauf et al., this volume, for an update and placement of Zone NN4). The overlap of *Triquetrorhabdulus carinatus* and *Discoaster druggii* indicates the presence of the lower Miocene NN2 *Discoaster druggii* Zone in Samples 608-43,CC and 608-44,CC.

Oligocene

A remarkable change in species composition of calcareous nannofossils occurs between Samples 608-44,CC and 608-45,CC. In contrast to the overlying samples, Samples 608-45,CC and 608-46,CC contain abundant *Dictyococcites bisectus, D. hesslandii*, and *Cyclicargolithus abisectus*, together with *Cyclicargolithus floridanus, Coccolithus pelagicus, C. miopelagicus, Sphenolithus ciperoensis*, and *S. moriformis*. A single specimen of *Helicosphaera recta* also occurs in Sample 608-45,CC. These two samples therefore belong to the uppermost Oligocene NP25 *Sphenolithus ciperoensis* Zone. The underlying Sample 608-48,CC contains a similar assemblage, but the overlap of common *Sphenolithus ciperoensis* with rare *S. distentus* in this sample assigns to it a late to middle Oligocene age (NP24 *Sphenolithus distentus* Zone). The fairly abundant occurrences of *Chiasmolithus grandis, Discoaster tani nodifer*, and *Reticulofenestra umbilica* in Sample 608-49,CC are interpreted as reworked.

Eocene

Calcareous nannofossils in Samples 608-50,CC through 608-52,CC are represented by abundant Eocene assemblages with relatively low species diversity. The assemblage consists mainly of *Coccolithus pelagicus, C. eopelagicus, Cyclicargolithus floridanus, Reticulofenestra umbilica, R. dictyoda, Calcidiscus formosus, Discoaster tani nodifer, D. barbadiensis*, and *D. saipanensis*, and is assigned to the *Isthmolithus recurvus* Zone (NP19). On the basis of the absence of *Isthmolithus recurvus* and the presence of *Chiasmolithus oamaruensis*, Sample 608-53,CC is assigned to the upper Eocene NP18 *Chiasmolithus oamaruensis* Zone. On the basis of the occurrence of *Chiasmolithus solitus* in Sample 608-57-3, 69–70 cm, the boundary between Zones NP17 and NP16 may be placed in Core 608-57. Therefore, the absolute age of the bottom sediments of Hole 608 approximates 42 Ma.

A middle Oligocene to upper Eocene hiatus occurs at this site. Between Samples 608-49,CC and 608-50,CC, Zones NP23 through part of NP19 are missing. One of the most reliable age indicators for the late Eocene, *Isthmolithus recurvus*, has previously been considered to occur only in sediments deposited in cold water. Bukry (1975) outlined the geographic distribution of *I. recurvus* at DSDP sites in the Pacific, Indian, and Atlantic oceans, and indicated that this species is typically absent at tropical sites. At the present site, which is located at about 42°N, abundant specimens of *I. recurvus* were found. This finding therefore supports Bukry's assertion about cold-water deposition.

A single specimen of *Braarudosphaera bigelowii* occurs in Sample 608-46-2, 64–65 cm. The geographic distribution of this species was discussed by Martini (1967) and Takayama (1972). *Braarudosphaera* can tolerate relatively high as well as relatively low salinities; they are most common in water less than 100 m deep, but rare in water 150 to 200 m keep (Takayama, 1972). The significance of the presence of Braarudosphaeraceae in deep-sea sediments has been discussed by Roth (1974). The specimen from Hole 608, considered to be a typical shallow-water species, is deemed to be reworked, but it may suggest the presence of turbidite sediments or the distribution of the *Braarudosphaera* chalk somewhere near Site 608.

Planktonic Foraminifers

All Quaternary and Pliocene samples from this site contain abundant, well-preserved planktonic foraminifers. Many upper Miocene samples, however, contain less abundant faunas with specimens of small average size and, in some cases, with moderate preservation. The position of this site, just south of the polar front during glacial maxima, has produced significant variations in the fauna between glacial and interglacial samples, but true polar faunas have not been recorded. The northerly position of this site is reflected in the absence of some subtropical species such as *Globorotalia miocenica*, and in the restrictions of others such as *Dentoglobigerina altispira*. Cooler-water forms such as *Neogloboquadrina pachyderma* (sinistral) and *N. atlantica* can, however, be found here in increased numbers. Because of this, not all the zones in Berggren's subtropical-temperature zonation (1973, 1977) can be identified (see Weaver, this volume).

The *Globorotalia truncatulinoides* Zone can be recognized with the first occurrence of *G. truncatulinoides* in Cores 608-5 and 608A-5. Within this zone pink *Globigerinoides ruber* was found in Sample 608-1,CC, and *Globorotalia hirsuta* occurs in Sample 608A-1,CC, indicating uppermost Quaternary in both cases. The faunas of this zone include large numbers of *Globigerina bulloides* and *N. pachyderma* (dextral), with increases in *G. truncatulinoides* during warm intervals and *N. pachyderma* (sinistral) and *Globigerina quinqueloba* during cold intervals. Other common species are *Globorotalia scitula, G. crassaformis, Globigerina glutinata, Globigerinoides ruber, Globigerina falconensis*, and *Orbulina universa*.

Zones PL4, PL5, and PL6 have proven difficult to recognize because of the absence of *Globorotalia miocenica* and the very rare occurrence of *D. altispira*. By comparison with Site 607, however, the transition from *Globorotalia puncticulata* to *G. inflata* should occur near the PL5/PL6 boundary. By this reasoning, the base of Zone PL6 should be in Cores 608-7 and 608A-8. *D. altispira* has been recorded in Samples 608-1,CC and 608-11,CC but not in samples from Hole 608A. Thus the base of Zone PL5 may lie in Core 608-10, but this datum cannot be recognized in Hole 608A and may be unreliable even in Hole 608, because *D. altispira* is near the limit of its geographic range at Site 608. The fauna of Zones PL4 through PL6 is more diverse than in the overlying Quaternary; *Globigerinoides sacculifer, G. trilobus, Globigerina decoraperta*, and *G. aperatura* are frequently present, and perhaps indicate a warmer-water regime than the warm intervals of the glacial period. *G. bulloides, Globorotalia crassaformis*, and *G. puncticulata* are commonly occurring species; *N. atlantica* (sinistral) is present below Zone PL6. The base of Zone PL4 is marked by the last occurrence of *Sphaeroidinellopsis seminulina* in Cores 608-11 and 608A-12.

Zone PL3 is easily recognized by the common occurrence of *S. seminulina* above the extinction of *G. margaritae*, which occurs in Cores 608-14 and 608A-14. The fauna of this zone is similar to that in Zones PL4 and PL6, but with the addition of *S. seminulina* and *Globorotalia* cf. *G. pliozea.*

Zone PL2 is absent in Hole 608, or at least restricted to Core 608-14, whereas, in Hole 608A, Core 608A-16 contains this zone. This strongly suggests the presence of a local hiatus in Hole 608, within Core 608-14. Zone PL2 continues to the base of Hole 608A, and contains a fauna similar to that in Zone PL3, with the addition of *G. margaritae.* As at the two previous sites, 606 and 607, *G. puncticulata* and *G. crassaformis* first appear near the base of Zone PL2, and not in PL1 as in the South Atlantic (Berggren, 1977).

Zone PL1, the overlap of *Globigerina nepenthes* with *Globorotalia margaritae*, is represented in only one sample in Hole 608 (608-14,CC) and within Core 608A-16. Sample 608-14,CC also contains *Globorotalia cibaoensis*, which suggests a position near the base of this zone. Thus the hiatus may also include the upper part of Zone PL1.

Samples 608-15,CC through 608-17,CC contain *Globorotalia* cf. *conomiozea*, and are thus assigned to the *G. conomiozea/G. mediterranea* Zone of Berggren (1977). *Globorotalia plesiotumida* is also present in this zone, and *N. acostaensis* and *N. continuosa* are dominantly sinistrally coiled. No specimens of *N. atlantica* were found at this level.

Below Core 608-17, *Globorotalia conoidea* occurs sporadically, together with *Neogloboquadrina pachyderma, N. continuosa*, and *N. acostaensis*, suggesting the *N. humerosa* Zone. Berggren (1977) did not define the base of this zone, but he suggested that it should approximate the first occurrence of the *Neogloboquadrina* plexus; neogloboquadrinids can be found at least down to Core 608-26. In this zone, specimens attributable to the *G. plesiotumida/G. merotumida* group are very common; the interval was not studied in detail.

The middle Miocene *Globorotalia mayeri* Zone was determined between Samples 608-27,CC and -32,CC: age-diagnostic species include the overlap of the zone fossil with *N. continuosa, G. menardii*, and *G. miotumida.* The base of the zone is defined by the first appearance of *G. mayeri* (see Table 3 for foraminiferal zonation of Eocene to late Miocene; see also Jenkins, this volume).

Samples 608-32,CC to 608-33,CC were determined to be from the middle Miocene *Orbulina suturalis* Zone, with the base of the zone defined by the first occurrence of the zone fossil, which is rare.

The *Praeorbulina glomerosa curva* Zone of the early Miocene is a very short interval of time, and is marked

Table 3. Planktonic foraminiferal zones, late Eocene–late Miocene, Hole 608.

Cores	Zones	Zonal markers
15–16	*Neogloboquadrina humerosa*	*N. humerosa* F.A.
17–26	Reworked lower Miocene	
27–31	*Globorotalia mayeri*	*G. mayeri* F.A.
32–33	*Orbulina suturalis*	*O. suturalis* F.A.
34	*Praeorbulina glomerosa curva*	*P. glomerosa curva* F.A.
39–35	*Globigerinoides trilobus*	*G. trilobus* F.A.
40–45	*Globorotalia kugleri*	*G. kugleri* F.A.
46–48	*Globigerina angulisuturalis*	*G. angulisuturalis* F.A.
49	*Globorotalia cerroazulensis*	*Globorotalia ampliapertura* F.A.
53–50	*Globigerina linaperta*	*Truncorotaloides topilensis* L.A.
54–57	*Truncorotaloides rohri*	

Note: F.A. = first appearance; L.A. = last appearance.

at this site by the extinction of *G. praescitula* within the zone. The base of the zone is marked by the appearance of the zone fossil.

Samples 608-36,CC to 608-39,CC have been assigned to the early Miocene *Globigerinoides trilobus* Zone; in the zone, *Catapsydrax dissimilis, Globorotalia nana*, and *Globigerinoides primordius* become extinct, and the first appearances include *Globorotalia bella, G. incognita*, and *Globorotalia praescitula*. The base of the zone is defined by the first appearance of *Globigerinoides trilobus*.

The late Oligocene *Globorotalia kugleri* Zone was recognized between Samples 608-45,CC and 608-40,CC; *G. euapertura* and *Globoquadrina tripartita* become extinct in the zone, whose base is marked by the appearance of *Globorotalia kugleri*. The late Oligocene *Globigerina angulisuturalis* Zone was recognized between Samples 608-48,CC and 608-46,CC; the zone fossil is common, but the base is not seen, because below Sample 608-48,CC there is an unconformity.

The fauna in Sample 608-49,CC has been tentatively assigned to the late Eocene *Globorotalia cerroazulensis* Zone, because of the presence of the zone fossil and *Globigerinatheka index, Globorotalia ampliapertura*, and *G. gemma;* there is no evidence of reworking.

The late Eocene *Globigerina linaperta* Zone has been recognized in Samples 608-53,CC to 608-50,CC; the base of the zone is defined by the extinction of *Truncatinuloides topilensis* and related taxa such as *T. pseudotopilensis* and *T. collacteus*.

Samples 608-57,CC and 608-54,CC have been assigned to the *T. rohri* Zone of the middle Eocene; the base of the zone is not defined at this site.

Benthic Foraminifers

Benthic foraminifers constitute less than 1% of the total foraminiferal fauna in the >63-μm fraction of the samples studied (all core-catcher samples and some additional samples), except in Sample 608-40-4, 47–49 cm, from a chalky conglomerate. All samples contained sufficient specimens for counts of 200 specimens.

All samples below 608-31,CC were dried at about 110°C for at least one hour, and then soaked in kerosene. Subsequently the kerosene was poured off, water added, and the samples were heated for 10 to 30 min. This treatment generally cleaned the fauna well. The preservation is good to moderate: good in the upper 200 m, and variable below. The aragonitic species *Hoeglundina elegans* is preserved in the mudline sample.

Relative abundances of the most common species and species groups are discussed in detail by Thomas (this volume). The diversity is between 40 and 50 species from Sample 608-29,CC upward; below that it is generally greater (between 45 and 60 species), except for samples in Cores 608-37 and 608-38. The fauna throughout the cored interval is indicative of oceanic depths, that is, more than about 2000 m (Douglas and Woodruff, 1981).The chalky conglomerate sample (608-40-4, 47–49 cm) as well as Samples 608-5,CC; 608-16,CC; 608-23,CC; 608-33,CC; 608-40,CC; 608-42,CC; and 608-49,CC contain numerous large, thick-walled, broken or corroded specimens. All these samples probably contain reworked material. The reworked fauna is not indicative of much shallower water. Generally, the transported specimens are large, robust specimens of species ordinarily present in the samples (e.g., *Stilostomella abyssorum, Stilostomella subspinosa, Oridorsalis umbonatus, Gyroidinoides soldanii, Globocassidulina subglobosa*).

The largest changes in the benthic foraminiferal fauna occur between Samples 608-32,CC and 608-38,CC. The faunal composition above this interval is essentially modern. This modern fauna contains *Nuttallides umbonifera, Epistominella exigua, Melonis pompilioides*, and *Cibicidoides wuellerstorfi*, together with long-ranging species. The fauna does not contain the "Oligocene survivors," a group of *Cibicidoides* species present from the middle to late Eocene through the Oligocene (*C. laurisae, C. havanensis, C. trinitatensis, C. grimsdalei, C. perlucidus*) and some agglutinant species commonly found in the same range (*Bolivinopsis cubensis, Vulvulina spinosa*).

Within the range of the modern fauna, the relative abundances of the common species show considerable fluctuations. There is no obvious correlation between fluctuations in abundance of benthic species and lithology in glacial cycles. *N. umbonifera* is present from Sample 608-5,CC through Sample 608-23,CC; it is common in Samples 608-5,CC, 608-13,CC, and 608-23,CC. *E. exigua* is abundant in the mudline sample, and fairly common (though variable) in samples down to 608-29,CC. The relative abundance of *Uvigerina peregrina* is highly variable.

From Sample 608-33,CC through Sample 608-38,CC, the benthic fauna shows great variability. Sample 608-33,CC contains a mixture of the modern fauna (with *C. wuellerstorfi* and the "Oligocene survivors"). The planktonic foraminifers are corroded and radiolarians are numerous. The sample may represent a time of carbonate dissolution and reworking. From Sample 608-37-2, 38–40 cm through Sample 608-38-4, 32–40 cm, the diversity drops dramatically to about 25 species, and up to 92% of the total benthic foraminiferal fauna consists of the single species *Bolivina spathulata*. In Sample 608-38,CC, *B. spathulata*, together with other bolivinid species, makes up 41% of the benthic fauna. Similar faunas have been described from restricted, oxygen-starved basins only (e.g., the eastern Mediterranean in the late Miocene: Van der Zwaan, 1982). The bolivinid species have delicate, thin-walled tests; it is not likely that they would survive transport and be well preserved, and the aberrant faunas do not resemble the transported fauna in the chalky conglomerate sample in Core 608-40. The abnormal conditions built up gradually, but they ended abruptly between Samples 608-37, 38–40 cm and 608-37-2, 38–40 cm. Local tectonic activity may have created small sub-basins that could have become stagnant during periods of generally sluggish bottom-water movements (see Thomas, this volume, for a detailed discussion).

With the exception of Cores 608-37 and 608-38, the faunas below Sample 608-33,CC are typical deep-sea faunas from the lower Miocene through middle to upper Eocene. *Stilostomella* and *Pleurostomella* species are common, as are the "Oligocene survivor" *Cibicidoides* species. The difference between the Oligocene and the upper Eocene is minor. The common species are present in the upper Eocene and continue in the Oligocene, as described by Corliss (1981). Several relatively rare species become extinct by the end of the Eocene; their last appearance cannot be accurately given, because they are rare (*Gavelinella micra, G. beccariiformis, Resigia westcotti, Alabamina dissonata*). *Nuttallides truempyi* is generally considered to be a reliable marker species for the Eocene/Oligocene boundary (Tjalsma and Lohmann, 1983). It has its last appearance in Sample 608-50-2, 100–102 cm. The co-occurrence of *N. truempyi* and *N. umbonifera* in all the Eocene samples suggests that the maximum age of the oldest sediments is latest middle Eocene.

Several benthic foraminiferal events recognized at Site 608 are also found in the equatorial Pacific (Thomas, 1985), but most events appear not to be coeval. An exception is the first appearance of *Cibicidoides wuellerstorfi* at about 15 Ma (see Thomas, this volume).

Diatoms

Middle Miocene, upper Pliocene, and Quaternary diatoms were observed in the sediments recovered from Site 608. Samples examined from other intervals were barren of diatoms. Generally, within the Pleistocene, rare to common, moderately preserved diatoms occur. The base of the *Pseudoeunotia doliolus* Zone (Burckle, 1977) is placed between Samples 608-2-2, 43–45 cm and 608-2-4, 48–50 cm on the basis of the last occurrence of *Nitzschia reinholdii* in Sample 608-2-4, 48–50 cm. The first occurrence of *Pseudoeunotia doliolus* in Sample 608-6,CC allows placement of the interval from Sample 608-2-4, 48–50 cm through Sample 608-6,CC in the *Nitzschia reinholdii* Zone of Burckle (1977).

Sample 608-5,CC contains reworked specimens of *Thalassiosira convexa* var. *convexa, Nitzschia jouseae*, and *Rhizosolenia praebergonii*. The *Nitzschia marina* Zone of Baldauf (1984) is recognized in the interval from Sample 608-7-2, 43–45 cm to Sample 608-8,CC. Samples examined from 608-11,CC through 608-28,CC are barren of biogenic silica. Common fragments of volcanic glass occur in Sample 608-9,CC.

Moderately preserved to well-preserved diatoms occur in Samples 608-29-5, 43–45 cm through 608-32,CC. The species present are indicative of warm to warm-temperate conditions. Samples 608-29-5, 43–45 cm through 608-30,CC are assigned to the middle Miocene *Coscinodiscus gigas* var. *diorama* Zone of Barron (1985) on the basis of the occurrence of *Denticulopsis hustedtii, Denticulopsis punctata* var. *hustedtii, Craspedodiscus coscinoduscus, Annellus californicus*, and *Actinocyclus ellipticus* stratigraphically above the last occurrence of *Coscinodiscus lewisianus*. This zonal assignment is supported by the first occurrences of *Coscinodiscus nodulifer* in Sample 608-30-5, 43–45 cm. This sample interval correlates with the *Denticulopsis nicobarica* Zone of Baldauf (1984).

Coscinodiscus lewisianus occurs in Samples 608-31-3, 43–45 cm through 608-32,CC, and allows placement of these samples in the middle Miocene *Coscinodiscus lewisianus* Zone of Schrader (1976). Samples 608-33,CC and 608-34,CC contain rare, poorly preserved diatoms not diagnostic of age. Samples examined from below Core 608-34 are barren of diatoms.

The uppermost six cores of Hole 608A contain, in general, few moderately preserved diatoms. Samples 608A-1,CC and 608A-2,CC are assigned to the *Pseudoeunotia doliolus* Zone of Burckle (1977). Samples 608A-3,CC through 608A-6,CC are assigned to the *Nitzschia reinholdii* Zone of Burckle (1977). Samples examined below 608A-10,CC are barren of diatoms.

Radiolarians

Samples from Miocene, upper Pliocene, and Pleistocene sediments of Hole 608 contain radiolarian assemblages. Only samples from Hole 608 have been examined (Table 4). In the Pliocene and Pleistocene cores, intervals with well-preserved, diverse assemblages alternate with intervals in which there are only robust, deep-living radiolarians, or in which all siliceous fossils are dissolved. The only radiolarian event observed in these cores is the last occurrence of *Stylatractus universus*, between Samples 608-2,CC and 608-1,CC.

Except for a few forms in Sample 608-11,CC, radiolarians are absent from Section 608-9-3 down through Core 608-28. Sample 608-29-2, 40–42 cm contains a few poorly preserved species from *Didymocyrtis antepenultima* Zone of the late Miocene. Seven samples between Sample 608-29,CC and Section 608-32-5 contain species confined to the middle Miocene zones *Diartus petterssoni* or *Dorcadospyris alata*. Below Core 608-33, all samples examined are barren of siliceous fossils.

PALEOMAGNETICS

Hole 608

Hydraulic piston coring and extended-core-barrel coring in Hole 608 provided over 510 m of sediment suitable for paleomagnetic study. Samples were taken at an interval of one sample per core section (one per 1.5 m), using 7-cm^3 plastic boxes in the upper portion of the sediment section. Below Core 608-33 (310 m) the sediment became too stiff to use the plastic boxes, and samples were taken by using a drill press with a diamond drill bit to cut oriented cores from the core sections.

Table 4. Abundance and preservation of Hole 608 radiolarians.

Sample (core-section, interval in cm)	Abundance[a]	Preservation[b]
1-4, 40–42	F	G
1,CC	F	M
2-3, 40–42	B	
2,CC	F	M
3-3, 40–42	B	
3,CC	C	G
4-3, 40–42	F	G
4,CC	B	
5-2, 40–42	B	
5,CC	C	G
6-2, 40–42	F	G
6,CC	F	M
7-2, 20–22	R	G
7,CC	F	G
8-2, 40–42	B	
8,CC	C	G
9-3, 40–42	B	
9,CC	B	
10-3, 40–42	B	
10,CC	B	
11,CC	R	G
All CC between 12 and 28	B	
29-2, 40–42	R	P
29-6, 40–42	F	G
29,CC	R	P
30-2, 40–42	F	M
30,CC	R	M
31-2, 40–42	F	G
31,CC	C	G
32-2, 40–42	F	M
32-5, 20–22	R	P
All CC below 33	B	

[a] C = 5000–10,000 specimens/slide; F = 1000–5000 specimens/slide; R = <1000 specimens/slide; B = barren.
[b] G = good; M = moderate; P = poor.

Progressive alternating-field demagnetization studies on pilot samples taken through the recovered section indicated that some reversed specimens initially exhibited a normal magnetization, but that such overprint secondary magnetizations were easily removed by treatment at 10 mT, leaving stable, univectorial magnetizations. On the basis of results of these demagnetization curves, the remaining samples were demagnetized at 10 mT.

The Custer orientation device was not used routinely at this site, so the declinations between cores are not consistent. For this reason, the inclination record alone was used to determine a polarity log. The polarity log is given elsewhere in this volume (Clements and Robinson). The depths of reversal boundaries are given in Table 5.

This hole is unique in that it contains a nearly complete record of the polarity-reversal sequence from the present back to the base of Chron C8 at 28.5 Ma. Lithostratigraphic and biostratigraphic evidence indicates that a major hiatus occurs at approximately 460 m sub-bottom. Unfortunately, the polarity record below 460 m is poor because of disturbed cores and poor recovery, and does not allow confident correlation with the time scale in this interval.

Two basalt samples were taken from Core 608-57. Only natural remanent magnetization (NRM) was measured, so as to allow magnetic viscosity and detailed thermal demagnetization to be studied on shore. Both samples gave NRM directions that were shallow and normal (+29°).

Hole 608A

Hydraulic piston coring in this hole yielded 146.4 m of sediment. The same paleomagnetic methods were employed as for Hole 608. The depths of the reversal boundaries are given in Table 5. The polarity correlations are straightforward down to a depth of 110 m. Below this, poorer magnetic data and complications with the biostratigraphic data make the correlations less certain.

It should be noted that an offset of up to 8 m exists between Holes 608 and 608A, as indicated by the relative depths of polarity reversals.

SEDIMENTATION RATES

The sedimentation rates at Site 608 were calculated on the basis of calcareous nannofossil, foraminiferal, and diatom zones, along with paleomagnetic stratigraphy (Table 6; see Baldauf et al., this volume, for an updated version). Figure 16 shows a time-depth curve to the middle Eocene for Hole 608, along with a separate plot for Hole 608A to the early Pliocene. A major hiatus is placed between Core 608-48 and Section 608-50-2, between upper Oligocene (NP24) and upper Eocene (NP10) sediments. It represents a time interval of up to 9.7 m.y., based on the nannofossil zonation. A short hiatus also exists in Core 608-14, with uppermost lower Pliocene above and lowermost lower Pliocene below. This hiatus was not seen in Hole 608A.

The upper part of the section (0–100 m sub-bottom), through the Quaternary and upper Pliocene, indicates that sedimentation rates in both holes were about 34 m/m.y. Much of this period, to 2.47 Ma, is represented by the alternating nannofossil oozes and marls of the glacial cycles. The rate is close to 30 m/m.y., as calculated from upper Quaternary conventional piston cores taken on the south flank of King's Trough (Weaver, 1983).

A sedimentation rate of 19.0 m/m.y. is calculated for the generally homogeneous nannofossil oozes and chalks of the middle and upper Miocene and lower Pliocene down to about 350 m (~15 Ma).

Between Cores 608-35 and 608-37 (~330–350 m), the time-depth curve levels out so that the gray green upper to lower Miocene chalks record sedimentation rates of 8.5 m/m.y.

The curve steepens slightly passing downward to the base of Core 608-48, at 454 m sub-bottom. Sedimentation rates over this upper Oligocene through lower Miocene interval average 10.0 m/m.y. Below the Eocene-Oligocene hiatus, sedimentation rates are slightly higher, so that, between the hiatus at 455 to 465 m and the basaltic basement at 515.4 m, rates for the middle and upper Eocene marly chalk sequence, with its volcaniclastic component, are calculated at 11.8 m/m.y.

GEOCHEMISTRY

Carbonate Bomb

Carbonate bomb samples were taken from lithologic Units I through VII, and the analytical results are plot-

Table 5. Reversal boundaries, Site 608.

Reversal	Age (Ma)	Core-section, cm level	Sub-bottom depth (m)[a]
Hole 608			
Brunhes	0.73	2-6, 98/3-1, 98	15.49/17.59
Jaramillo (top)	0.91	3-1, 98/3-2, 98	17.59/19.09
(bottom)	0.98	3-3, 98/3-4, 88	20.59/21.99
Cobb Mtn. (top)	—	3-4, 88/3-5, 98	21.99/23.59
(bottom)	—	3-5, 98/3-6, 98	23.59/25.09
(top)	—	5-4, 98/5-5, 98	41.29/42.79
(bottom)	—	5-6, 130/6-1, 98	44.60/46.39
Olduvai (top)	1.66	6-4, 98/6-5, 98	50.89/52.39
(bottom)	1.88	6-6, 98/7-1, 98	53.89/55.99
Matuyama/Gauss	2.47	10-1, 98/10-2, 98	84.79/86.29
Kaena (top)	2.92	10-6, 98/11-6, 98	92.29/94.39
(bottom)	2.99	11-5, 99/11-6, 98	100.39/101.89
Mammoth (top)	3.08	12-1, 65/12-1, 98	103.66/103.99
(bottom)	3.18	12-3, 98/12-4, 98	106.99/108.49
Gauss/Gilbert	3.40	12-5, 30/12-5, 98	109.31/109.99
Chron 6/Chron 7	6.70	19-3, 98/19-4, 25	170.09/170.96
Chron 7/Chron 8	7.41	20-5, 25/20-5, 98	181.96/182.69
Chron 8/Chron 9	7.90	21-3, 25/21-3, 87	188.56/189.18
Chron 9/Chron 10	8.50	22-4, 75/22-4, 98	199.66/200.39
Chron 10/Chron C5	8.92	23-2, 98/23-3, 98	206.99/208.49
Chron C5/Chron C5A	11.55	29-1, 98/29-2, 30	263.09/263.91
Chron C5A/Chron C5AA	12.83	31-3, 90/31-4, 24	285.21/286.05
Chron C5AA/Chron C5AB	13.20	32-5, 106/33-1, 50	297.97/301.01
Chron C5AD/Chron C5B	14.87	34-5, 88/34-6, 94	316.99/318.56
Chron C5B/Chron C5C	16.22	36-2, 128/36-3, 6	332.09/332.37
Chron C5C/Chron C5D	17.57	37-4, 96/37-5, 10	344.37/345.01
Chron C5D/Chron C5E	18.56	38-4, 25/38-4, 40	353.26/353.41
Chron C5E/Chron C6	19.35	39-3, 59/39-4, 126	361.61/363.87
Chron C6/Chron C6A	20.88	42-2, 32/42-3, 33	388.73/390.24
Chron C6A/Chron C6AA	21.90	42-4, 16/43-1, 34	391.57/396.85
Chron C6AA/Chron C6B	22.57	44-2, 24/44-2, 102	407.85/408.61
Chron C6B/Chron C6C	23.27	45-6, 123/46-1, 6	424.44/425.37
Chron C8/Chron C9	28.15	48-3, 138/48-4, 33	448.89/450.39
Hole 608A			
Brunhes	0.73	3-4, 120/3-5, 94	17.71/18.95
Jaramillo (top)	0.91	3-6, 114/4-1, 98	20.65/22.59
(bottom)	0.98	4-1, 98/4-2, 98	22.59/24.09
Olduvai (top)	1.66	7-4, 98/7-6, 98	55.89/57.39
(bottom)	1.88	7-5, 98/7-6, 98	57.39/58.89
(top)		9-2, 98/9-3, 98	72.09/73.59
(bottom)		9-4, 98/9-5, 98	75.09/76.59
Matuyama/Gauss	2.47	11-3, 98/11-4, 35	92.79/93.66
Gauss/Gilbert	3.40	12-4, 35/12-4, 98	103.26/103.89

Note: — indicates no age estimate available.

[a] Midpoint depths of samples in third column.

Table 6. Site 608, datum levels used to construct Figure 16.

Number	Datum level	Age (Ma)
Hole 608		
1	Top of *Emiliania huxleyi*	0.28
2	Top of *Pseudoemiliania lacunosa*	0.47
3	Top of *Nitzschia reinholdii*	0.65
4	Matuyama/Brunhes	0.73
5	Top of Jaramillo	0.91
6	Bottom of Jaramillo	0.98
7	Top of *Helicosphaera sellii*	1.37
8	Top of *Calcidiscus macintyrei*	1.45
9	Top of Olduvai	1.66
10	Bottom of *Globorotalia truncatulinoides*	1.78
11	Bottom of *Pseudoeunotia doliolus*	1.80
12	Bottom of Olduvai	1.88
13	Top of discoasters	1.90
14	Bottom of *Globorotalia inflata* (PL6)	2.20
15	Top of *Discoaster pentaradiatus*	2.40
16	Top of Gauss	2.47
17	Top of *Dentoglobigerina altispira*	2.90
18	Bottom of Kaena	2.99
19	Top of Mammoth	3.08
20	Top of *Sphaeroidinellopsis seminulina*	3.10
21	Bottom of Mammoth	3.18
22	Gauss/Gilbert	3.40
23	Top of *Globorotalia margaritae*	3.40
24	Top of *Reticulofenestra pseudoumbilica*	3.50
25	Top of *Amaurolithus tricorniculatus*	3.70
26	Bottom of *Globorotalia margaritae*	5.30
27	Top of *Discoaster quinqueramus*	5.6
28	Bottom of *Globorotalia conomiozea*	6.5
29	Chron 6/7	6.70
30	Chron 7/8	7.41
31	Chron 8/9	7.90
32	Chron 9/10	8.50
33	Bottom of *Discoaster quinqueramus*	8.20
34	Top of *Discoaster hamatus*	8.85
35	Chron 10/C5	8.92
36	Bottom of *Discoaster hamatus*	10.00
37	Chron C5/C5A	11.55
38	Top of *Cyclicargolithus floridanus*	11.60
39	Chron C5A/C5AA	12.83
40	Top of *Coscinodiscus lewisianus*	12.90
41	Chron C5AA/C5AB	13.20
42	Top of *Sphenolithus heteromorphus*	14.40
43	Chron C5AD/C5B	14.87
44	Bottom of *Orbulina suturalis*	15.20
45	Bottom of *Cibicidoides wuellerstorfi*	15.4–15.6
46	Bottom of *Praeorbulina glomerosa curva*	16.1
47	Chron C5B/C5C	16.22
48	Top of *Sphenolithus belemnos*	17.40
49	Chron C5C/C5D	17.57
50	Chron C5D/C5E	18.56
51	Chron C5E/C6	19.35
52	Chron C6/C6A	20.88
53	Bottom of *Globigerinoides trilobus*	21.80
54	Chron C6A/C6AA	21.90
55	Chron C6AA/C6B	22.57
56	Chron C6B/C6C	23.27
57	Bottom of *Globorotalia kugleri*	24.60
58	Chron C8/C9	28.15
59	Top of *Sphenolithus distentus*	28.10
60	Bottom of *Sphenolithus ciperoensis*	32.5
61	Bottom of *Isthmolithus recurvus*	37.8
62	Bottom of *Globorotalia cerroazulensis*	37.7
63	Bottom of *Chiasmolithus oamaruensis*	40.0
64	Bottom of *Globorotalia linaperta*	41.3
Hole 608A		
1	Top of *Emiliania huxleyi*	0.28
2	Top of *Pseudoemiliania lacunosa*	0.47
3	Matuyama/Brunhes	0.73
4	Top of Jaramillo	0.91
5	Bottom of Jaramillo	0.98
6	Top of *Helicosphaera sellii*	1.37
7	Top of *Calcidiscus macintyrei*	1.45
8	Top of Olduvai	1.66
9	Bottom of *Globorotalia truncatulinoides*	1.78
10	Bottom of Olduvai	1.88
11	Top of discoasters	1.90
12	Bottom of *Globorotalia inflata* (PL6)	2.20
13	Top of *Discoaster pentaradiatus*	2.40
14	Gauss/Matuyama	2.47
15	Top of *Sphaeroidinellopsis seminulina*	3.10
16	Gilbert/Gauss	3.40
17	Top of *Globorotalia margaritae*	3.40
18	Top of *Reticulofenestra pseudoumbilica*	3.50
19	Top of *Globigerina nepenthes*	3.90

ted in Figure 17. The glacial cycles of Unit I show fluctuations in carbonate content from as low as 45% to up to 96%. Values remain above 90% in most of the nannofossil ooze of Unit II, but show greater variation in Units III through V, ranging from 70 to 95%. The few values from Units VI and VII indicate a marked drop in the $CaCO_3$ content. However, the 4% value from Unit VII is thought to be anomalously low in the light of X-ray diffraction results.

Interstitial Water

At this site, analyses of chlorinity, Ca^{2+}, and Mg^{2+} were carried out on board, in addition to the pH, alkalinity, and salinity analyses (Fig. 18). All curves show predictable trends similar to those at other sites. The Ca^{2+} and Mg^{2+} values are linearly correlated (Fig. 19). The only feature of interest is the slight fluctuation in the curves within Unit IVB (Fig. 18), where the calcium

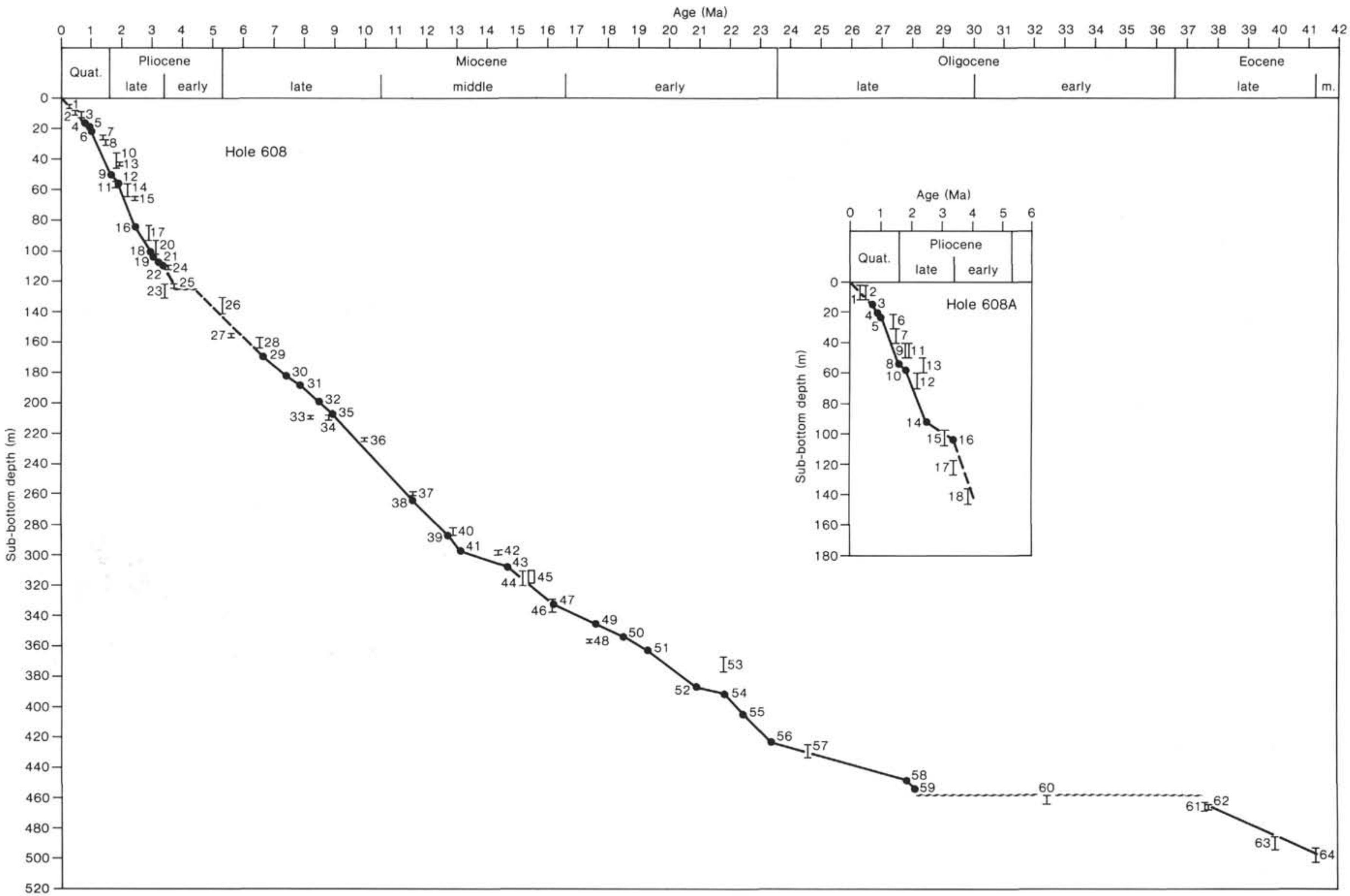

Figure 16. Time-versus-depth plot for cores taken at Hole 608. Cores taken at Hole 608A are plotted in the inset figure. The datum levels used to construct the curves are given in Table 6.

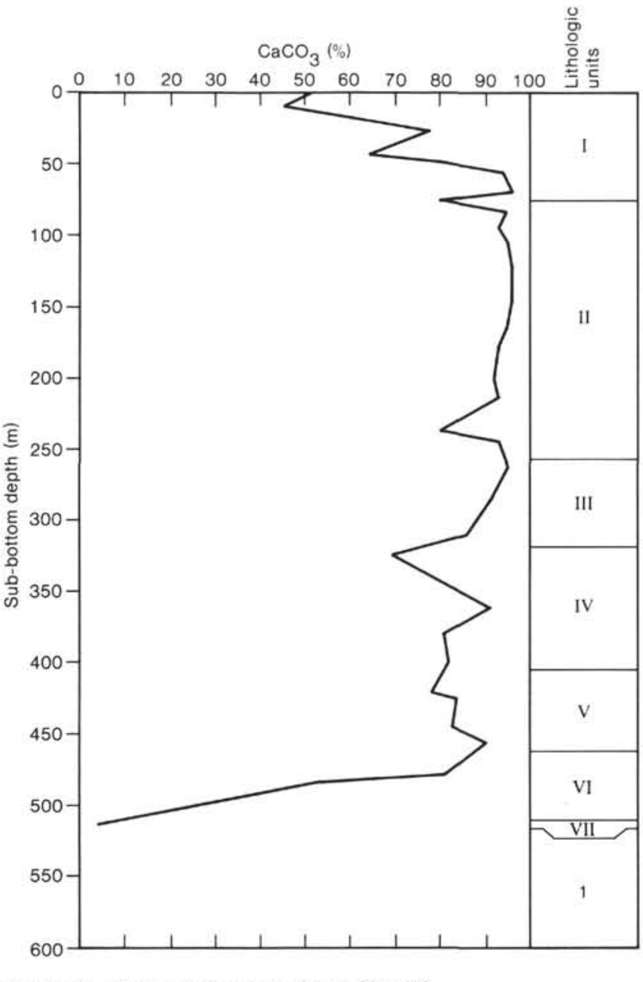

Figure 17. Carbonate bomb analyses, Site 608.

concentration remains constant and magnesium increases slightly. This may have been caused by the presence of reworked dolomite in this subunit (see Sediment Lithology section).

SUMMARY AND CONCLUSIONS

Site 608 sampled almost completely the sedimentary section to basement on the southern flank of the King's Trough complex (42°50.2′N; 23°05.2′W). From the seafloor (at 3526 m) to about 150 m sub-bottom, a complete stratigraphic section apparently was recovered through overlapping double VLHPC coring in two holes (608 and 608A). Beyond that depth, Hole 608 was continuously XCB-cored to basement at 515.4 m sub-bottom (Fig. 6). Two cores were then taken in the basaltic basement, to a terminal depth of 530.9 m. Overall recovery averaged 81% in Hole 608 and 98% in Hole 608A. Very low recoveries in isolated cores in the deepest 100 m of Hole 608 are responsible for the decreased recovery in that hole. In general, core recovery with the XCB was greater than 90%, and for the most part the cores are free of drilling disturbance.

The sedimentary section extends in age from the late Quaternary (NN21) to the late middle Eocene (NP16). The paleomagnetic stratigraphy obtained from this site can be considered unique for the North Atlantic, in that a complete record of polarity reversals was obtained back to Chron C8 (28.5 Ma). As many as 64 datum levels are available for the combined biostratigraphy and paleomagnetic stratigraphy of Hole 608 (Table 6, Fig. 16).

The sediment immediately above the relatively fresh pillow lava basalt of basement is a dolomite-bearing calcareous mudstone passing upward into dolomitic marlstone of lithologic Unit VII, and is dated as NP16 on nannofossil evidence. Isolated nannofossils preserved in partly recrystallized sediment within the basalt suggest the same age. The apparent absolute age of about 42 Ma agrees well with the age of magnetic Chron C18, upon which the site is located; estimates of the age of this Chron range from 41.29 to 43.6 Ma (Berggren, Kent, and Van Couvering, in press).

Only one major hiatus has been detected from shipboard biostratigraphic and paleomagnetic studies, at a sub-bottom depth of about 460 m. Nannofossil evidence suggests that the hiatus separates nannofossil Zone NP24 (late Oligocene), in Sample 608-48,CC, from Zone NP19 (late Eocene), in Sample 608-50,CC. Sample 608-49,CC, between the two, contains a mixed Eocene and Oligocene assemblage, and is considered reworked. Benthic foraminiferal evidence is in agreement with the nannofossil evidence. Planktonic foraminiferal evidence indicates that the hiatus separates sediments of the late Eocene *Globorotalia cerroazulensis* Zone in Sample 608-49,CC from the *G. linaperta* Zone in Sample 608-50,CC. These two lines of evidence suggest that the hiatus may span up to 9.7 m.y. (28.1-37.8 Ma, nannofossils), but, on the other hand, may span no more than 8.1 m.y. (28.1-36.6 Ma, planktonic foraminifers). The placing here of the contact above Sample 608-50,CC is in keeping with the lithologies as described in what follows, and it most probably occurs in the upper part of Core 608-50.

The upper Eocene sediments below the hiatus are green, marly nannofossil chalks (lithologic Unit VI) containing volcaniclastic turbidites and volcanic ash layers. The topmost core of the unit, 608-50, shows no evidence of sediment deformation. Above the hiatus, on the other hand, in Core 608-49 (454.1-461.7 m sub-bottom) the upper Oligocene sediments are chalk conglomerates (suggestive of debris-flow processes) and pinkish marly nannofossil flaser chalks. These chalks are interpreted as evidence of regional tectonic activity. The remaining upper Oligocene marly nannofossil chalks of lithologic Unit V (to about 406 m sub-bottom, the Oligocene/Miocene boundary), are typically pelagic with no microfaulting or flaser chalk development.

A further interval, similarly interpreted as resulting from some regional tectonic event, occurs within the lower Miocene chalk sequence (lithologic Unit IV). Again, flaser chalks and chalk conglomerates occur, along with conspicuous microfaulting that displays clear slickenside surfaces. The chalks of the base and top of this lithologic unit (Subunits IVC and IVA) are gray green, whereas the intervening Subunit IVB is tan to brown, which may reflect its content of dolomite, as detected by X-ray diffraction. Benthic foraminiferal evidence suggests sluggish, restricted bottom-water conditions in the early Mi-

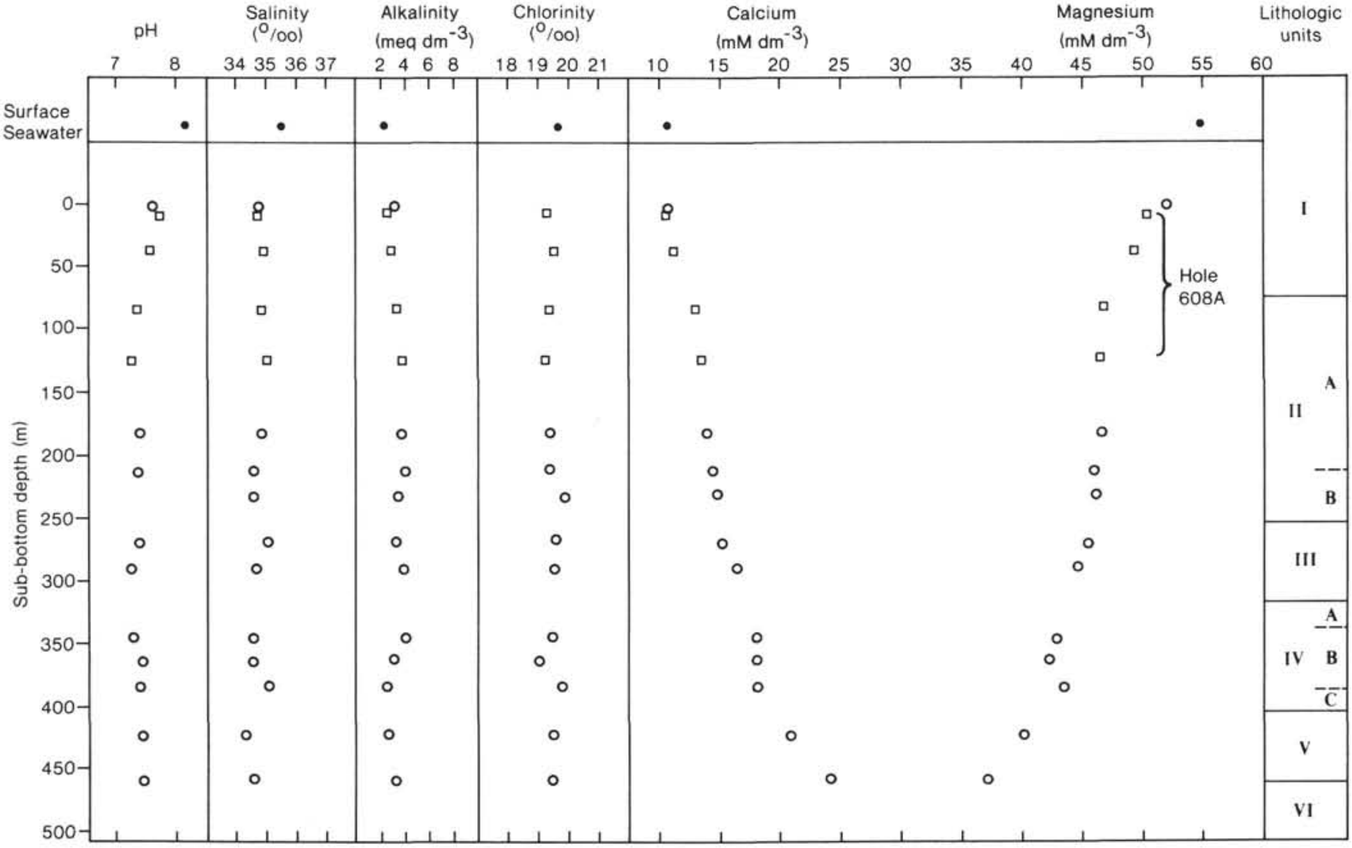

Figure 18. Interstitial water analyses, Site 608. □ = Hole 608A; ○ = Hole 608.

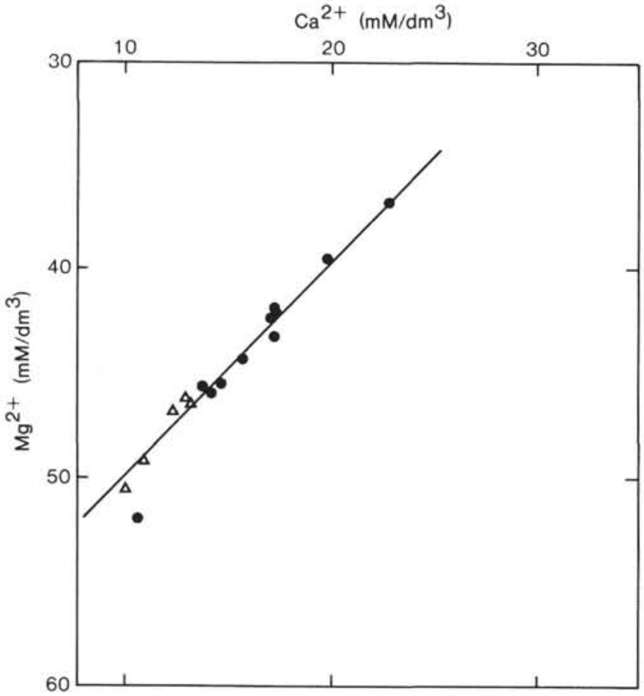

Figure 19. Plot of Mg^{2+} versus Ca^{2+} concentrations in interstitial waters, Site 608. Δ = Hole 608A; ● = Hole 608.

ocene (Subunit IVB). Flaser chalks become less common uphole and downhole from the center of Subunit IVB, where chalk conglomerate, interpreted as debris-flow material, is present at 369 to 375 m sub-bottom. Sedimentation rates over this early Miocene period were probably erratic, but they averaged 10 m/m.y., except for a slowing in lithologic Unit IVA to 8.5 m/m.y.

The sediments of the middle Miocene are white nannofossil chalks with green intervals (lithologic Unit III, 257 to 320 m sub-bottom). These grade upsection into a thick upper Miocene and lower Pliocene sequence of homogeneous white nannofossil chalks (softening to oozes), which is interrupted only by pyritized fractures and burrows or isolated pelagic turbidites (lithologic Unit II, 76–257 m sub-bottom). Throughout the middle Miocene, the site was clearly a location of generally more stable tectonic conditions than during deposition of lithologic Unit IV. Sediments accumulated at average rates of about 19.0 m/m.y., almost twice the rates in the lower parts of the sequence. This appears to be accounted for by evidence of local reworking and signs of slope sedimentation (pelagic turbidites, a hiatus occurring in one hole only, major reworking of foraminifers in Cores 608-17 through 608-26). Vertical transport distances for displaced material must not have been great, because no major bathymetric displacement of benthic foraminifers has been found in the drilled sequence.

The first indications of glacial–interglacial carbonate cycles and of ice rafting occur at about 76 m sub-bottom, correlating with the end of the Gauss Chron (2.47 Ma). Nannofossil ooze to marl alternations develop upsection into nannofossil marl to calcareous mud cycles. Carbonate concentrations reach values as low as 45% in some of the mud intervals, reflecting their content of ice-rafted terrigenous material in these intervals. Glacial erratics, some almost as large as the diameter of the core liner (6.5 cm), are disseminated throughout the upper Pliocene and Quaternary section. Most are basaltic, metamorphic (gneiss, schist), or igneous (mostly granite), but shales and mudstones are also present. Sedimentation rates increased considerably through this glacial–interglacial period, to about 34 m/m.y., a reflection, presumably, of ice-rafted sediment input.

Holes 608 and 608A appeared well-correlated through paleomagnetic, biostratigraphic, and lithologic tie-lines (Ruddiman et al., this volume). At the time of drilling, however, we suspected that either sediment slumping occurred at the site during the Quaternary, as at deeper levels, or downhole drilling contamination had caused some of the observed perturbations. We concluded that a complete Quaternary to upper Pliocene section was recovered. Some suspicion remained, though, that additional sediment was added by drilling contamination to the section cored with the VLHPC (see Ruddiman et al.; Takayama and Sato, this volume).

The major events in the geologic history of this site appear traceable in a regional sense through the seismic records. The primary reflectors are as follows:

The basement to sediment reflector, which represents the first sedimentation (dolomitic mudstone and marlstone) on 42-Ma pillow lava basalts.

An acoustically stratified to transparent sediment reflector representing the Eocene/Oligocene hiatus. The acoustic change reflects the passage upward from the marly nannofossil chalks of lithologic Unit VI, with their volcaniclastic interbeds, to the marly nannofossil chalks of Unit V, through the flaser chalks and chalk conglomerate of Core 608-49. The reflector is disconformable with basement, and is clearly tectonic in character.

The top of an acoustically more coherent seismic unit within a thick transparent acoustic interval. This probably represents a contact of undeformed, unfractured, untectonized middle Miocene and lower Pliocene chalks with lower Miocene chalks that have suffered soft-sediment deformation and microfaulting. This reflector is disconformable with overlying seismic units.

The base of the uppermost acoustically stratified unit, which appears to represent the initiation of cyclic glacial sedimentation in the region.

The tectonic events interpreted from the drilled sedimentary section correlate reasonably well, as to age, with those previously proposed by Kidd et al. (1982) for the region from geophysical studies and from dredge and rock-core sampling within the King's Trough complex. Two major tectonic events had been proposed by these authors:

1. After initial formation of the main hot-spot-ridge edifice between 56 and 34 Ma, a regional intraplate volcanic event was thought to have uplifted the crest of the ridge to subaerial depths, so that tuffs and ashes were deposited near sea level. This event was thought to have been brought about by major intrusion of trachytic rocks along fault planes, and the trachytes were dated at 32 to 34 Ma. The ridge-flank location of Site 608 appears to have recorded these events, but only partially. Because of its young crustal age (magnetic Chron C18), the lowermost sediments record only part of the Eocene history, but do confirm the existence of a nearby source of volcaniclastic material, presumably the ridge, between 42 and 38 Ma. The Eocene/Oligocene hiatus is primarily tectonic in character, and spans the period of trachyte intrusion.

Sediments deposited during the period between about 28 and 23 Ma, the late Oligocene, are predominantly pelagic, and represent a period of relatively stable tectonic conditions. Isolated occurrences of reworked *Braarudosphaera* (calcareous nannofossil) indicate the existence of a very shallow region (less than 200 m water depth) near the site. The lack of obviously displaced benthic foraminifers presumably reflects the relative stability of the slopes during that period.

2. An intraplate rifting event at about Chron C6A (21 Ma) was the second tectonic interval proposed by Kidd et al. (1982) and earlier authors (Searle and Whitmarsh, 1978). This was believed to have brought about the formation of the internal, anomalously deep, troughs, by rifting and subsidence along fault scarps. The Site 608 sequence shows evidence of tectonic instability in the form of flaser chalks and microfaulting in lithologic Unit IV. Flaser chalks and microfaulting become most abundant, giving an impression of maximum disturbance of the sediments, in Core 608-40. This core is dated at about 20 Ma (NN3), and contains a chalk conglomerate, interpreted as a debris flow. Detailed consideration of the regional implications of the events dated at Site 608 is left to the synthesis chapters (Kidd and Ramsay, this volume), where the results of shore-based studies on geophysical and dredge-haul data are also presented.

REFERENCES

Baldauf, J. G., 1985. Cenozoic diatom biostratigraphy and paleoceanography of the Rockall Plateau region, North Atlantic, DSDP Leg 81. *In* Roberts, D. G., Schnitker, D., et al., *Init. Repts. DSDP*, 81: Washington (U.S. Govt. Printing Office), 439–477.

Barron, J. A., 1985. Neogene planktic diatom biostratigraphy. *In* Bolli, H. M., Saunders, J. B., and Perch-Nielsen, K. (Eds.), *Plankton Stratigraphy:* Cambridge, U.K. (Cambridge University Press), pp. 763–809.

Berggren, W. A., 1973. The Pliocene timescale calibration of planktonic foraminiferal and calcareous nannoplankton zonation. *Nature*, 243:391–397.

________, 1977. Late Neogene planktonic foraminiferal biostratigraphy of the Rio Grande Rise (South Atlantic). *Mar. Micropaleontol.*, 2:251–265.

Berggren, W. A., Kent, D., and Flynn, J. J., in press. Paleogene geochronology and chronostratigraphy. *In* Snelling, N. J. (Ed.), *Geochronology and the Geological Record*, J. Geol. Soc. London Mem.

Berggren, W. A., Kent, D. V., and Van Couvering, J. A., in press. Neogene geochronology and chronobiostratigraphy. *In* Snelling, N. J. (Ed.), *Geochronology and the Geological Record*, J. Geol. Soc. London Mem.

Bukry, D., 1973. Low-latitude coccolith biostratigraphic zonation. *In* Edgar, N. T., Saunders, J. B., et al., *Init. Repts. DSDP*, 15: Washington (U.S. Govt. Printing Office), 685–703.

———, 1975. Coccolith and silicoflagellate stratigraphy, northwestern Pacific Ocean, Deep Sea Drilling Project Leg 32. *In* Larson, R. L., Moberly, R., et al., *Init. Repts. DSDP*, 32: Washington (U.S. Govt. Printing Office), 677-701.

Burckle, L. H., 1977. Pliocene and Pleistocene diatom datum levels from the equatorial Pacific. *Quat. Geol.*, 7:330-340.

Cann, J. R., 1971. Petrology of basement rocks from Palmer Ridge, N.E. Atlantic. *Phil. Trans. R. Soc. London*, Ser. A., 268:605-664.

Corliss, B. H., 1981. Deep-sea benthic foraminiferal faunal turnover near the Eocene/Oligocene boundary. *Micropaleontology*, 27:356-378.

Douglas, R., and Woodruff, F., 1981. Deep sea benthic foraminifera. *In* Emiliani, C. (Ed.), *The Sea* (Vol. 7): *The Oceanic Lithosphere:* New York (Wiley-Interscience), 1233-1327.

Garrison, R. E., and Kennedy, W. J., 1977. Origin of solution seams and flaser structures in Upper Cretaceous chalks of southern England. *Sed. Geol.*, 19:107-137.

Kidd, R. B., Searle, R. C., Ramsay, A. T. S., Prichard, H., and Mitchell, J., 1982. The geology and formation of King's Trough, northeast Atlantic Ocean. *Mar. Geol.*, 48:1-30.

Laughton, A. S., 1965. Bathymetry of the northeastern Atlantic Ocean and recent geophysical studies. *In* Whittard, W. F., and Bradshaw, R. (Eds.), *Submarine Geology and Geophysics:* London (Butterworth), pp. 175-176.

Le Pichon, X., and Sibuet, J. C., 1971. Western extension of the boundary between European and Iberian plates during the Pyrenean Orogeny. *Earth Planet. Sci. Lett.*, 12:83-88.

Martini, E., 1967. Nannoplankton aus Umlagerungserscheinungen im Persischen Golf und im nordlichen Arabischen Meer. *Neues Jahrb. Geol. Paleont. Monatsch.*, 10:597-607.

Matthews, D. H., Laughton, A. S., Pugh, D. J., Jones, E. J. W., Sunderland, J., et al., 1969. Crustal structure and origin of Peake and Freen deeps, N.E. Atlantic. *Geophys. J. R. Astron. Soc.*, 18:517-542.

Mimran, Y., 1975. Fabric deformation induced in Cretaceous chalks by tectonic stresses. *Tectonophysics*, 26:309-316.

Ramsay, A. T. S., 1970. The pre-Pleistocene stratigraphy and paleontology of the Palmer Ridge area, N.E. Atlantic. *Mar. Geol.*, 9: 261-285.

Roth, P. H., 1974. Calcareous nannofossils from the northwestern Indian Ocean, Leg 24, Deep Sea Drilling Project. *In* Fisher, R. L., Bunce, E. T., et al., *Init. Repts. DSDP*, 24: Washington (U.S. Govt. Printing Office), 969-994.

Schrader, H. J., 1976. Cenozoic marine planktonic diatom biostratigraphy of the southern Pacific Ocean. *In* Hollister, C. D., Craddock, C., et al., *Init. Repts. DSDP*, 35: Washington (U.S. Govt. Printing Office), 605-671.

Searle, R. C., and Whitmarsh, R. B., 1978. The structure of King's Trough, northeast Atlantic, from bathymetric, seismic and gravity studies. *Geophys. J. R. Astron. Soc.*, 53:259-287.

Stebbins, J., and Thompson, G., 1978. The nature and petrogenesis of intra-oceanic alkaline eruptive and plutonic rocks: King's Trough, northeast Atlantic. *J. Volc. Geotherm. Res.*, 4:323-361.

Takayama, T., 1972. A note on the distribution of *Braarudosphaera bigelowi* (Gran and Braarud) Deflandre in the bottom sediments of Sendai Bay, Japan. *Trans. Proc. Paleontol. Soc. Japan*, N. S., 87: 429-435.

Thomas, E., 1985. Late Eocene to Recent deep-sea benthic foraminifers from the central equatorial Pacific Ocean. *In* Mayer, L., Theyer, F., et al., *Init. Repts. DSDP*, 85: Washington (U.S. Govt. Printing Office), 655-694.

Tjalsma, R. C., and Lohmann, G. P., 1983. Paleocene-Eocene abyssal benthic foraminifera from the Atlantic Ocean. *Micropaleontology Spec. Publ.*, 4.

Van der Zwaan, G. J., 1982. Paleoecology of late Miocene Mediterranean foraminifera. *Utrecht Micropaleontol. Bull.*, 26.

Vogt, P. R., and Avery, O. E., 1974. Detailed magnetic surveys in the northeast Atlantic and Labrador Sea. *J. Geophys. Res.*, 79:363-389.

Weaver, P. P. E., 1983. An integrated stratigraphy of the King's Trough flank area. *Oceanol. Acta*, 6:451-456.

Williams, C. A., and McKenzie, D., 1971. The evolution of the northeast Atlantic. *Nature*, 232:168-173.

SITE 608 HOLE CORE 1 CORED INTERVAL 0.0–7.0 m

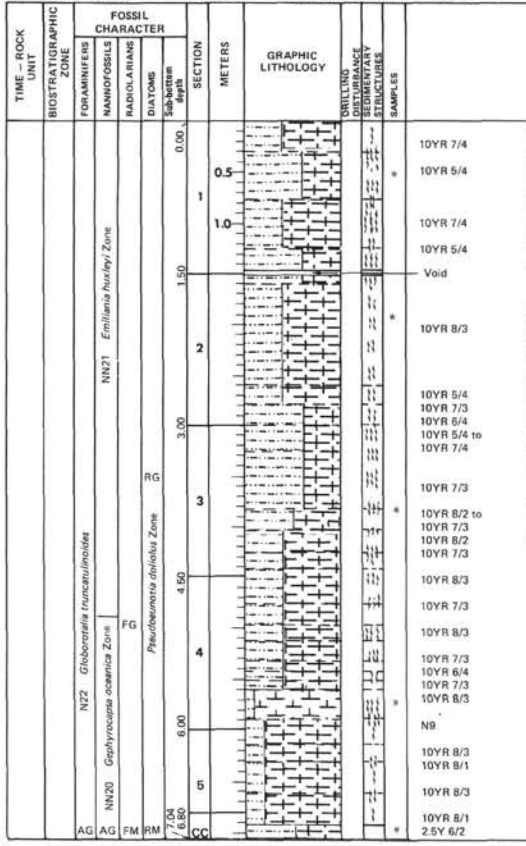

LITHOLOGIC DESCRIPTION

MARLY FORAMINIFERAL NANNOFOSSIL OOZE, mostly alternating layers (with gradational contacts) of very light brown (10YR 8/3), light brown (10YR 7/4), and brown (10YR 5/4 and 10YR 6/4). 5.59 to 5.89 m white (N9) NANNOFOSSIL OOZE. Bioturbation evident throughout.

Erratic piece of schist, 0.49 m. At 4.57 m piece of quartzite.

SMEAR SLIDE SUMMARY (%)

	1, 50 D	2, 50 D	3, 83 D	4, 129 D	CC,23 D
Texture:					
Sand	15	–	TR	TR	5
Silt	70	20	25	30	40
Clay	15	80	75	70	55
Composition:					
Quartz	40	25	35	12	35
Feldspar	5	5	5	3	10
Mica	TR	TR	–	–	–
Heavy minerals	TR	–	–	–	TR
Clay	15	10	TR	TR	10
Foraminifers	25	20	12	3	15
Calc. nannofossils	15	40	48	82	30
Diatoms	–	–	TR	–	–

ORGANIC CARBON AND CARBONATE (%)

	1, 50
Organic carbon	–
Carbonate	51

SITE 608 HOLE CORE 2 CORED INTERVAL 7.0–16.6 m

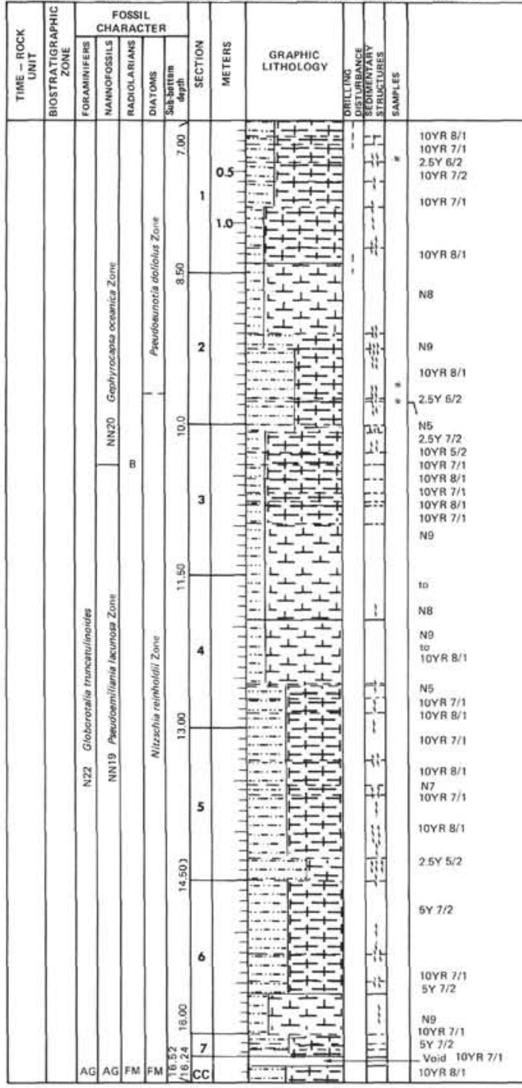

LITHOLOGIC DESCRIPTION

MARLY FORAMINIFERAL NANNOFOSSIL OOZE, mostly alternating layers (with gradational contacts) of very light brown (10YR 8/1) and light brown (10YR 7/1).

NANNOFOSSIL OOZE, 8.24 to 9.19, 10.96 to 12.56, and 15.61 to 16.02 m, white (N9) and very light gray (N8). Frequently bounded by sharp contacts.

Bioturbation mostly at color contrasts. Greenish gray (5Y 6/1) layer at 10.67 m. Erratic pieces of basalt(?) 9.10 to 10.00 m and 14.29 to 14.50 m.

SMEAR SLIDE SUMMARY (%)

	1, 38 M	2, 111 D	2, 127 D
Texture:			
Sand	–	–	30
Silt	–	100	70
Clay	–	–	–
Composition:			
Quartz	30	30	10
Feldspar	–	10	–
Clay	–	10	5
Foraminifers	20	15	18
Calc. nannofossils	50	35	77

ORGANIC CARBON AND CARBONATE (%)

Section-Interval (cm)	2-111
Carbonate	45

SITE 608 HOLE CORE 3 CORED INTERVAL 16.6–26.2 m

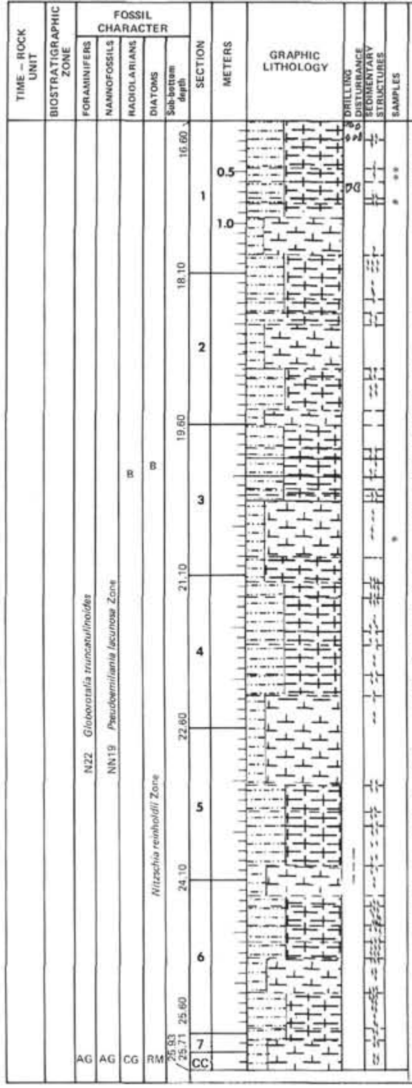

LITHOLOGIC DESCRIPTION

MARLY FORAMINIFERAL NANNOFOSSIL OOZE, mostly layers (with gradational contacts) of very light brown (10YR 8/1) and light brown (2.5Y 7/2, 10YR 7/2, 10YR 7/1, 5Y 8/1).

NANNOFOSSIL OOZE, white (N9) and very light gray (N8): 17.53 to 17.90, 18.70 to 19.13, 19.44 to 19.60, 20.35 to 20.90, 22.26 to 23.13, 23.98 to 24.25, 24.84 to 25.20, 25.67 to 25.93 m.

SMEAR SLIDE SUMMARY (%)

	1, 51 D	1, 48 M	1, 80 D	3, 110 D
Texture:				
Sand	7	–	–	–
Silt	40	–	–	–
Clay	53	–	–	–
Composition:				
Quartz	30	15	60	20
Feldspar	5	–	–	–
Mica	TR	–	–	–
Clay	15	5	–	–
Foraminifers	20	60	10	5
Calc. nannofossils	30	20	30	75

ORGANIC CARBON AND CARBONATE (%)

	1, 50
Organic carbon	–
Carbonate	57

SITE 608 HOLE CORE 4 CORED INTERVAL 26.2–35.8 m

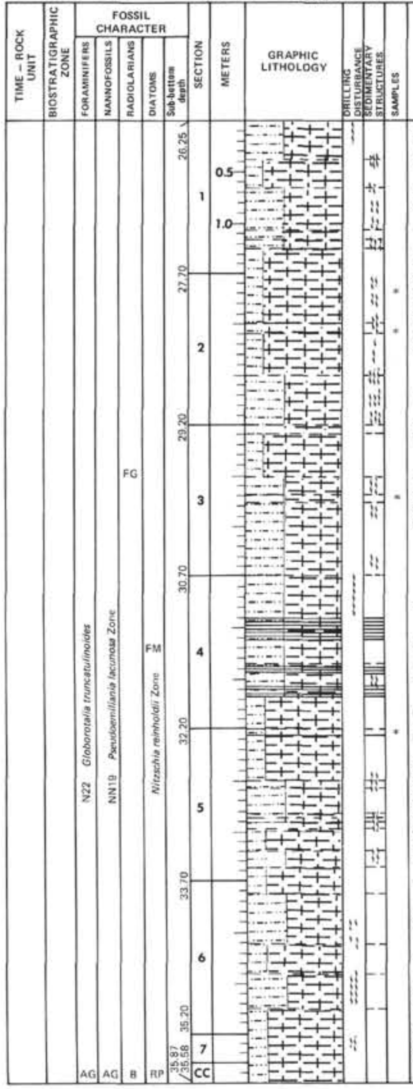

LITHOLOGIC DESCRIPTION

MARLY FORAMINIFERAL NANNOFOSSIL OOZE, mostly alternating shades of gray (5Y 7/2, 10YR 7/1, N7 to N8). Contacts gradational. Distinct bands of light gray (10YR 7/1) from 31.10 to 31.84 m.

FORAMINIFERAL NANNOFOSSIL OOZE, white (N9) alternating with above darker, marly layers. Contacts gradational.

Note: recovery ~100%.

SMEAR SLIDE SUMMARY (%)

	2, 14 D	3, 71 D	4, 149 D	2, 65 D
Composition:				
Quartz	20	17	20	–
Feldspar	–	TR	1	–
Heavy minerals	–	TR	–	–
Clay	10	–	–	–
Foraminifers	20	15	12	–
Calc. nannofossils	50	73	67	–
Diatoms	TR	–	–	–

ORGANIC CARBON AND CARBONATE (%)

	2, 14
Organic carbon	–
Carbonate	78

SITE 608 HOLE CORE 5 CORED INTERVAL 35.8–45.4 m

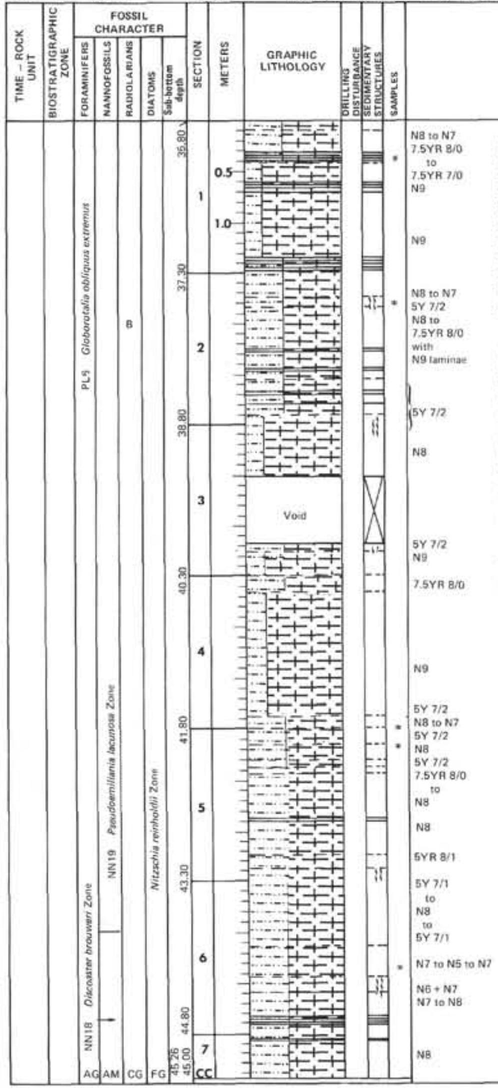

LITHOLOGIC DESCRIPTION

FORAMINIFERAL NANNOFOSSIL OOZE, mostly alternating layers of white (N9), very light gray (N8), light grayish brown (5Y 7/2), and light gray (7.5YR 8/0). All contacts gradational except where laminae present. Darker gray (7.5YR 7/0) laminae evident 36.10 to 37.30 m. Light greenish gray (5G 7/1) laminae evident 38.48 to 38.58 and 42.66 to 42.68 m. Faint white (N9) laminae at 38.04 to 38.05 and 38.23 to 38.26 m. Thin layers of pale green (5G 7/2), bluish gray (7.5YR 7/0), and pale blue (5PB 7/2) 44.66 to 44.85 m. Generally less color contrast than overlying cores.

SMEAR SLIDE SUMMARY (%):

	1, 30 D	2, 27 D	4, 143 D	5, 12 D	6, 73 M
Texture:					
Sand	—	—	—	—	1
Silt	5	7	4	2	7
Clay	95	93	96	98	92
Composition:					
Quartz	11	25	43	18	38
Feldspar	TR	TR	1	TR	TR
Volcanic glass	1	—	TR	—	2
Pyrite	—	TR	—	—	—
Carbonate unspec.	TR	—	—	TR	TR
Foraminifers	11	12	17	15	13
Calc. nannofossils	77	65	70	67	46
Diatoms	TR	—	—	—	TR
Sponge spicules	—	—	TR	—	—

ORGANIC CARBON AND CARBONATE (%):

	6, 73
Organic carbon	—
Carbonate	64

SITE 608 HOLE CORE 6 CORED INTERVAL 45.4–55.0 m

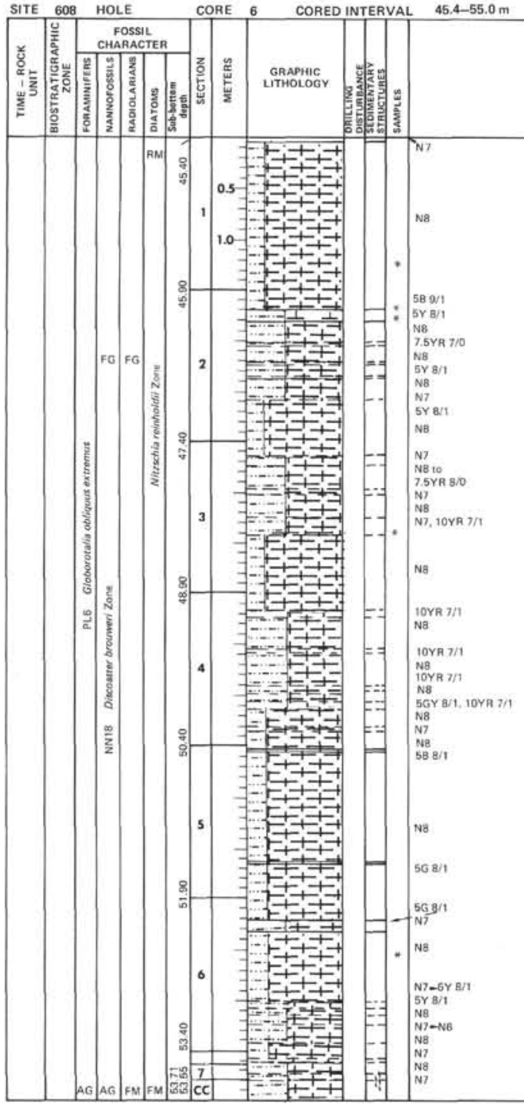

LITHOLOGIC DESCRIPTION

FORAMINIFERAL NANNOFOSSIL OOZE, dominantly very light gray (N8). Occasional layers of light gray (N7), yellowish gray (5Y 8/1), and light grayish brown (10YR 7/1). Couplets of light gray (N7) and light grayish brown (10YR 7/1) occur 47.54 to 48.31 m. Layers of bluish gray (7.5YR 7/0), light blue gray (7.5YR 8/0), and light greenish gray (5GY 8/1 and 5G 8/1) occur 46.44, 47.87, 49.97, 50.44, 51.55, and 52.13 m.

NANNOFOSSIL OOZE, bluish white (5B 9/1), 46.10 m.

SMEAR SLIDE SUMMARY (%):

	1, 120 D	2, 20 M	2, 27 D	3, 83 M	6, 53 D
Texture:					
Sand	—	—	—	—	—
Silt	1	2	1	3	3
Clay	99	98	99	97	97
Composition:					
Quartz	15	25	30	28	15
Feldspar	TR	TR	TR	TR	TR
Volcanic glass	—	—	TR	TR	—
Pyrite	—	—	—	1	—
Carbonate unspec.	—	—	TR	TR	TR
Foraminifers	12	6	15	16	11
Calc. nannofossils	73	69	55	55	74
Sponge spicules	—	TR	—	—	—

ORGANIC CARBON AND CARBONATE (%):

	3, 83
Organic carbon	—
Carbonate	81

SITE 608 HOLE CORE 7 CORED INTERVAL 55.0–64.6 m

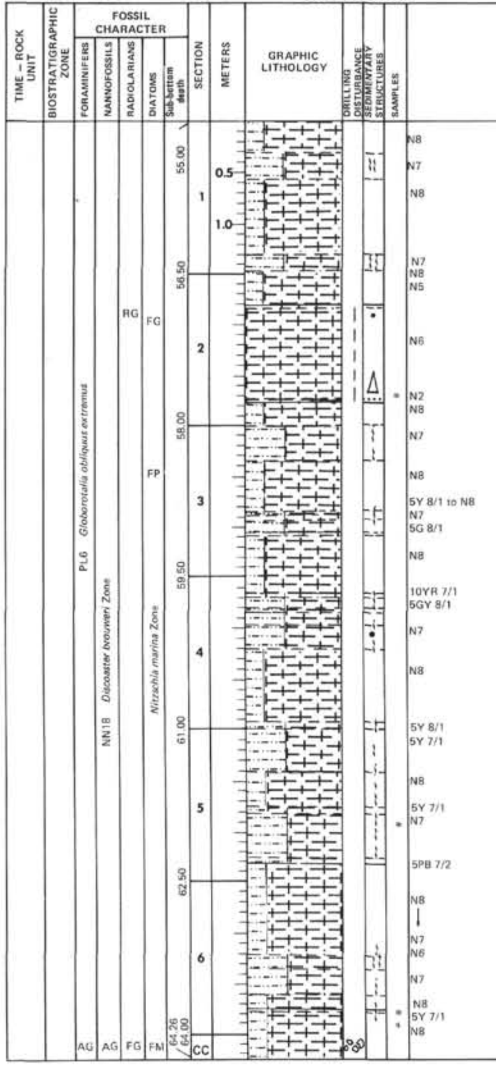

LITHOLOGIC DESCRIPTION

FORAMINIFERAL NANNOFOSSIL OOZE, mostly alternating layers of very light gray (N8), light gray (N7), and light tannish gray (10YR 7/1 and 5Y 7/1).

FORAMINIFERAL SAND, gray (N6) to grayish black (N2) 56.81 to 57.64 m. This interval watery and details of structure probably blurred by coring and splitting process. Some evidence of fining upwards.

Dropstones at 57.04 and 60.09 m.

SMEAR SLIDE SUMMARY (%):

	2, 116	5, 86	6, 127	6, 137
	M	M	M	D
Texture:				
Silt	5	10	–	1
Clay	95	90	100	99
Composition:				
Quartz	6	25	6	20
Feldspar	TR	TR	TR	1
Volcanic glass	1	–	TR	–
Pyrite	–	1	–	TR
Carbonate unspec.	3	1	–	1
Foraminifers	22	12	16	12
Calc. nannofossils	68	61	78	67
Sponge spicules	–	–	TR	–
Silicoflagellates	–	–	TR	–

ORGANIC CARBON AND CARBONATE (%):

	2, 41
Organic carbon	–
Carbonate	94

SITE 608 HOLE CORE 8 CORED INTERVAL 64.6–74.2 m

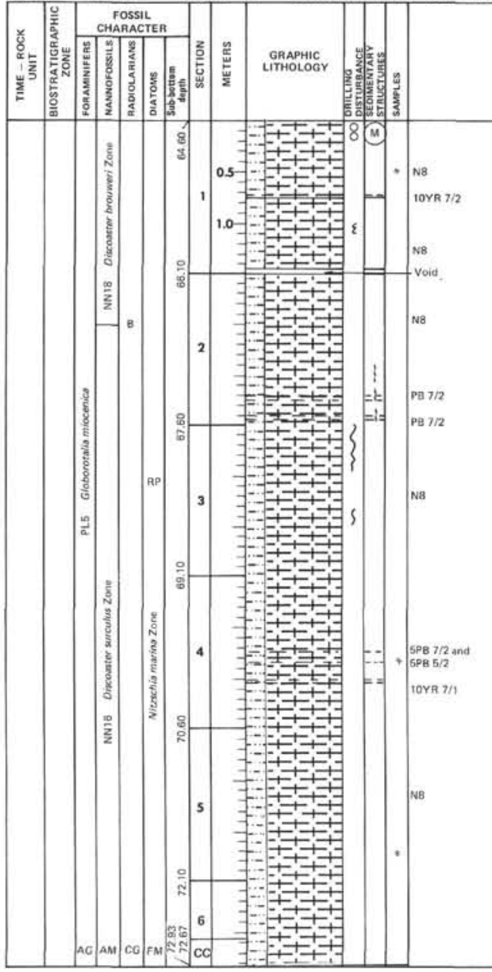

LITHOLOGIC DESCRIPTION

FORAMINIFERAL NANNOFOSSIL OOZE, very light gray (N8). Occasional layers of light brownish gray (10YR 7/2), light tannish gray (10YR 7/1), pale blue (5PB 7/2) and grayish blue (5PB 5/2). Bivalve shell (diameter ~ 0.5 cm) at 64.69 m. Gray (N6) streaks at 45° between 70.60 and 71.40 m.

SMEAR SLIDE SUMMARY (%):

	1, 50	4, 82	5, 120
	D	M	D
Texture:			
Silt	1	5	–
Clay	99	95	100
Composition:			
Quartz	18	22	5
Feldspar	TR	1	1
Pyrite	–	TR	–
Carbonate unspec.	1	–	TR
Foraminifers	10	42	15
Calc. nannofossils	31	36	79

ORGANIC CARBON AND CARBONATE (%):

	4, 81
Organic carbon	–
Carbonate	96

SITE 608 HOLE CORE 9 CORED INTERVAL 74.2–83.8 m

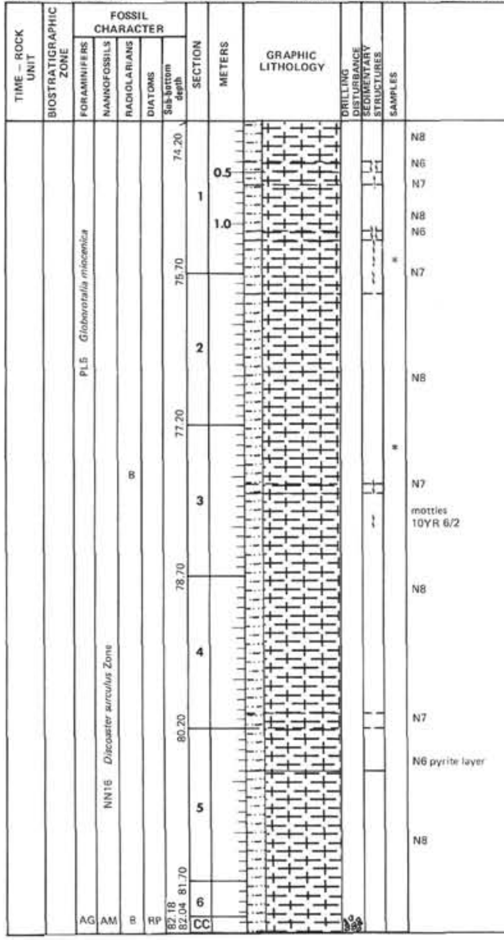

LITHOLOGIC DESCRIPTION

FORAMINIFERAL NANNOFOSSIL OOZE, gray (N6) to dominantly very light gray (N8).

SMEAR SLIDE SUMMARY (%):

	1, 136 M	3, 18 D
Texture:		
Silt	1	2
Clay	99	98
Composition:		
Quartz	18	20
Feldspar	TR	TR
Volcanic glass	1	–
Foraminifers	19	12
Calc. nannofossils	62	68

ORGANIC CARBON AND CARBONATE (%):

	1, 136
Organic carbon	–
Carbonate	80

SITE 608 HOLE CORE 10 CORED INTERVAL 83.8–93.4 m

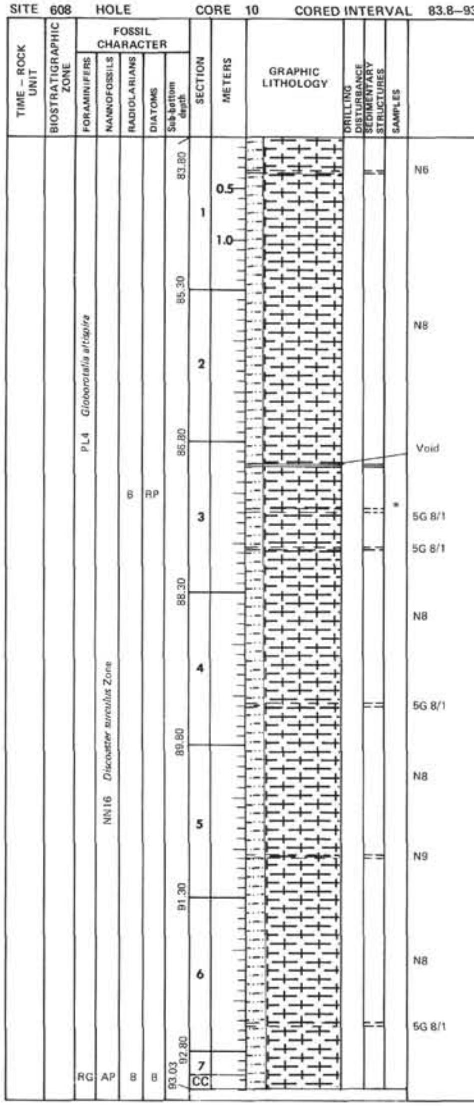

LITHOLOGIC DESCRIPTION

FORAMINIFERAL NANNOFOSSIL OOZE, dominantly very light gray (N8), with thin layers of white (N9), gray (N6) and light greenish gray (5G 8/1).

SMEAR SLIDE SUMMARY (%):

	3, 60 D
Texture:	
Silt	1
Clay	99
Composition:	
Quartz	17
Feldspar	TR
Carbonate unspec.	TR
Foraminifers	14
Calc. nannofossils	69

ORGANIC CARBON AND CARBONATE (%):

	1, 30
Organic carbon	–
Carbonate	95

SITE 608 HOLE CORE 11 CORED INTERVAL 93.4–103.0 m

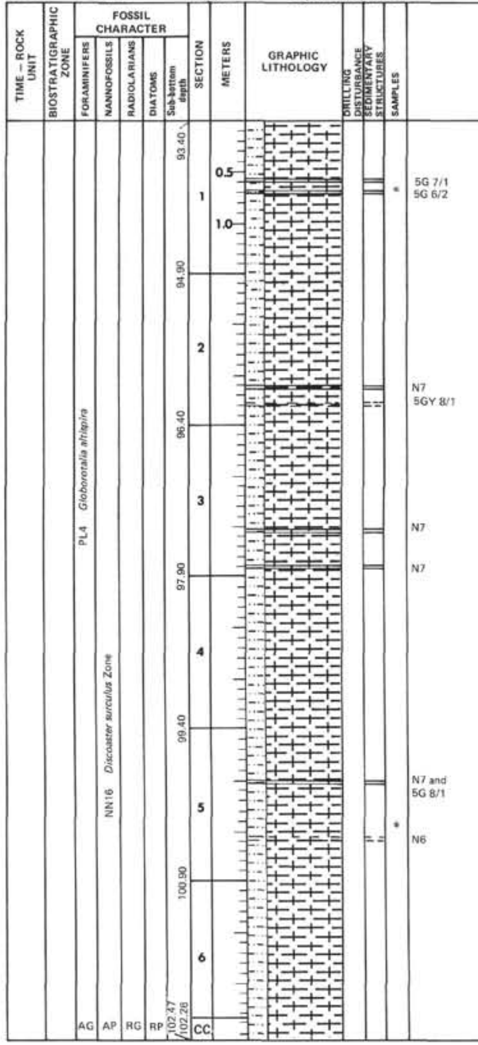

LITHOLOGIC DESCRIPTION

FORAMINIFERAL NANNOFOSSIL OOZE, very light gray (N8). Faint laminae of gray and green (5G 7/1, 5G 6/2, 5GY 8/1). Multiple laminae of light gray (N7).

SMEAR SLIDE SUMMARY (%):

	1, 69 M	5, 90 D
Texture:		
Silt	2	2
Clay	98	98
Composition:		
Quartz	12	20
Feldspar	1	TR
Volcanic glass	TR	–
Carbonate unspec.	2	TR
Foraminifers	27	18
Calc. nannofossils	68	56

ORGANIC CARBON AND CARBONATE (%):

	2, 111
Organic carbon	–
Carbonate	93

SITE 608 HOLE CORE 12 CORED INTERVAL 103.0–112.6 m

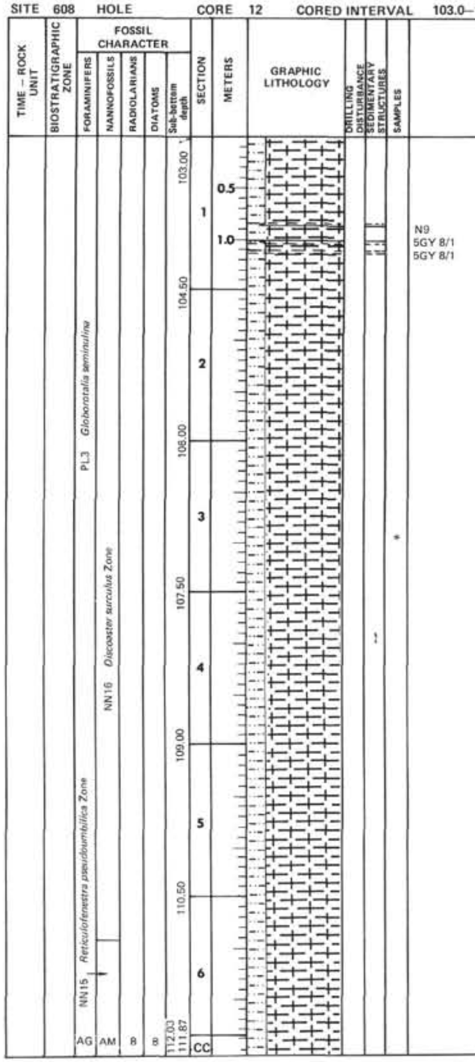

LITHOLOGIC DESCRIPTION

FORAMINIFERAL NANNOFOSSIL OOZE, very light gray (N8)

SMEAR SLIDE SUMMARY (%):

	3, 90 D
Texture:	
Silt	2
Clay	98
Composition:	
Quartz	9
Feldspar	1
Foraminifers	11
Calc. nannofossils	79

ORGANIC CARBON AND CARBONATE (%):

	2, 110
Organic carbon	–
Carbonate	95

SITE 608 HOLE CORE 13 CORED INTERVAL 112.6–122.2 m

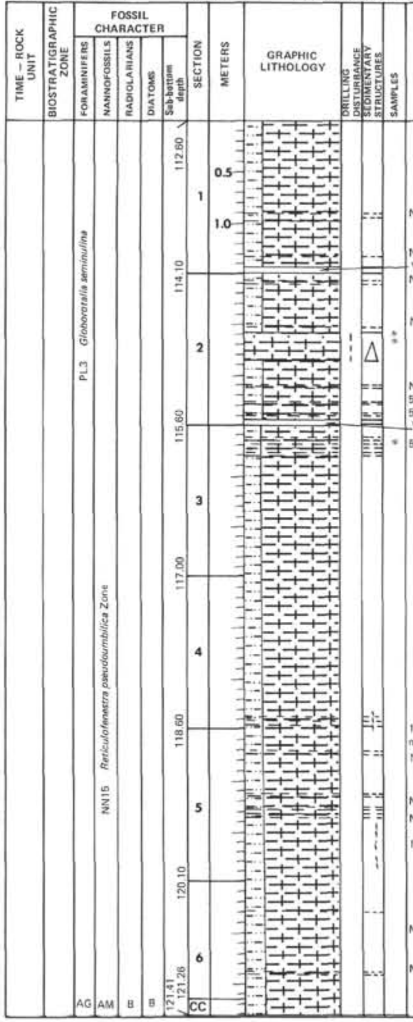

LITHOLOGIC DESCRIPTION

FORAMINIFERAL NANNOFOSSIL OOZE, white (N9) and very light gray (N8). Occasional layers and multiple laminations of light gray (N7), and mottles of gray (N5–6). Multiple green (5G 8/1) laminations 115.75 to 115.91 m.

Watery NANNOFOSSIL FORAMINIFERAL SAND 114.69–114.95 m. Sequence fines upward.

SMEAR SLIDE SUMMARY (%):

	2, 57 M	2, 61 M	3, 15 M
Composition:			
Quartz	15	5	15
Feldspar	–	–	TR
Heavy minerals	–	TR	10
Clay	–	–	5
Pyrite	10	–	–
Foraminifers	10	50	10
Calc. nannofossils	65	45	60

SITE 608 HOLE CORE 14 CORED INTERVAL 122.2–131.8 m

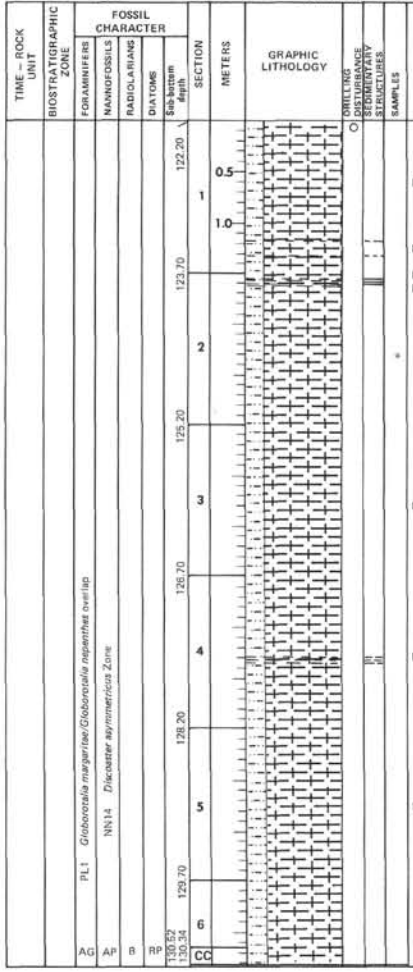

LITHOLOGIC DESCRIPTION

NANNOFOSSIL OOZE, white (N9), rare gray (N5–7) layers and laminae.

SMEAR SLIDE SUMMARY (%):

	2, 80 D
Composition:	
Quartz	23
Clay	2
Foraminifers	7
Calc. nannofossils	68

ORGANIC CARBON AND CARBONATE (%):

	2, 80
Organic carbon	–
Carbonate	96

SITE 608 HOLE CORE 15 CORED INTERVAL 131.8–141.4 m

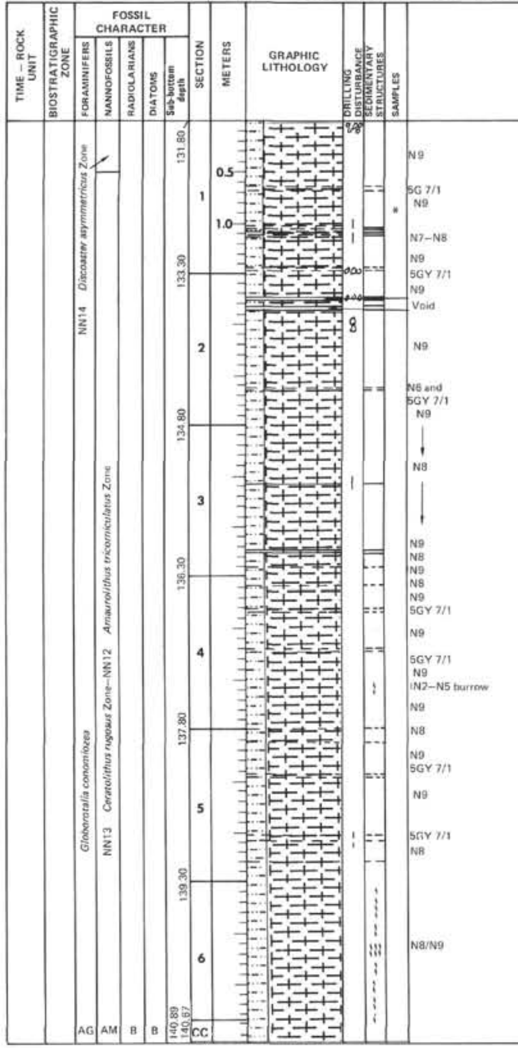

LITHOLOGIC DESCRIPTION

NANNOFOSSIL OOZE, mostly white (N9) with frequent layers of very light gray (N8). Occasional laminae of light gray (N7) and greenish gray (5G 7/1).

SMEAR SLIDE SUMMARY (%):

	1, 80
	D
Composition:	
Quartz	25
Clay	TR
Foraminifers	5
Calc. nannofossils	70

SITE 608 HOLE CORE 16 CORED INTERVAL 141.4–151.0 m

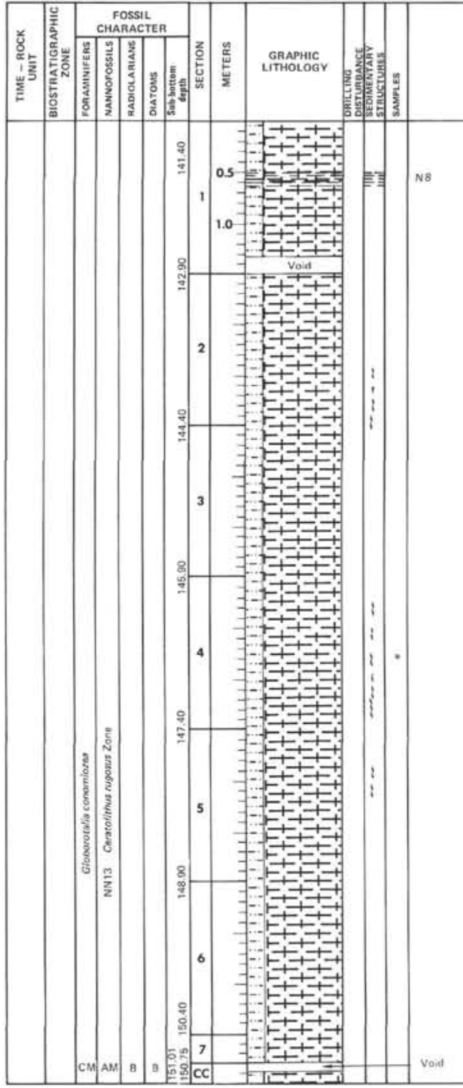

LITHOLOGIC DESCRIPTION

NANNOFOSSIL OOZE, white (N9) with multiple very light gray (N8) laminae 141.92–142.05 m. Burrow mottling throughout various shades of gray.

SMEAR SLIDE SUMMARY (%):

	4, 75
	D
Composition:	
Quartz	22
Clay	3
Foraminifers	8
Calc. nannofossils	67

ORGANIC CARBON AND CARBONATE (%):

	3, 75
Organic carbon	–
Carbonate	96

SITE 608 HOLE CORE 17 CORED INTERVAL 151.0–156.5 m

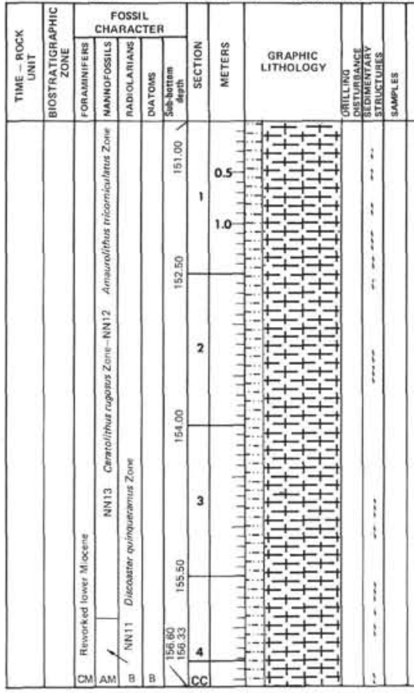

LITHOLOGIC DESCRIPTION

NANNOFOSSIL OOZE, white (N9) with burrow mottling of various shades of gray.

SITE 608 HOLE CORE 18 CORED INTERVAL 156.5–166.1 m

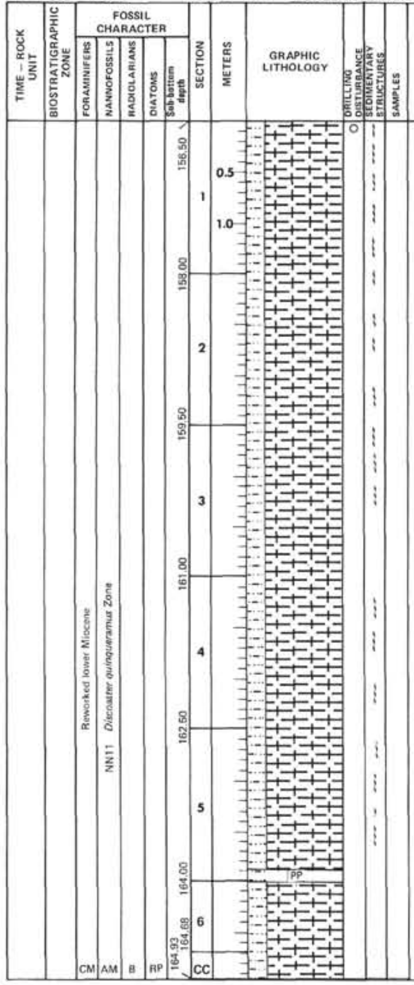

LITHOLOGIC DESCRIPTION

NANNOFOSSIL OOZE, white (N9) with occasional gray (N4–7) mottles.

SMEAR SLIDE SUMMARY (%):

	4, 90
Composition:	
Quartz	15
Heavy minerals	TR
Pyrite	TR
Foraminifers	2
Calc. nannofossils	83

ORGANIC CARBON AND CARBONATE (%):

	4, 90
Organic carbon	–
Carbonate	95

SITE 608 HOLE CORE 19 CORED INTERVAL 166.1–175.7 m

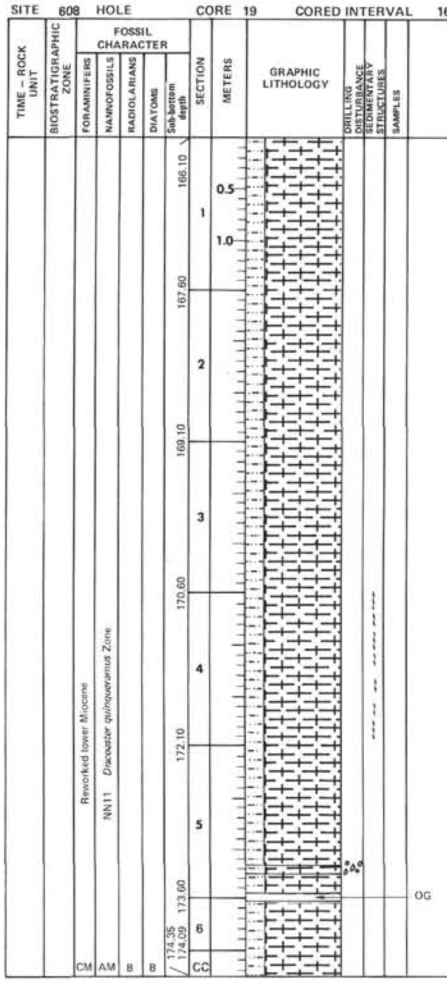

LITHOLOGIC DESCRIPTION

NANNOFOSSIL OOZE, white (N9). Burrow mottling evident 170.60–172.10 m.

NANNOFOSSIL CHALK, white (N9), brecciated, 172.25–172.32 m.

SITE 608 HOLE CORE 20 CORED INTERVAL 175.7–185.3 m

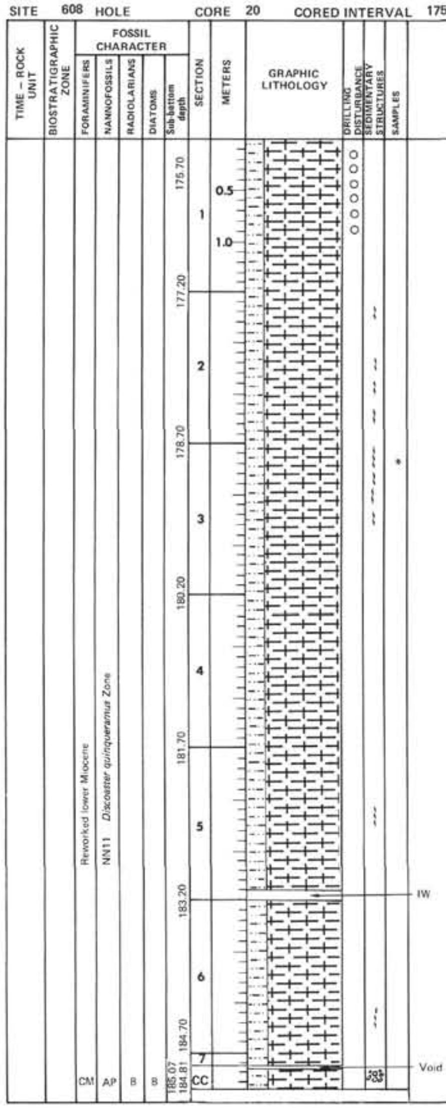

LITHOLOGIC DESCRIPTION

NANNOFOSSIL OOZE, white (N9).

SMEAR SLIDE SUMMARY (%):

	3, 20
Composition:	
Quartz	20
Heavy minerals	TR
Foraminifers	2
Calc. nannofossils	78

ORGANIC CARBON AND CARBONATE (%):

	3, 20
Organic carbon	–
Carbonate	93

SITE 608 HOLE CORE 21 CORED INTERVAL 185.3–194.9 m

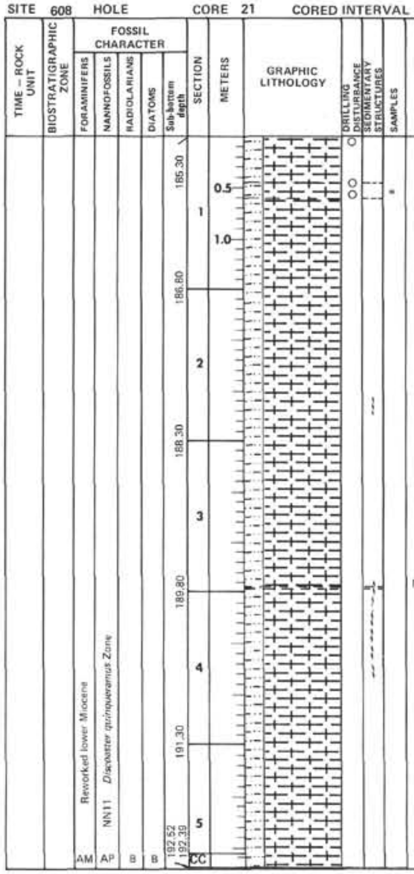

LITHOLOGIC DESCRIPTION

NANNOFOSSIL OOZE, white (N8)

FORAMINIFERAL NANNOFOSSIL OOZE, white (N9), 85.77–85.92 m.

SMEAR SLIDE SUMMARY (%):

	1, 57
	D
Composition:	
Quartz	15
Heavy minerals	TR
Foraminifers	15
Calc. nannofossils	70

N6

SITE 608 HOLE CORE 22 CORED INTERVAL 194.9–204.5 m

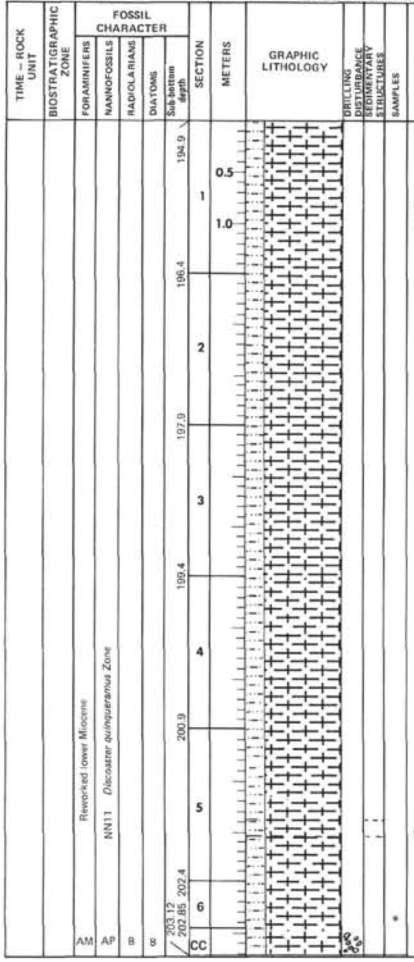

LITHOLOGIC DESCRIPTION

FORAMINIFERAL NANNOFOSSIL OOZE, white (N9) to very light gray (N8). Sediment firm, becoming chalky.

N9 to
N8

SMEAR SLIDE SUMMARY (%):

	6, 36
	D
Composition:	
Quartz	30
Feldspar	TR
Foraminifers	10
Calc. nannofossils	60

ORGANIC CARBON AND CARBONATE (%):

	6, 36
Organic carbon	–
Carbonate	92

N8

SITE 608 HOLE CORE 23 CORED INTERVAL 204.5–214.1 m

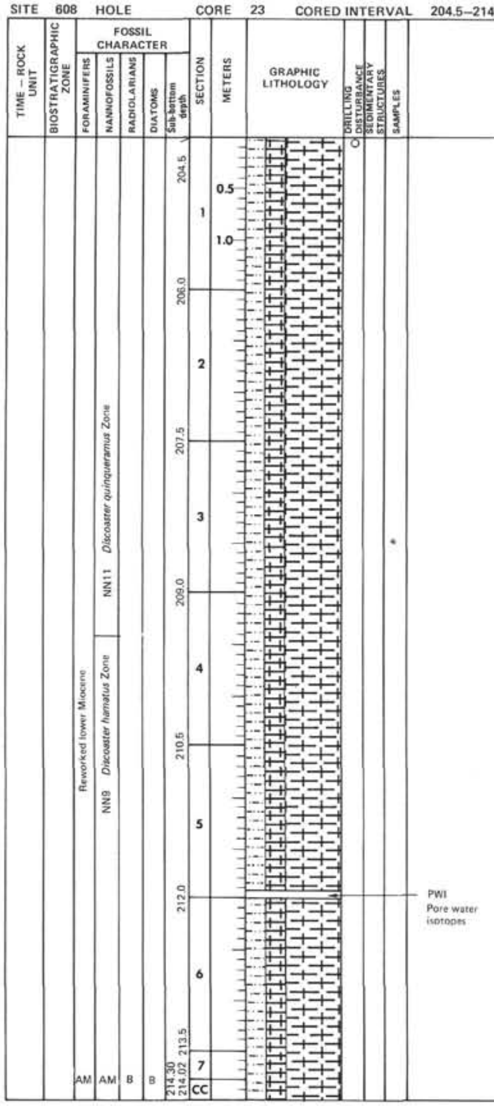

LITHOLOGIC DESCRIPTION

NANNOFOSSIL OOZE, white (N9) with occasional chalky intervals. Sediment stiffness increases noticeably below 212 m.

note: this core recovered >100%

SMEAR SLIDE SUMMARY (%):

	3, 96
	D
Composition:	
Quartz	30
Feldspar	1
Clay	5
Carbonate unspec.	1
Foraminifers	5
Calc. nannofossils	58

SITE 608 HOLE CORE 24 CORED INTERVAL 214.1–223.7 m

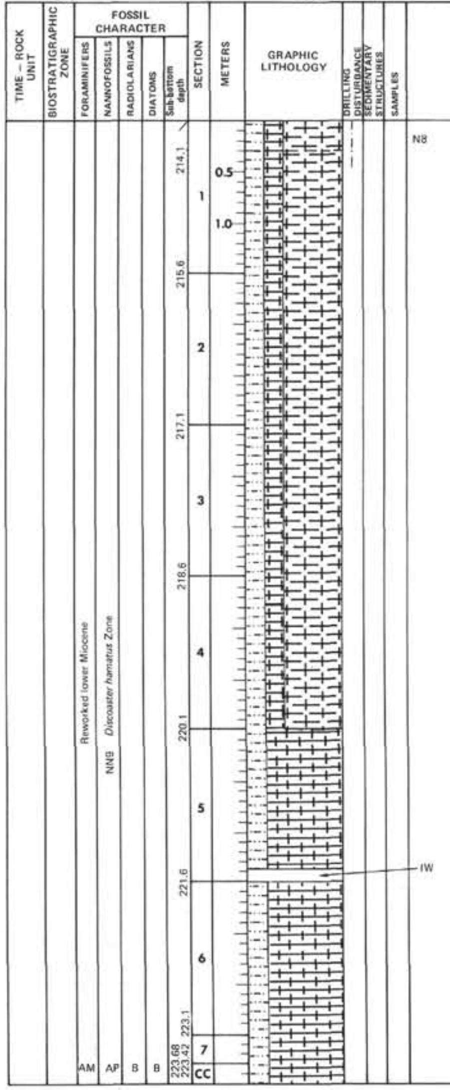

LITHOLOGIC DESCRIPTION

NANNOFOSSIL OOZE/CHALK, white (N9). This core changes from ~20% chalk at the top to mostly chalk by 220.1 m.

SMEAR SLIDE SUMMARY (%):

	1, 15
	D
Composition:	
Quartz	23
Feldspar	1
Clay	7
Carbonate unspec.	3
Foraminifers	4
Calc. nannofossils	62

ORGANIC CARBON AND CARBONATE (%):

	1, 15
Organic carbon	–
Carbonate	93

SITE 608 HOLE CORE 25 CORED INTERVAL 223.7–233.3 m

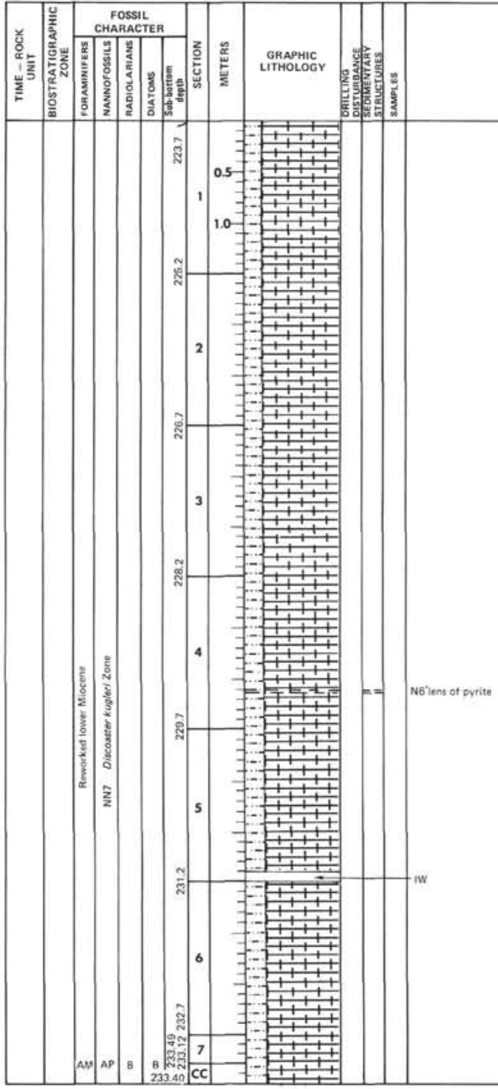

LITHOLOGIC DESCRIPTION

NANNOFOSSIL CHALK, white (N9).

Note: this core recovered 100%.

SMEAR SLIDE SUMMARY (%):

	1, 75
Composition:	
Quartz	22
Feldspar	1
Clay	6
Carbonate unspec.	3
Foraminifers	8
Calc. nannofossils	60

SITE 608 HOLE CORE 26 CORED INTERVAL 233.3–242.9 m

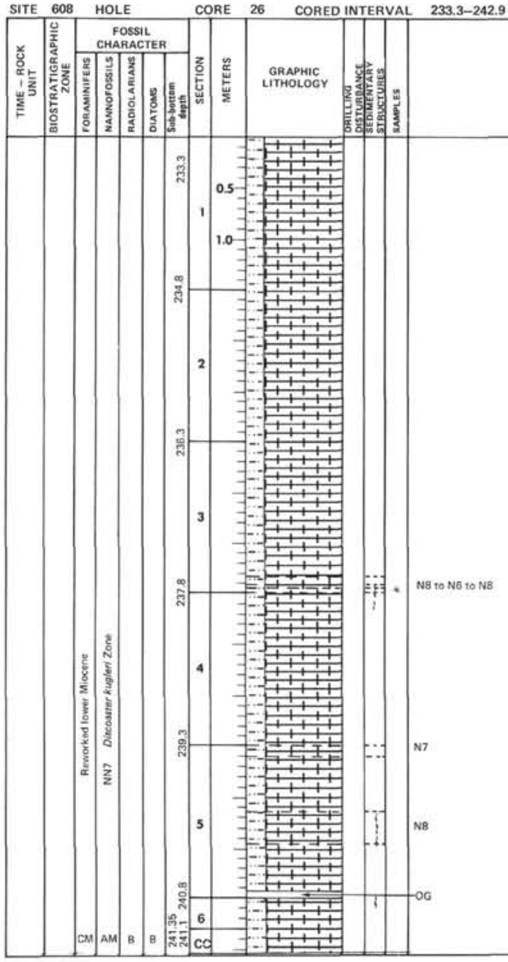

LITHOLOGIC DESCRIPTION

NANNOFOSSIL CHALK, white (N9).

Note: beginning at 237.8 m cores split with saw. Sediment frequently fractured but fractures appear natural because fracture faces darkened with pyrite.

SMEAR SLIDE SUMMARY (%):

	3, 143 M
Composition:	
Quartz	35
Feldspar	TR
Clay	8
Carbonate unspec.	2
Foraminifers	3
Calc. nannofossils	52

ORGANIC CARBON AND CARBONATE (%):

	3, 143
Organic carbon	–
Carbonate	80

SITE 608 HOLE CORE 27 CORED INTERVAL 242.9–252.5

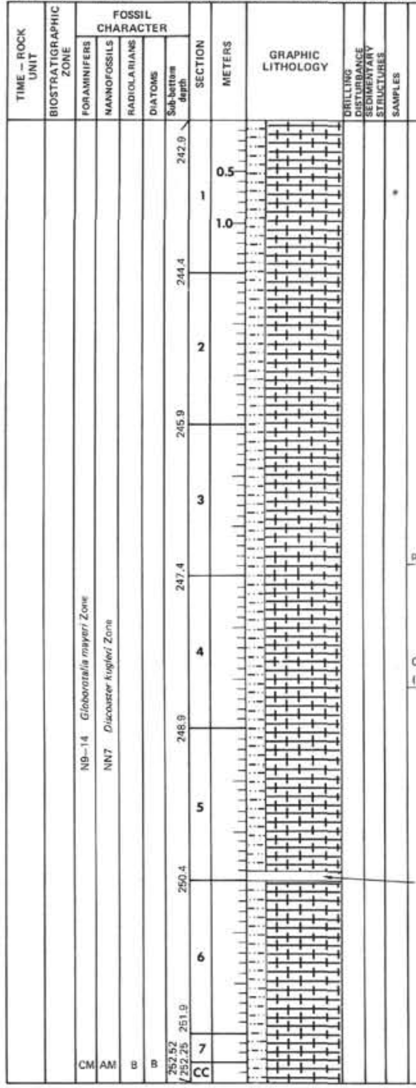

LITHOLOGIC DESCRIPTION

NANNOFOSSIL CHALK, white (N9)

SMEAR SLIDE SUMMARY (%):

	1, 66
	D
Composition:	
Quartz	9
Feldspar	1
Carbonate unspec.	1
Foraminifers	4
Calc. nannofossils	85

ORGANIC CARBON AND CARBONATE (%):

	2, 65
Organic carbon	–
Carbonate	93

patch of N5

$CaCO_3$ nodules (~2mm diameter)

PWI

SITE 608 HOLE CORE 28 CORED INTERVAL 252.5–262.1 m

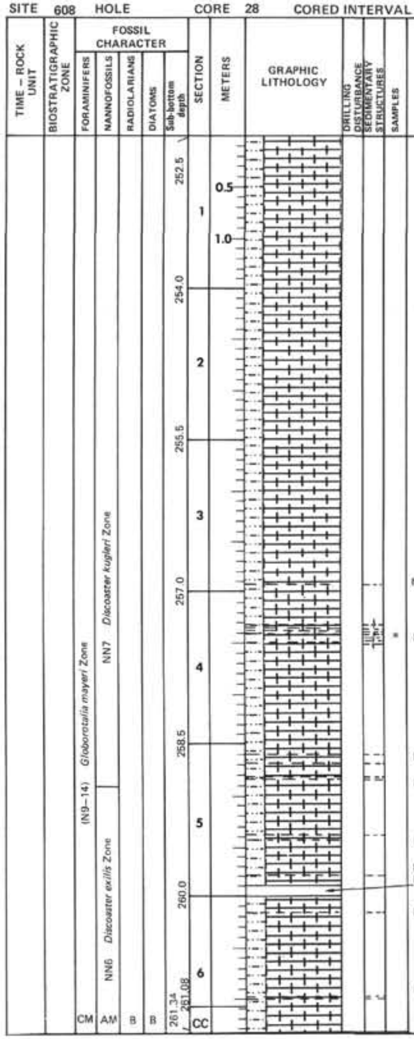

LITHOLOGIC DESCRIPTION

NANNOFOSSIL CHALK, white (N9) with gray (N5 to N8) laminae below 256.9 m.

SMEAR SLIDE SUMMARY (%):

	4, 42
	M
Composition:	
Quartz	20
Heavy minerals	TR
Volcanic glass	TR
Pyrite	1
Carbonate unspec.	1
Foraminifers	5
Calc. nannofossils	73
Sponge spicules	TR

N5

N8 to 5G 6/1

N8

N8

N8

N8
PP sample

N7

N7

SITE 608 HOLE CORE 29 CORED INTERVAL 262.1–271.7 m

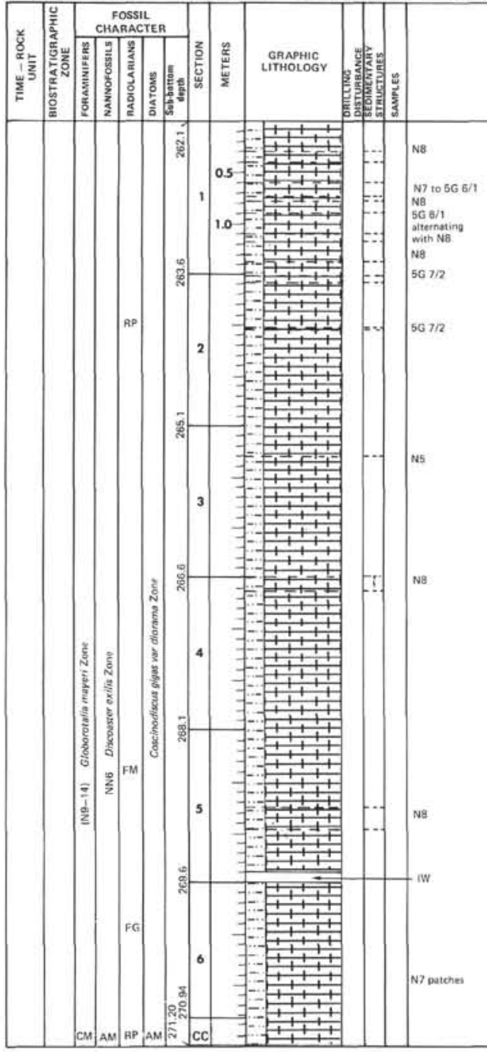

LITHOLOGIC DESCRIPTION

NANNOFOSSIL CHALK, white (N9) with several layers of gray (N5–8). Interval 262.7 to 263.5 m marked by alternating laminae of very light gray (N8), light gray (N7), and greenish gray (5G 6/1). Pale green (5G 7/2) laminae at 263.6 to 264.3 m.

SMEAR SLIDE SUMMARY (%):

	1, 65
	D
Composition:	
Quartz	30
Feldspar	TR
Carbonate unspec.	1
Foraminifers	4
Calc. nannofossils	65

ORGANIC CARBON AND CARBONATE (%):

	1, 115
Organic carbon	–
Carbonate	95

SITE 608 HOLE CORE 30 CORED INTERVAL 271.7–281.3 m

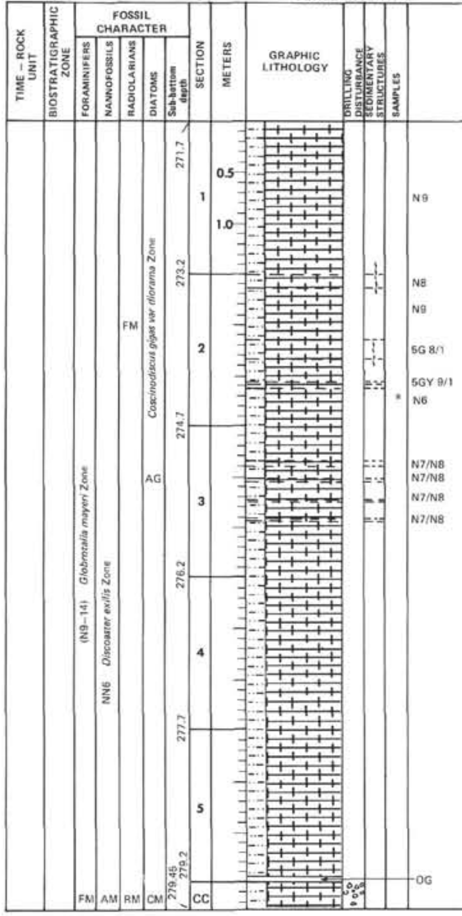

LITHOLOGIC DESCRIPTION

NANNOFOSSIL CHALK, 271.7 to 273.2 m, white (N9). Dominantly greenish white (5GY 9/1) at 274.2 to 279.45 m.

Laminae of gray (N6–8) and light green gray (5GY 8/1) at 273.2 to 275.7 m.

SMEAR SLIDE SUMMARY (%):

	1, 106
Composition:	
Quartz	23
Feldspar	TR
Foraminifers	9
Calc. nannofossils	68

SITE 608 HOLE CORE 31 CORED INTERVAL 281.3–290.9 m

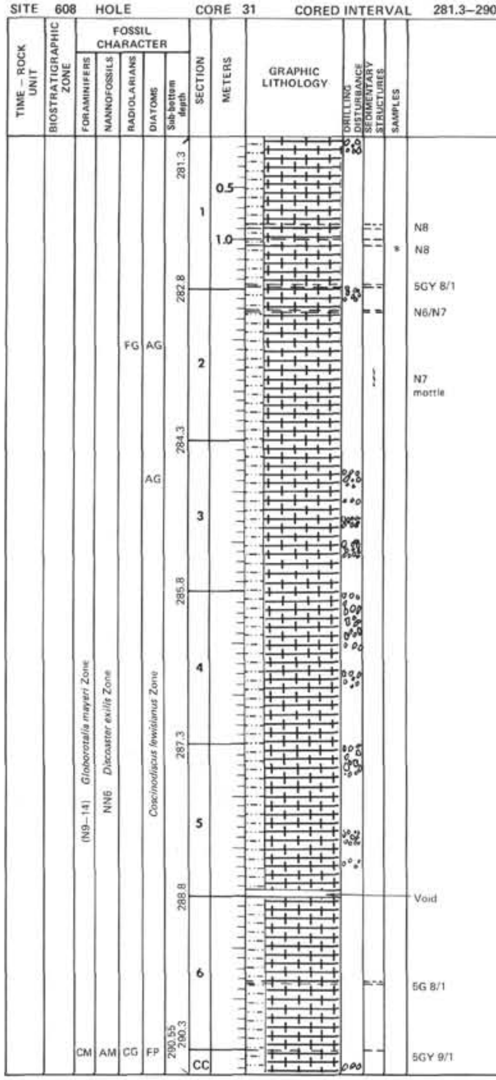

LITHOLOGIC DESCRIPTION

White (N9) NANNOFOSSIL CHALK. Occasional laminae of gray (N6–8) and light greenish gray (5GY 8/1 and 5G 8/1). Greenish white (5GY 9/1) below 290.3 m.

Sediment frequently brecciated.

SMEAR SLIDE SUMMARY (%):

	1, 106 D
Composition:	
Quartz	5
Foraminifers	5
Calc. nannofossils	90

ORGANIC CARBON AND CARBONATE (%):

Organic carbon	–
Carbonate	92

SITE 608 HOLE CORE 32 CORED INTERVAL 290.9–300.5 m

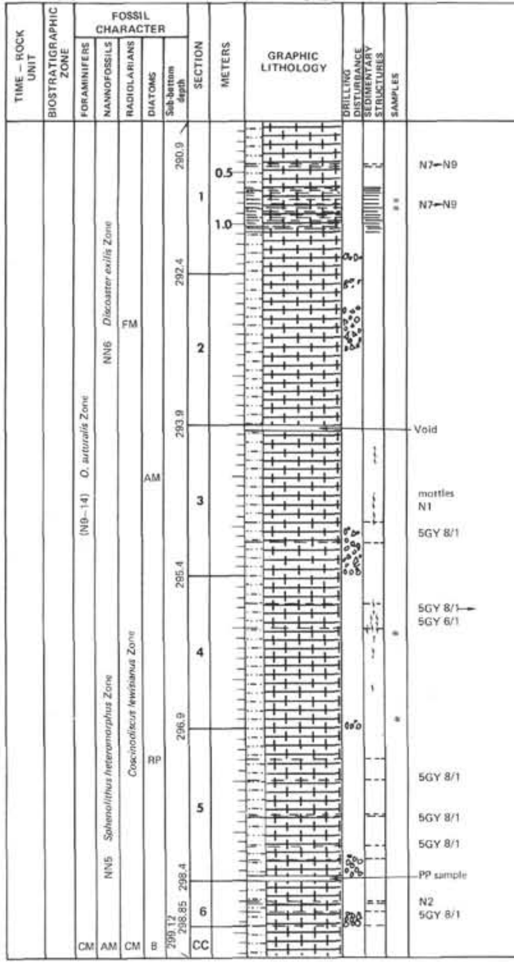

LITHOLOGIC DESCRIPTION

White (N9) NANNOFOSSIL CHALK. Pale green (5GY 8/1) intervals common below 294.8 m. Sequence of light gray (N7), white (N9), and very light gray (N8) laminae between 291.3 and 292.0 m.

White (N9) NANNOFOSSIL OOZE, 293.96 to 294.77 m.

SMEAR SLIDE SUMMARY (%):

	1, 78 M	1, 79 M	4, 50 D	4, 133 D
Composition:				
Quartz	5	10	10	15
Feldspar	–	–	TR	–
Pyrite	–	–	–	TR
Foraminifers	5	5	5	5
Calc. nannofossils	90	85	80	80
Radiolarians	–	–	TR	–
Sponge spicules	–	–	TR	–

SITE 608 HOLE CORE 33 CORED INTERVAL 300.5–310.1 m

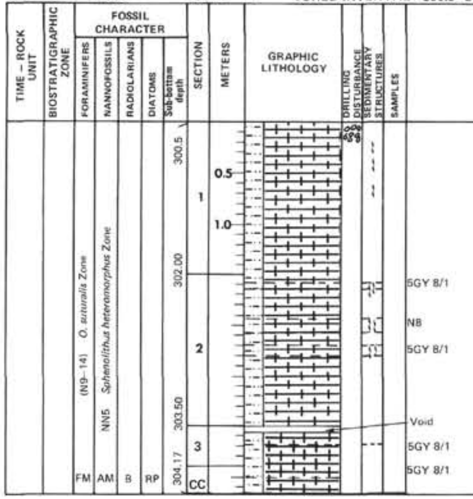

LITHOLOGIC DESCRIPTION

White (N9) NANNOFOSSIL CHALK. Several layers of very light green (5GY 8/1).

SMEAR SLIDE SUMMARY (%):

	1, 143
	D
Composition:	
Quartz	20
Clay	TR
Volcanic glass	5
Carbonate unspec.	40
Foraminifers	2
Calc. nannofossils	33

SITE 608 HOLE CORE 34 CORED INTERVAL 310.1–319.7 m

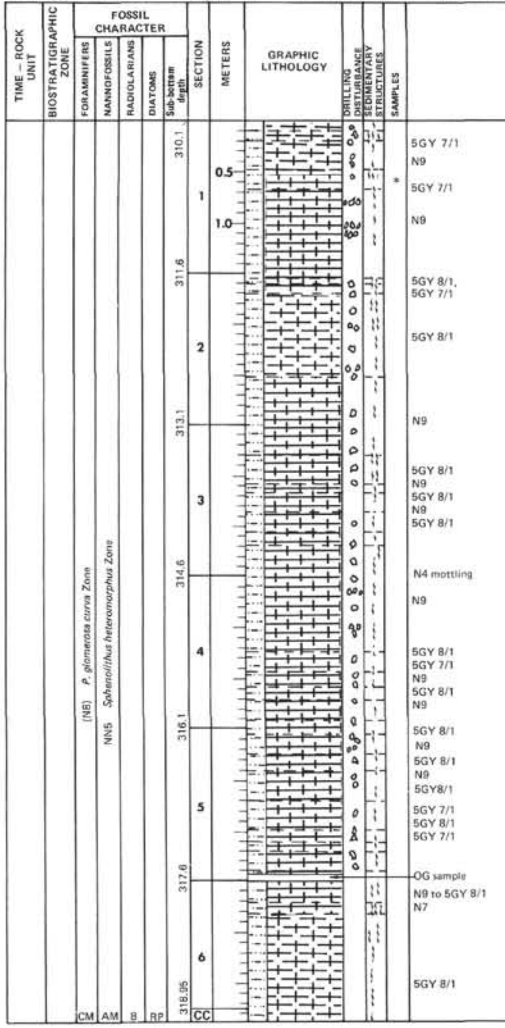

LITHOLOGIC DESCRIPTION

NANNOFOSSIL CHALK, dominantly white (N9) at 310.1 to 315.3 m, with occasional light greenish gray (5GY 8/1) intervals. Dominantly light greenish gray (5GY 8/1) with occasional white (N9) below 315.3 m.

Zoophycos burrows frequent throughout core.

SMEAR SLIDE SUMMARY (%):

	1, 54
	D
Composition:	
Quartz	19
Volcanic glass	2
Carbonate unspec.	TR
Foraminifers	1
Calc. nannofossils	78

ORGANIC CARBON AND CARBONATE (%):

	1, 53
Organic carbon	–
Carbonate	86

SITE 608 HOLE CORE 35 CORED INTERVAL 319.7–329.3 m

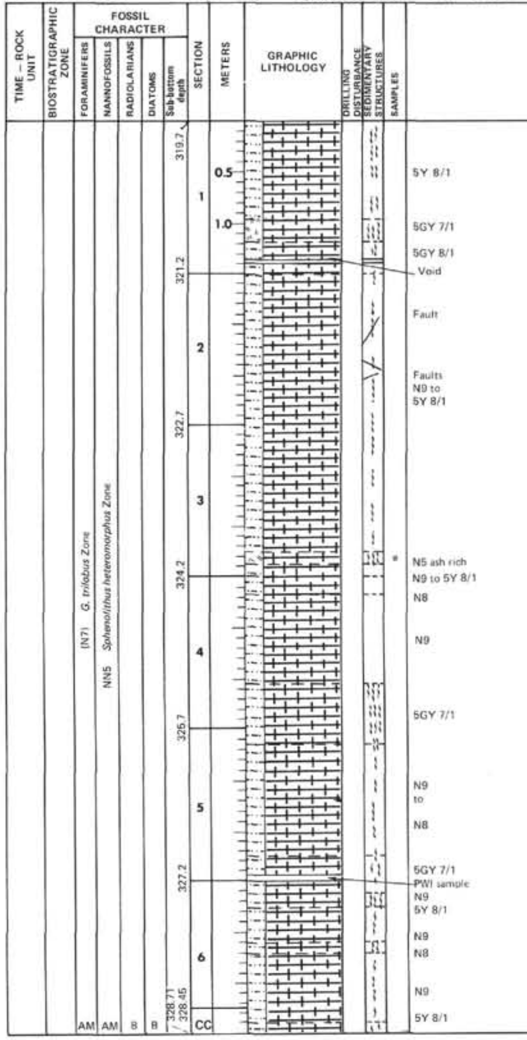

LITHOLOGIC DESCRIPTION

FORAMINIFERAL NANNOFOSSIL CHALK, mostly white (N9) to yellowish gray (5Y 8/1), light greenish gray (5GY 8/1), and light gray (N8, 5Y 7/1). Occasional *Zoophycos* burrows, especially in Section 1.

Volcanic ash and glass common ~320.7 and ~324.0 m.

Microfaults and slickensides evident, 321.6 to 322.2 m.

SMEAR SLIDE SUMMARY (%):

	3, 140 M
Composition:	
Quartz	15
Clay	TR
Volcanic glass	15
Foraminifers	1
Calc. nannofossils	69

ORGANIC CARBON AND CARBONATE (%):

	3,130
Organic carbon	—
Carbonate	69

SITE 608 HOLE CORE 36 CORED INTERVAL 329.3–338.9 m

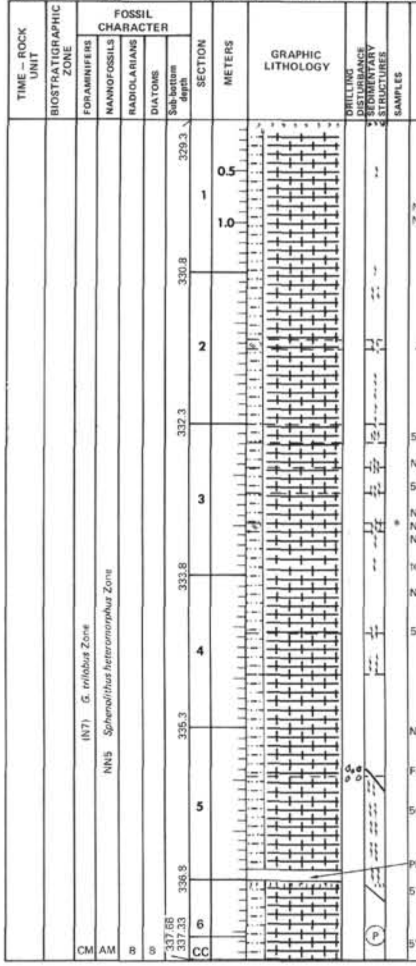

LITHOLOGIC DESCRIPTION

FORAMINIFERAL NANNOFOSSIL CHALK, white (N9) to various shades of gray (N8, 5Y 8/1, 5GY 8/1).

Microfault at ~335.8 and 336.9 m. Two intervals where burrows show subhorizontal streaming (~332.8 and ~337.0 m). At upper interval *Zoophycos* burrows crosscut subhorizonational burrows.

Volcanic ash present ~331.5 and ~333.3 m.

SMEAR SLIDE SUMMARY (%):

	3, 95 D	2, 70 M
Composition:		
Quartz	10	18
Feldspar	TR	–
Clay	–	TR
Volcanic glass	TR	12
Carbonate unspec.	6	5
Foraminifers	17	5
Calc. nannofossils	67	60

SITE 608 HOLE CORE 37 CORED INTERVAL 338.9–348.5 m

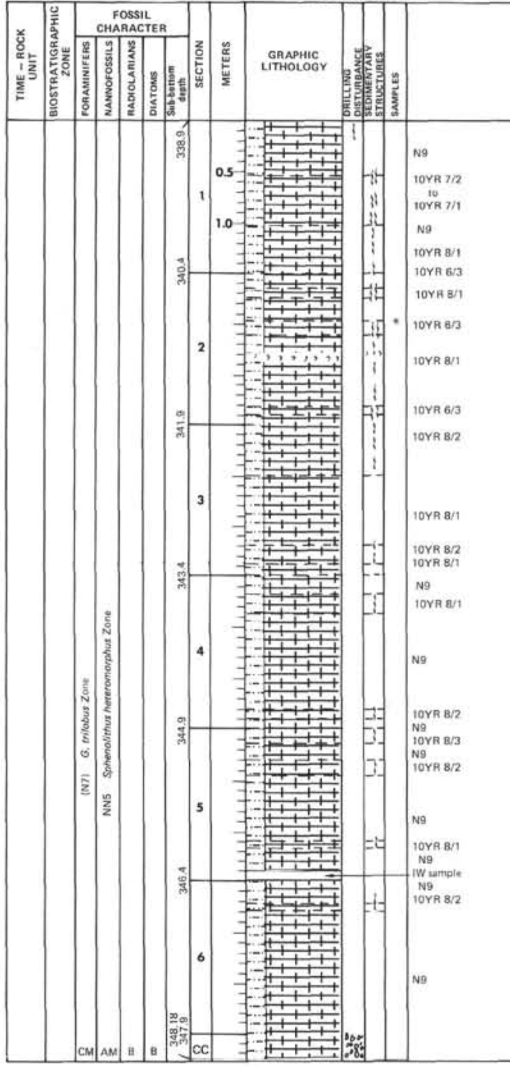

LITHOLOGIC DESCRIPTION

FORAMINIFERAL NANNOFOSSIL CHALK, white (N9 and 10YR 8/1, 10YR 8/2), light gray (10YR 7/1–10YR 7/2) and pale brown (10YR 6/3).

SMEAR SLIDE SUMMARY (%):

	2, 54 D
Composition:	
Quartz	20
Feldspar	TR
Volcanic glass	TR
Carbonate unspec.	3
Foraminifers	13
Calc. nannofossils	64

ORGANIC CARBON AND CARBONATE (%):

	2, 54
Organic carbon	–
Carbonate	79

SITE 608 HOLE CORE 38 CORED INTERVAL 348.5–358.1 m

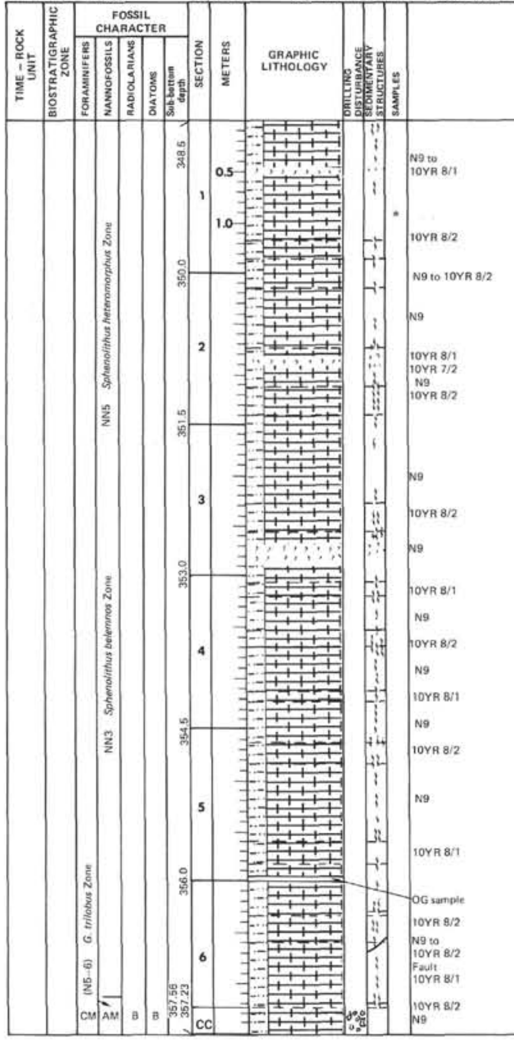

LITHOLOGIC DESCRIPTION

White (N9) to very faint tan (10YR 8/1, 8/2) FORAMINIFERAL NANNOFOSSIL CHALK.

Fault with slickensides at 356.7 m.

SMEAR SLIDE SUMMARY (%):

	1, 85 D
Composition:	
Quartz	15
Feldspar	1
Volcanic glass	TR
Carbonate unspec.	2
Foraminifers	12
Calc. nannofossils	70

SITE 608 HOLE CORE 39 CORED INTERVAL 358.1–367.7 m

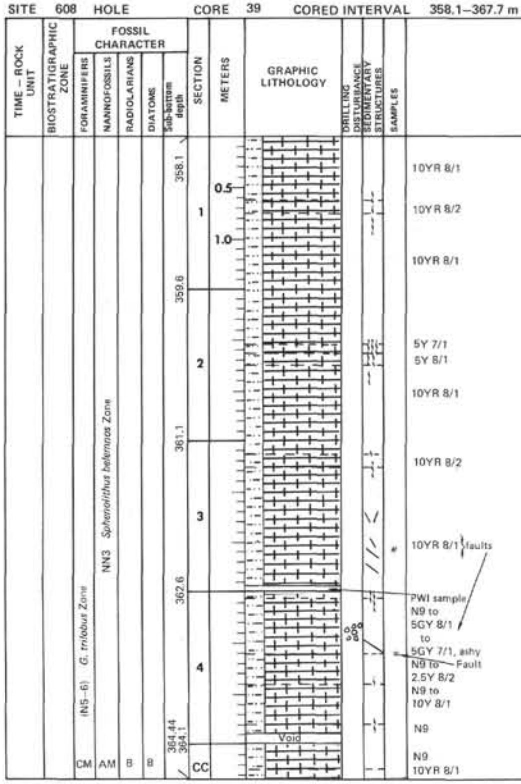

LITHOLOGIC DESCRIPTION

FORAMINIFERAL NANNOFOSSIL CHALK, mostly white (N9) to very faint tan (10YR 8/1, 10YR 8/2).

Sediment faulted: 359.5 m, 361.8 to 362.4 m, 363.2 m.

SMEAR SLIDE SUMMARY (%):

	3, 49 D	4, 58 M
Composition:		
Quartz	32	5
Feldspar	1	–
Volcanic glass	–	2
Carbonate unspec.	1	–
Foraminifers	3	10
Calc. nannofossils	65	83

ORGANIC CARBON AND CARBONATE (%)

	3, 49
Organic carbon	–
Carbonate	91

SITE 608 HOLE CORE 40 CORED INTERVAL 367.7–377.3 m

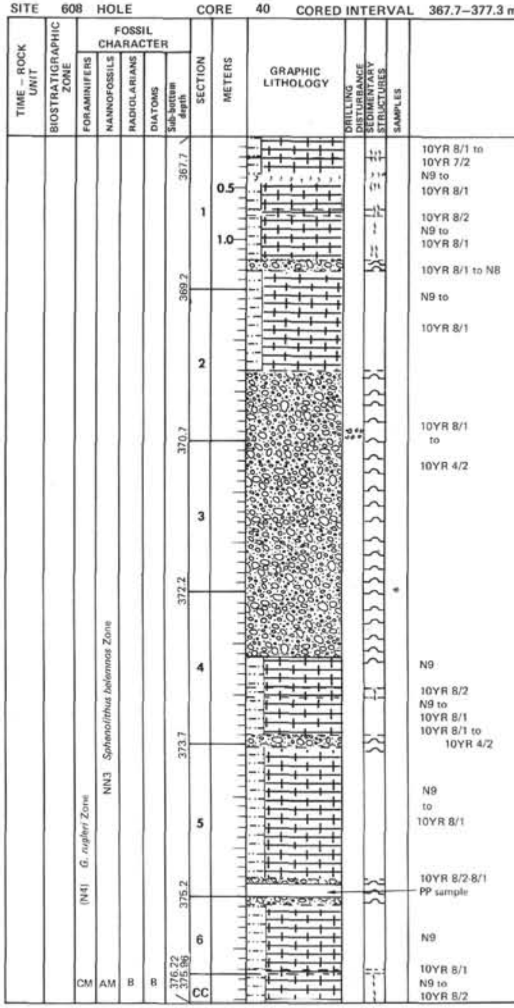

LITHOLOGIC DESCRIPTION

FORAMINIFERAL NANNOFOSSIL CHALK, mostly white *(N9) to very faint tan (10YR 8/1 to 10YR 8/2).*

CHALKY CONGLOMERATE, mixed layers of very light brown (10YR 8/1) and brown (7.5YR 4/2). Matrix is generally darker and clasts are lighter. Conglomerate intervals appear 369.91 to 370.01 m, 370.02 to 372.83 m, 373.60 to 373.74 m, and 375.05 to 375.29 m. Clasts are sub-angular to rounded chalk, volcanic-rich chalk and marly chalk. Some clasts have truncated burrows and are similar to overlying lithology.

SMEAR SLIDE SUMMARY (%):

	3, 147 D
Composition:	
Quartz	27
Feldspar	TR
Carbonate unspec.	1
Calc. nannofossils	72

SITE 608 HOLE CORE 41 CORED INTERVAL 377.3–386.9 m

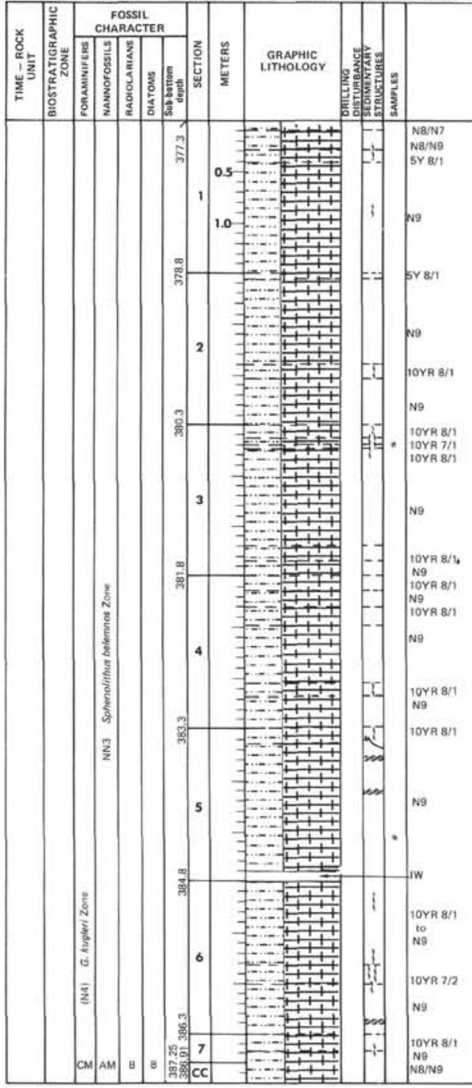

LITHOLOGIC DESCRIPTION

MARLY NANNOFOSSIL CHALK, mostly alternating white (N9) and very faint tan (10YR 8/1).

Sharp, angular contact at 383.4 m.

Note: this core 100% recovery.

SMEAR SLIDE SUMMARY (%):

	3, 18	5, 106
	D	D
Composition:		
Quartz	45	53
Feldspar	TR	TR
Volcanic glass	TR	–
Carbonate unspec.	1	TR
Foraminifers	–	2
Calc. nannofossils	54	47

ORGANIC CARBON AND CARBONATE (%):

	3, 16
Organic carbon	–
Carbonate	81

SITE 608 HOLE CORE 42 CORED INTERVAL 386.9–396.5 m

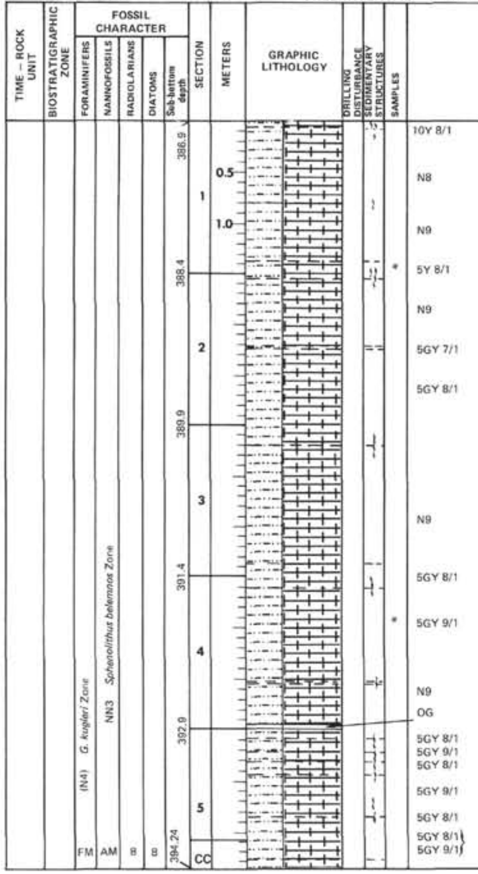

LITHOLOGIC DESCRIPTION

MARLY NANNOFOSSIL CHALK, mostly white (N9), light greenish gray (5GY 8/1, 5GY 9/1).

SMEAR SLIDE SUMMARY (%):

	1, 140	4, 40
	D	D
Composition:		
Quartz	46	42
Volcanic glass	TR	TR
Carbonate unspec.	3	TR
Foraminifers	1	–
Calc. nannofossils	49	58

SITE 608 HOLE CORE 43 CORED INTERVAL 396.5–406.1 m

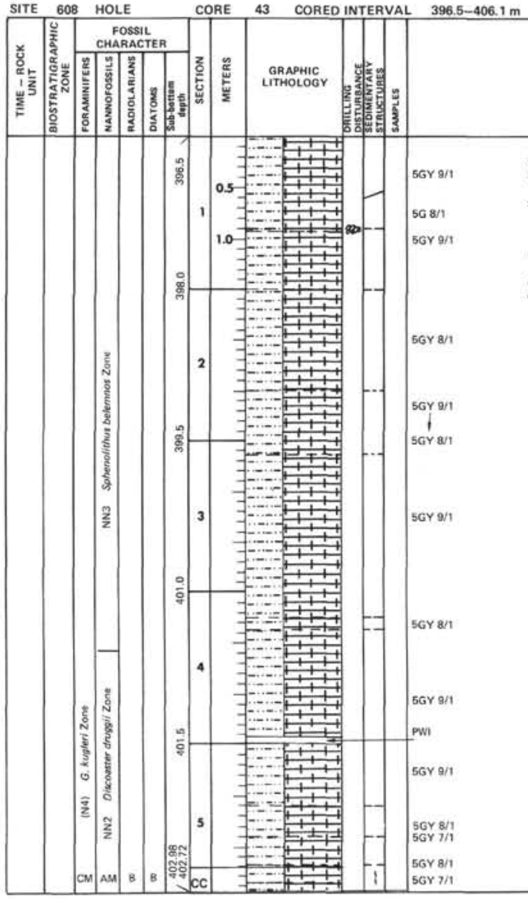

LITHOLOGIC DESCRIPTION

Greenish white (5GY 9/1) and light greenish gray (5GY 8/1) MARLY NANNOFOSSIL CHALK.

Slickensides along fracture at 397.0 to 397.1 m.

ORGANIC CARBON AND CARBONATE (%):

	3, 12
Organic carbon	–
Carbonate	82

SITE 608 HOLE CORE 44 CORED INTERVAL 406.1–415.7 m

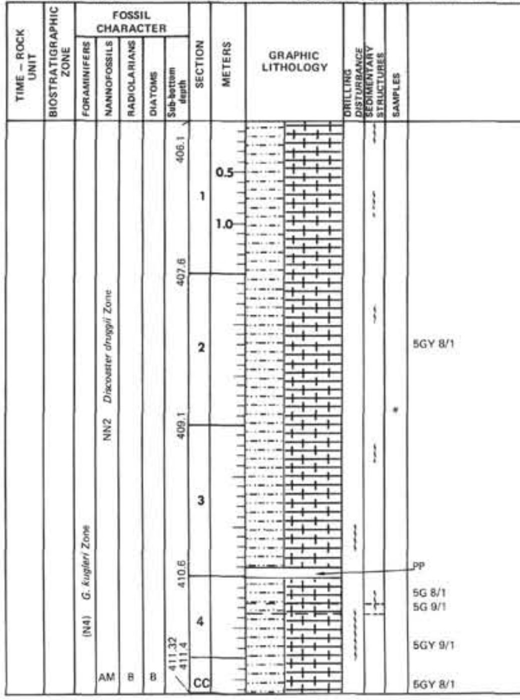

LITHOLOGIC DESCRIPTION

MARLY NANNOFOSSIL CHALK, mostly light greenish gray (5GY 8/1).

SMEAR SLIDE SUMMARY (%):

	2, 130
	D
Composition:	
Quartz	28
Carbonate	4
Foraminifers	2
Calc. nannofossils	66

SITE 608 HOLE CORE 45 CORED INTERVAL 415.7–425.3 m

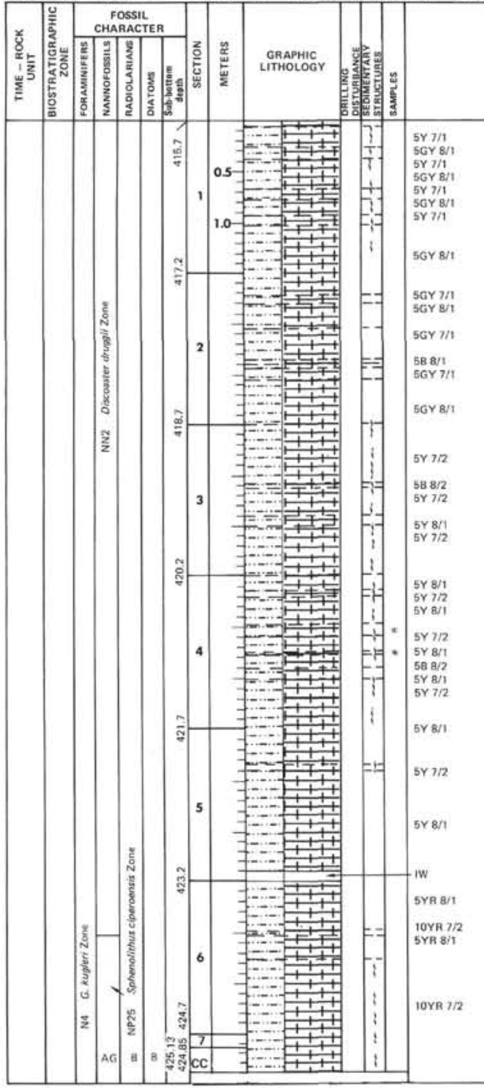

LITHOLOGIC DESCRIPTION

MARLY NANNOFOSSIL CHALK, dominantly light grayish green (5GY 8/1), pinkish gray (5YR 8/1), light tannish gray (10YR 7/2), light gray (5Y 7/2) and yellowish gray (5Y 8/1).

SMEAR SLIDE SUMMARY (%):

	4, 54	4, 77
	D	M
Composition:		
Quartz	45	30
Feldspar	1	1
Carbonate unspec.	6	7
Foraminifers	TR	TR
Calc. nannofossils	48	62

ORGANIC CARBON AND CARBONATE (%):

	4, 54
Organic carbon	–
Carbonate	78

SITE 608 HOLE CORE 46 CORED INTERVAL 425.3–434.9 m

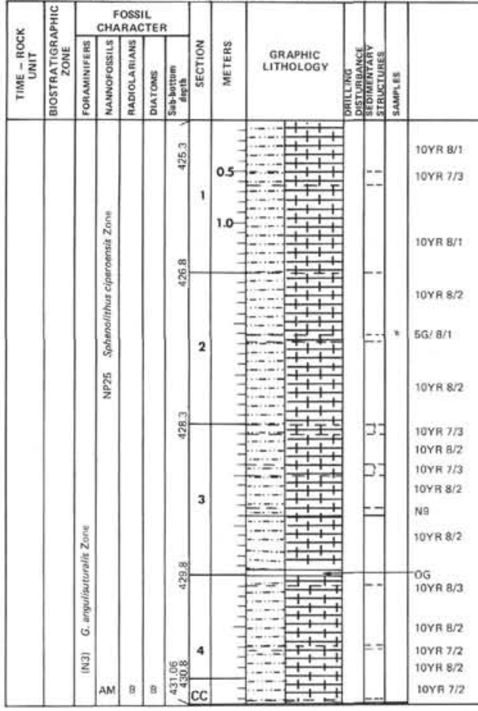

LITHOLOGIC DESCRIPTION

MARLY NANNOFOSSIL CHALK, tannish white (10YR 8/1, 10YR 8/2) and light gray (10YR 7/2) to very pale brown (10YR 7/3)

SMEAR SLIDE SUMMARY (%):

	2, 64
	M
Composition:	
Quartz	35
Feldspar	TR
Carbonate unspec.	5
Foraminifers	1
Calc. nannofossils	59

ORGANIC CARBON AND CARBONATE (%):

	1, 65
Organic carbon	–
Carbonate	84

SITE 608 HOLE CORE 47 CORED INTERVAL 434.9–444.5 m

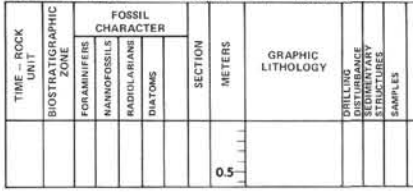

LITHOLOGIC DESCRIPTION

Total recovery: 1 cm MARLY NANNOFOSSIL CHALK

SITE 608 HOLE CORE 48 CORED INTERVAL 444.5–454.1 m

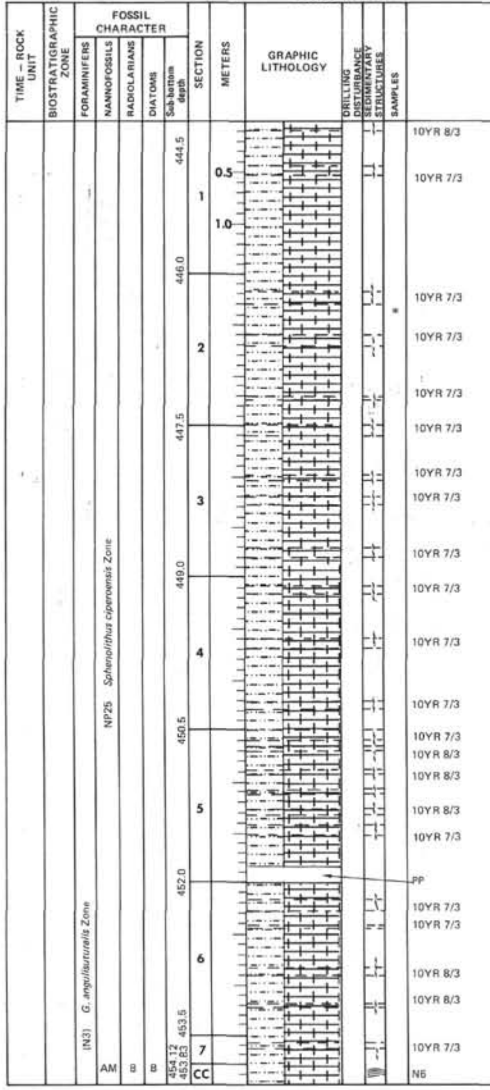

LITHOLOGIC DESCRIPTION

MARLY NANNOFOSSIL CHALK, mostly tannish white (10YR 8/2) alternating with layers of very pale brown (10YR 7/3). Below 450.6 m alternating layers are lighter (10YR 8/3).

Burrow mottles become progressively flattened in this core. By 453.6 m they show first signs of "smearing". Filamentous, wavy bedding structure at ~453.9 m.

SMEAR SLIDE SUMMARY (%):

	2, 30
	D
Composition:	
Quartz	28
Feldspar	TR
Carbonate unspec.	2
Foraminifers	1
Calc. nannofossils	69

ORGANIC CARBON AND CARBONATE (%):

	1, 65
Organic carbon	–
Carbonate	83

SITE 608 HOLE CORE 49 CORED INTERVAL 454.1–461.7 m

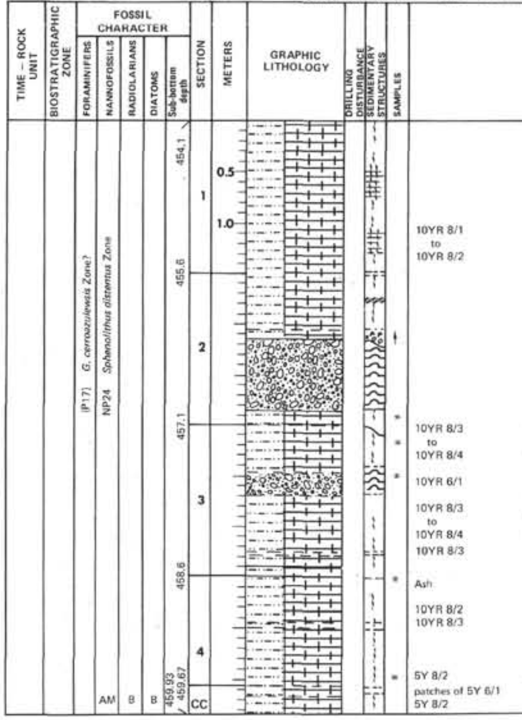

LITHOLOGIC DESCRIPTION

MARLY NANNOFOSSIL CHALK, white (10YR 8/1–10YR 8/2) and very pale brown (10YR 8/3–10YR 8/4). From 455.6 to 456.15 m chalk has numerous sand to fine gravel sized clasts of dispersed volcanic ash.

VOLCANIC ASH-BEARING MARLY CHALK CONGLOMERATE, 456.15 to 456.94 m and 457.58 to 457.78 m. Interval 456.15 to 456.25 m sequence fines upward. Upper conglomerate bounded by sharp contacts. Clasts are chalk, up to 3 cm across, subangular to (predominantly) rounded.

SMEAR SLIDE SUMMARY (%):

	2, 136	3, 20	3, 50	4, 3	4, 95
	D	D	M	M	D
Composition:					
Quartz	10	22	15	27	13
Feldspar	5	TR	–	2	2
Clay	20	–	–	–	18
Volcanic glass	–	–	10	7	2
Carbonate unspec.	5	2	20	3	15
Foraminifers	–	2	5	2	–
Calc. nannofossils	60	74	50	59	50

ORGANIC CARBON AND CARBONATE (%):

	2, 65
Organic carbon	–
Carbonate	90

SITE 608 HOLE CORE 50 CORED INTERVAL 461.7–467.3 m

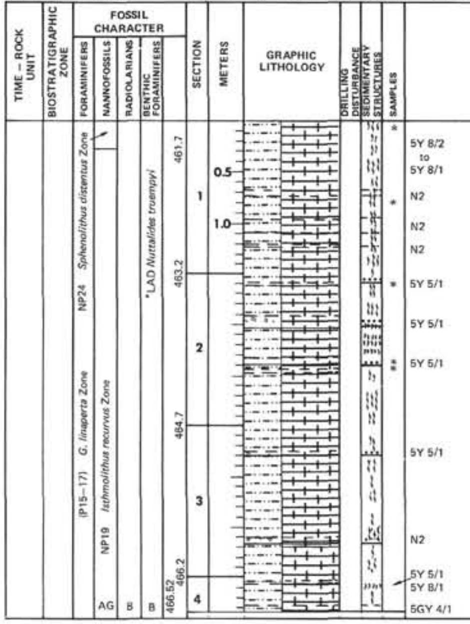

LITHOLOGIC DESCRIPTION

Yellowish white (5Y 8/1) MARLY NANNOFOSSIL CHALK with beds of very dark gray (N2) and dark green (5Y 5/1) VOLCANICLASTIC NANNOFOSSIL CHALK and GLASSY TUFF.

SMEAR SLIDE SUMMARY (%):

	1, 72 D	1, 10 D	2, 10 M	2, 87 M	2, 89 M
Composition:					
Quartz	10	13	30	15	10
Feldspar	5	2	5	–	5
Heavy minerals	TR	–	–	–	–
Clay	5	18	25	35	35
Volcanic glass	25	2	20	35	35
Carbonate unspec.	–	15	5	10	10
Foraminifers	5	–	–	–	–
Calc. nannofossils	50	50	15	5	5
Shell fragments	–	–	–	TR	TR

SITE 608 HOLE CORE 51 CORED INTERVAL 467.3–473.3 m

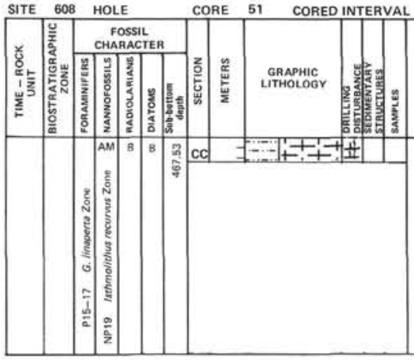

LITHOLOGIC DESCRIPTION

MARLY NANNOFOSSIL CHALK, pale green/gray (5GY 8/1). Fragments of chalk bedded in ooze.

SITE 608 HOLE CORE 52 CORED INTERVAL 473.3–482.9 m

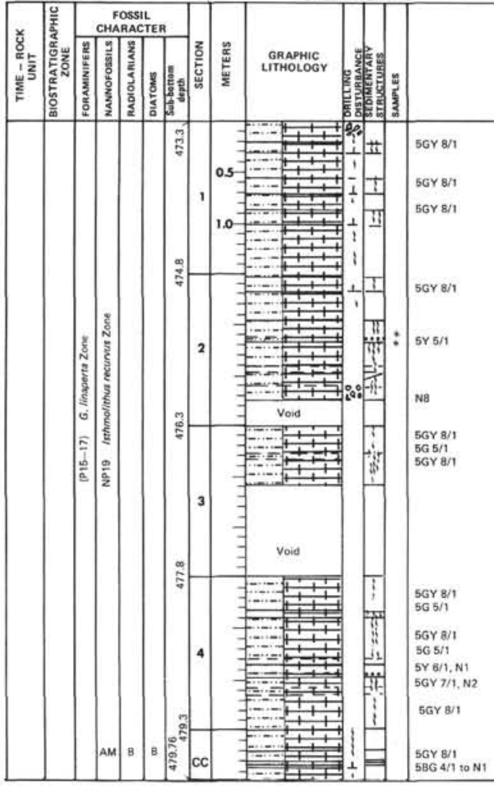

LITHOLOGIC DESCRIPTION

MARLY NANNOFOSSIL CHALK, dominantly light greenish gray (5GY 8/1). Soft sediment of mixed lithology extensively flowed-in around blocks of chalk. Blocks commonly broken by faulting; well-developed slickensides occur at 475.8 and 478.1 to 478.2 m.

Dark gray (5Y 5/1) and dark green (5G 5/1) layers are frequent. At least two appear graded (475.4 and 478.7 m). Uppermost is volcanic glass bearing.

SMEAR SLIDE SUMMARY (%):

	2, 63 M	2, 64 M
Composition:		
Quartz	15	20
Feldspar	15	20
Heavy minerals	–	TR
Clay	20	20
Volcanic glass	5	5
Carbonate unspec.	15	15
Calc. nannofossils	30	20

ORGANIC CARBON AND CARBONATE (%):

	4, 70
Organic carbon	–
Carbonate	81

SITE 608 HOLE CORE 53 CORED INTERVAL 482.9–492.5 m

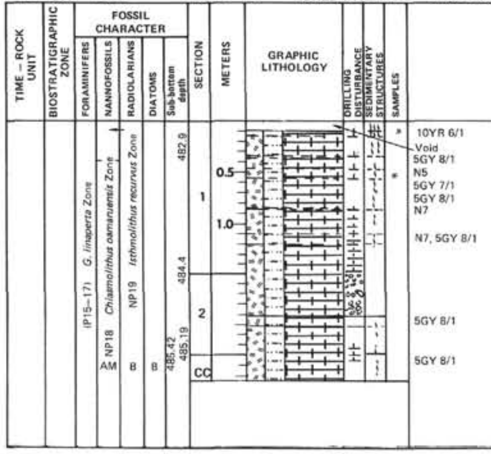

LITHOLOGIC DESCRIPTION

VOLCANIC GLASS BEARING MARLY NANNOFOSSIL CHALK, mostly light greenish gray (5GY 8/1) with occasional layers of darker gray (N5, N7, 10YR 6/1, 5GY 7/1). Section fragmented by drilling.

SMEAR SLIDE SUMMARY (%):

	1, 8 D	1, 52
Composition:		
Quartz	20	5
Heavy minerals	–	TR
Clay	15	5
Volcanic glass	10	20
Carbonate unspec.	20	5
Foraminifers	–	TR
Calc. nannofossils	35	65

ORGANIC CARBON AND CARBONATE (%):

	1, 53
Organic carbon	–
Carbonate	54

SITE 608 HOLE CORE 54 CORED INTERVAL 492.5–502.1 m

TIME – ROCK UNIT	BIOSTRATIGRAPHIC ZONE	FOSSIL CHARACTER: FORAMINIFERS	FOSSIL CHARACTER: NANNOFOSSILS	FOSSIL CHARACTER: RADIOLARIANS	FOSSIL CHARACTER: DIATOMS	Sub-bottom depth	SECTION	METERS
		P14 T. *rohri* Zone	NP17 *Discoaster saipanensis* Zone			492.5	1	0.5 1.0
						494.0	2	
						495.5	3	
						497.0	4	
						498.5		
			AP	B	B	499.05	5	

GRAPHIC LITHOLOGY / DRILLING DISTURBANCE / SEDIMENTARY STRUCTURES / SAMPLES

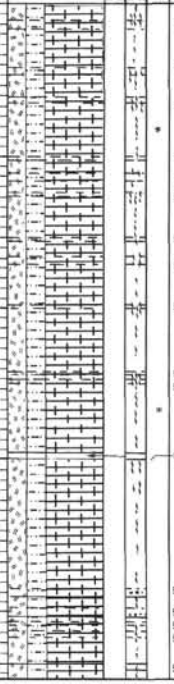

2.5Y 7/2
N7–N4
5YR 4/1
5GY 6/1
10YR 5/1
5Y 7/1
5Y 7/1
5Y 7/1
5Y 7/1
5Y 4/1
5Y 4/1
OG
5YR 4/1
5YR 4/1
5Y 6/1
5Y 6/1
5YR 4/1

LITHOLOGIC DESCRIPTION

VOLCANIC GLASS-BEARING MARLY NANNOFOSSIL CHALK, very light greenish gray (5GY 8/1) to ~496 m. Yellowish white (10YR 8/2) to ~498.5 m, followed by very light greenish gray (5GY 8/1) to very light gray (N8) to 499.05 m. Throughout are layers of gray to dark brown (5YR 4/1). Layers at 498.3 and 498.5 m are graded, fining upward.

SMEAR SLIDE SUMMARY (%):

	1, 120 D	3, 100 D
Composition:		
Quartz	10	5
Feldspar	20	25
Heavy minerals	TR	TR
Volcanic glass	20	20
Zeolite	TR	–
Foraminifers	5	5
Calc. nannofossils	45	45

SITE 608 HOLE CORE 55 CORED INTERVAL 502.1–507.7 m

TIME – ROCK UNIT	BIOSTRATIGRAPHIC ZONE	FOSSIL CHARACTER: FORAMINIFERS	FOSSIL CHARACTER: NANNOFOSSILS	FOSSIL CHARACTER: RADIOLARIANS	FOSSIL CHARACTER: DIATOMS	SECTION	METERS
		T. rohri Zone P14	NP17 *Discoaster saipanensis* Zone			CC	
			AM	B	B		

GRAPHIC LITHOLOGY / DRILLING DISTURBANCE / SEDIMENTARY STRUCTURES / SAMPLES

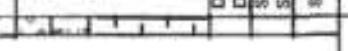

LITHOLOGIC DESCRIPTION

7 cm of very pale brown (10YR 8/2) MARLY NANNOFOSSIL CHALK

SITE 608 HOLE CORE 56 CORED INTERVAL 507.7–511.7 m

TIME – ROCK UNIT	BIOSTRATIGRAPHIC ZONE	FOSSIL CHARACTER: FORAMINIFERS	FOSSIL CHARACTER: NANNOFOSSILS	FOSSIL CHARACTER: RADIOLARIANS	FOSSIL CHARACTER: DIATOMS	SECTION	METERS
		T. rohri Zone P14	AM	B	B	CC	
			NP17 *Discoaster saipanensis* Zone				

GRAPHIC LITHOLOGY / DRILLING DISTURBANCE / SEDIMENTARY STRUCTURES / SAMPLES

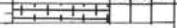

LITHOLOGIC DESCRIPTION

Total recovery: 15–20 cm^3 of light gray (10YR 7/1) VOLCANIC GLASS-BEARING MARLY NANNOFOSSIL CHALK in Core Catcher.

SMEAR SLIDE SUMMARY (%):

	CC
Composition:	
Quartz	4
Feldspar	1
Clay	18
Volcanic glass	1
Carbonate unspec.	11
Calc. nannofossils	65

SITE 608 HOLE CORE 57 CORED INTERVAL 511.7–514.7 m

TIME – ROCK UNIT	BIOSTRATIGRAPHIC ZONE	FOSSIL CHARACTER: FORAMINIFERS	FOSSIL CHARACTER: NANNOFOSSILS	FOSSIL CHARACTER: RADIOLARIANS	FOSSIL CHARACTER: DIATOMS	Sub-bottom depth	SECTION	METERS
		T. rohri Zone (P14)	NP17 *Discoaster saipanensis* Zone			511.7	1	0.5 1.0
						513.2	2	
						514.7	3	
		NP16 *Discoaster tani nodifer* Zone	AM	B	B	515.7		

GRAPHIC LITHOLOGY / DRILLING DISTURBANCE / SEDIMENTARY STRUCTURES / SAMPLES

10YR 6/2
10YR 8/2
10YR 8/2
10YR 6/2
10YR 8/2
10YR 8/2
10YR 6/2
10YR 8/2
10YR 6/2
10YR 8/2
10YR 8/2
10YR 8/2
10YR 8/2
10YR 8/2
10YR 6/3, N3
10YR 7/3–10YR 8/4 and 10YR 8/6
10YR 5/2 and 10YR 6/2
Void
10YR 7/3–10YR 8/4 and 10YR 8/6
10YR 5/2 and 10YR 6/2
10YR 6/3
Basalt
Carbonate vein
Basalt

LITHOLOGIC DESCRIPTION

VOLCANIC GLASS-BEARING MARLY NANNOFOSSIL CHALK, dominantly light brownish gray (10YR 6/2) to light yellowish brown (10YR 6/4) to 514.3 m.

At 514.3 to 515.44 m DOLOMITIC MARLSTONE, dark grayish brown (10YR 4/2) to pale brown (10YR 6/3). At 514.3 to 514.7 m faint layers of very pale brown (10YR 7/3–10YR 8/4) and yellow (10YR 8/6). At 514.9 to 515.0 m two layers of dark reddish brown (5YR 3/4) sandwiched by layers of light gray (10YR 7/2).

Note: recovery here 150% (see operations section).

SMEAR SLIDE SUMMARY (%):

	1, 23 M	2, 10 D	2, 112 D
Composition:			
Quartz	5	3	–
Feldspar	–	–	2
Heavy minerals	–	–	TR
Clay	10	12	70
Volcanic glass	–	–	3
Carbonate unspec.	67	69	20*
Calc. nannofossils	18	16	1
Opaque oxides	–	–	4

* = 20% dolomite

ORGANIC CARBON AND CARBONATE (%):

	2, 111
Organic carbon	–
Carbonate	4

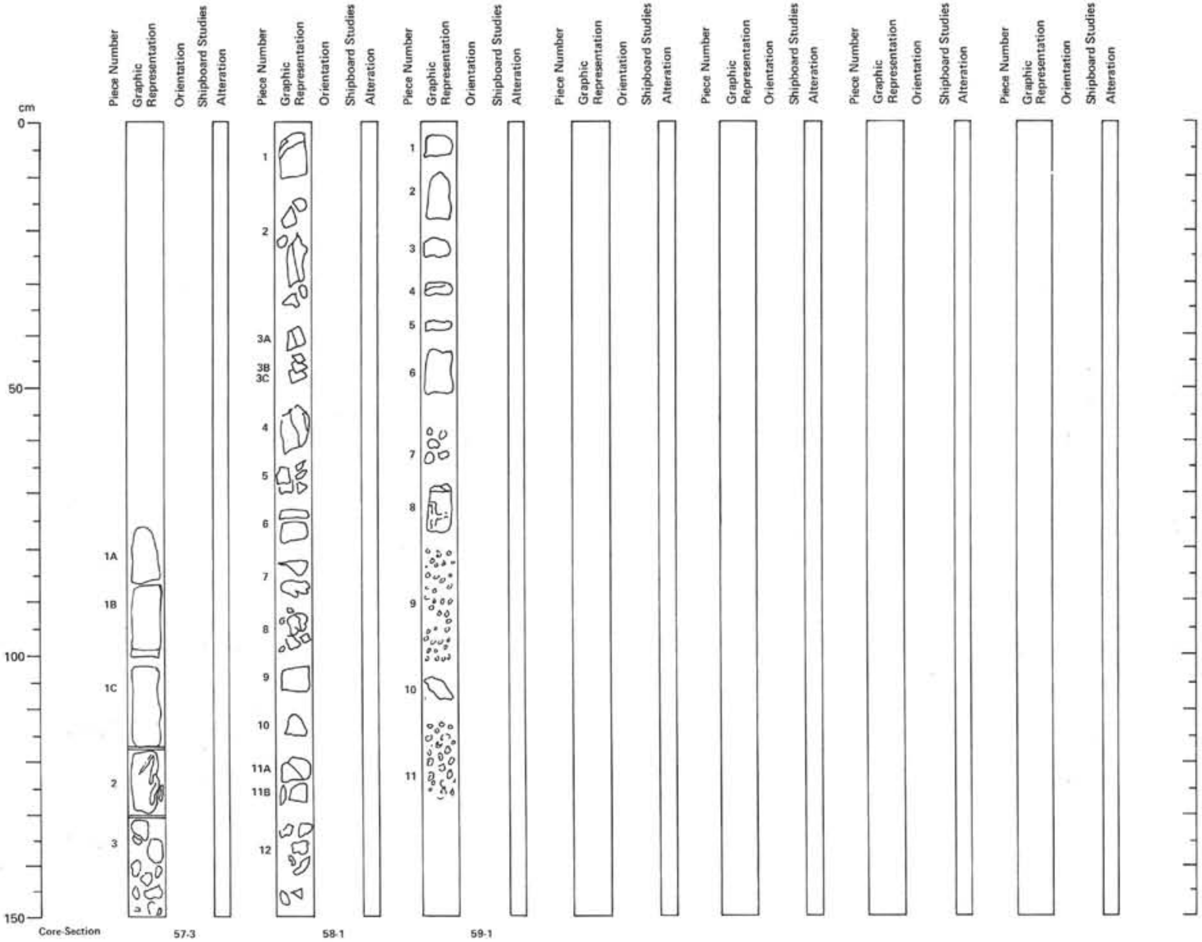

94-608-57-3 Depth: 515.4–516.2 m

Pieces 1–3: DOMINANT LITHOLOGY: BASALT.
Macroscopic description: All fragments are fine-grained and relatively fresh with fresh clinopyroxene phenocrysts (up to 3 mm) and 1 mm vesicles. The uppermost portion of Piece 1A has a 1–2 mm glass rind. Calcite veins are common with a large vein in Piece 1B containing nannofossils.

TS 85 cm (Piece 1A): Fine- to medium-grained basalt, doleritic in texture, made up of plagioclase and clinopyroxene laths. Phenocrysts are fresh, Ti-rich, augitic clinopyroxenes, and calcite-pseudomorphs after plagioclase. Vesicles and some fractures are filled with green, microcrystalline silica, calcite, and chlorite. Approximate composition: 37% plagioclase laths, 37% clinopyroxene laths, 10% calcite, 7% alteration minerals (hematite), 5% opaque oxides (magnetite) and 5% microcrystalline silica.

94-608-58-1 Depth 514.7–521.3 m

Pieces 1–12: DOMINANT LITHOLOGY: BASALT. Macroscopic description: The majority of the fragments are fine-grained, relatively fresh basalt with small weathered olivine phenocrysts (up to 3 mm) and 1 mm vesicles. Larger basalt fragments (1–4, 11) have thick calcite veins (up to 4 cm). Some fragments are calcite (2, 3C, 5, 8, 11) most likely from fractured veins. 1–2 mm alteration rind (green) is present on Piece 7A. Fragments in Piece 12 are volcanic tuff with non-fossiliferous calcite. Pieces in this section are suspected downhole contaminants.

TS 104 cm (Piece 9): Fine-grained basalt, doleritic in texture made up of clinopyroxene and plagioclase. Phenocrysts are augitic clinopyroxenes, calcite pseudomorphs after plagiclase. Common vesicles lined with a green, microcrystalline silica and occassionally filled with secondary calcite. Large (1 cm) phenocryst composed of several calcite crystals surrounded by many small vesicles and alteration minerals. Approximate composition: 35% plagioclase, 25% pyroxene, 15% calcite, 10% reddish-brown alteration minerals, 8% interstitial opaque oxides, 5% olivine and 2% microcrystalline silica.

TS 45–47 cm: Clinopyroxene, plagioclase, chlorite, with phenocrysts of olivine.

94-608-59-1 Depth: 521.3–530.9 m

Pieces 1–11: DOMINANT LITHOLOGY: BASALT.
Macroscopic description: Most fragments are fine-grained, relatively fresh vesicular basalt. Some vesicles (up to 2 mm) are lined with a blue/green microcrystalline (silica?) coating. Calcite veins in Pieces 2, 4, and 8 show a reddish-brown alteration zone along the edges and often contain fragments of basalt. Pieces in Sections 9–11 appear highly altered and are probably mixed with wash material.

TS 13 cm (Piece 2): Fine-grained basalt. Fair thin section. Doleritic in texture, made up of plagioclase, with interstitial pyroxene and opaque oxides. Phenocrysts are fresh clinopyroxene, calcite-pseudomorphs after plagioclase. Approximate composition: 43% plagioclase laths, 35% interstitial pyroxenes, 10% opaque oxides, 5% calcite, 5% reddish-brown alteration minerals, and 2% microcrystalline silica.

SITE 608 HOLE A CORE 1 CORED INTERVAL 0.0–2.4 m

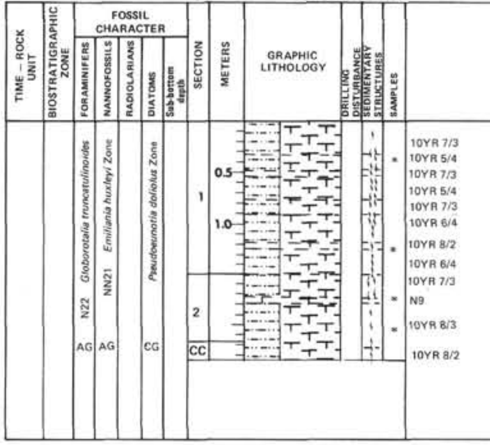

LITHOLOGIC DESCRIPTION

MARLY NANNOFOSSIL OOZE, alternating layers of brown (10YR 6/4, 10YR 5/4) and light to very light brown (10YR 6/4 to 10YR 8/2).

White (N9) FORAMINIFERAL NANNOFOSSIL OOZE, 1.73 to 1.79 m.

SMEAR SLIDE SUMMARY (%)

	1, 42	1, 124	2, 28	2, 58
	D	D	D	D
Composition:				
Quartz	30	25	15	25
Feldspar	–	5	–	–
Heavy minerals	TR	–	–	TR
Clay	5	5	TR	5
Volcanic glass	10	5	1	5
Foraminifers	7	15	20	8
Calc. nannofossils	48	45	65	56
Diatoms	TR	–	–	TR
Radiolarians	TR	–	TR	TR
1%				

SITE 608 HOLE A CORE 2 CORED INTERVAL 2.4–12.0 m

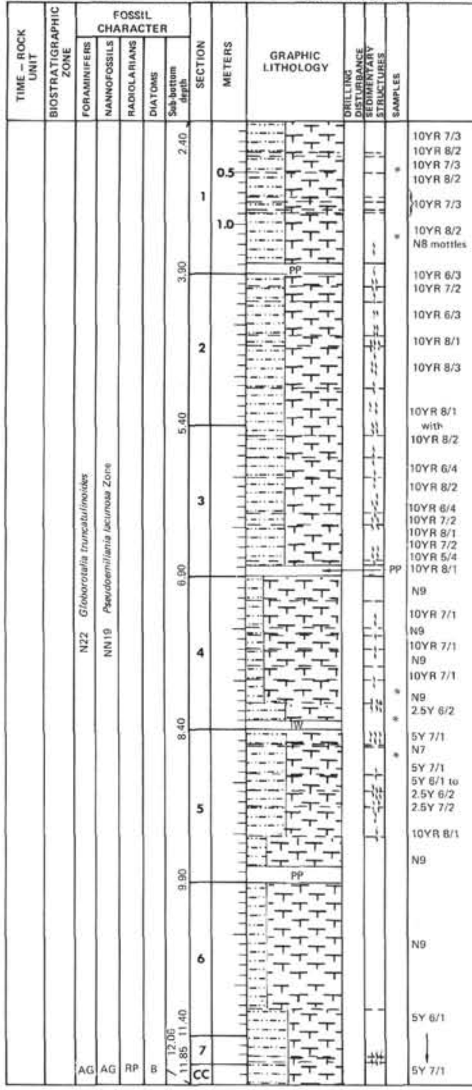

LITHOLOGIC DESCRIPTION

Dominantly shades of white (N9) and tan (10YR 8/1–10YR 8/2) FORAMINIFERAL NANNOFOSSIL OOZE, alternating with pale brown (10YR 7/1), dark green/olive (5Y 6/1), and brown (10YR 6/3–10YR 6/4) layers.

MARLY FORAMINIFERAL NANNOFOSSIL OOZE at 3.90 to 6.90 m.

ASH-BEARING FORAMINIFERAL NANNOFOSSIL OOZE, dark green olive (2.5Y 6/2) at 8.14 to 8.38 m.

Note: >100% recovery.

SMEAR SLIDE SUMMARY (%)

	1, 44	1, 110	4, 110	4, 138	5, 20
	D	D	D	D	M
Composition:					
Quartz	25	20	5	10	30
Feldspar	TR	2	1	5	5
Mica	–	–	–	–	TR
Heavy minerals	TR	1	–	1	–
Clay	5	5	4	5	5
Volcanic glass	5	5	–	5	–
Foraminifers	20	12	10	20	20
Calc. nannofossils	45	65	80	54	40
Radiolarians	–	TR	–	–	–

SITE 608 HOLE A CORE 3 CORED INTERVAL 12.0–21.6 m

TIME – ROCK UNIT	BIOSTRATIGRAPHIC ZONE	FORAMINIFERS	NANNOFOSSILS	RADIOLARIANS	DIATOMS	Sub-bottom depth	SECTION	METERS
		N22 *Globorotalia truncatulinoides*	NN19 *Pseudoemiliania lacunosa* Zone		*Nitzschia reinholdii* Zone	12.0	1	0.5 1.0
						13.5	2	
						15.0	3	
						16.5	4	
						18.0	5	
						19.5	6	
						21.0 21.78	7	
		AG	AG		AG	21.56	CC	

GRAPHIC LITHOLOGY / DRILLING DISTURBANCE / SEDIMENTARY STRUCTURES / SAMPLES

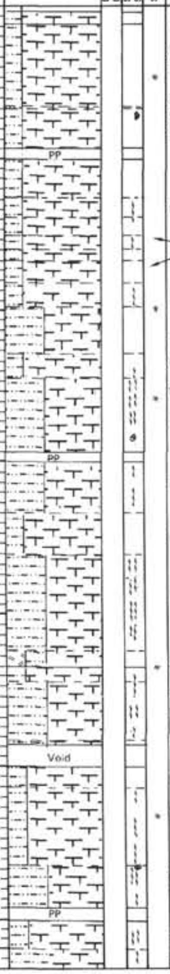

LITHOLOGIC DESCRIPTION

10YR 6/2
N9
to
10YR 6/1
N8
dropstone
N9 to
10YR 6/1
N7
N7
N5
↓
N8
N8
10YR 6/1
to
10YR 7/1
Pumice
10YR 7/1
N9 to
N8
10YR 8/1 to
10YR 6/2
N9 to N8
10YR 6/2
to
10YR 8/1
N8
N8
N8 to
10YR 7/2
dropstone
2.5Y 6/2
N8 to
2.5Y 6/2
2.5Y 7/2 to 8/2

FORAMINIFERAL NANNOFOSSIL OOZE and NANNOFOSSIL OOZE, mostly white (N9) to gray (10YR 6/1) alternating with MARLY FORAMINIFERAL NANNOFOSSIL OOZE, gray (10YR 6/1, N5–N8) to light brownish gray (10YR 6/2, 2.5Y 6/2).

Note: >100% recovery.

SMEAR SLIDE SUMMARY (%):

	1, 70 M	2, 149 D	3, 84 D	5, 47 D	6, 50 D
Composition:					
Quartz	5	10	15	5	5
Feldspar	1	TR	5	1	TR
Heavy minerals	TR	–	5	TR	–
Clay	–	5	5	TR	–
Volcanic glass	–	5	2	2	2
Foraminifers	5	20	20	25	30
Calc. nannofossils	89	60	48	67	63
Diatoms	–	–	–	TR	–

SITE 608 HOLE A CORE 4 CORED INTERVAL 21.6–31.2 m

TIME – ROCK UNIT	BIOSTRATIGRAPHIC ZONE	FORAMINIFERS	NANNOFOSSILS	RADIOLARIANS	DIATOMS	Sub-bottom depth	SECTION	METERS
		N22 *Globorotalia truncatulinoides/Globorotalia tosaensis* overlap	NN19 *Pseudoemiliania lacunosa* Zone		*Nitzschia reinholdii* Zone	21.6	1	0.5 1.0
						23.1	2	
						24.6	3	
						26.1	4	
						27.6	5	
						29.1	6	
						30.6 31.43	7	
		AG	AG		AG	31.16	CC	

GRAPHIC LITHOLOGY / DRILLING DISTURBANCE / SEDIMENTARY STRUCTURES / SAMPLES

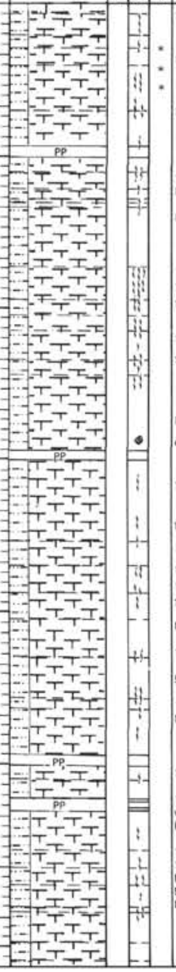

LITHOLOGIC DESCRIPTION

2.5Y 6/2
10YR 7/1
10YR 8/1
N9 to N8
10YR 7/1
to
10YR 8/1
N9
↓
10YR 8/1
10YR 8/1
10YR 7/1
N8
N9
10YR 7/1
10YR 8/1
10YR 6/1
10YT 6/2
10YR 8/1
N9
dropstone
10YR 8/1
↓
10YR 7/1
N9
10YR 8/1
10YR 7/1
10YR 8/1
N9
↓
10YR 8/1
5Y 7/2
10YR 8/1
N9
↓
10YR 8/1
10YR 8/1
with N7
laminae
10YR 7/1
10YR 8/1
N9
5Y 8/1
N9
5YR 8/1
10YR 8/1

Top 9 cm brown (2.5Y 6/2) MARLY FORAMINIFERAL NANNOFOSSIL OOZE. Remainder FORAMINIFERAL NANNOFOSSIL OOZE, alternating various shades of tan and gray with white.

Note: >100% recovery.

SMEAR SLIDE SUMMARY (%):

	2, 46	2, 65	2, 75
Composition:			
Quartz	15	25	15
Feldspar	–	–	TR
Clay	–	TR	TR
Volcanic glass	–	TR	–
Carbonate unspec.	–	TR	–
Foraminifers	12	10	12
Calc. nannofossils	73	65	73
Diatoms	TR	TR	–
Radiolarians	TR	–	–

SITE 608 HOLE A CORE 5 CORED INTERVAL 31.2–40.8 m

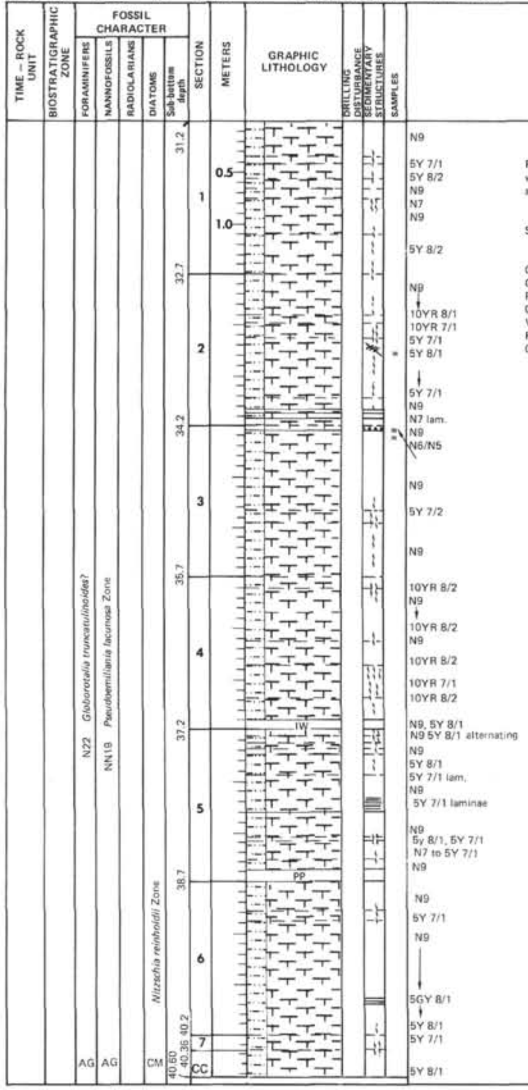

LITHOLOGIC DESCRIPTION

FORAMINIFERAL NANNOFOSSIL OOZE, alternating white (N9), gray (N7) and various shades of tan, olive and gray (5Y 7/1, 10YR 8/2).

SMEAR SLIDE SUMMARY (%):

	2, 70 D	3, 1 M	3, 3 M
Composition:			
Quartz	30	10	15
Feldspar	TR	–	–
Clay	TR	–	–
Volcanic glass	10	–	–
Foraminifers	10	40	50
Calc. nannofossils	50	50	35

SITE 608 HOLE A CORE 6 CORED INTERVAL 40.8–50.4 m

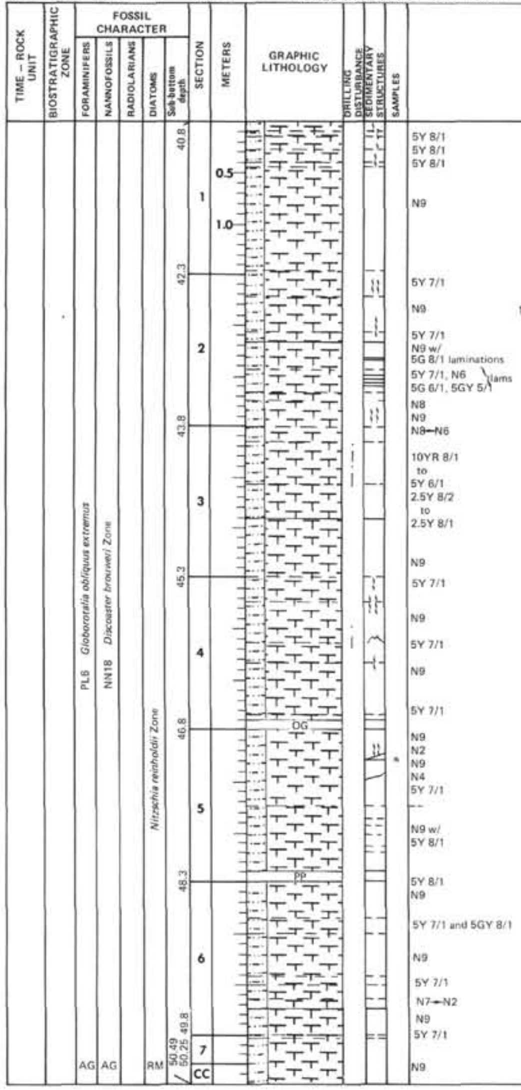

LITHOLOGIC DESCRIPTION

Dominantly FORAMINIFERAL NANNOFOSSIL OOZE, white (N9) alternating with shades of tan (5Y 8/1, 10YR 8/1) and olive (5Y 7/1, 5Y 6/1).

Two intervals of NANNOFOSSIL FORAMINIFERAL SAND with sharp lower contacts (44.3 to 44.7 m and 49.4 to 49.6 m).

Note: >100% recovery.

SMEAR SLIDE SUMMARY (%):

	5, 28 M
Composition:	
Quartz	3
Feldspar	TR
Clay	1
Volcanic glass	TR
Pyrite	2
Carbonate unspec.	2
Foraminifers	65
Calc. nannofossils	27

SITE 608 HOLE A CORE 7 CORED INTERVAL 50.4–60.0 m

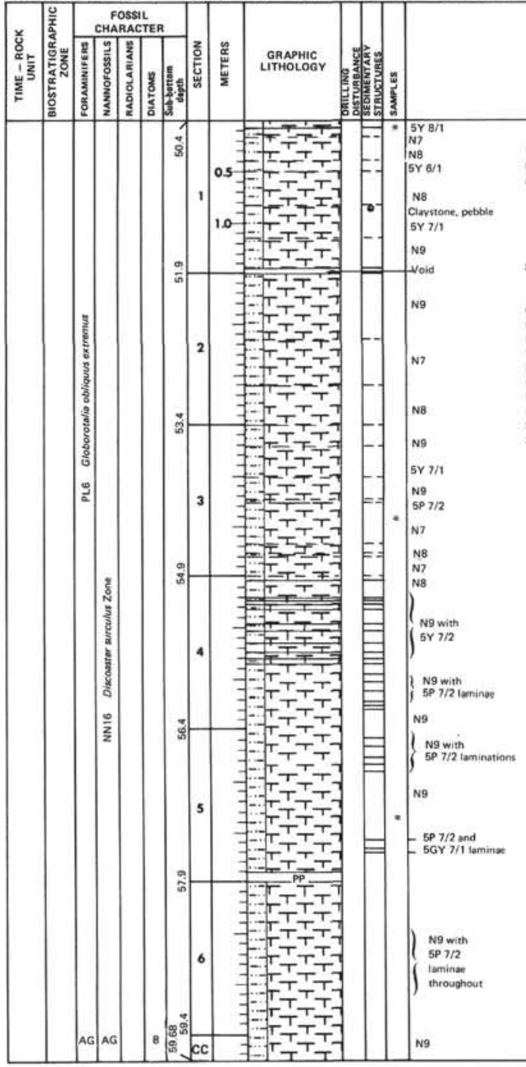

LITHOLOGIC DESCRIPTION

FORAMINIFERAL NANNOFOSSIL OOZE, dominantly light gray (N7) to white (N9). Light olive brown (5Y 7/2) and pale purple (5P 7/2) laminae abundant below 54.9 m.

SMEAR SLIDE SUMMARY (%):

	1, 10 D	3, 89 M	5, 87 D
Composition:			
Quartz	3	31	8
Feldspar	TR	–	TR
Volcanic glass	TR	–	–
Pyrite	–	3	–
Carbonate unspec.	TR	–	TR
Foraminifers	11	16	12
Calc. nannofossils	86	50	80
Sponge spicules	–	TR	–
Silicoflagellates	–	TR	–

SITE 608 HOLE A CORE 8 CORED INTERVAL 60.0–69.6 m

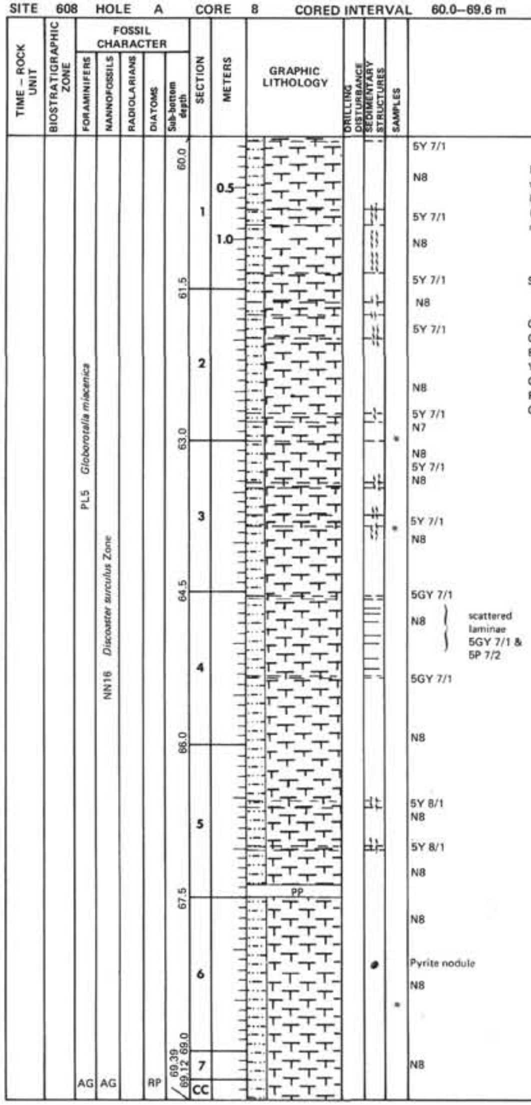

LITHOLOGIC DESCRIPTION

FORAMINIFERAL NANNOFOSSIL OOZE, dominantly very light gray (N8) with occasional bands of pale olive brown (5Y 7/1). Scattered laminae of light green gray (5GY 7/1) and pale purple (5P 7/2) between 64.5 and 65.4 m.

SMEAR SLIDE SUMMARY (%):

	2, 145 D	3, 82 D	6, 106 D
Composition:			
Quartz	36	12	13
Feldspar	1	1	TR
Volcanic glass	TR	TR	–
Carbonate unspec.	TR	TR	TR
Foraminifers	16	16	10
Calc. nannofossils	47	71	77

SITE 608 HOLE A CORE 9 CORED INTERVAL 69.6–79.2 m

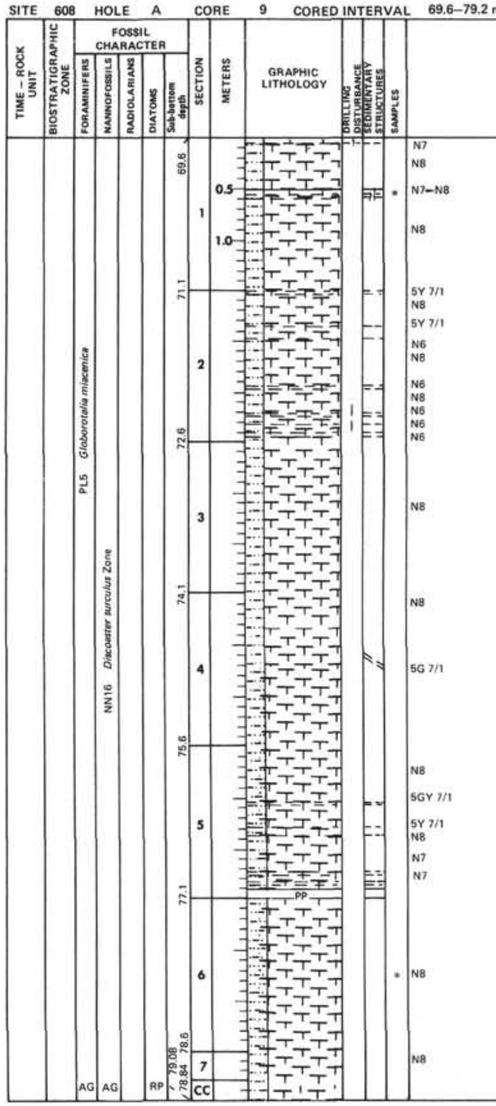

LITHOLOGIC DESCRIPTION

Very light gray (N8) FORAMINIFERAL NANNOFOSSIL OOZE with light gray (N6–7) and yellowish gray (5Y 7/1) laminae throughout.

SMEAR SLIDE SUMMARY (%):

	1, 50 M	6, 77 D
Composition:		
Quartz	34	21
Feldspar	TR	TR
Carbonate unspec.	TR	TR
Foraminifers	18	12
Calc. nannofossils	48	67

SITE 608 HOLE A CORE 10 CORED INTERVAL 79.2–88.8 m

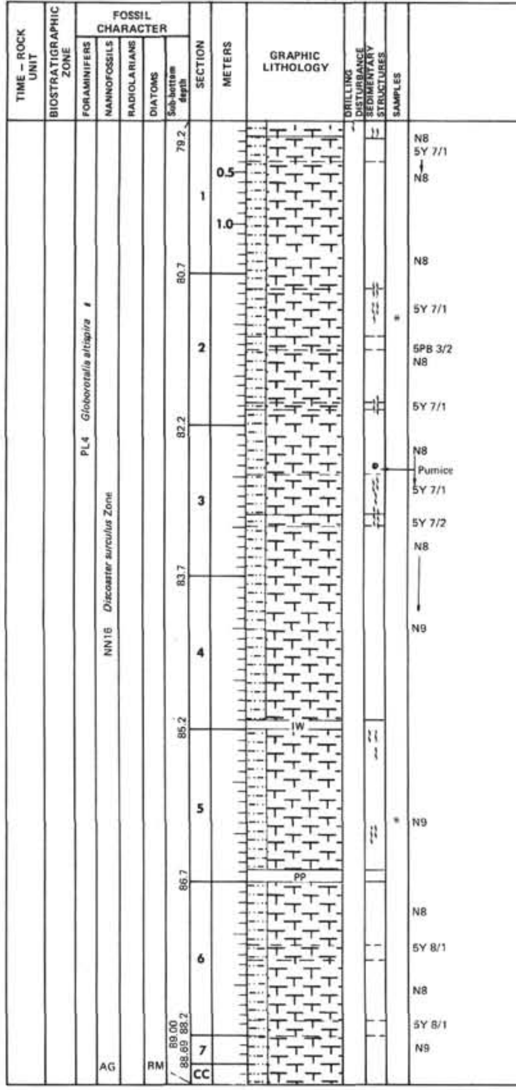

LITHOLOGIC DESCRIPTION

Very light gray (N8) to white (N9) FORAMINIFERAL NANNOFOSSIL OOZE. Occasional gradual changes to yellowish white (5Y 8/1) and light yellowish gray (5Y 7/1).

Note: recovery >100%.

SMEAR SLIDE SUMMARY (%):

	2, 42	5, 84
Composition:		
Quartz	5	8
Feldspar	TR	TR
Volcanic glass	TR	–
Carbonate unspec.	TR	TR
Foraminifers	10	12
Calc. nannofossils	85	80

SITE 608 HOLE A CORE 11 CORED INTERVAL 88.8–98.4 m

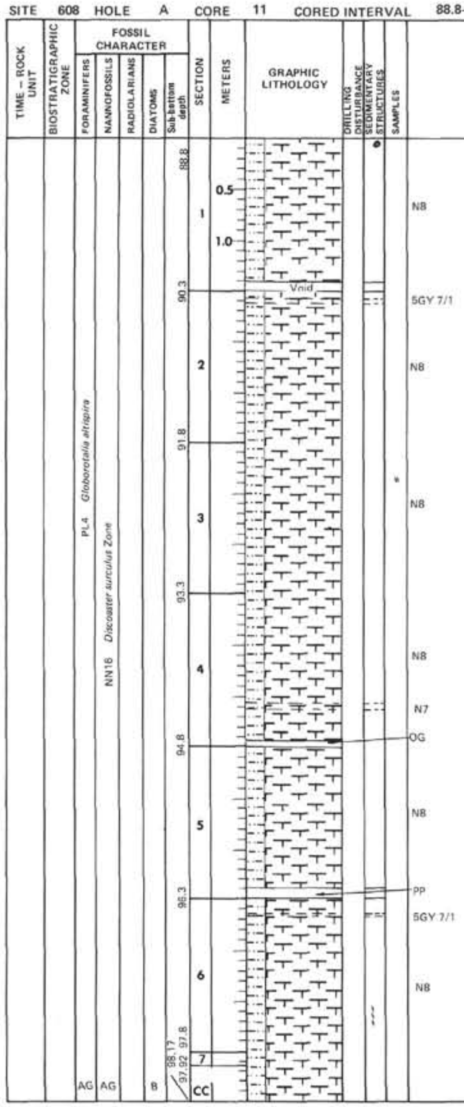

LITHOLOGIC DESCRIPTION

Very light gray (N8) FORAMINIFERAL NANNOFOSSIL OOZE

SMEAR SLIDE SUMMARY (%):

	3, 30 D
Composition:	
Quartz	17
Feldspar	TR
Foraminifers	16
Calc. nannofossils	67

SITE 608 HOLE A CORE 12 CORED INTERVAL 98.4–108.0 m

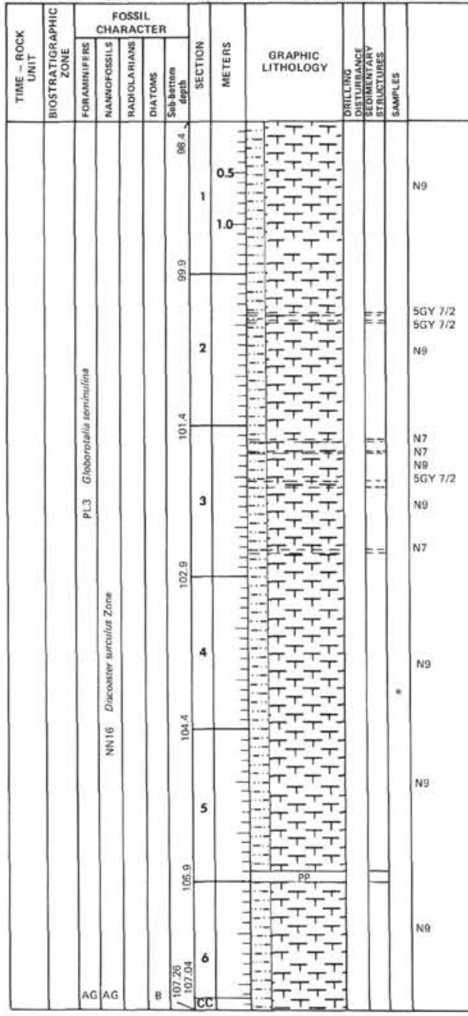

LITHOLOGIC DESCRIPTION

White (N9) FORAMINIFERAL NANNOFOSSIL OOZE

SMEAR SLIDE SUMMARY (%):

	4, 110 D
Composition:	
Quartz	2
Feldspar	TR
Pyrite	TR
Foraminifers	17
Calc. nannofossils	81

SITE 608 HOLE A CORE 13 CORED INTERVAL 108.0–117.6 m

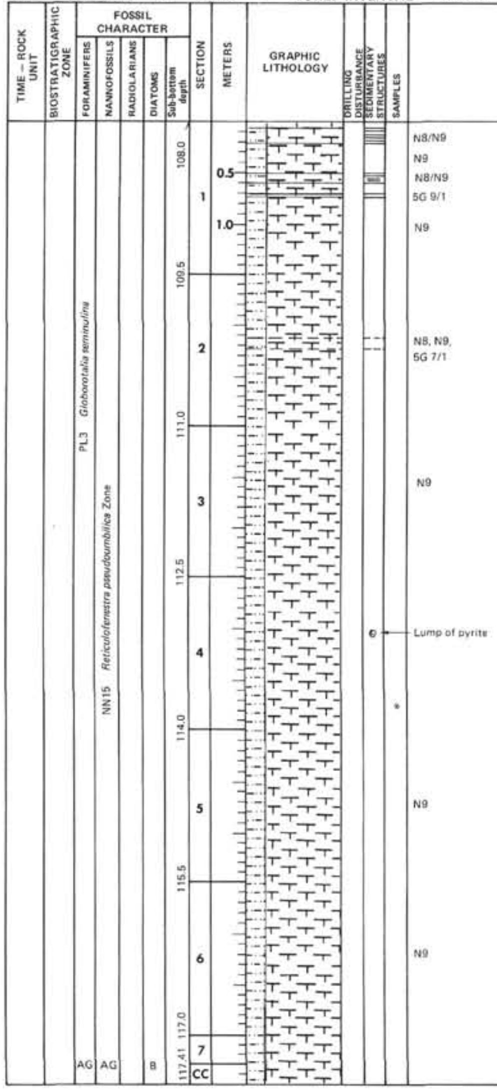

LITHOLOGIC DESCRIPTION

White (N9) FORAMINIFERAL NANNOFOSSIL OOZE. Laminae of very light gray (N8) and very light green (5G 9/1) 108.0 to 108.8 m.

SMEAR SLIDE SUMMARY (%):

	4, 130 D
Composition:	
Quartz	3
Feldspar	TR
Foraminifers	19
Calc. nannofossils	78

SITE 608 HOLE A CORE 14 CORED INTERVAL 117.6–127.2 m

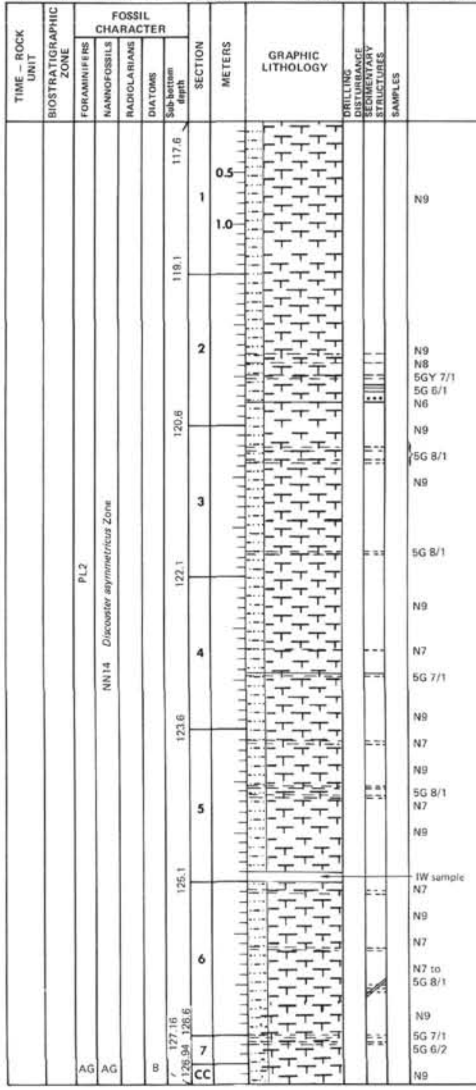

LITHOLOGIC DESCRIPTION

White (N9) FORAMINIFERAL NANNOFOSSIL OOZE with occasional light gray (N7) and light green (5G 6/2 to 5G 8/1) laminae.

Two laminae slightly offset by microfault at 126.1 m.

NANNOFOSSIL FORAMINIFERAL SAND 119.9 to 120.4 m. Sand coarsens and darkens (to N6) toward sharp contact at base.

SMEAR SLIDE SUMMARY (%):

	6, 73 D	2, 109 M
Composition:		
Quartz	2	–
Feldspar	TR	TR
Foraminifers	20	80
Calc. nannofossils	78	10
Fish remains	–	TR

SITE 608 HOLE A CORE 15 CORED INTERVAL 127.8–136.8 m

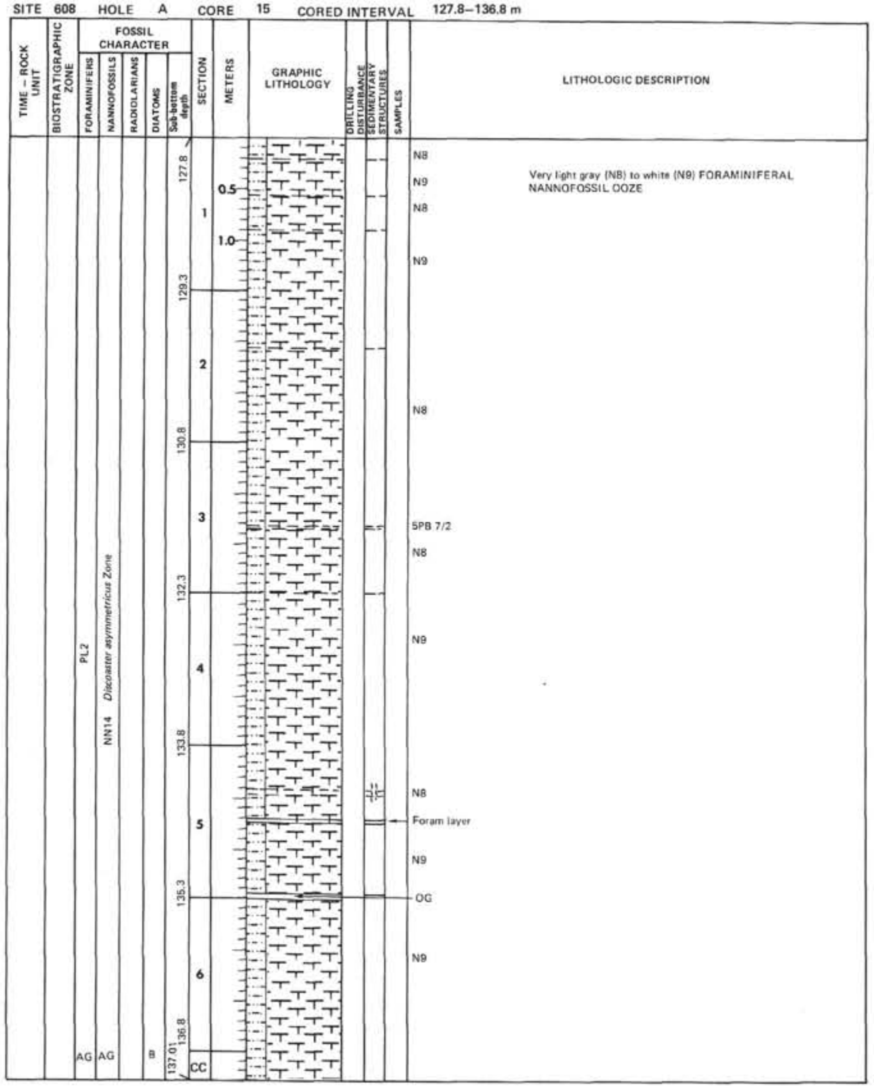

Very light gray (N8) to white (N9) FORAMINIFERAL NANNOFOSSIL OOZE

SITE 608 HOLE A CORE 16 CORED INTERVAL 136.8–146.4 m

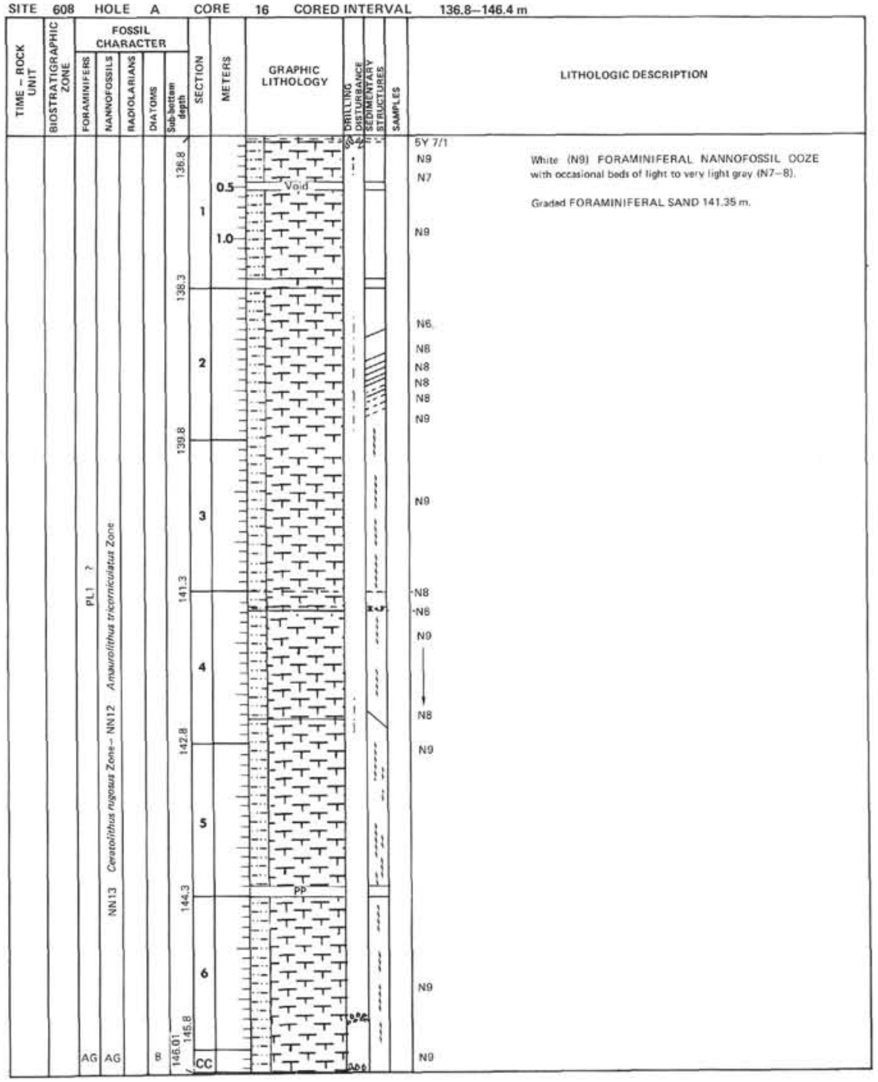

White (N9) FORAMINIFERAL NANNOFOSSIL OOZE with occasional beds of light to very light gray (N7–8).

Graded FORAMINIFERAL SAND 141.35 m.

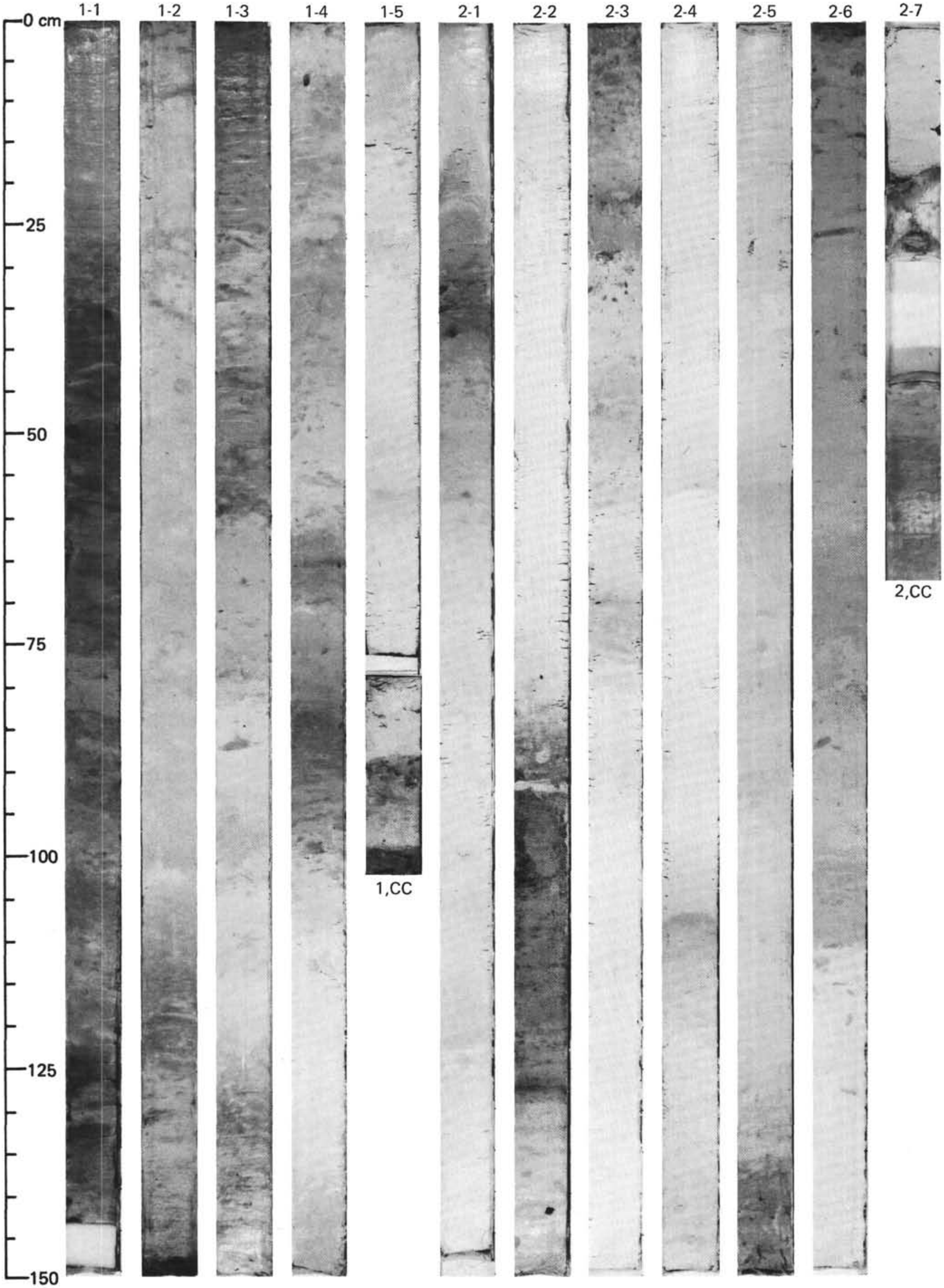
0 cm
25
50
75
100
125
150
1-1
1-2
1-3
1-4
1-5
1,CC
2-1
2-2
2-3
2-4
2-5
2-6
2-7
2,CC

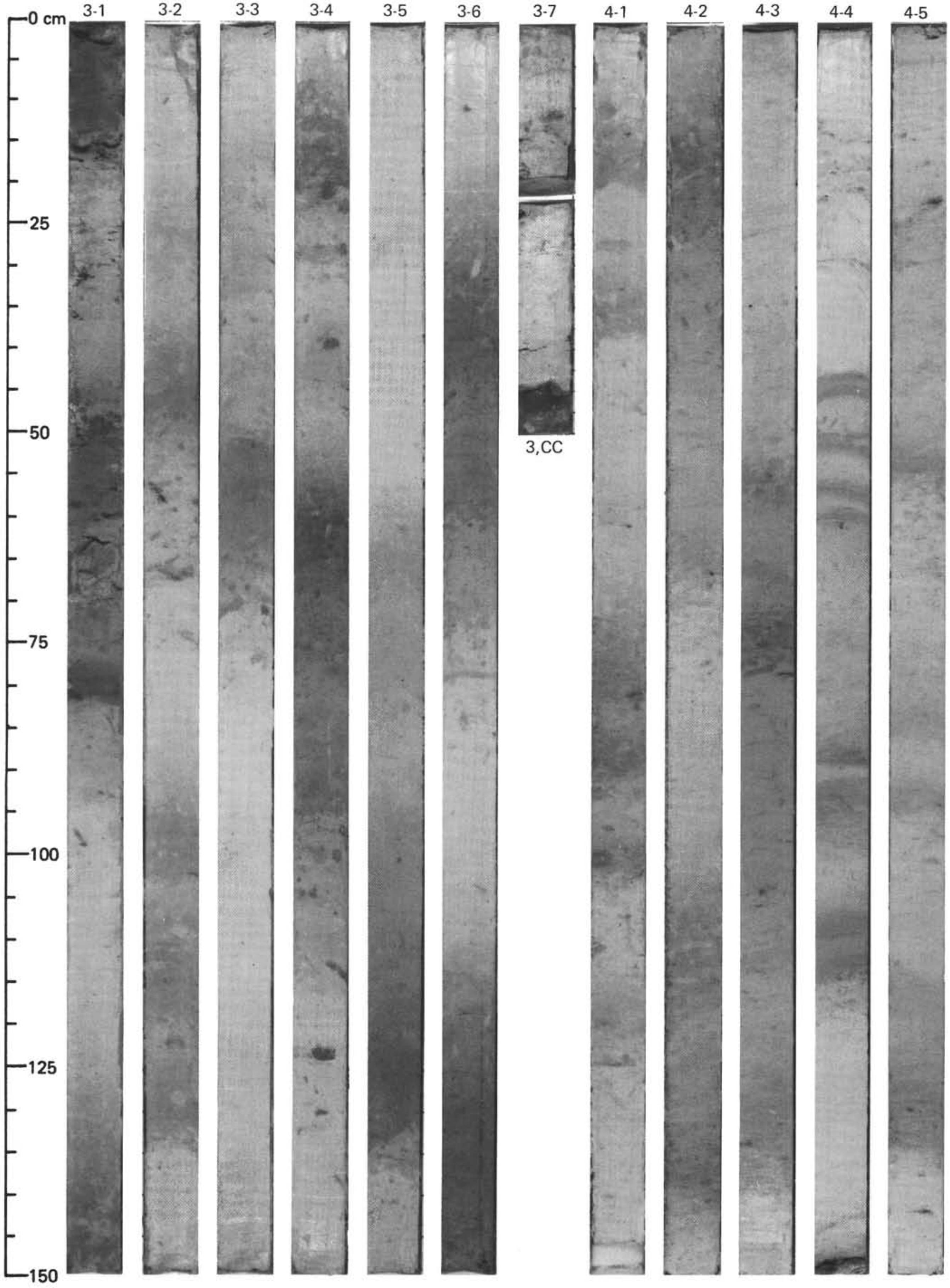
0 cm
25
50
75
100
125
150
3-1
3-2
3-3
3-4
3-5
3-6
3-7
3,CC
4-1
4-2
4-3
4-4
4-5

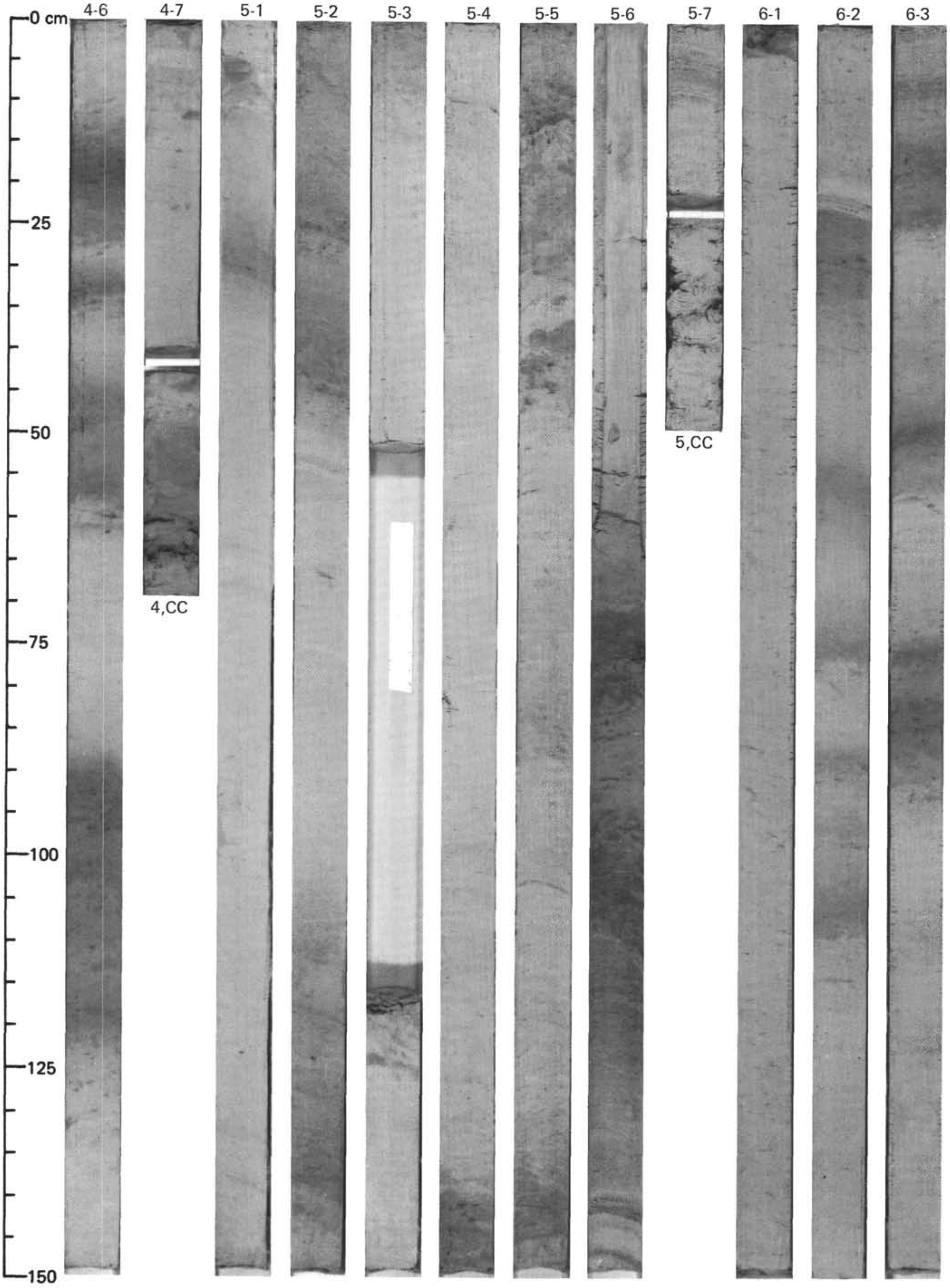
0 cm
25
50
75
100
125
150
4-6
4-7
4,CC
5-1
5-2
5-3
5-4
5-5
5-6
5-7
5,CC
6-1
6-2
6-3

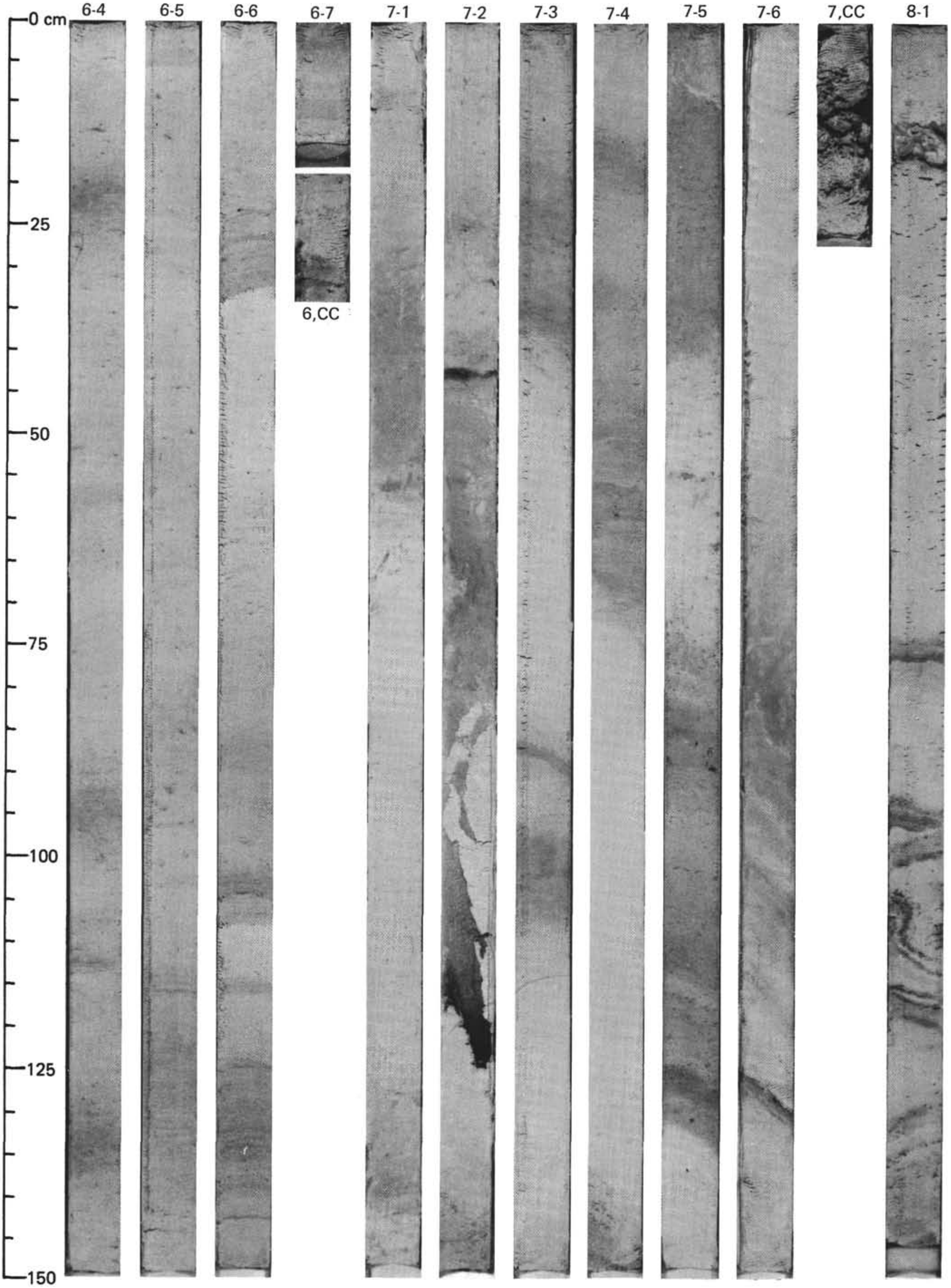
0 cm
25
50
75
100
125
150
6-4
6-5
6-6
6-7
6,CC
7-1
7-2
7-3
7-4
7-5
7-6
7,CC
8-1

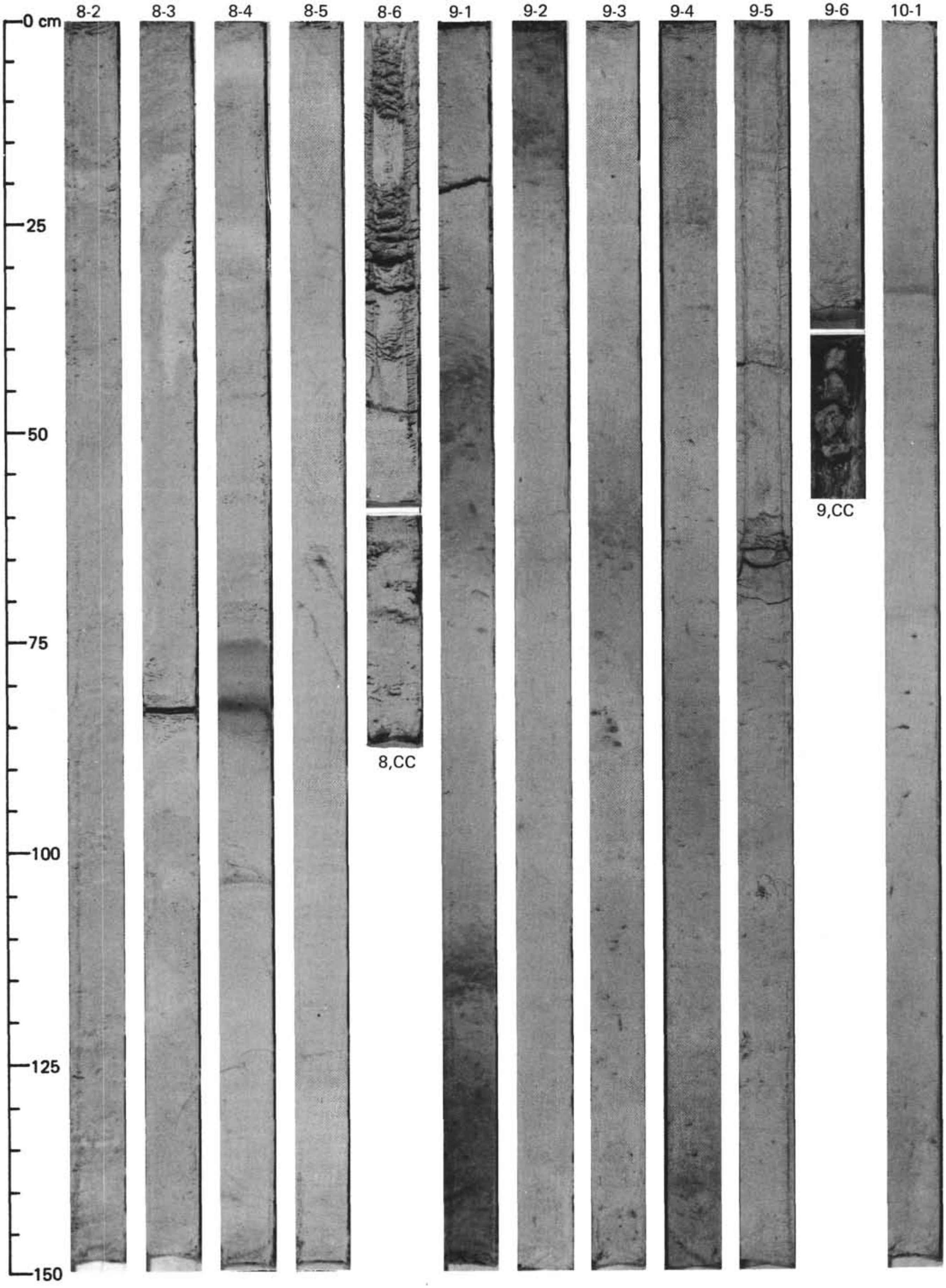
0 cm
25
50
75
100
125
150
8-2
8-3
8-4
8-5
8-6
8,CC
9-1
9-2
9-3
9-4
9-5
9-6
9,CC
10-1

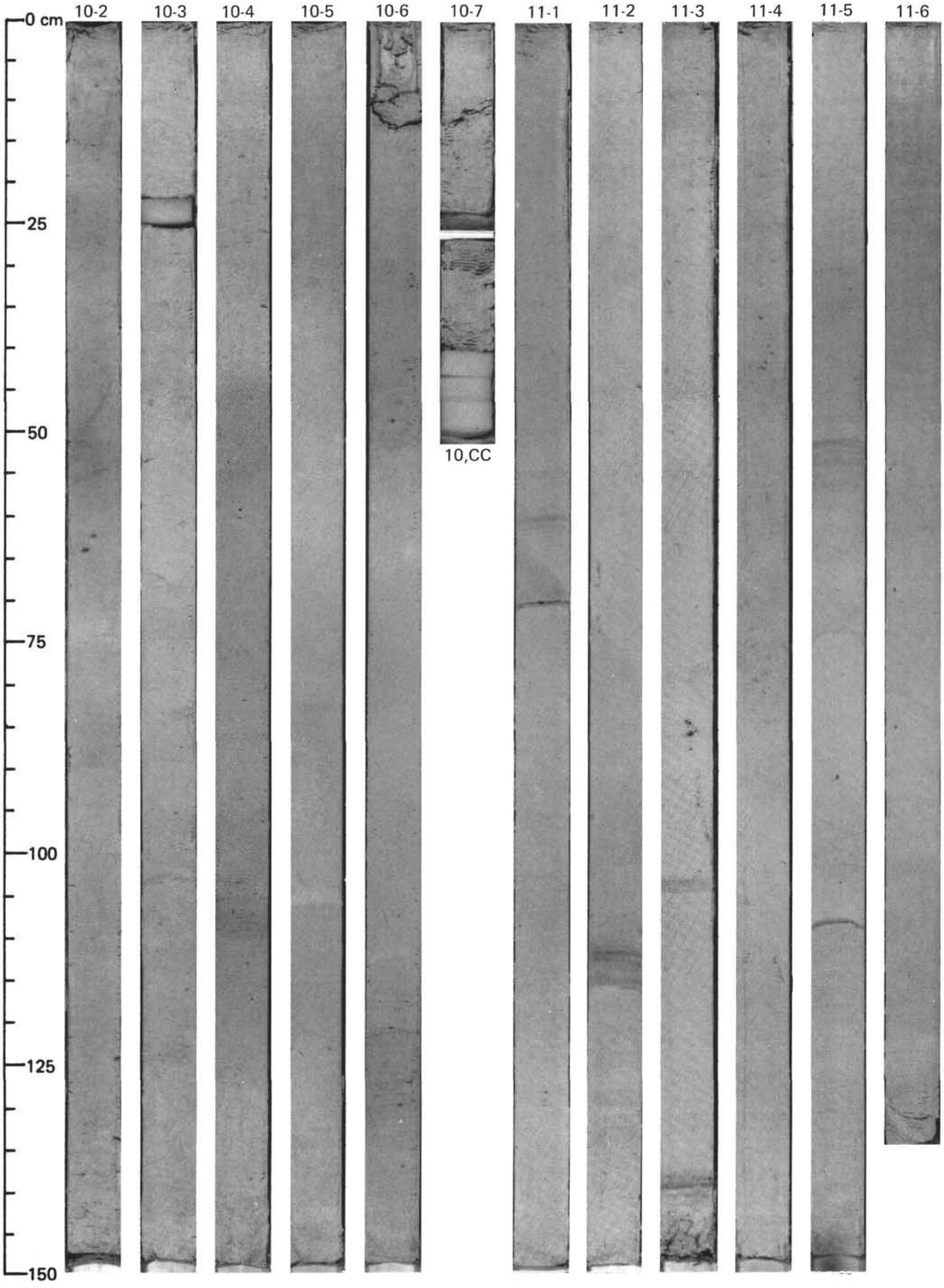
0 cm
25
50
75
100
125
150
10-2
10-3
10-4
10-5
10-6
10-7
10,CC
11-1
11-2
11-3
11-4
11-5
11-6

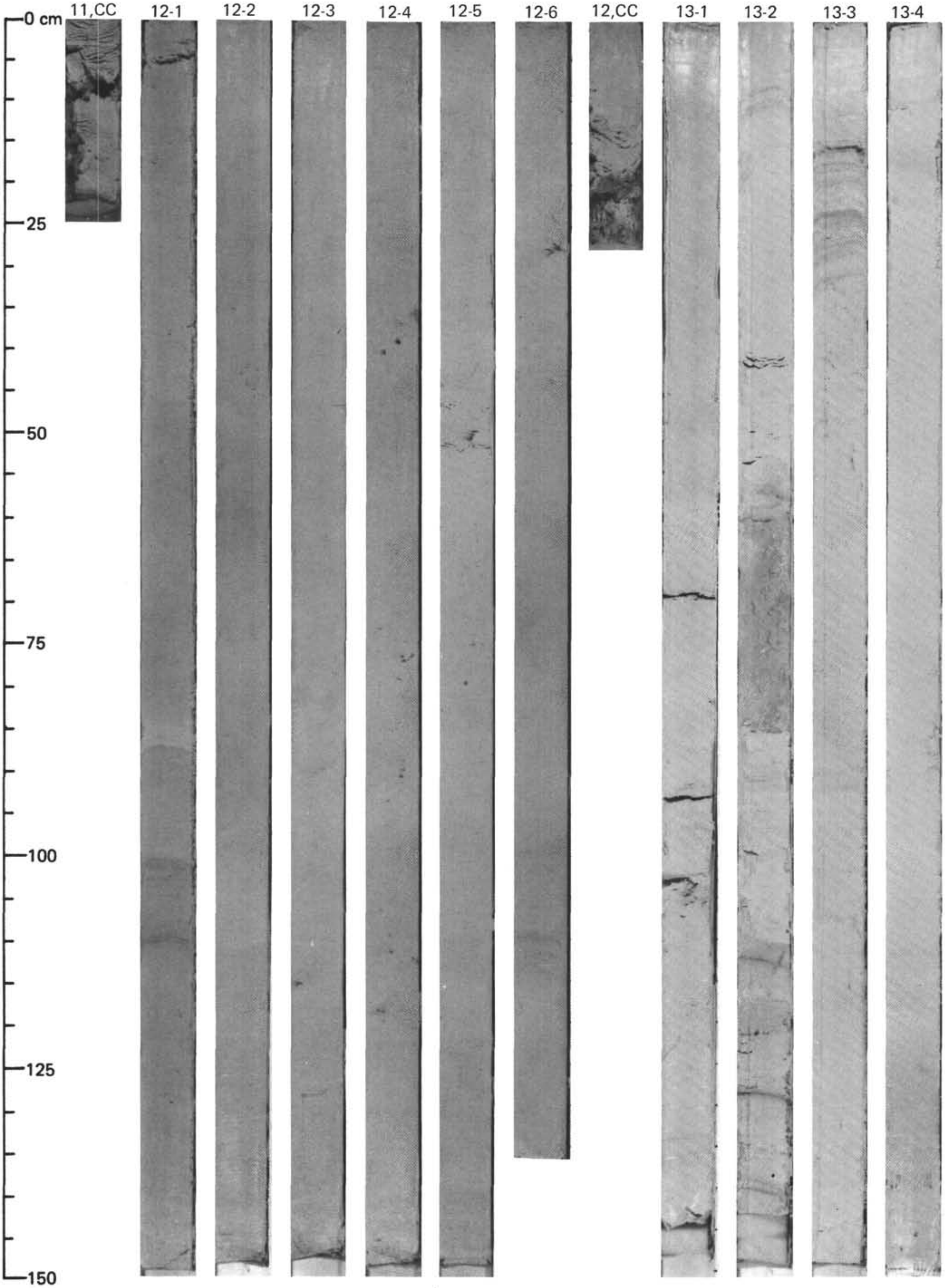
0 cm
25
50
75
100
125
150
11,CC
12-1
12-2
12-3
12-4
12-5
12-6
12,CC
13-1
13-2
13-3
13-4

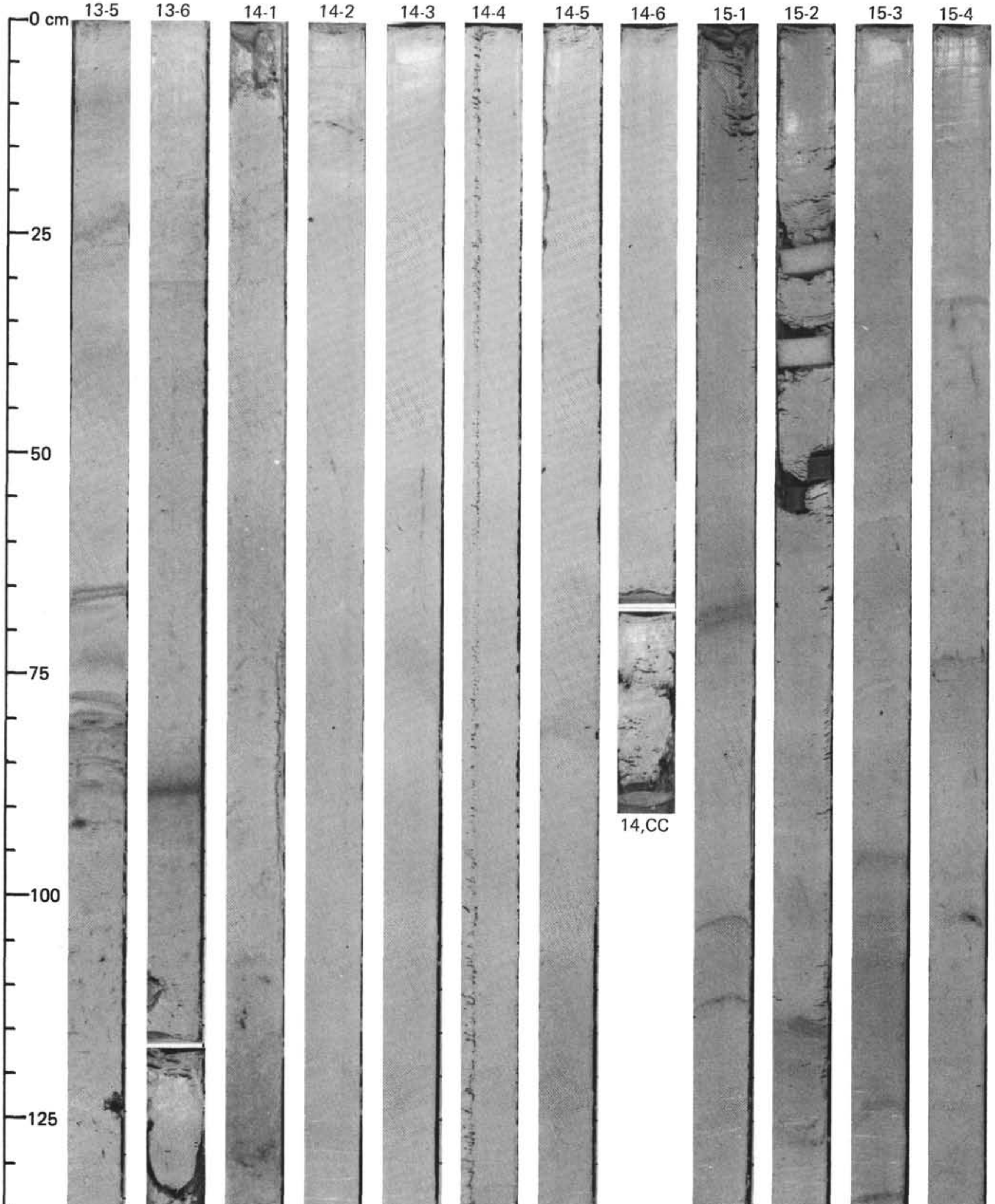
0 cm
25
50
75
100
125
150
13-5
13-6
13,CC
14-1
14-2
14-3
14-4
14-5
14-6
14,CC
15-1
15-2
15-3
15-4

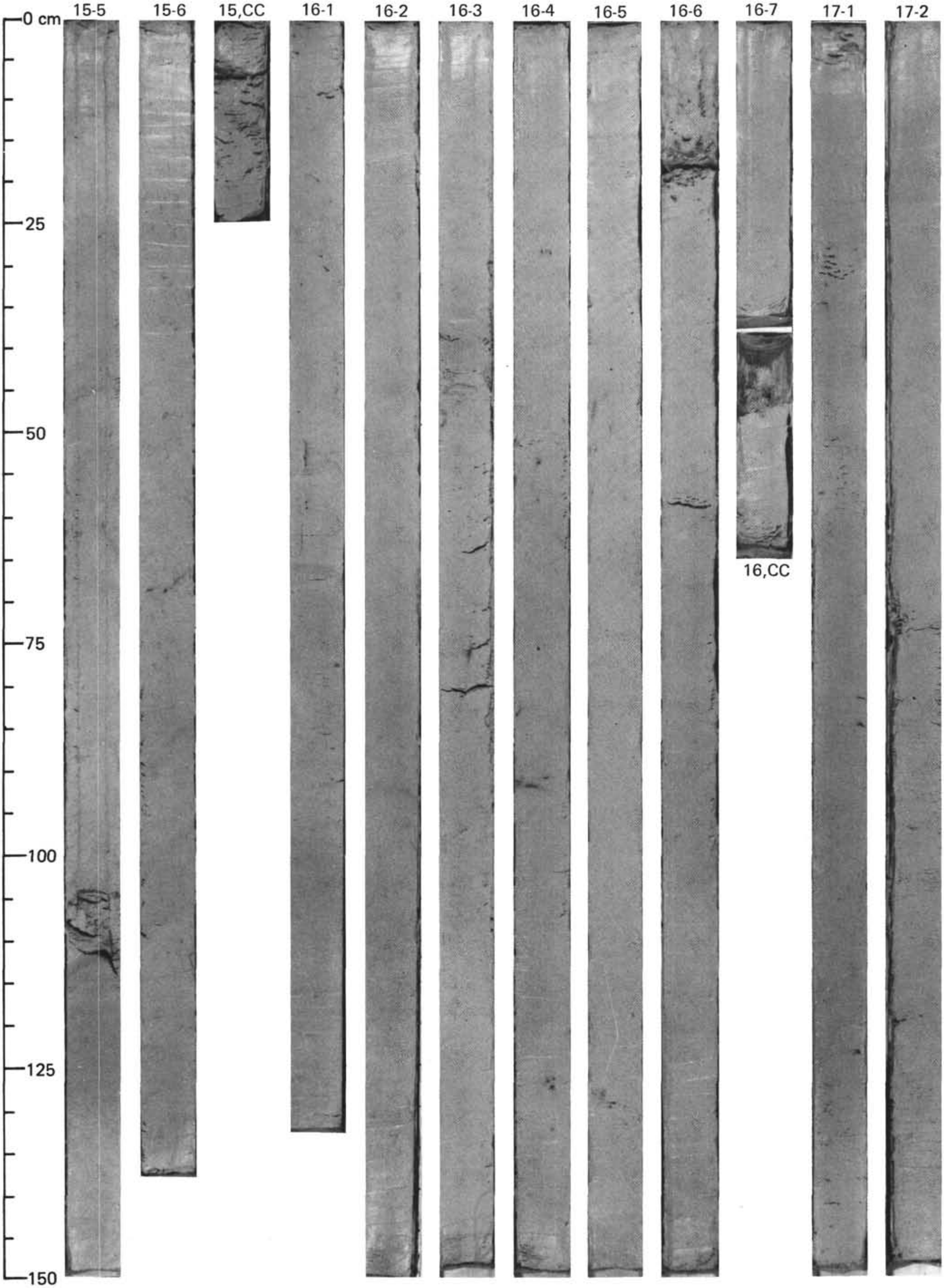
0 cm
25
50
75
100
125
150
15-5
15-6
15,CC
16-1
16-2
16-3
16-4
16-5
16-6
16-7
16,CC
17-1
17-2

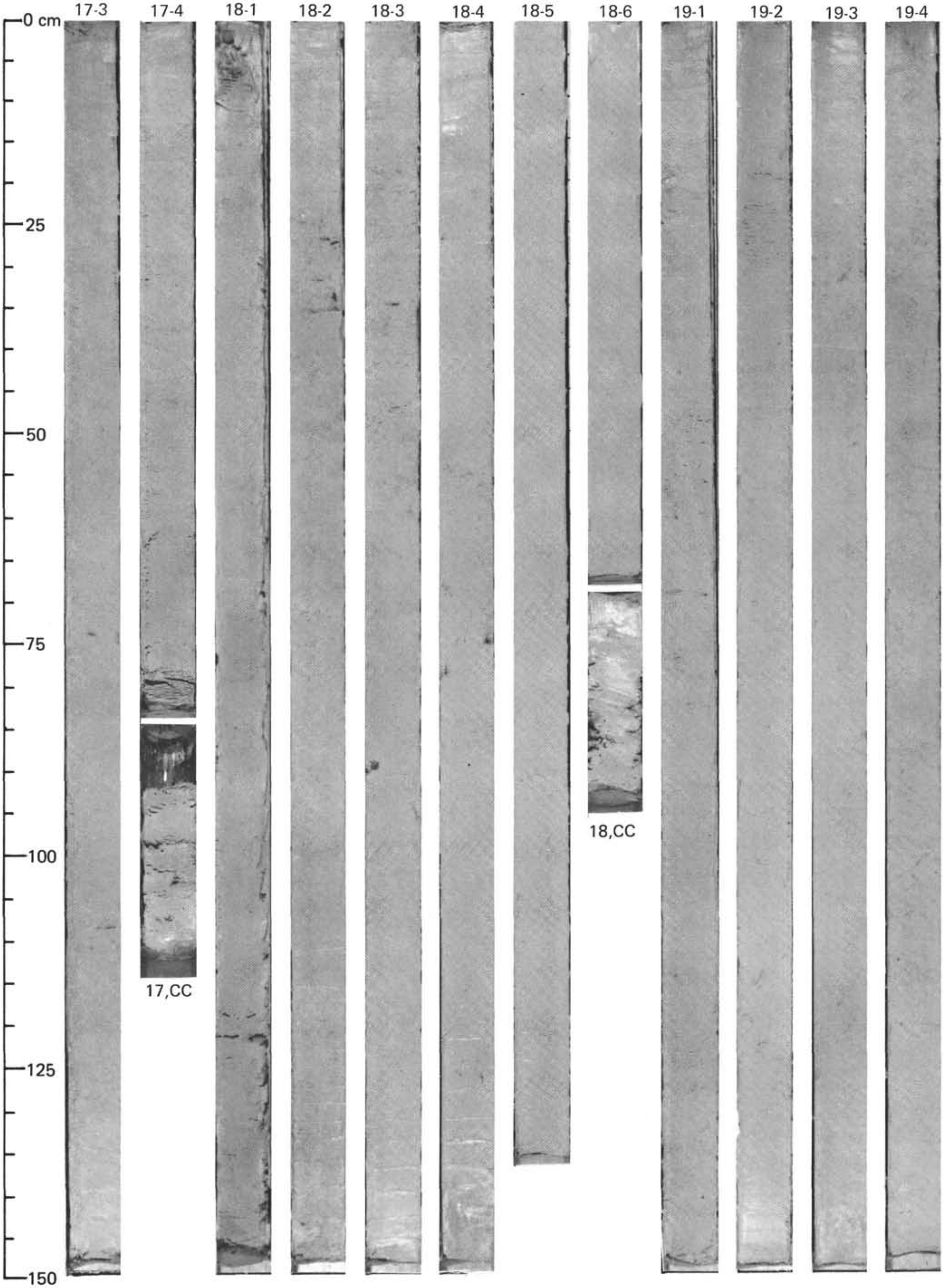
0 cm
25
50
75
100
125
150
17-3
17-4
17,CC
18-1
18-2
18-3
18-4
18-5
18-6
18,CC
19-1
19-2
19-3
19-4

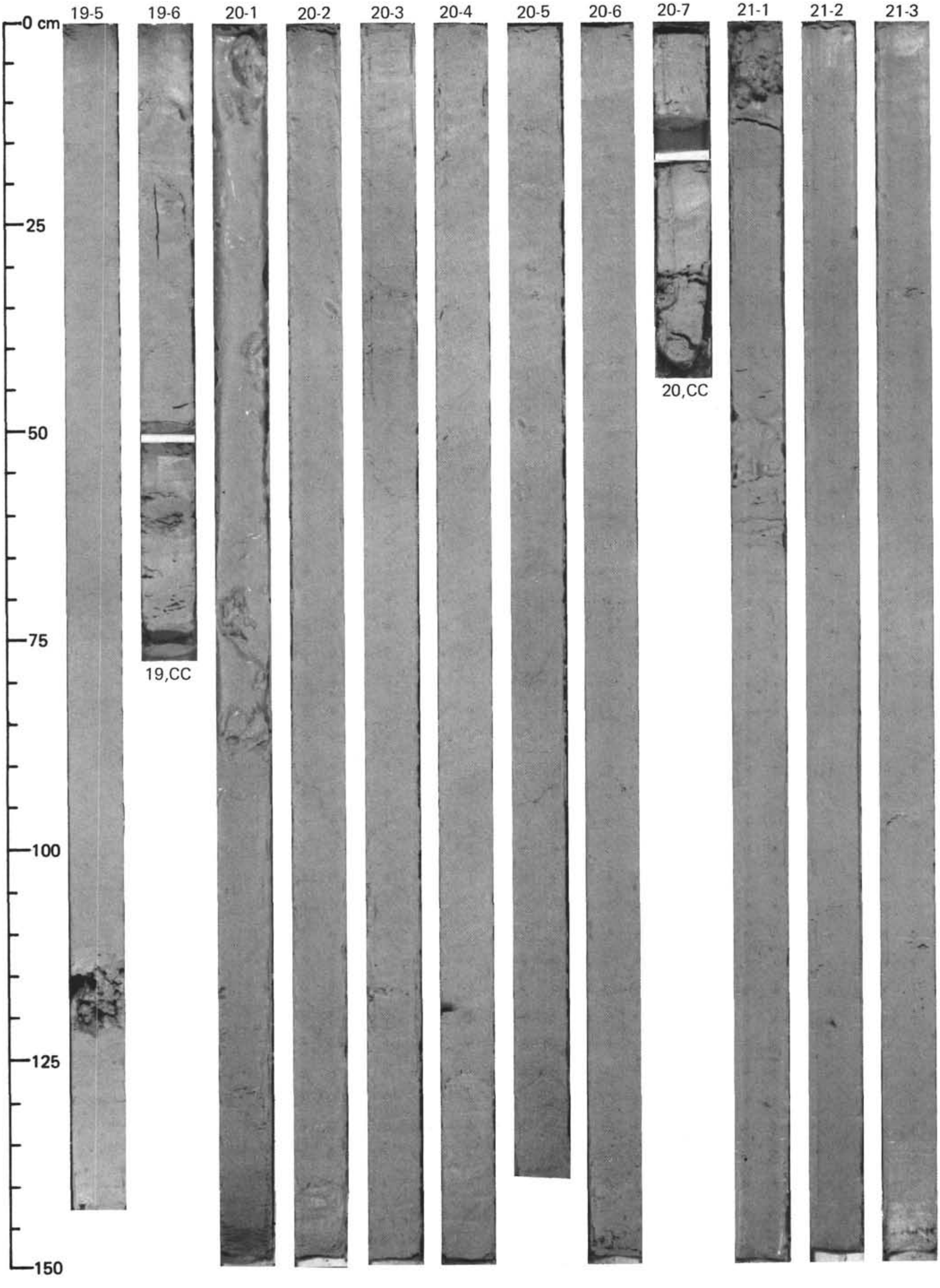
0 cm
25
50
75
100
125
150
19-5
19-6
20-1
20-2
20-3
20-4
20-5
20-6
20-7
21-1
21-2
21-3
19,CC
20,CC

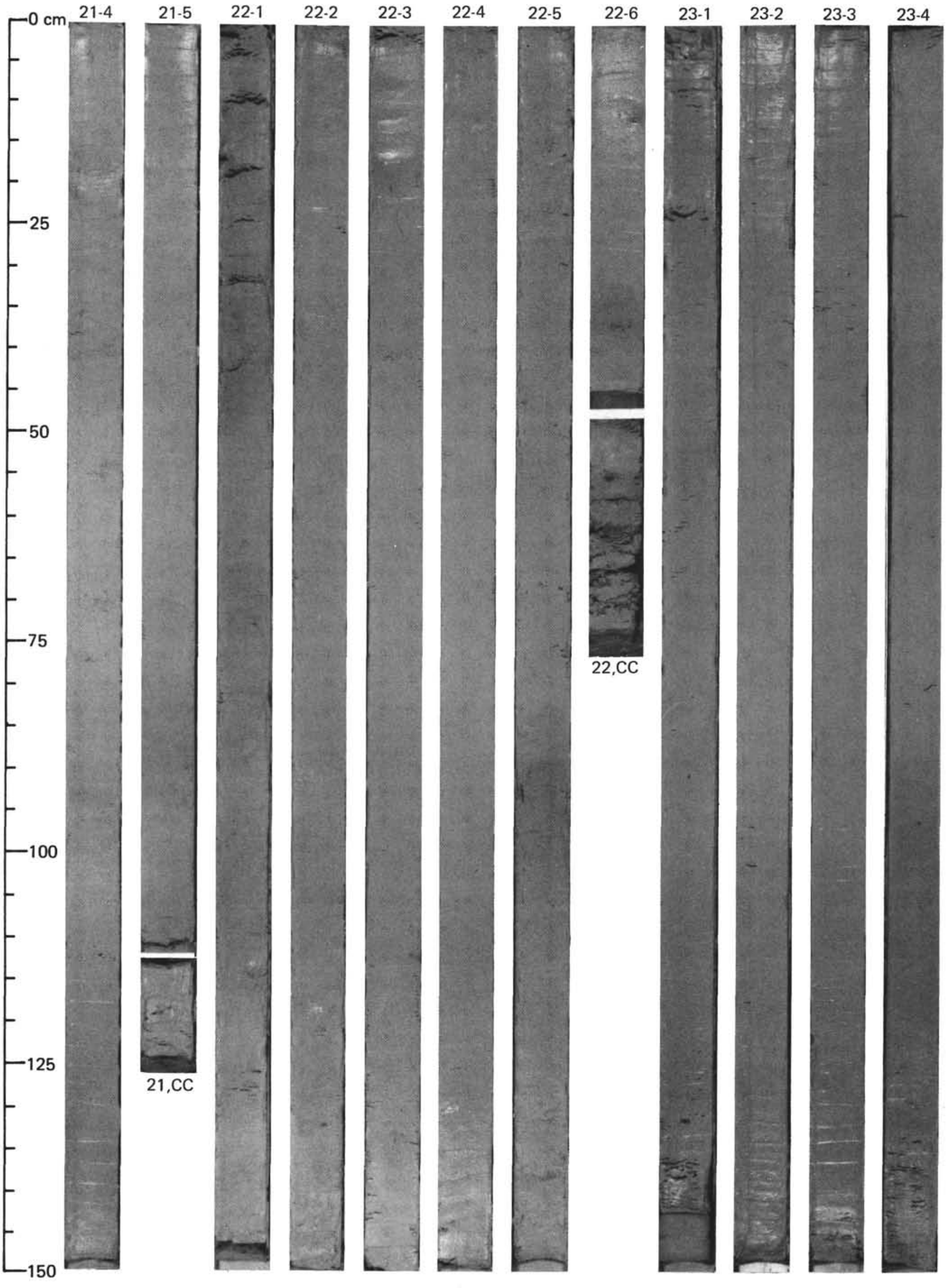
0 cm
25
50
75
100
125
150
21-4
21-5
21,CC
22-1
22-2
22-3
22-4
22-5
22-6
22,CC
23-1
23-2
23-3
23-4

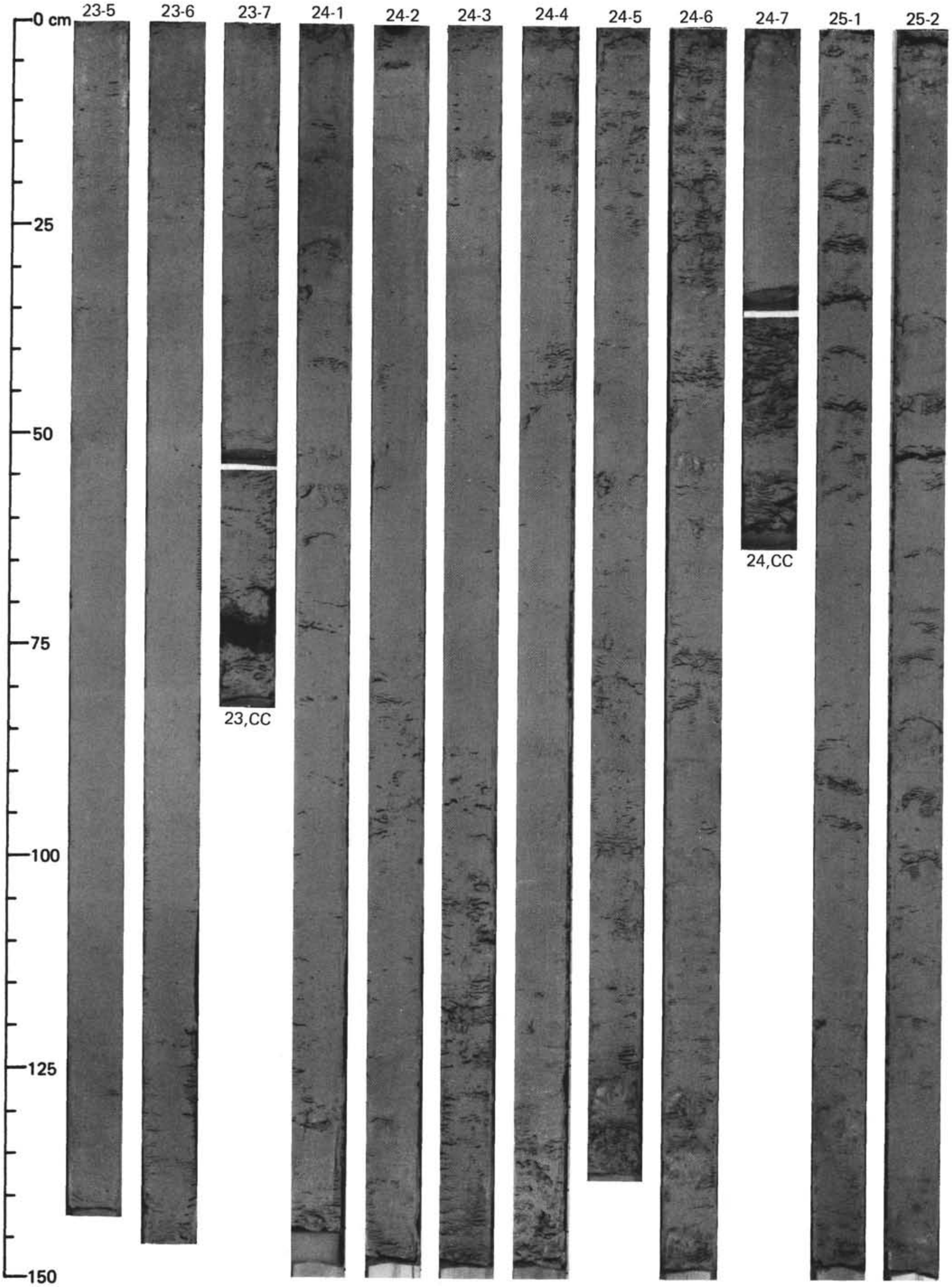
0 cm
25
50
75
100
125
150
23-5
23-6
23-7
23,CC
24-1
24-2
24-3
24-4
24-5
24-6
24-7
24,CC
25-1
25-2

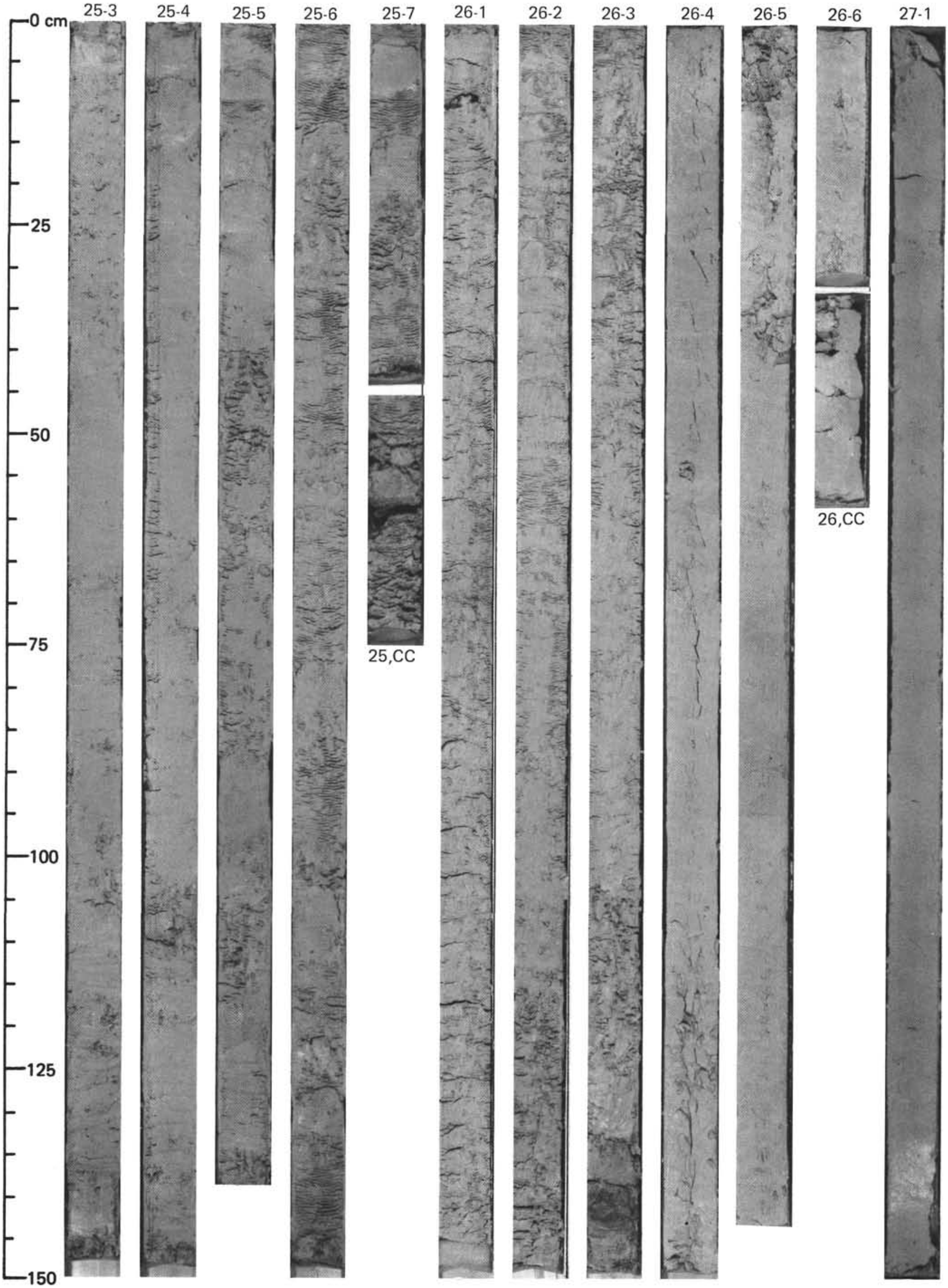
0 cm
25
50
75
100
125
150
25-3
25-4
25-5
25-6
25-7
26-1
26-2
26-3
26-4
26-5
26-6
27-1
25,CC
26,CC

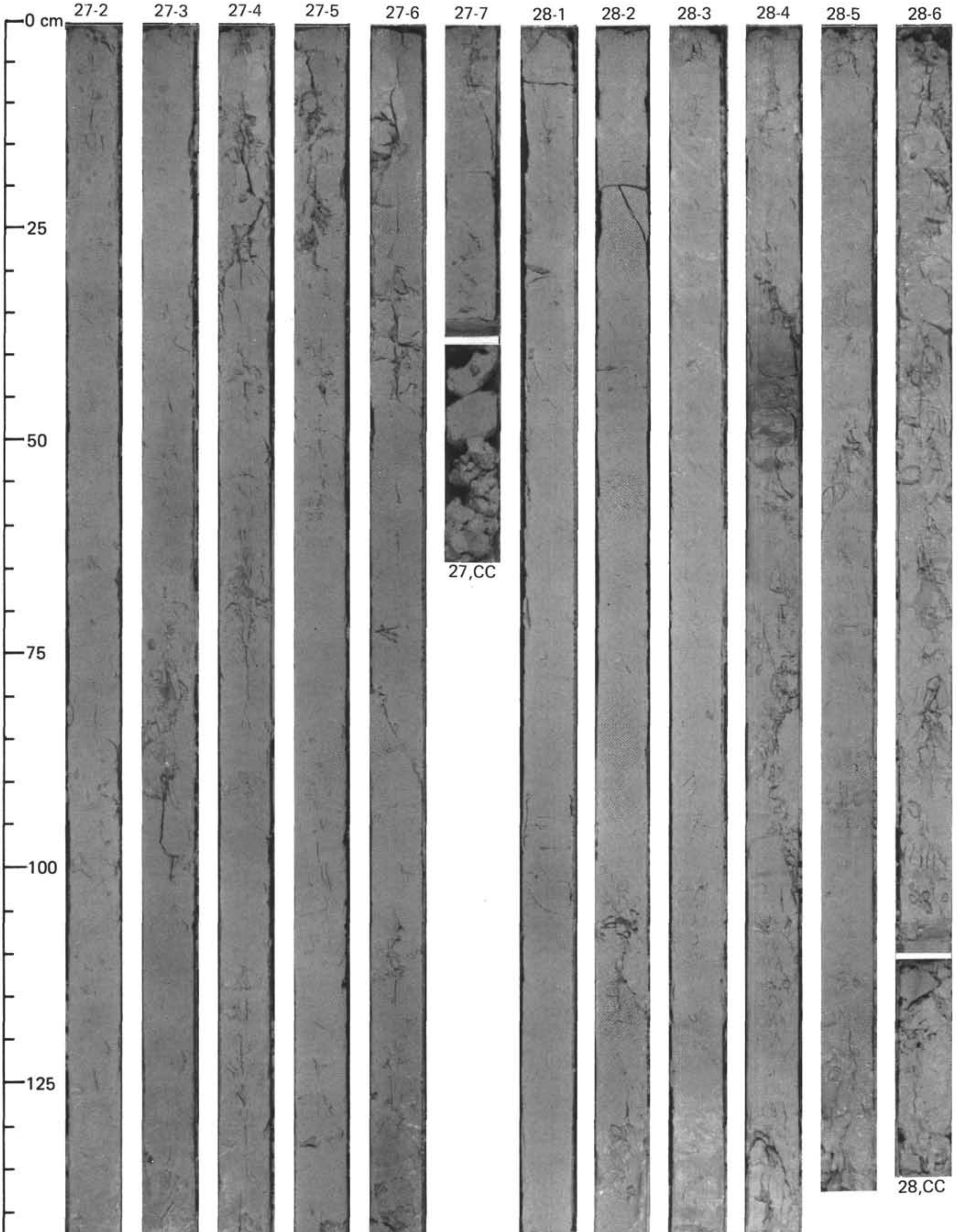
0 cm
25
50
75
100
125
150
27-2
27-3
27-4
27-5
27-6
27-7
27,CC
28-1
28-2
28-3
28-4
28-5
28-6
28,CC

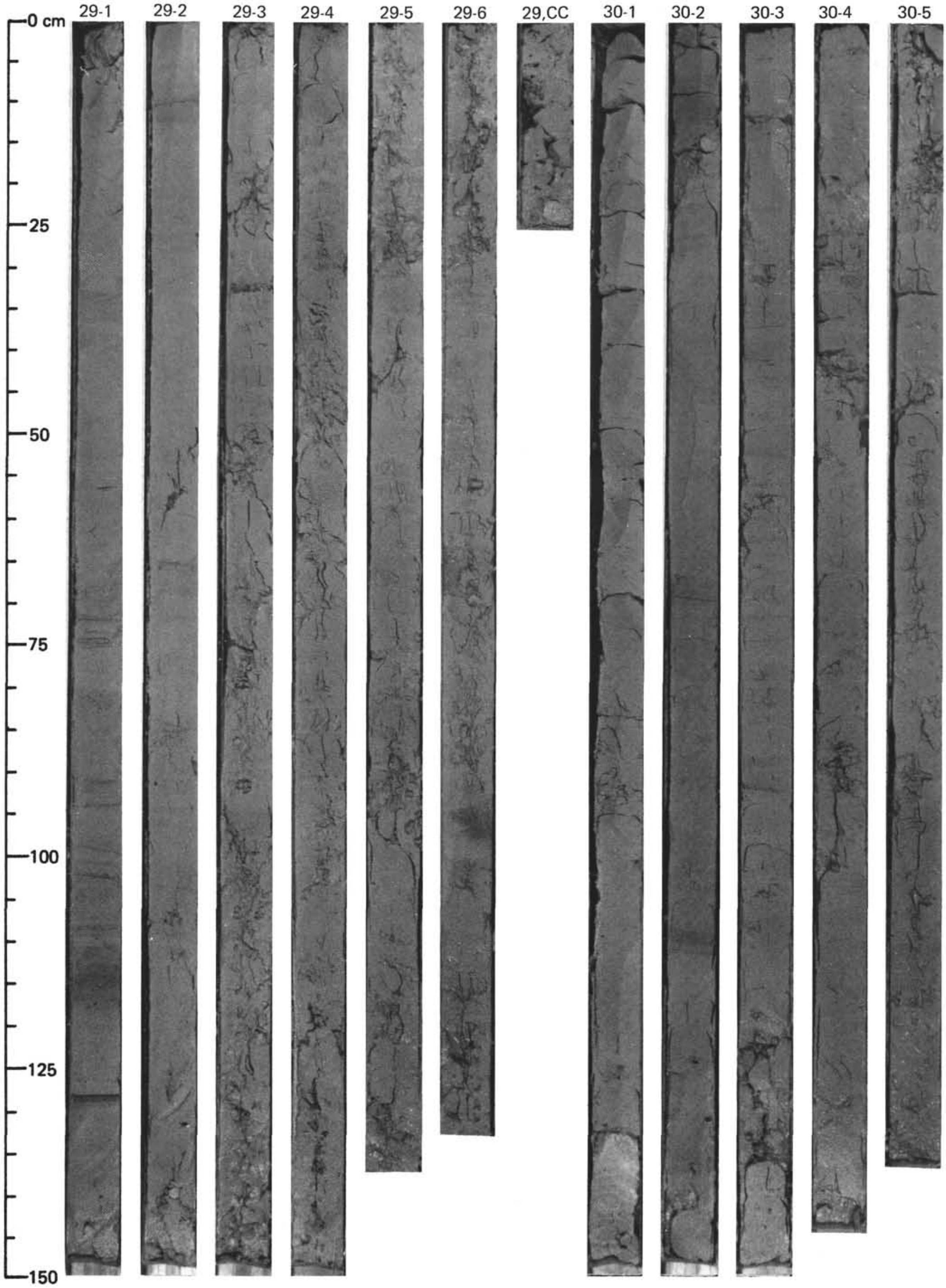

0 cm
25
50
75
100
125
150
29-1
29-2
29-3
29-4
29-5
29-6
29,CC
30-1
30-2
30-3
30-4
30-5

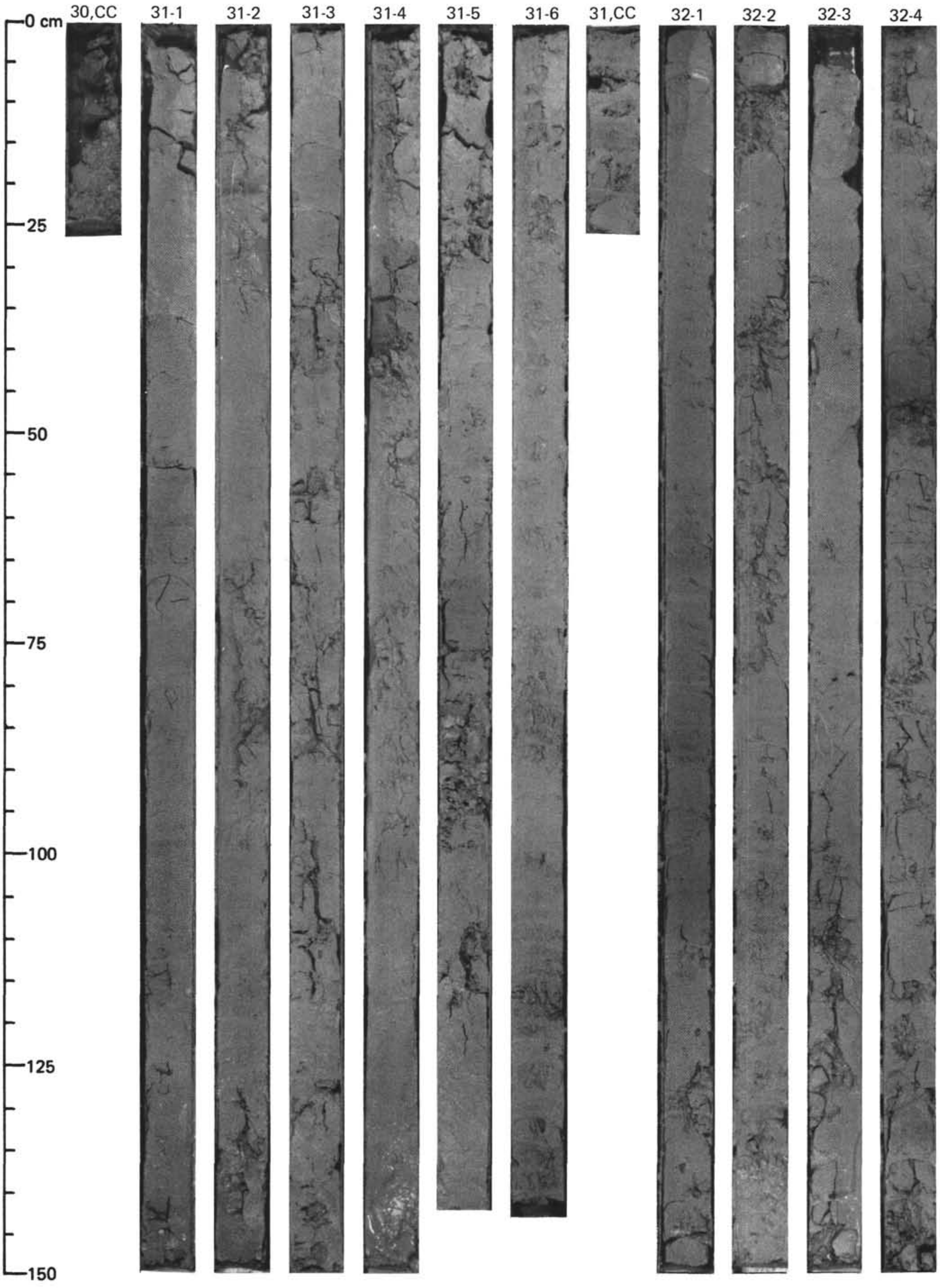
30,CC
31-1
31-2
31-3
31-4
31-5
31-6
31,CC
32-1
32-2
32-3
32-4
0 cm
25
50
75
100
125
150

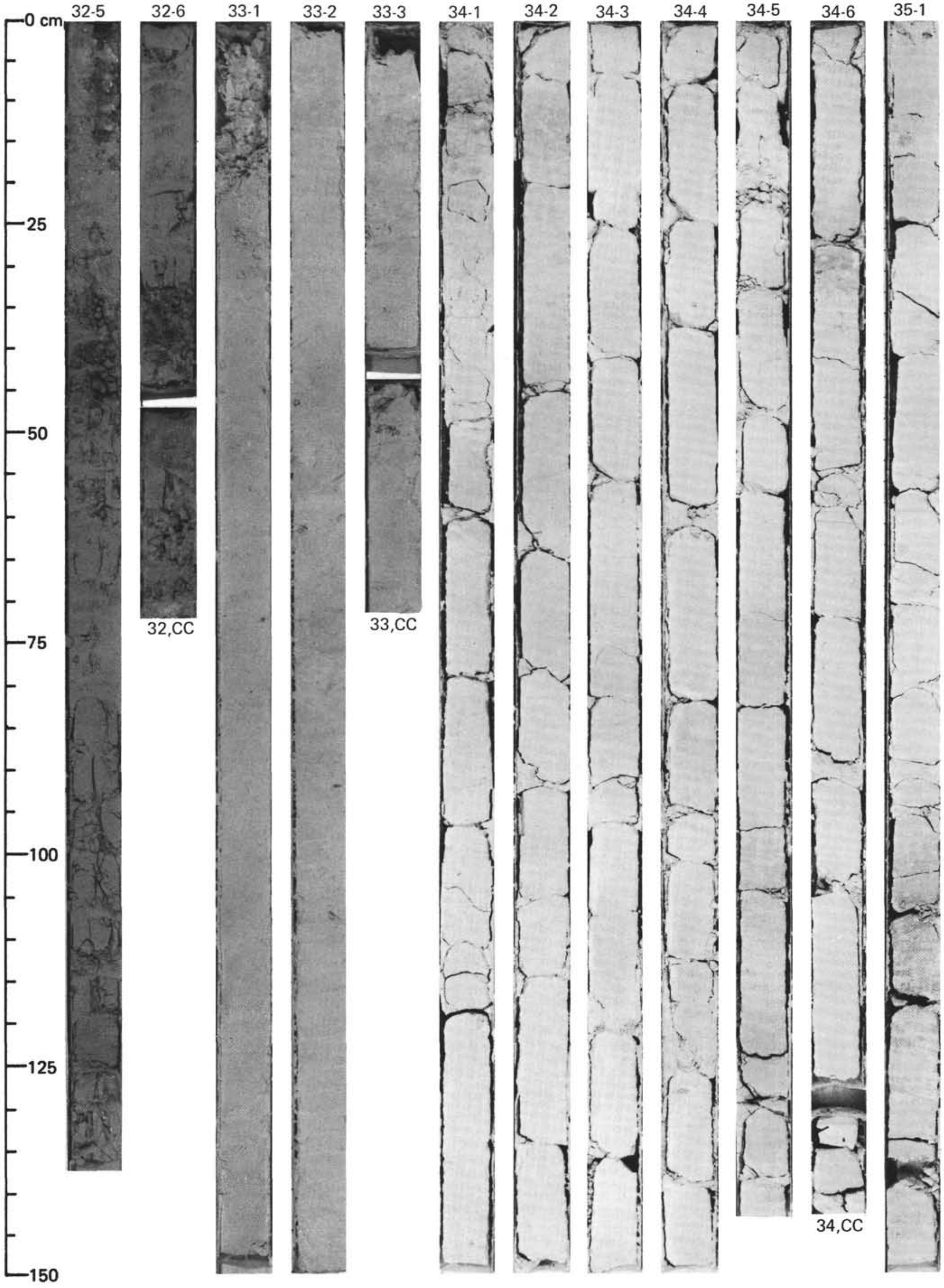
0 cm
25
50
75
100
125
150
32-5
32-6
33-1
33-2
33-3
34-1
34-2
34-3
34-4
34-5
34-6
35-1
32,CC
33,CC
34,CC

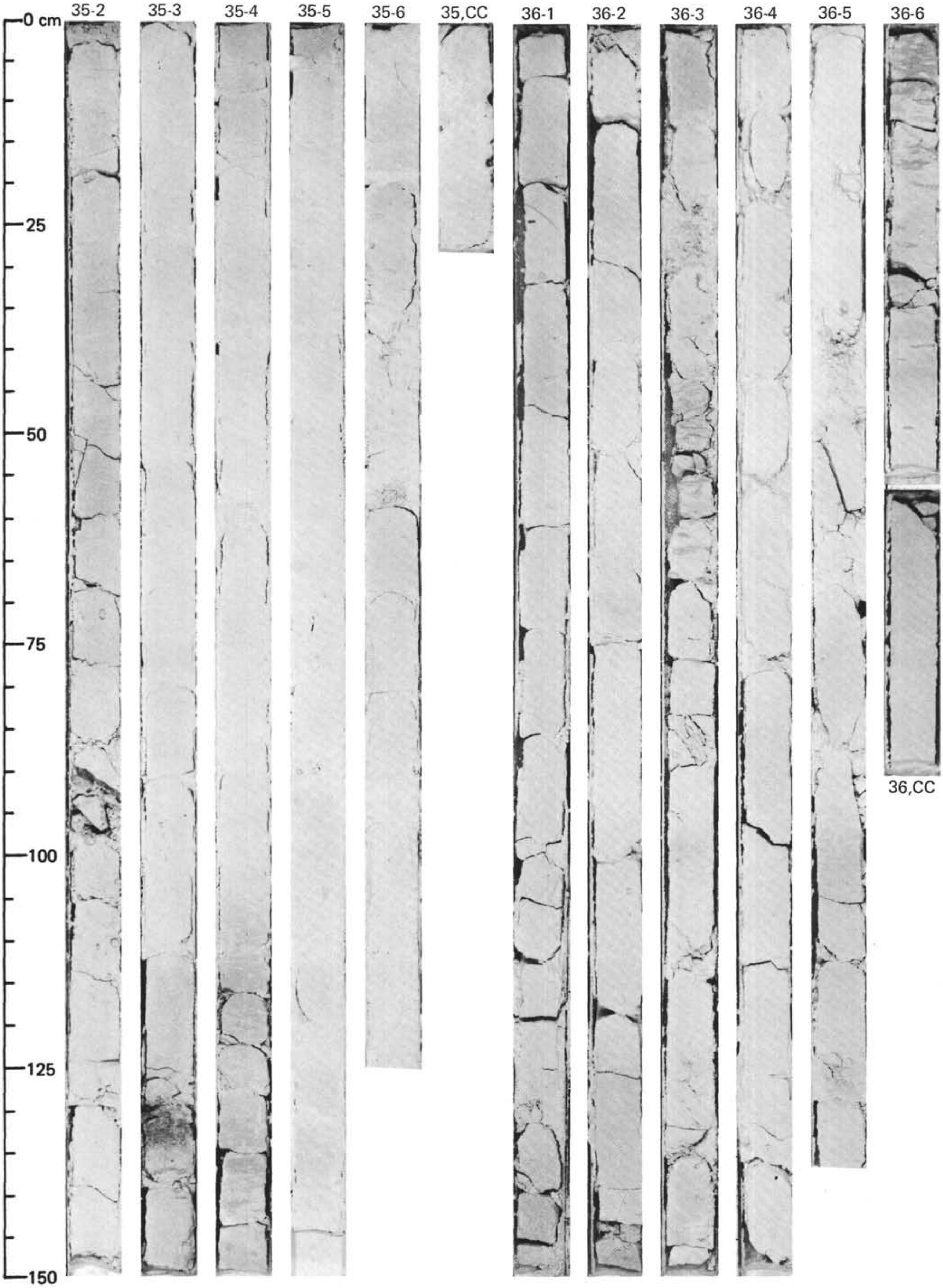
0 cm
25
50
75
100
125
150
35-2
35-3
35-4
35-5
35-6
35,CC
36-1
36-2
36-3
36-4
36-5
36-6
36,CC

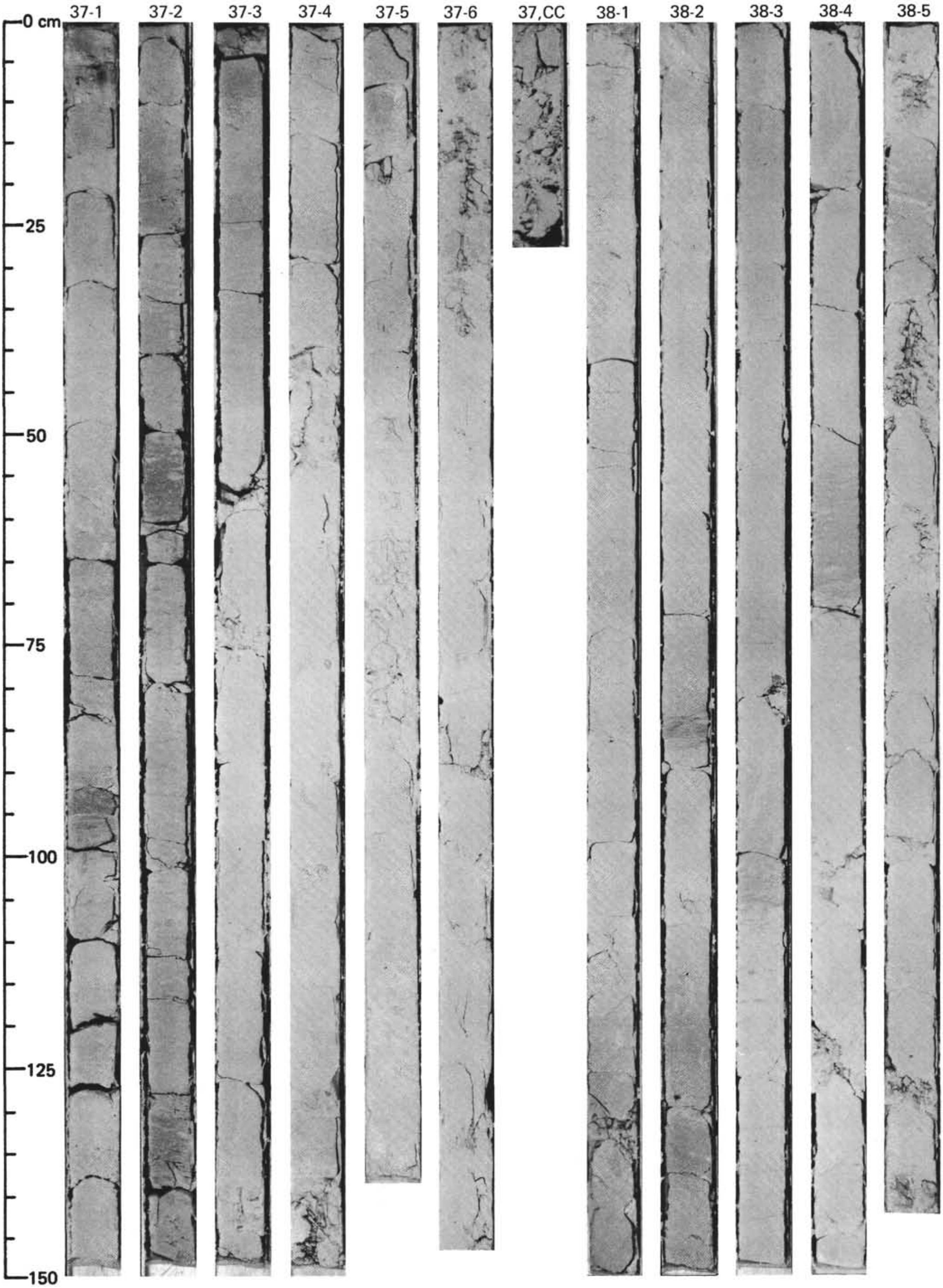
37-1
37-2
37-3
37-4
37-5
37-6
37,CC
38-1
38-2
38-3
38-4
38-5
0 cm
25
50
75
100
125
150

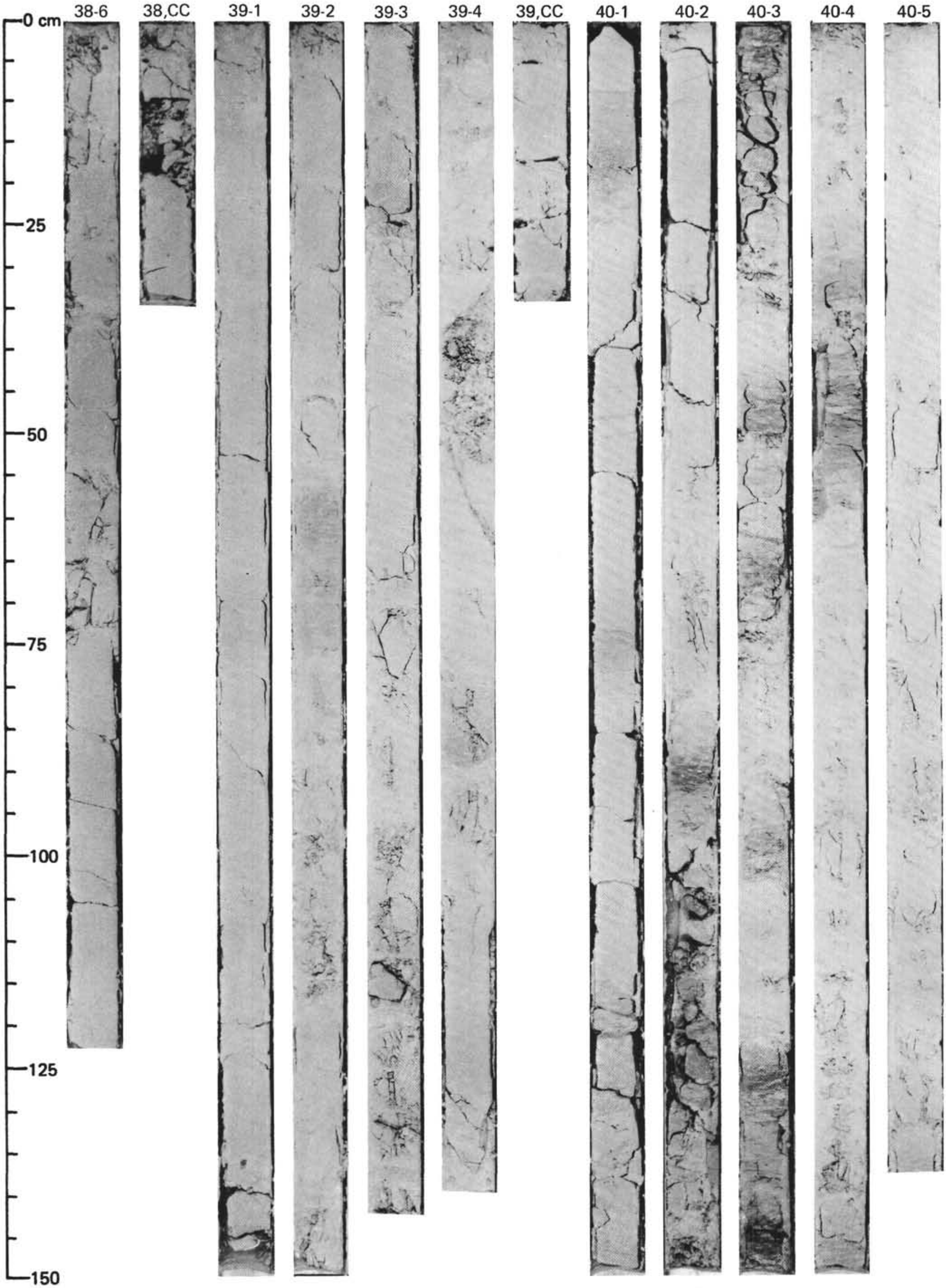
38-6
38,CC
39-1
39-2
39-3
39-4
39,CC
40-1
40-2
40-3
40-4
40-5
0 cm
25
50
75
100
125
150

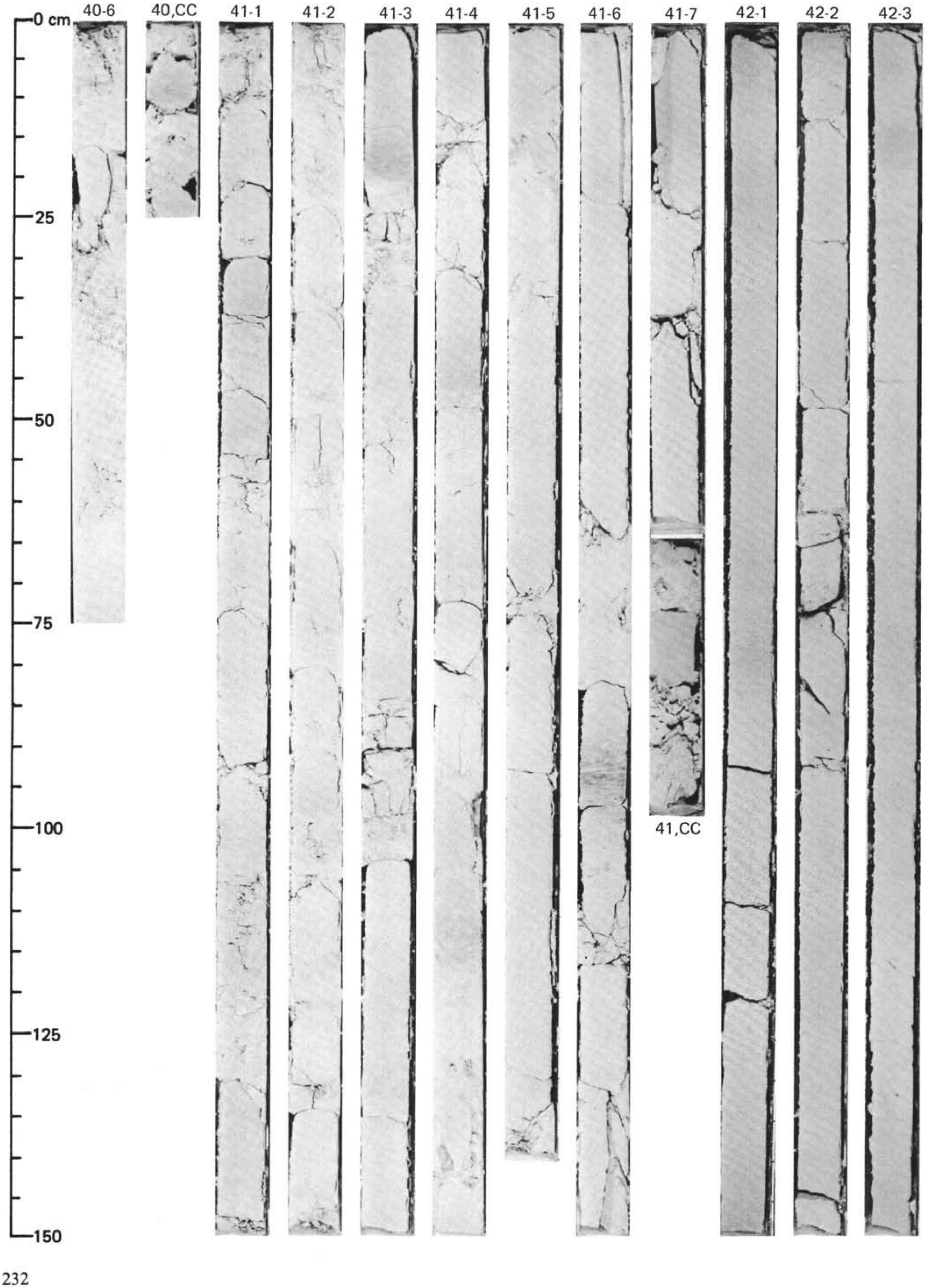
0 cm
25
50
75
100
125
150
40-6
40,CC
41-1
41-2
41-3
41-4
41-5
41-6
41-7
41,CC
42-1
42-2
42-3

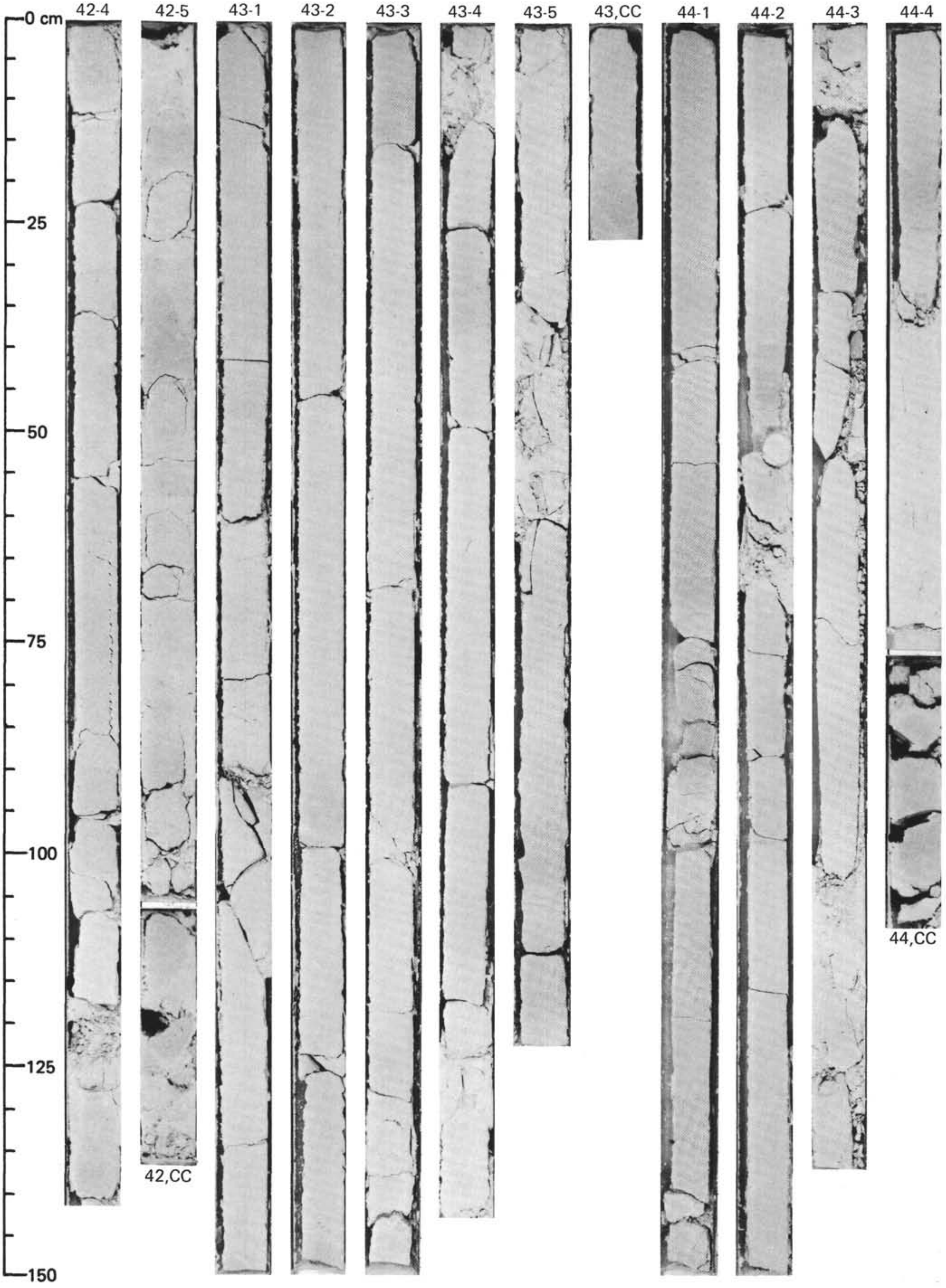
0 cm
25
50
75
100
125
150
42-4
42-5
42,CC
43-1
43-2
43-3
43-4
43-5
43,CC
44-1
44-2
44-3
44-4
44,CC

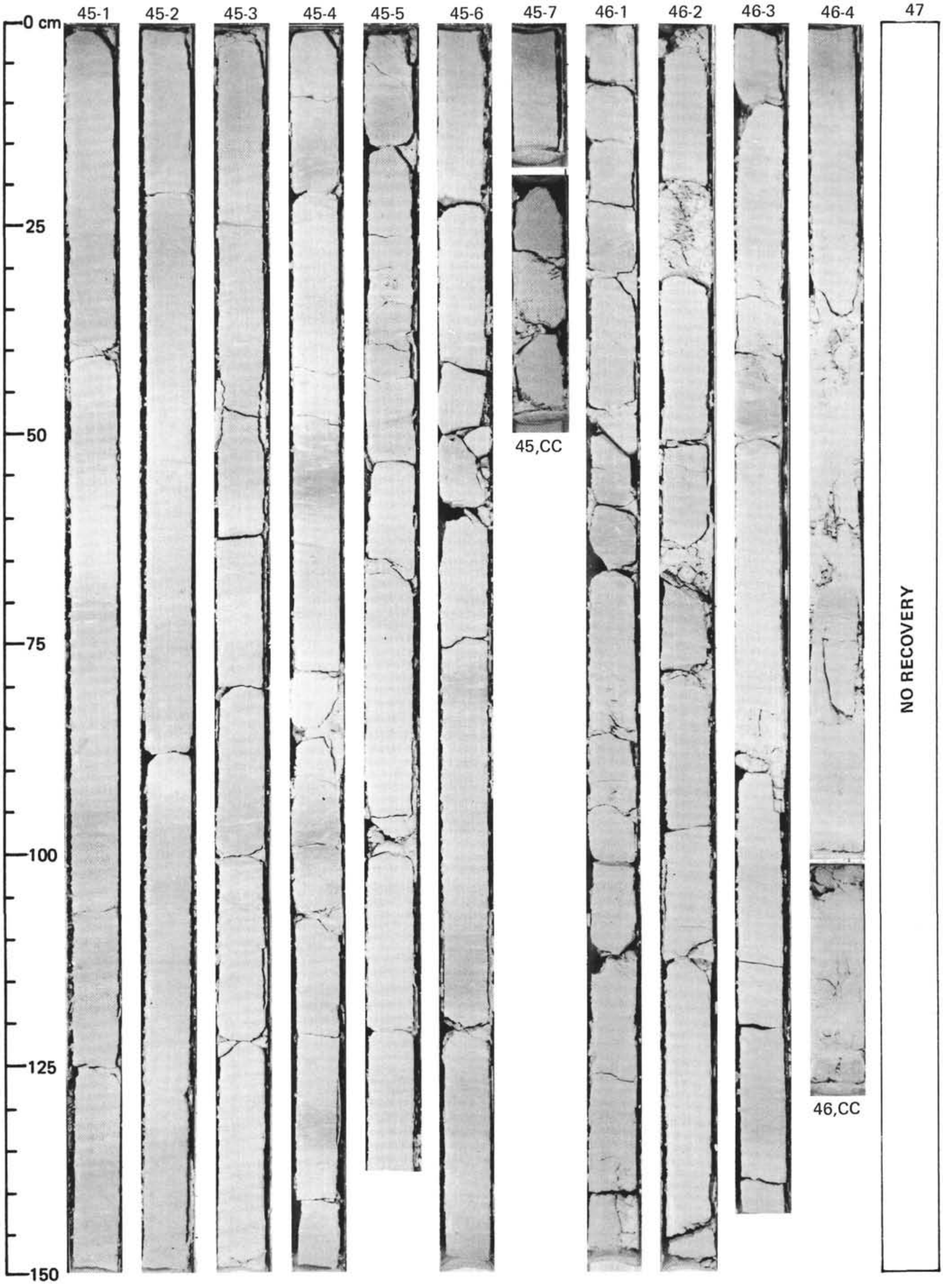
0 cm
25
50
75
100
125
150
45-1
45-2
45-3
45-4
45-5
45-6
45-7
45,CC
46-1
46-2
46-3
46-4
46,CC
47
NO RECOVERY

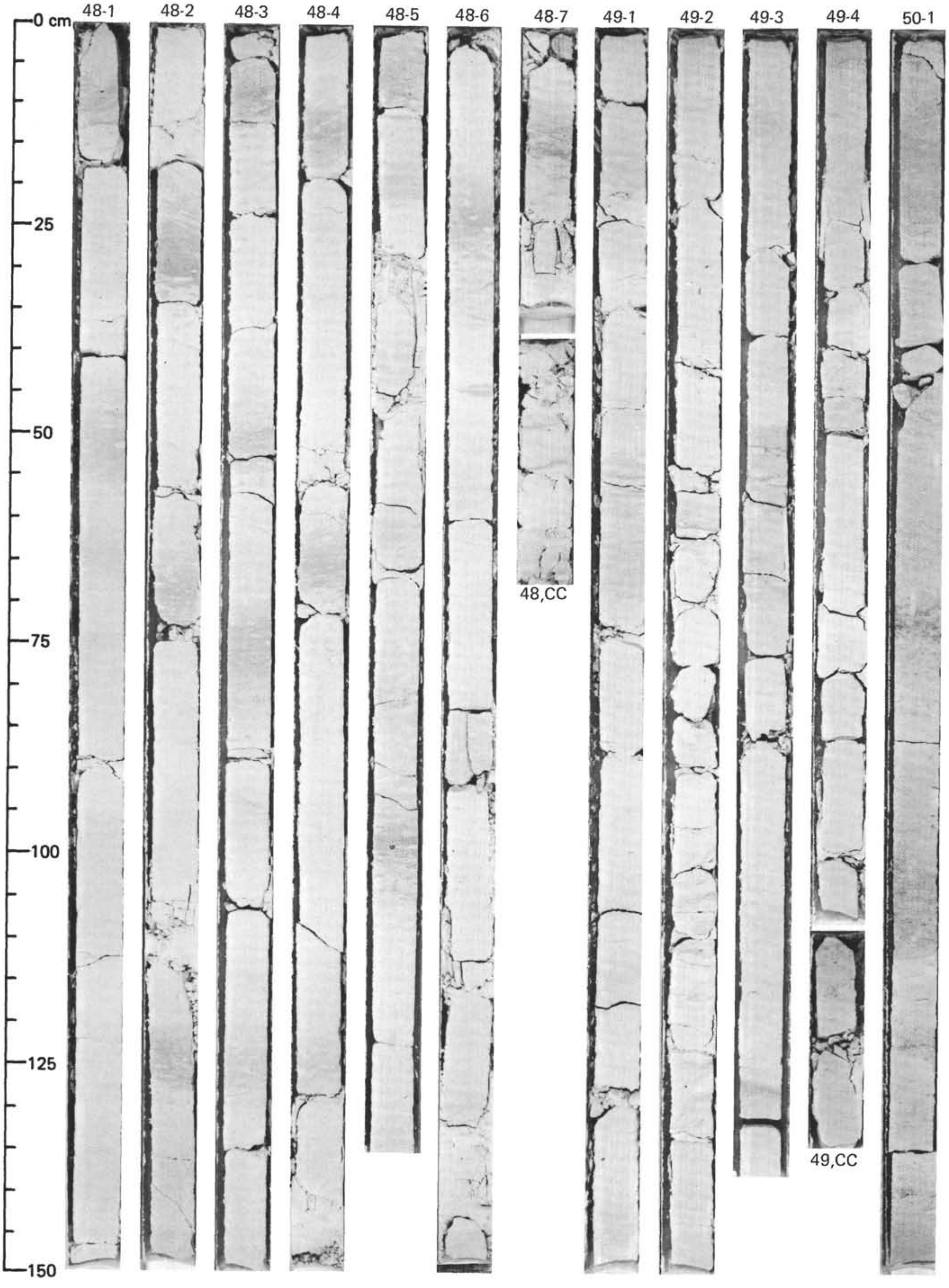
0 cm
25
50
75
100
125
150
48-1
48-2
48-3
48-4
48-5
48-6
48-7
48,CC
49-1
49-2
49-3
49-4
49,CC
50-1

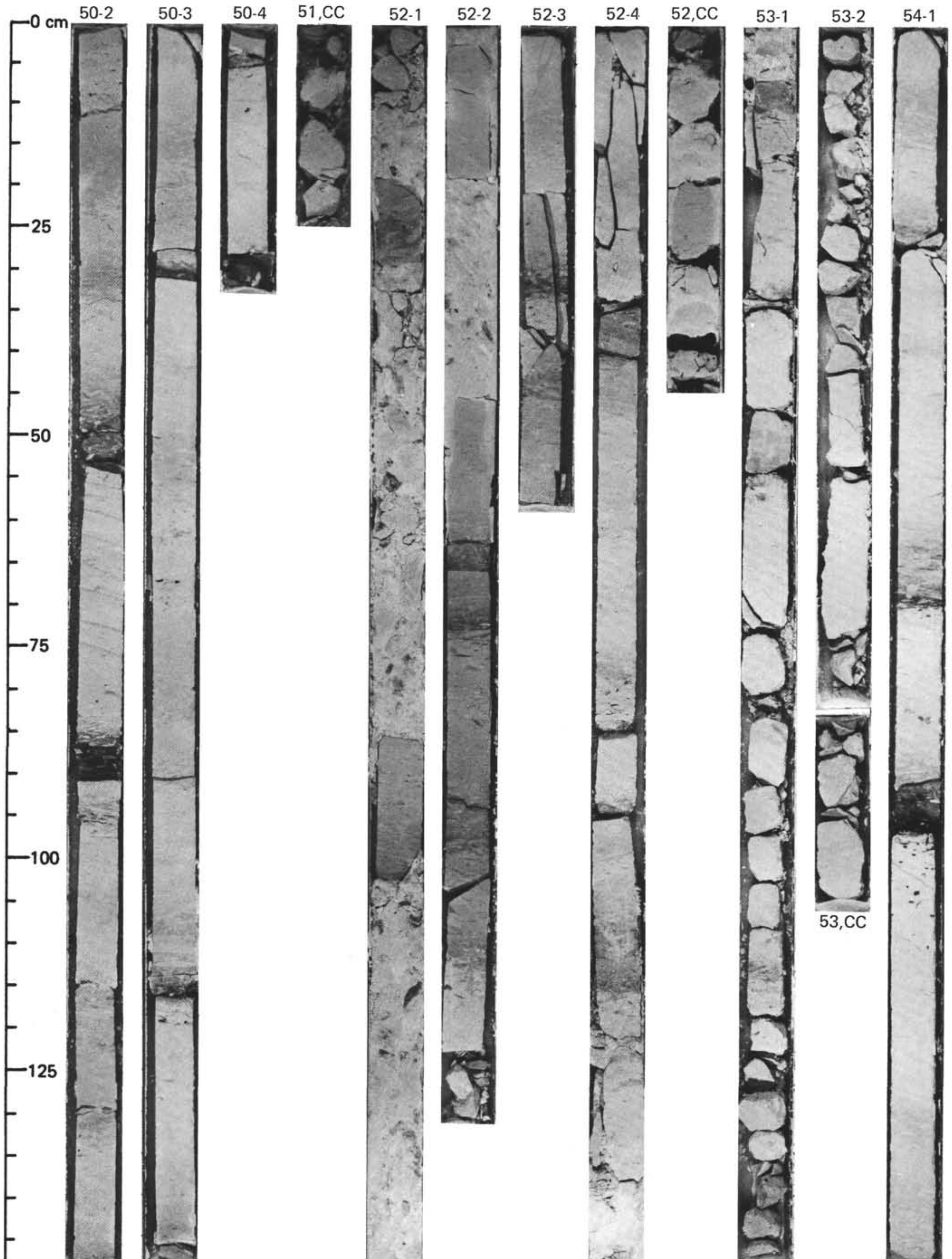
0 cm
25
50
75
100
125
150
50-2
50-3
50-4
51,CC
52-1
52-2
52-3
52-4
52,CC
53-1
53-2
53,CC
54-1

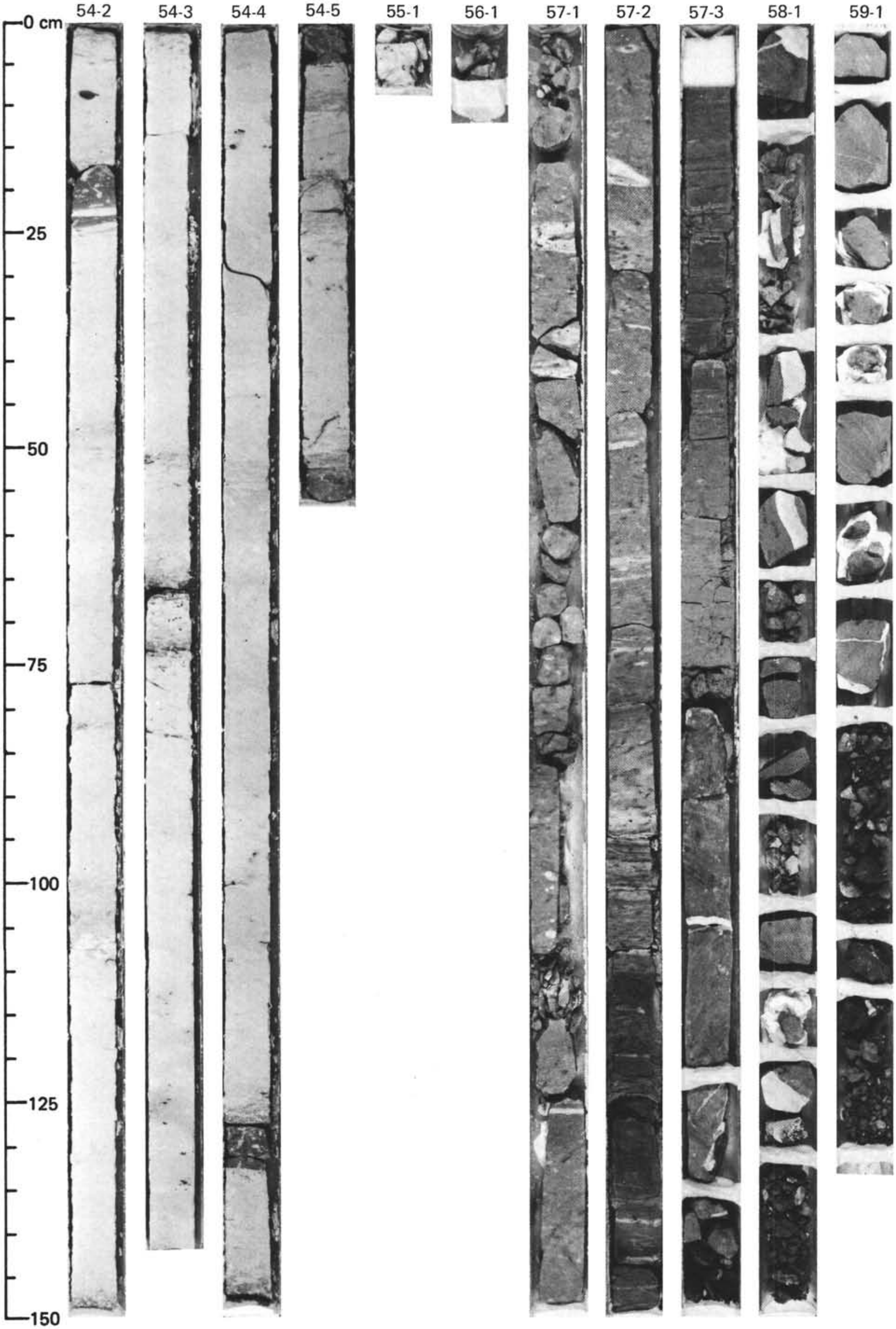
0 cm
25
50
75
100
125
150
54-2
54-3
54-4
54-5
55-1
56-1
57-1
57-2
57-3
58-1
59-1

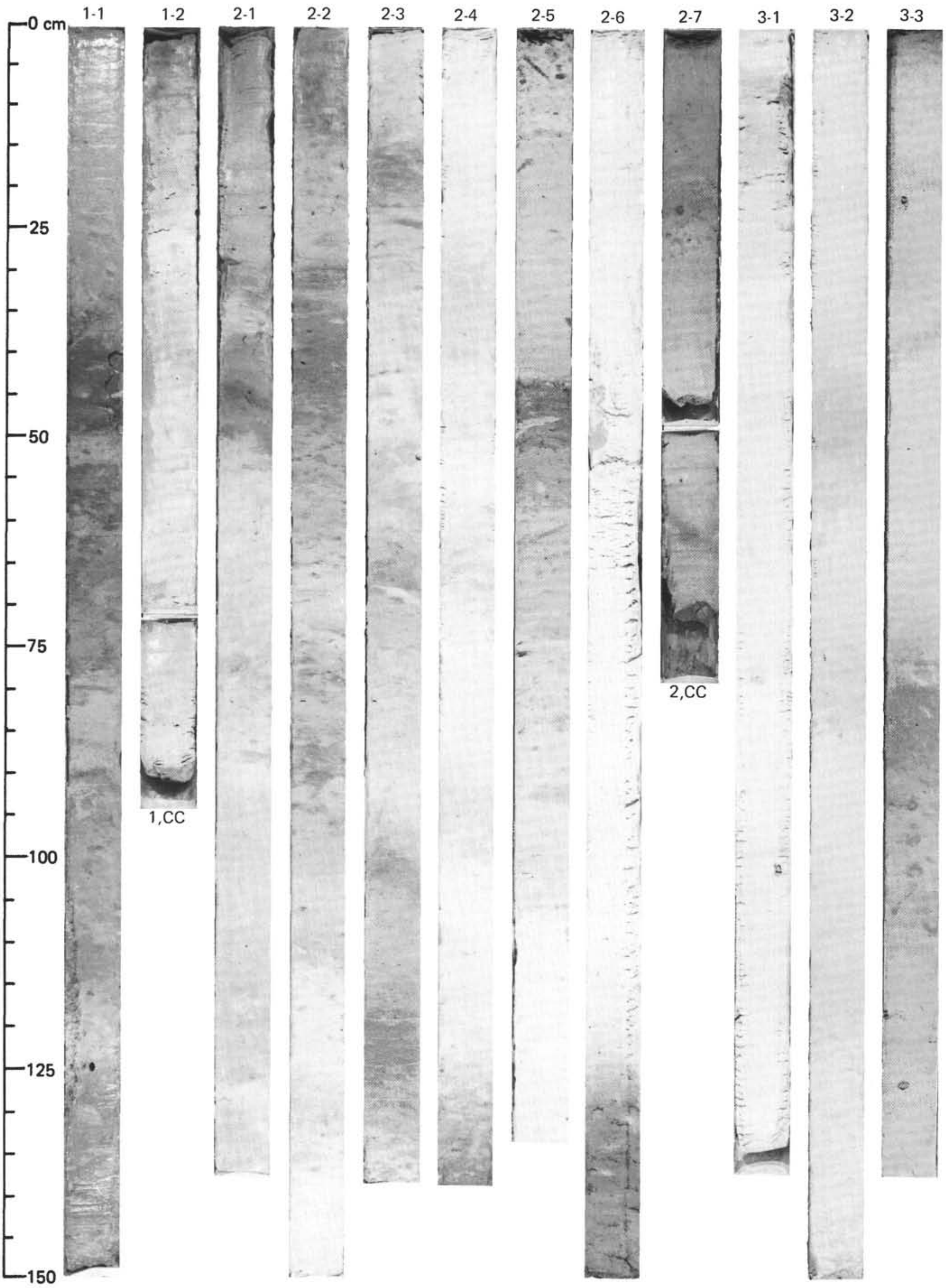
0 cm
25
50
75
100
125
150
1-1
1-2
1,CC
2-1
2-2
2-3
2-4
2-5
2-6
2-7
2,CC
3-1
3-2
3-3

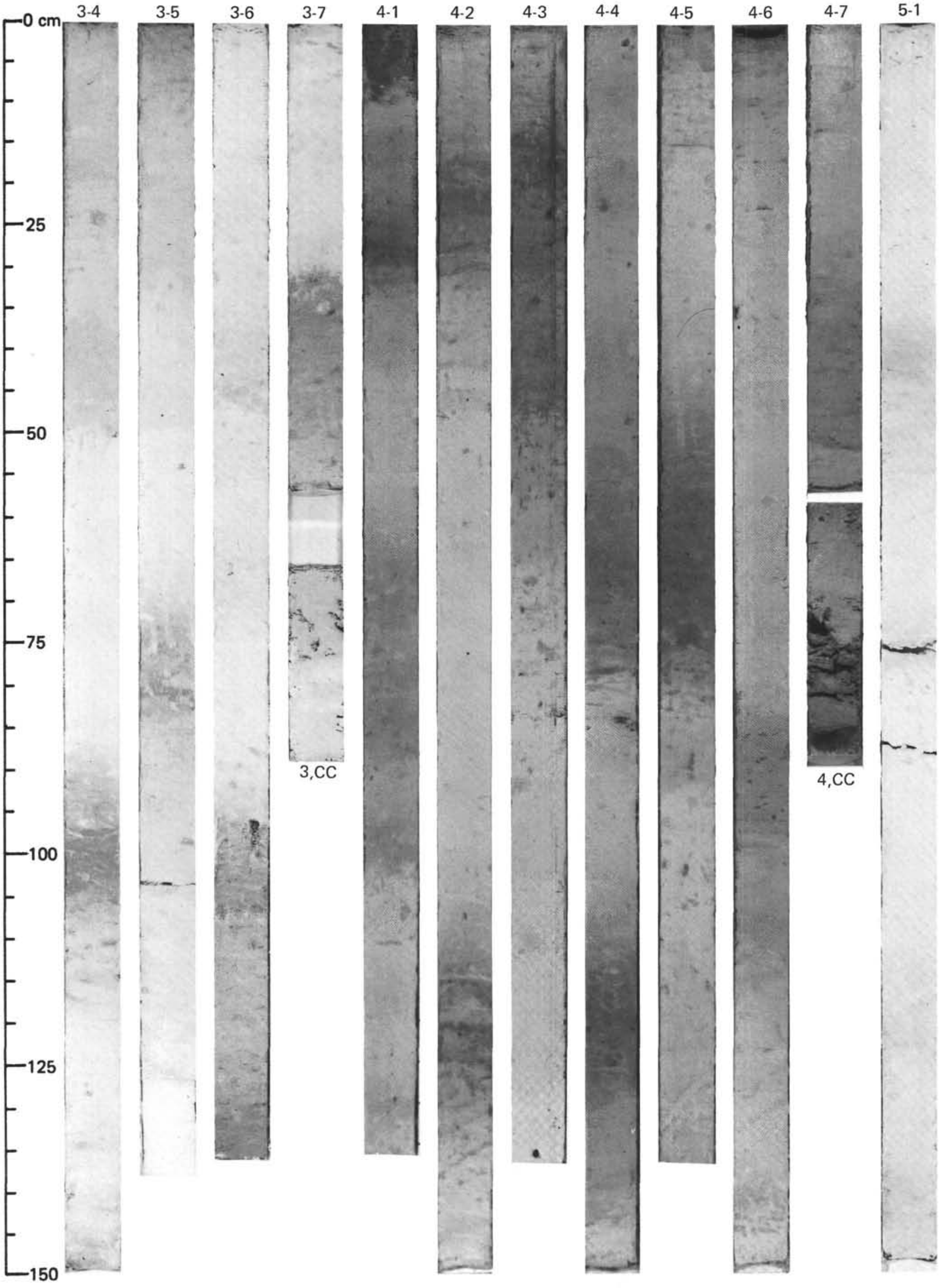
0 cm
25
50
75
100
125
150
3-4
3-5
3-6
3-7
4-1
4-2
4-3
4-4
4-5
4-6
4-7
5-1
3,CC
4,CC

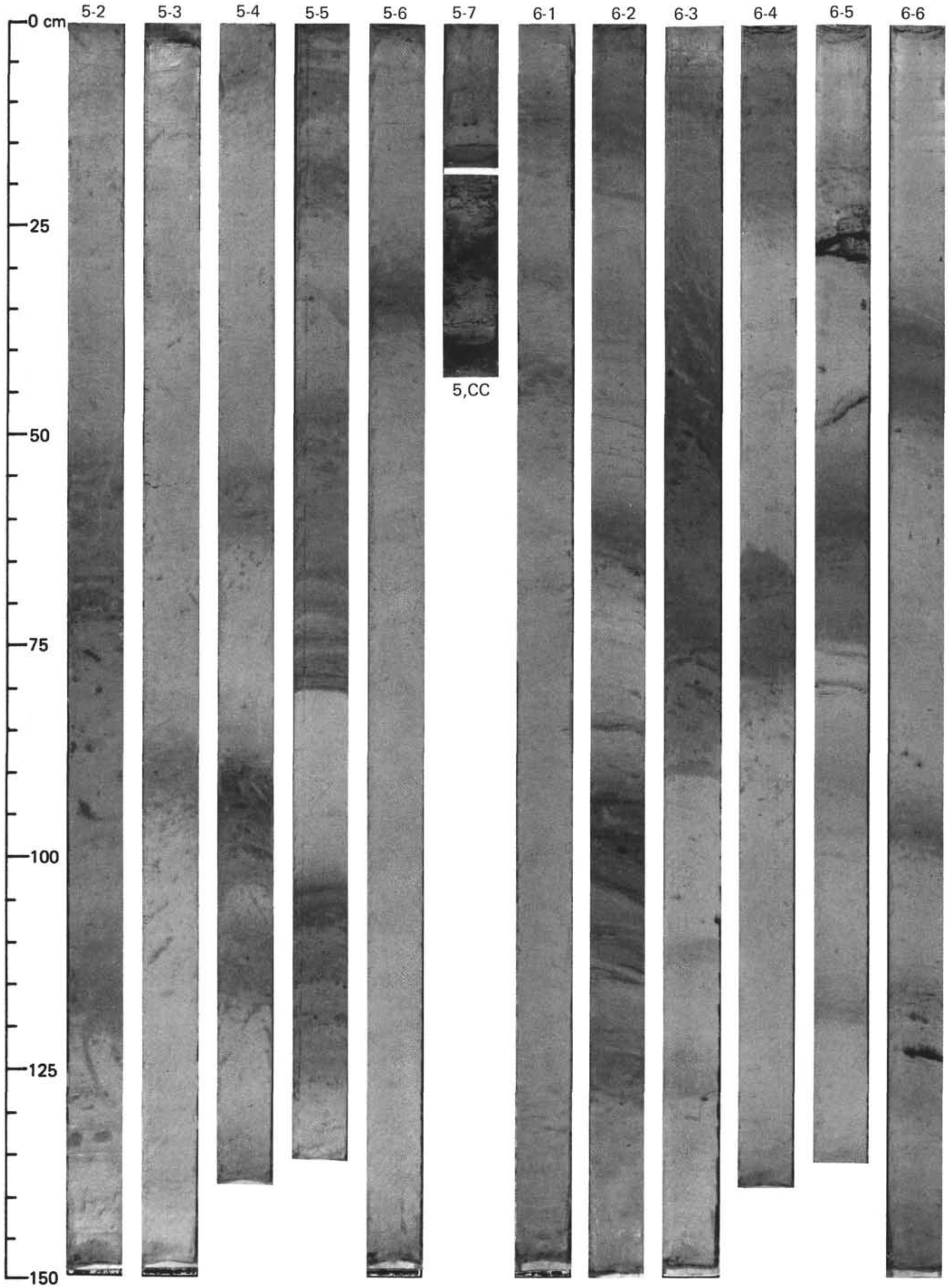
0 cm
25
50
75
100
125
150
5-2
5-3
5-4
5-5
5-6
5-7
5,CC
6-1
6-2
6-3
6-4
6-5
6-6

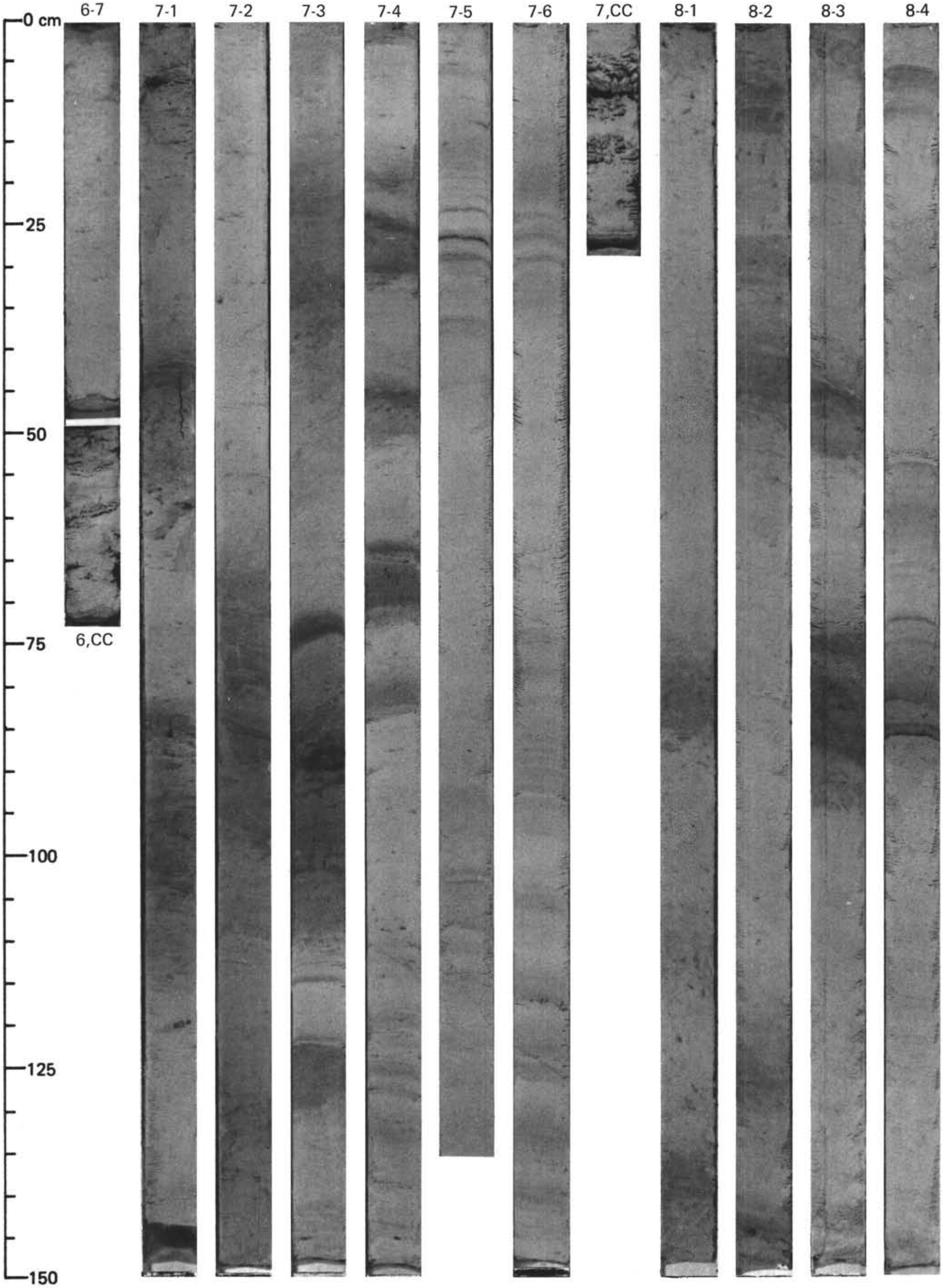
0 cm
25
50
75
100
125
150
6-7
6,CC
7-1
7-2
7-3
7-4
7-5
7-6
7,CC
8-1
8-2
8-3
8-4

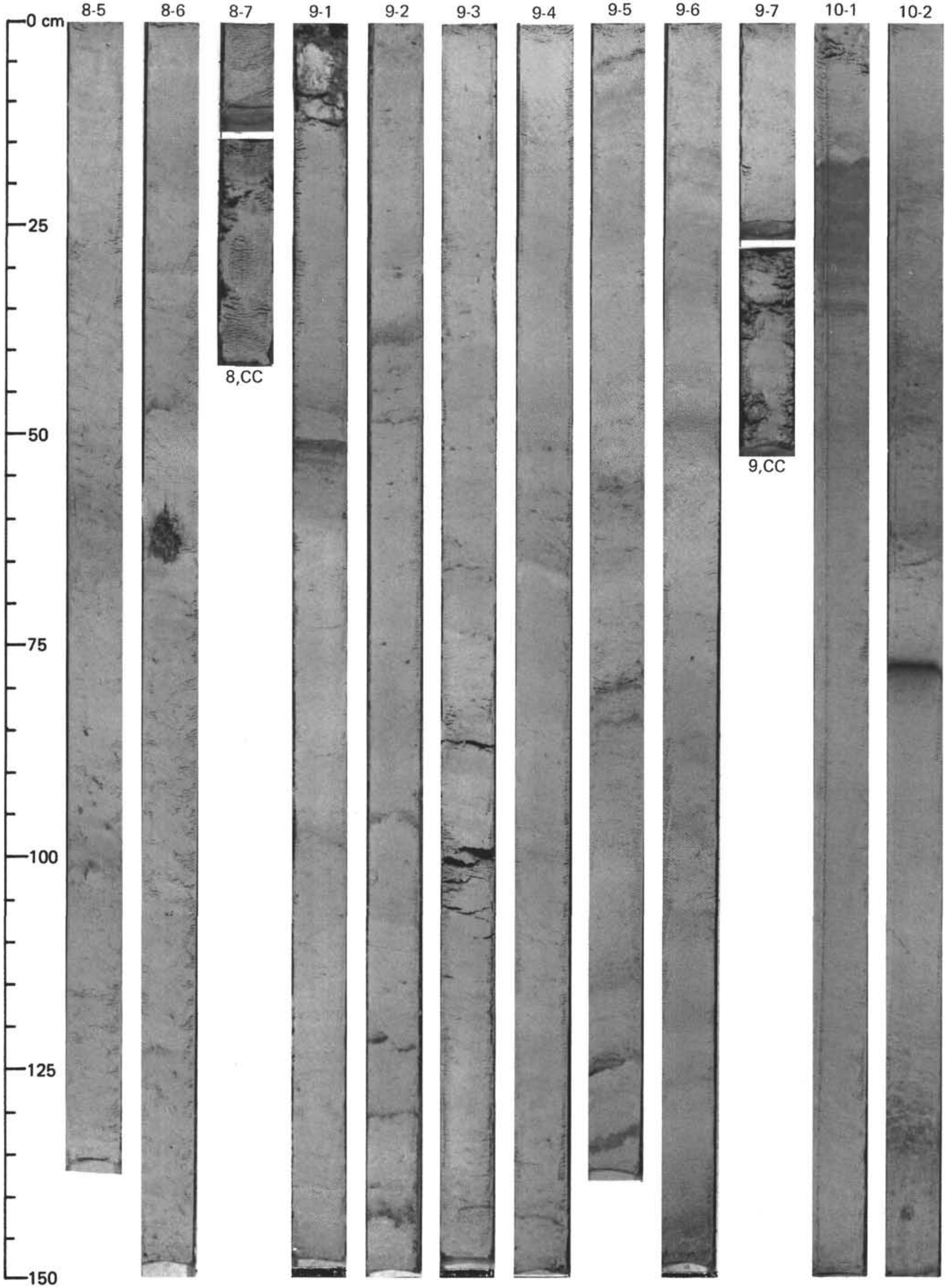
0 cm
25
50
75
100
125
150
8-5
8-6
8-7
9-1
9-2
9-3
9-4
9-5
9-6
9-7
10-1
10-2
8,CC
9,CC

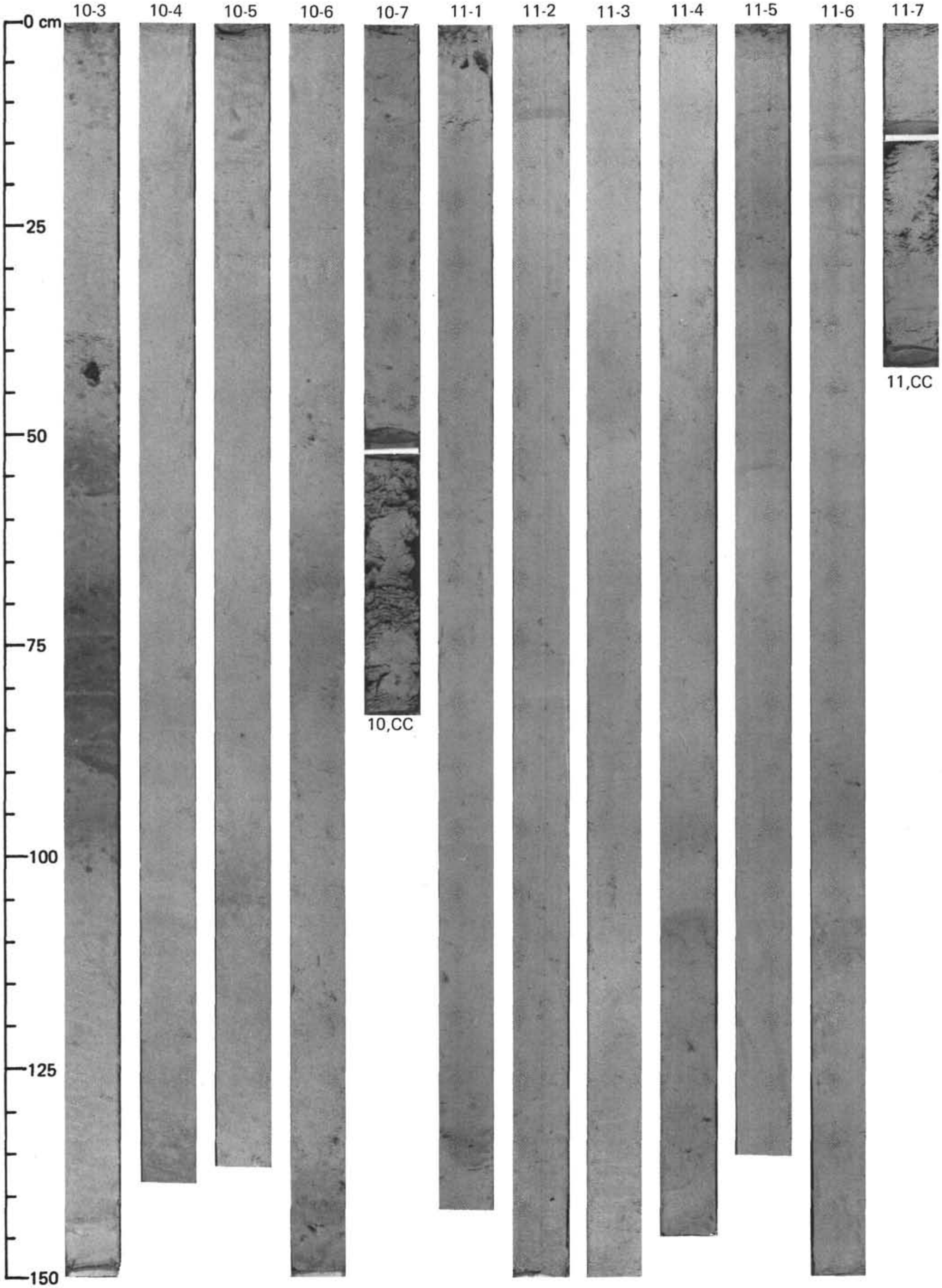
0 cm
25
50
75
100
125
150
10-3
10-4
10-5
10-6
10-7
11-1
11-2
11-3
11-4
11-5
11-6
11-7
10,CC
11,CC

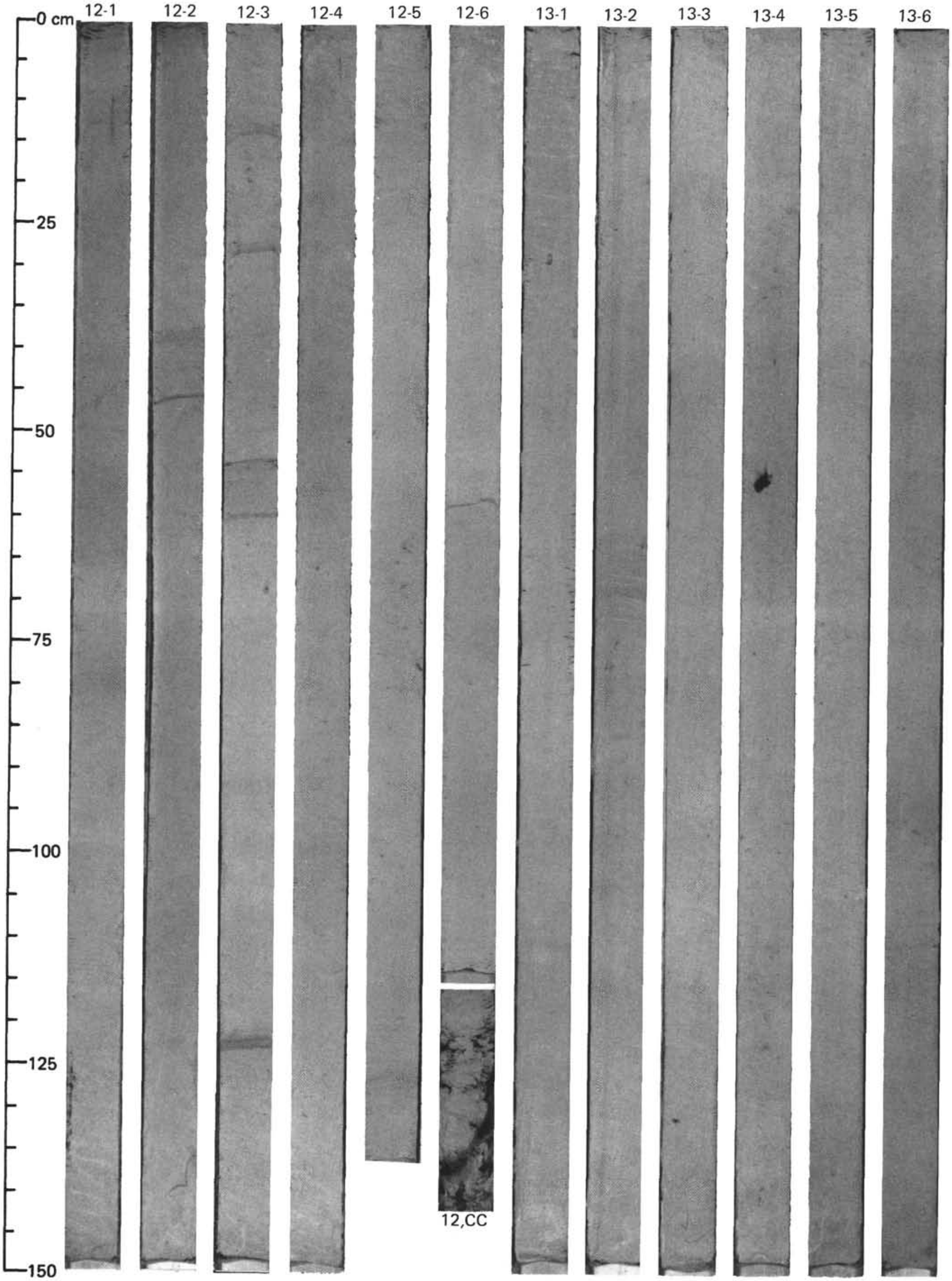
0 cm
25
50
75
100
125
150
12-1
12-2
12-3
12-4
12-5
12-6
12,CC
13-1
13-2
13-3
13-4
13-5
13-6

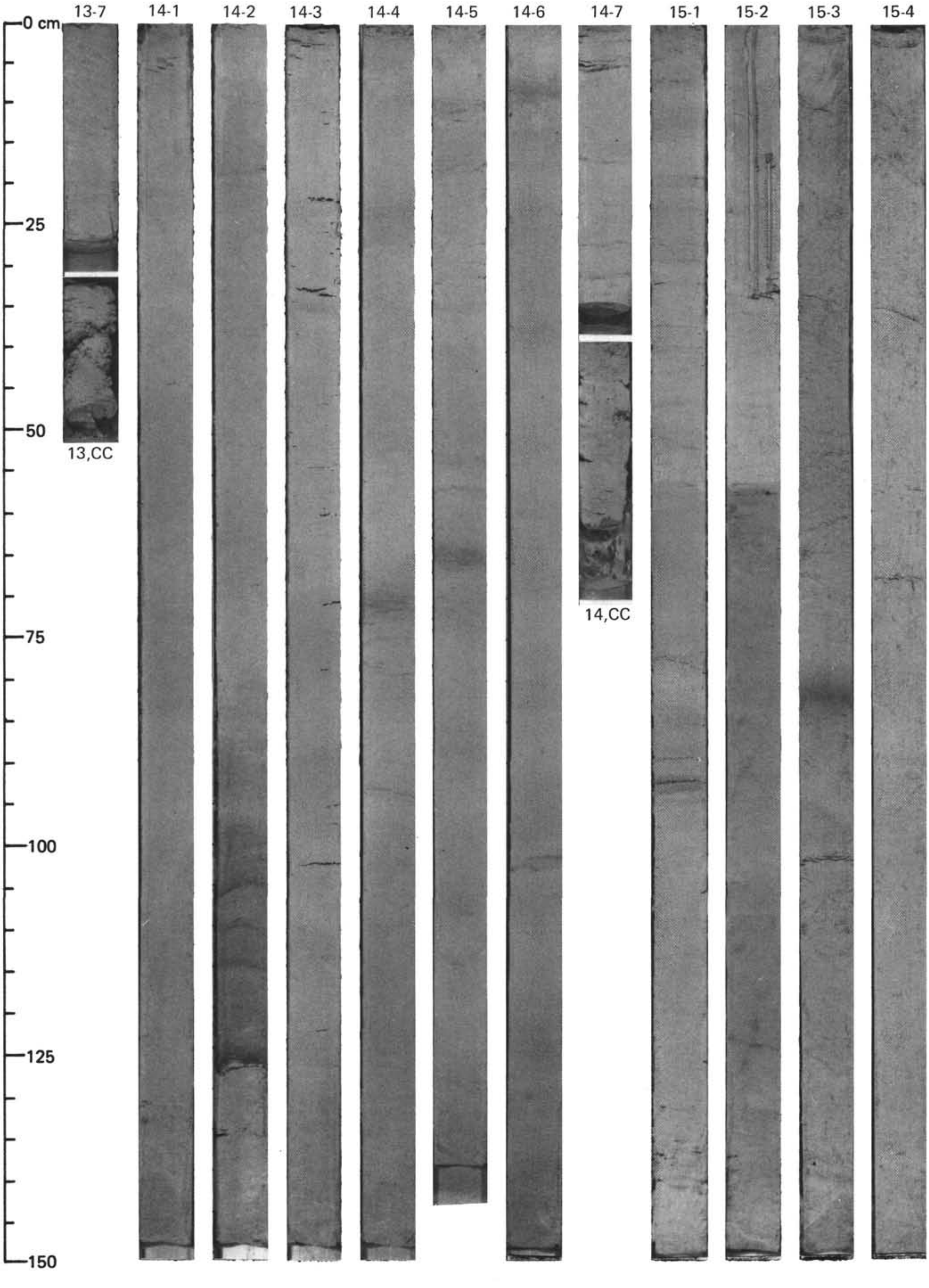
0 cm
25
50
75
100
125
150
13-7
14-1
14-2
14-3
14-4
14-5
14-6
14-7
15-1
15-2
15-3
15-4
13,CC
14,CC

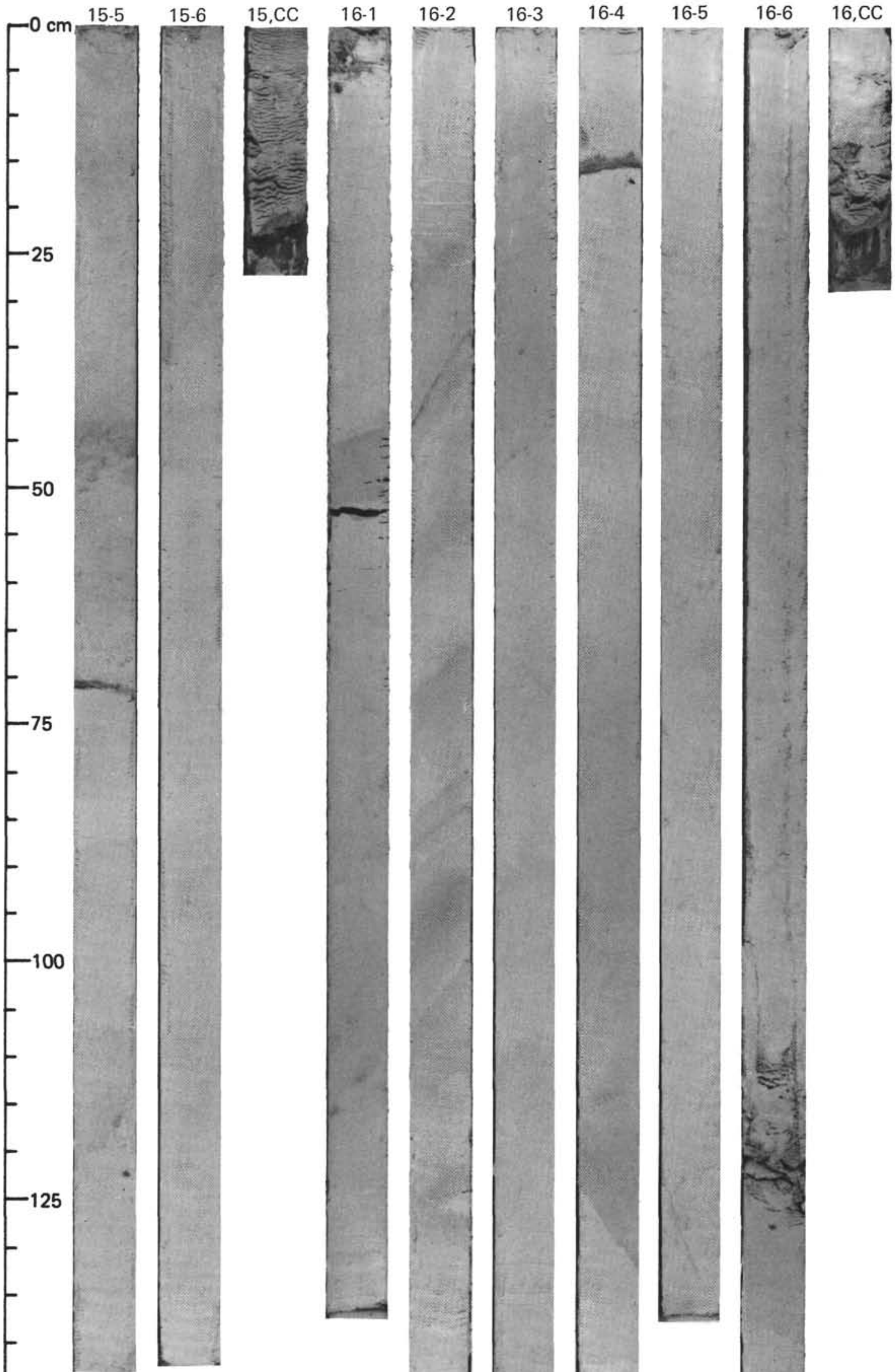
15-5
15-6
15,CC
16-1
16-2
16-3
16-4
16-5
16-6
16,CC
0 cm
25
50
75
100
125
150